NASA TECHNICAL TRANSLATION

NASA TT F-751

NASA TT F-751

(NASA TT F-751) STABILITY AND OSCILLATION OF ELASTIC SYSTEMS: MODERN CONCEPTS, PARADOXES AND ERRORS (Scientific Translation Service) 426 p HC $8.75 CSCL 20K N70-14626 thru N70-14628 Unclas 25078

RECEIVED NOV 1970 NASA ST FACILITY INPUT BRANCH

STABILITY AND OSCILLATION OF ELASTIC SYSTEMS: MODERN CONCEPTS, PARADOXES AND ERRORS

Second Edition

by Ya. G. Panovko and I. I. Gubanova

"Nauka" Press, Moscow, 1967

NATIONAL AERONAUTICS AND SPACE ADMINISTRATION • WASHINGTON, D. C. • NOVEMBER 1972

ANNOTATION

This book discusses contemporary problems such as "jumps" in elastic systems, problems of aeroelasticity, problems of frictional self-oscillations, and self-synchronization, giving only the elementary data on these questions.

The first part examines the stability of equilibrium shapes of elastic systems. Stability loss in the case of similar equilibrium shapes, the disappearance of stable equilibrium shapes, and the disappearance of any forms of equilibrium are discussed. The error made by Euler in analyzing stability loss is pointed out, and Mises' truss is used as an example of stability loss in the case of similar equilibrium shapes.

The second part deals with problems of oscillations of linear systems, including systems with a fractional number of degrees of freedom, as well as free oscillations of a cantilever in the field of centrifugal forces. Four methods of solving the problem of the action of periodic instantaneous impulses are presented. The Tacoma catastrophe is analyzed and used as an example of aeroelastic oscillations. Problems of nonlinear system oscillations include the vibration maintenance of rotation, the Sommerfeld effect, and self-oscillations of a quasi-system with dry friction.

PRECEDING PAGE BLANK NOT FILMED

FOREWORD TO THE FIRST EDITION

Many books, both textbooks and monographs, have been devoted to the /7* stability and oscillations of elastic systems. This book is neither a textbook nor a monograph. The authors have written it as a "book for reading" and a collection of synopses devoted to selected problems of elasticity theory and the theory of oscillations of elastic and incompletely elastic systems. Consequently, this book is divided into two parts, and each section is devoted to its own individual topic, falling more or less far beyond the limits of the usual educational courses.

In part of the sections some paradoxical results and erroneous solutions are discussed, but the majority of the sections are devoted to contemporary problematics — the problems which are being actively discussed in the periodical literature and which are represented in special monographs but are still not elucidated in textbooks ("jumps" in elastic systems, the effect of following loads, the problems of aeroelasticity, the problems of frictional self-oscillations and self-synchronization, and so on). Here only elementary data are given; the authors have strived for an extremely simplified and most transparent statement of the individual problems. Of course, this approach has imparted a certain sketchiness to the exposition, but it was very difficult to overcome it within the limits of the modest extent of the present book.

Thus, the book is composed of individual accounts rather "mixed" in their content; because of this fact, it was not possible to achieve just a single level of complexity but a smooth increase in it. The book is calculated for a broad circle of readers who have mastered the laws of theoretical mechanics and strength of materials in the schedule of courses of engineering universities — students and graduate students of engineering universities and also

*Numbers in the margin indicate pagination in the original foreign text.

PRECEDING PAGE BLANK NOT FILMED

young engineers who are involved in computational-design and research work.

References to the literature are cited at the end of each section and /8
are accompanied by short commentaries.

The authors are deeply grateful to V. I. Feodos'yev and I.K. Smitko for a number of useful remarks made by them while becoming familiar with the manuscript.

G. Yu. Dzhanelidze devoted a large amount of attention to the manuscript; his valuable advice helped eliminate many inadequacies of the discussion. This remarkable person and scientist passed away when the production of the book was nearing its end. The authors will keep forever a grateful memory of the deceased.

Riga, January, 1964.

Ya. G. Panovko,
I. I. Gubanova

FOREWORD TO THE SECOND EDITION

The former structure of the book has been completely maintained in the present edition, but a number of new sections are included (Sect. 2, 12, 13, 14, 20, 23, 29, 30, 33, 34, 36), and Sect. 5, 7, 8, 17, 19, 21, 22, 32, have been significantly supplemented. In addition, small errors which slipped into the first edition have been corrected. The authors are sincerely grateful to those individuals who have helped with their advice to improve and supplement the book, and in particular, L. I. Balabukh for a number of subtle remarks and valuable advice.

Leningrad — Riga,
March, 1966.

Ya. G. Panovko
I. I. Gubanova

TABLE OF CONTENTS

Forword to the First Edition v

Forword to the Second Edition vi

PART 1

THE STABILITY OF EQUILIBRIUM SHAPES OF ELASTIC SYSTEMS

Introduction 1

Chapter I. The Loss of Stability Upon the Appearance of Similar Equilibrium Shapes 5

§ 1. Euler's Error 5

§ 2. The Effect of Subcritical Compression of a Bar on the Critical Value of the Compressive Force . . 11

§ 3. One Version of the Application of the Energy Method 17

§ 4. Loads Whose Values Depend on the Displacements . 22

Chapter II. Loss of Stability Upon the Appearance of Non-Similar Equilibrium Shapes 43

§ 5. The Mises' Truss 43

§ 6. The Stability of a Fluted Strip 51

§ 7. More Examples of Systems with Jumps; Discussion of the Results 58

Chapter III. Stability Loss Upon the Disappearance of Stable Equilibrium Shapes 70

§ 8. Tracking Loads. Static Statement of the Problem . 70

§ 9. Tracking Loads. Dynamic Statement of the Problem . 80

§10. Tracking Loads. A System with Two Degrees of Freedom 87

§11. The History of the Problem 91

Chapter IV. Stability Losses When Any Forms of Equilibrium Disappear 96

§ 12. General Stability of High Buildings 97
§ 13. Characteristics of "Deformation Calculations" . . 104
§ 14. Two Discussions (Solutions of R. Lorenz and V. E. Vlasov) 113
§ 15. Stability Losses of a Rod Under Tension 125
§ 16. Critical Internal Pressure for a Spherical Shell . 136
§ 17. Rotation of a Flexible Shaft in a Rigid Tube-Shell . 140

Chapter V. Buckling of Not Fully Elastic Rods 153
§ 18. Elastic-Plastic Buckling; Classical Concept . . . 153
§ 19. Elastic-Plastic Buckling; Present-Day Concept . . 160
§ 20. Buckling of a Rod in a Statically Indeterminate System 167
§ 21. Stability Loss in the Case of Material Creep . . 175

PART 2

OSCILLATIONS OF ELASTIC SYSTEMS

Introduction 184

Chapter VI. Certain Problems of Oscillations of Linear Systems 187
§ 22. System with a Fractional Number of Degrees of Freedom 187
§ 23. Free Oscillations of a Cantilever in the Field of Centrifugal Forces 192
§ 24. Equal-Frequency Shock Absorber 197
§ 25. Comments on the Formulas of Rayleigh and Grammel . 201
§ 26. Lagrange Errors 214
§ 27. Formula of A. N. Krylov 224
§ 28. Four Methods of Solving the Problem of the Action of Periodic Instantaneous Impulses 233
§ 29. Superpositions: Variations of Using It in Problems of Forced Oscillations 244
§ 30. The "Inverse" Form of Differential Equations of Oscillations 252
§ 31. Terminology Information: Impedance, Receptance, Admittance, Response, Anti-Resonance 259

§ 32. Parametric Excitation of Oscillations 269
§ 33. Destabilizing Action of the Forces of Viscous Friction 285
§ 34. Linear Realizations of Dry Friction Forces . . . 292
§ 35. Paradox Connected with Damping Coverings . . . 302
§ 36. Damping of Pipeline Oscillations by Coriolis Forces 309

Chapter VII. Dynamic Action of a Moving Load 314
§ 37. Brief Historical Sketch 314
§ 38. Bresse Error 322
§ 39. A Travelling Bending Wave 327
§ 40. Action of an Infinite Strip of a Moving Load . . 332

Chapter VIII. Aeroelastic Oscillations 338
§ 41. Dynamic Problems of Aeroelasticity Theory . . . 338
§ 42. "Classical" Flutter 341
§ 43. Tacoma Catastrophe; Separation Flutter 351

Chapter IX. Problems of Nonlinear System Oscillations . . 358
§ 44. Vibration Maintenance of Rotation 358
§ 45. Dynamics of the Boisse-Sarda Regulator 365
§ 46. Sommerfeld Effect 372
§ 47. Self Oscillations; Method of Slowly Changing Amplitudes 383
§ 48. Self Oscillations of a Quasi-System with Dry Friction 393
§ 49. Discontinuous Self Oscillations in the Case of Dry Friction 400
§ 50. Delta Method 406

PART 1

THE STABILITY OF EQUILIBRIUM SHAPES OF ELASTIC SYSTEMS

Ya. G. Panovko and I.I. Gubanova

INTRODUCTION

/9

The term "stability" is, according to the expression of one contemporary scientist, "strongly overworked and has a variable definition." This remark is valid not only for the concept of the stability of motion as a whole but also for the narrower problem of the stability of equilibrium shapes of elastic systems. In the latter case, stability does not completely and wholly characterize how an elastic system is capable of maintaining a specific equilibrium shape under the action of a given load. However, the loss of this capability as a function of the system's properties can be expressed in various ways, and several completely different phenomena are understood by loss of stability.

The principles of the theory of the stability of equilibrium shapes of elastic systems were propounded by Euler more than two centuries ago. According to Euler's conception, the existence of similar (i.e., as near to the original as desired) displaced equilibrium shapesin the case of a constant

load serves as the criterion of the instability of an equilibrium shape. It is possibly understood that just this new equilibrium shape is stable, and the original shape is unstable. Such a statement of the problem assumes that the loss of stability is expressed in the system's transition to a similar equilibrium shape and that any negligibly small perturbation of the original equilibrium shape is sufficient for this transition.

Of course, the possibility of the existence of displaced equilibrium shapes depends on the load level, as this is established, for example, in the case of the solution of the problem of buckling of a centrally compressed bar. Stable and unstable equilibrium states for this case are represented by the curves in Figure 0.1- the points of the heavy lines correspond to the stable states, and the unstable states are denoted by small crosses. The characteristic deflection v is plotted along the abscissa, and the values of the compressive force P are plotted along the ordinate. /10

In the case of forces such that $P < P_{crit}$ there exists a unique equilibrium state when $v = 0$ (the bar's axis is straight). In the case of $P = P_{crit}$ a branching of the equilibrium shapes (bifurcation) occurs, and in the case of $P > P_{crit}$ the displaced shapes become stable. It is assumed here that the system's shape is determined only by the characteristic displacement v, and the higher multinodal equilibrium shapes are not represented.

Within the framework of Euler's conception, it has proven possible to solve any important problems concerning the stability of bar systems, plates, and shells. However, it turned out later that the Eulerian statement of the problem is not universal, and the loss of stability in a number of cases is expressed not as a transition to similar equilibrium shapes but in some other way. One can point out three classes of such cases, which are illustrated by the typical P — v graphs in Figures 0.2 — 0.4.

For some systems, the connection between the quantities P and v has the form illustrated in Figure 0.2. If in the case of a monotonic increase in the /11

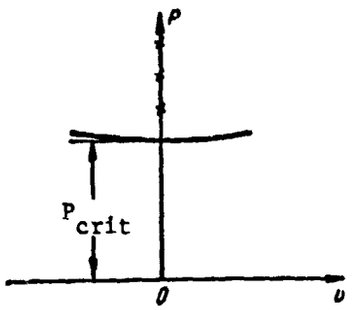

Fig. 0.1. Adjacent equilibrium shapes appear at $P = P_{crit}$.

load P the value P_{crit} is reached, there occurs a "jump" of a representative point (v, P) to a different branch of the curve. In such systems the stability loss consists of a sharp transition to a new (dissimilar) equilibrium shape.

There also exist mechanical systems for which the unperturbed shape is the unique equilibrium shape. However, it is stable only up to a specific load level $P = P_{crit}$ (Figure 0.3), and therefore, when $P \geq P_{crit}$ the departure of the system from a state of rest to motion is practically inevitable, as is indicated by the dashed lines. The stability of such systems is in general impossible to ascertain by a statistical investigation, and only the dynamical method offers a conclusion as to the stability in such cases.

A typical P — v diagram is illustrated in Figure 0.4 for systems which do not in general possess equilibrium shapes in the case of loads exceeding a certain level which is dependent on the system's properties. If we assume the conditions of monotonic loading, the left-hand part of the graph (the ascending branch of the curve) corresponds to stable equilibrium states, and the right-hand part (the descending branch of the curve) corresponds to unstable equilibrium

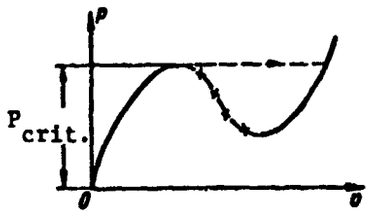

Fig. 0.2. A jump onto the right-hand ascending branch of the curve occurs at $P = P_{crit}$.

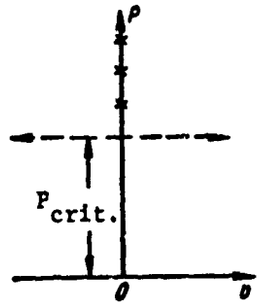

Fig. 0.3. Only points of the ordinate correspond to equilibrium states; when $P > P_{crit}$, these states are unstable.

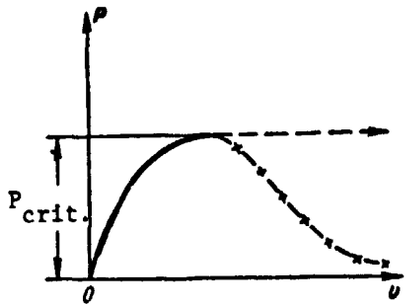

Fig. 0.4. When $P > P_{crit}$, there are no equilibrium states. Sometimes the ascending branch of the curve approaches the straight line $P = P_{crit}$ asymtotically.

states. If the load reaches the value P_{crit}, an unrestricted increase in the displacements occurs, as is shown by the dashed line.

The present part of the book consists of five chapters, and the first four are devoted to the problems of the elasticity of elastic systems. The division into chapters was associated with those distinctive features of the appearance of instability which one can see from a comparison of the P — v curves and Figures 0.1 -- 0.4.

The problems of the stability of incompletely elastic systems are discussed in Chapter V.

N74-14627

CHAPTER I

THE LOSS OF STABILITY UPON THE APPEARANCE OF SIMILAR EQUILIBRIUM SHAPES

The synopses appearing in this chapter refer to case of stability loss pointed out by Euler. The error which was spoken of in Section 1 is interesting not only as an historical curiosity,(*) it gives a convenient occasion for a useful probing into the essence of the matter. The effect of subcritical compression on the critical value of the compressive force, which is usually not taken into account, is discussed in Section 2, and a curious peculiarity of one of the widely used versions of the energy method is dis- sed in Section 3. Cases of stability loss are described in Section ...e case of loads whose magnitude varies as the configuration of the ... c system changes; in particular, here the loss of stability of the lifting surfaces of aircraft (divergence) and the loss of stability of pipe ducts are schematically described.

§ 1. Euler's Error

Leonard Euler (1707 - 1783) left an indelible mark in mechanics and in mathematics. Adademician S. I. Vavilov wrote: "Along With Peter I and Lomonosov, Euler became a good spirit of our Academy, who determined its honor, its greatness and its productivity."

Euler is the founder of the theory of stability of equilibrium shapes of elastic systems. He turned his attention to this problem repeatedly, starting /13 in 1744; Euler wrote the last of his papers devoted to the problems of the

*An interesting collection of such cur'osities is brought together in Lecat's book "The Errors of Mathematicians From Antiquity to Our Times" (Brussel, 1935.) Among the authors whose errors are cited in this book are Jacob and Johann Bernoulli, Galileo, d'Alembert, Cauchy, Lagrange, Laplace, Newton, and Euler.

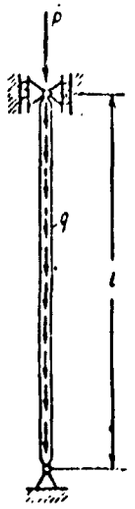

Fig. 1.1. A uniformly distributed load q is acting on the column in addition to the compressive force P.

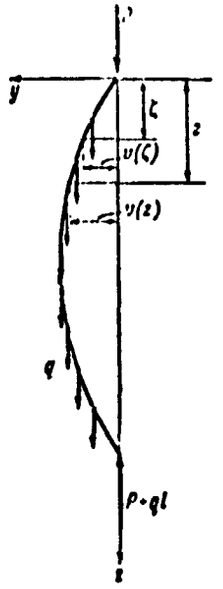

Fig. 1.2. Layout adopted by Euler for the forces acting on the column.

buckling of bars in 1778, when he was seventy years old. In this section, we will discuss the error which crept into one of Euler's papers on buckling; Euler himself subsequently noticed and corrected this error.

In a paper of 1744, Euler, proceeding from the exact differential equation of a curved shaft, establishes the significance of the critical force for a hinge-supported bar which is compressed at its ends.

In his next publication (1757) he obtains the same result using a linearized differential equation. The concluding part of this publication is devoted to the problem of the stability of the straight equilibrium shape of a bar loaded not only by compressive forces at its ends, but also by a longitudinal uniformly distributed load (Figure 1.1). However, the solution which he gave for this problem contained a significant error. We will trace Euler's calculations, adopting the following notation: q is the intensity of the distributed load, P is the compressive force at the upper end of the bar, z is the coordinate of the instantaneous cross-section of the bar whose deflection in the case of buckling is equal to v(z), and ζ is the abscissa of the instantaneous cross-section, which varies within the limits [0, z].

An element of the load q dζ causes a bending moment-q dζ [v(z) — v (ζ)] in the cross-section with abscissa z; the total bending moment at this cross-section is equal to the sum of the moments of all the forces located between the upper end of the bar and the cross-section under discussion (Figure 1.2):

$$M(z)=-\int_0^z q\,[v(z)-v(\zeta)]\,d\zeta-Pv(z) \tag{1.1}$$

On the other hand,

$$M(z)=EI\frac{d^2v}{dz^2}, \tag{1.2}$$

and the integro-differential equation of the bar's curved axis takes the form

$$EJ\frac{d^2v}{dz^2}+q\int_0^z[v(z)-v(\zeta)]\,d\zeta+Pv(z)=0. \tag{1.3}$$

We will transform the integral appearing in Equation (1.3):

$$\begin{aligned}\int_0^z[v(z)-v(\zeta)]\,d\zeta&=v(z)\,z-\int_0^z v(\zeta)\,d\zeta=\\&=zv(z)-[\zeta v(\zeta)]_0^z+\int_0^z\zeta\frac{dv}{d\zeta}\,d\zeta=\\&=zv(z)-zv(z)+\int_0^z\zeta\frac{dv}{d\zeta}\,d\zeta=\int_0^z\zeta\frac{dv}{d\zeta}\,d\zeta.\end{aligned} \tag{1.4}$$

Then we obtain in place of Equation (1.3)

$$EJ\frac{d^2v}{dz^2}+q\int_0^z\zeta\frac{dv}{d\zeta}\,d\zeta+Pv(z)=0 \tag{1.5}$$

or, after differentiation with respect to the z coordinate,

$$EJ\frac{d^3v}{dz^3}+qz\frac{dv}{dz}+P\frac{dv}{dz}=0. \tag{1.6}$$

We note that this equation follows directly from the equation for the transverse force Q; however, in Euler's time this expression was not known (the differential dependence between the bending moment and the transverse force

$Q = \frac{dM}{dz}$ was not established until the middle of the 19th century). /15

Equation (1.6) is of the third order, and therefore its solution will contain three constants. The paradoxical nature of Equation (1.6) has already appeared here, since its solution must satisfy the four boundary conditions

$$v = 0, \quad \frac{d^2v}{dz^2} = 0 \tag{1.7}$$

at $z = 0$ and $z = 1$. Evidently, it is impossible to satisfy all four conditions, since there are only three constants at our disposal. Such disagreement in the number of boundary conditions of a problem and the number of constants indicates the incorrectness of the basic Equation (1.6).

The error (if the reader has not already noticed it) consists of what we will explain below. In any case, Euler did not at first give any attention to the indicated disagreement and continued the solution by simply omitting the last of the boundary conditions (1.7). We will not cite this solution of Equation (1.6), since Euler gave it for a case in which the quantity q is small; of course, this solution was erroneous, although it resulted in the correct value for the critical force P_{crit} in the limiting case $q = 0$.

From 1727 to 1741, Euler worked at the Petersburg Academy of Sciences. Toward the end of this period, the conditions for the scientists of the Academy were very difficult in Russia, and many of the foreign scientists hurriedly abandoned Petersburg "wiping away bitter tears" (in Lomonosov's words). Euler availed himself of a proposal by the Prussian King Frederick II and moved to Berlin in order to work at the Berlin Academy of Sciences. Here Euler lived for 25 years, but nearly half of the papers which he wrote during this period were published in the Proceedings of the Petersberg Academy. Among these papers are the investigations of the buckling which we spoke of above.

In 1766, Euler responded to an invitation of Catherine II and returned to Petersberg, where he lived right up until his death. Here already in his

Fig. 1.3. Transverse reactions arise in the case of a buckling caused by the load q.

declining years Euler in 1778 returned again to the problem of buckling. In the problem discussed above, he assumed that there is no compressive force in the upper cross-section and investigated the solution of the differential equation

/16

$$EJ\frac{d^3v}{dz^3} + qz\frac{dv}{dz} = 0. \qquad (1.8)$$

This time the error assumed in setting up the equation was stated in the most sensitive manner, and it was precisely determined that there do not exist any equilibrium shapes, except the linear, for any values of the load q. From this, Euler concluded that such a bar cannot in general lose its stability.

This result, which is contradictory to common sense, caused doubt to Euler himself, and after several months work he advanced a critique of his own preceding work. Euler calls his conclusion regarding the unrestricted stability of a bar loaded by its own weight "not only paradoxical but very suspicious" and asserts that the analytic solution which he derived earlier evidently contains an error. However, Euler still did not see what the error consisted of.

Euler completely clarified the matter only in his next publication, which dates from 1778. He noted that in setting up Equation (1.1) the moment produced by the horizontal reaction N is omitted. If $q = 0$, there will actually not be any horizontal reactions; however, when $q \neq 0$, the appearance of horizontal reactions follows inevitably from the equilibrium conditions of the entire bar (Figure 1.3). Therefore, if one takes account of the moment Nz of the horizontal reaction, the correct differential equation

$$EJ\frac{d^3v}{dz^3} + qz\frac{dv}{dz} = N. \qquad (1.9)$$

is obtained in place of Equation (1.8). Since the value of N is not known, one can treat it as the force constant, the one which was missing earlier for satisfying all four boundary conditions of the problem. Euler constructs the subsequent solution in the form of a power series. Although an error of a purely computational nature crept into Euler's calculations, the result refuted his previous conclusion as to the unrestricted stability of the bar under discussion. /17

The correct solution

$$\frac{q_{crit}\,l^3}{EJ} = 18.6 \qquad (1.10)$$

was given almost one hundred and fifty years later by A. N. Dinnik(*).

A detailed analysis of Euler's papers on the theory of buckling was given in 1938 by Ye. L. Nikolai (**); the following words appear in his article, where the history cited above is expounded in detail: "the paradox clarified with such brilliance by Euler ..., is instructive and deserves attention. The resolution of this paradox consists, as we will see, of the simple observation that if the freedom of the bar's ends to translate in the transverse direction is restrained by any conditions, corresponding transverse reactions should be applied to the bar's ends. This fact is sometimes overlooked. We will repeatedly encounter again in the history of the

*Aleksandr Nikolayevich Dinnik (1876 - 1950) was an Academician of the Ukrainian SSR Academy of Sciences (from 1929). In 1946 he was chosen as a Member of the USSR Academy of Sciences. The most important investigations of A. N. Dinnik are associated with the problem of the stability of elastic systems and also with the contact problem of the theory of elasticity.

**Evgeniy Leopol'dovich Nikolai (1880 - 1950) was from 1917 up until his death a professor at the Leningrad Polytechnic Institute. A number of important results in the theory of elasticity and oscillations of elastic systems are due to him.

theory of stability of elastic systems the error initially assumed by Euler in his 1757 memoir and straightened out by him in 1778. Thus, in the problem of the stability of a bar simultaneously subjected to compression and torsion, we will find this same error in the papers of Greenhill and Grammel." (See E. L. Nikolai's "Treatise on Mechanics", Moscow, 1955, pp. 452 - 453).

The papers of Greenhill and Grammel are related to the problem of the stability of a straight bar under the effect of compressive forces and torsional moments applied to its ends. See Section 11 concerning these papers.

§ 2. The Effect of Subcritical Compression of a Bar on the Critical Value of the Compressive Force

Analogous to a flexible bar with a rectilinear axis, a compressed twisted spring loses its stability when a critical value of the compressive force is reached. One of the simplest solutions of this characteristic problem is based on the replacement of the spring by the equivalent bar; the critical force /18 for the equivalent bar is determined from Euler's equation. But in determining the critical force for such a bar it is necessary to take into account the fact that in Euler's equation

$$P_{crit} = \frac{\pi^2 EJ}{(\mu l)^2} \qquad (2.1)$$

(EJ is the rigidity upon deflection, and μ is the length coefficient), we should, strictly speaking, take l to mean not the initial length of the bar (i.e., its length in the unloaded state) but a somewhat shorter length which the bar has at the instant it loses stability. It is understood that if we are speaking of a calculation of the stability of a real bar, the identification of two very similar dimensions cannot entail any kind of sensitive error. But it is necessary to take into account the subcritical compression in those cases in which Euler's equation is applied to an equivalent bar which replaces some compressed twisted spring.

The following simplified statement of the equivalent problem is of interest precisely from this point of view. The discussion is devoted to a

compressed bar made of a very pliant material which obeys Hooke's law without restriction; it is taken into consideration that at the instant of stability loss the bar's length l is less than its initial length l_0 by the amount

$$\Delta l = \frac{P_{crit}\, l_0}{EF}$$

where EF is the compressive rigidity, which we will assume to be constant during the process of compression and l_0 is the bar's initial length. Thereupon, Euler's equation (2.1) is transformed into the equation

$$P_{crit} = \frac{\pi^2 EJ}{\left[\mu\left(l_0 - \frac{P_{crit}\, l_0}{EF}\right)\right]^2} \qquad (2.2)$$

from which it is necessary to find the critical force P_{crit}. Let us introduce the following notation: $p = \frac{P_{crit}}{EF}$ is the dimensionless critical stress, i.e., the ratio of the critical stress (P_{crit} : F) to the modulus of elasticity; $\lambda_0 = \mu l_0 \sqrt{\frac{F}{J}}$ is the bar's initial flexibility. Then Equation (2.2) will take the form

$$p(1 - p)^2 = \frac{\pi^3}{\lambda_0^2} \qquad (2.3)$$

Then it is necessary to find p from this cubic equation, after which the critical force is determined by a multiplication of the value found for p by the compressive rigidity EF. /19

We will trace out the properties of the roots of Equation (2.3) for three different levels of accuracy of the solution.

The crudest assumption is that p is so small in comparison with unity that one can neglect p inside the brackets of Equation (2.3). At this level of linear approximation, we obtain

$$p = \frac{\pi^2}{\lambda_0^2} \qquad (2.4)$$

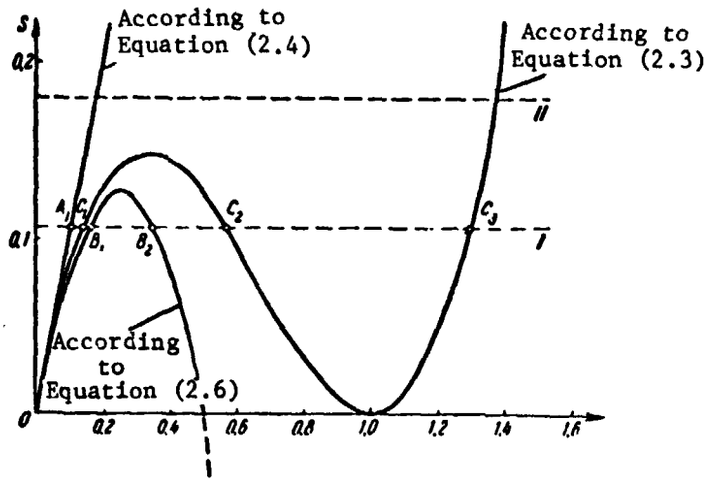

Fig. 2.1. Dependence of the left-hand sides S of Equations (2.3), (2.4) and (2.6) on the parameter p. The right-hand side of these equations depends on the initial flexibility λ_0 and is represented by the dashed lines I and II.

in place of Equation (2.3), i.e., Euler's equation. A more accurate approach turns out to be the quadratic approximation, which is obtained if one replaces

$$(1 - p)^2 \approx 1 - 2p. \tag{2.5}$$

in Equation (2.3). Then we will have

$$p - 2p^2 = \frac{\pi^2}{\lambda_0^2} \tag{2.6}$$

in place of Equation (2.3). Finally, the completely exact approach is the solution of the cubic equation (2.3) in its unmodified form.

The left-hand sides S(p) of Equations (2.4), (2.6), and (2.3) are presented graphically in Figure 2.1 as a function of the sought-after value p. In the case of very small values of p the curves are practically indistinguishable. However, as p increases, an increasing difference develops which is, moreover, not just of a quantitative nature but of a qualitative nature.

In order to determine the roots of each of the equations (2.4), (2.6), and (2.3), we will represent the right-hand side of these equations in the form of a horizontal line separated from the abscissa by a distance $\frac{\pi^2}{\lambda_0^2}$, and then we will note the abscissas of the intersection points of this straight line with the corresponding curves. In the case in which the right-hand side is represented by the dashed lines I (Figure 2.1), the linear approximation gives a unique value for the critical parameter p (the point A_1), the quadratic approximation gives two such values (the points B_1 and B_2), and the exact solution gives three values (the points, C_1, C_2, C_3).

Of course, in the case of multivalued solutions practical significance should be assigned only to the smallest roots, i.e., the points B_1 and C_1. /20 As long as the initial flexibility λ_0 is large and the horizontal straight line is located close to the abscissa, the points A_1, B_1 and C_1 are not too far from one another and all the approximations give similar results.

However, if the initial flexibility λ_0 is small, the horizontal straight line is situated higher and perhaps even above old maxima of the curves of Equations (2.6) and (2.3) (the dashed straight line II). In this case, a marked disagreement develops among the three solutions being considered; in general there are no real solutions in the quadratic approximation (i.e., as if the impossibility of instability loss is confirmed). Thus, the different levels of approximations may lead to results which differ quantitatively and even qualitatively.

It is very interesting that the solution of the complete Equation (2.3) possesses an amazing property, namely, a discontinuous dependence of the critical parameter p on the bar's initial flexibility. We will trace out the variation of the critical parameter p in the case of a gradual decrease in the /21 initial flexibility λ_0, using Equation (2.3). The horizontal lines on Figure 2.2 represent the sequence of smallest roots of Equation (2.3). As is evident, when the flexibility decreases, the critical parameter p first

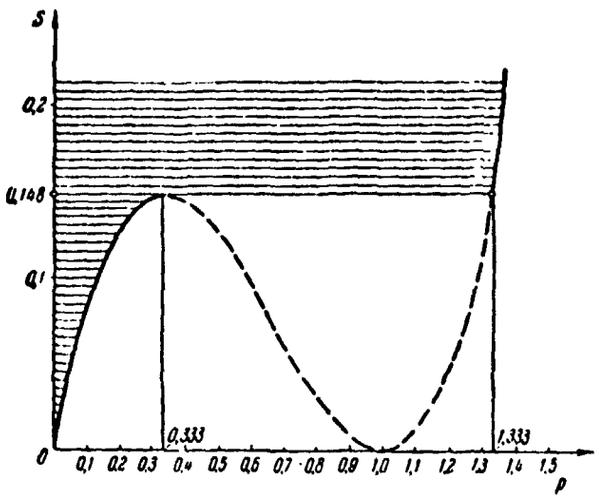

Fig. 2.2. The horizontal segments determine the critical values of the parameters p for various values of the initial flexibility λ_0.

increases monotonically but at a certain value of the initial flexibility $\lambda_0 = \lambda_0^*$ the critical value of the parameter p undergoes a jump from the value p = 0.333 to the value p = 1.333; upon a further decrease in the initial flexibility λ_0 the critical value of p again increases monotonically.

Simple calculations show that the jump occurs at a value of the initial flexibility of

$$\lambda_0^* = 8.162. \qquad (2.7)$$

Of course, this flexibility is very small and for the overwhelming majority of design materials is many times less than the value of the flexibility which limits from below the region of applicability of Euler's theory. However, if one assumes that materials will appear in the future with an exceeding high limit of proportionality, it will become necessary to use in place of the usual hyperbola of Euler (the curve a in Figure 2.3) the corrected curve containing a discontinuity (curve b in Figure 2.3). As is evident, even in the case of unrestricted validity of Hook's law, Euler's hyperbola becomes more and more inapplicable in cases of small flexibility. /22

As was pointed out at the start of this section, what has been expounded above has a direct relationship to the problem of the stability of twisted compression springs.

More than half a century ago, E. Hurlbrink investigated the stability of such a spring by replacing it with an equivalent bar having an initially straight axis. E. Hurlbrink used Euler's method, but he took into consideration

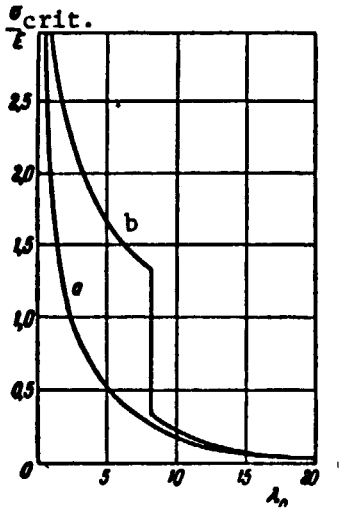

Fig. 2.3. Euler's hyperbola (a) and the more accurate curve (b).

the fact that due to the compression by the force P_{crit} the equivalent bar's length differs significantly at the instant of stability loss from its initial length.

On the basis of these ideas a quadratic equation was derived for the critical value of the load, and it was discovered that there exists a region of values of the parameters of springs in which stability loss in general becomes impossible. In 1924 R. Grammel(*) turned to this problem and characterized the existence of the indicated region as "a remarkable and technically very interesting fact." A year later Biezeno and Koch refined the solutions by taking into account the effect of the transverse force on the deflection; having obtained a cubic equation for the critical load, Biezeno and Koch established that a spring can lose stability for any values of its parameters.

The graph in Figure 2.1 clearly illustrates how at different levels of /23 approximation significantly discordant results can be obtained. One can say that the quadratic parabola illustrated in the graph expresses the existence of the Hurlbrink-Grammel solutions and the cubic parabola expresses the existence of the Biezeno — Koch solution (**).

(*) Richard Grammel (1889 — 1964) was a professor at the Stuttgart Technical Academy and the author of a number of investigations in the area of the mechanics of a solid body and the applied theory of elasticity.

(**) In 1946 N. A. Chernyshev investigated the stability of a twisted spring upon compression, without drawing on the concept of an equivalent bar and treating the spring as a three-dimensional bar with an axis of double curvature; having been restricted by the quadratic approximation, N. A. Chernyshev naturally came to the conclusion that there are springs which do not lose their stability.

The Biezeno — Koch solution has been discussed in the book of K. Biezeno and R. Grammel entitled "Engineering Dynamics" (Gostekhizdat, Leningrad — Moscow, 1950, Vol. 1, pp. 799 — 805) and also in S. T. Timoshenko's book "The Stability of Elastic Systems" (Gostekhizdat, Moscow, 1955, pp. 179 — 182). See the paper by N. A. Chernyshev entitled "The Stability of Compression Springs" in the book "New Methods for the Calculation of Springs" (Mashgiz, Moscow, 1946); also see the paper by V. M. Makushin entitled "Critical Values of Loads in the Case of Two-Dimensional Equilibrium Shapes of Compressed Bars" (in the book "Strength Calculations in Mechanical Engineering" edited by S. D. Ponomarev, Mashgiz, Moscow, 1950, Vol. 3, Chapt. 22).

§ 3. One Version of the Application of the Energy Method

The investigation of the Eulerian type of stability loss (i.e., a stability loss which is associated with branching of the equilibrium shapes) has not always been successfully completed by the method which Euler himself used, mainly the method of setting up and integrating exactly the differential equation of the problem. Even for compressed bars in the general case of the variability of the moment of inertia along the bar's length, it is necessary to solve the equation of the buckling by this or another approximate method. One of the most widespread and useful of these methods is the energy method, which permits a roundabout way (without integration of the problem's equation) of determining approximately (but with a high degree of accuracy) the values of the critical loads.

The effectiveness of the energy method in solving problems of elasticity theory is generally well known. The method was introduced by Kirchhoff(*) in

(*) Gustav Robert Kirchhoff (1824 — 1887) was a professor of physics at Heidelberg University (1854 — 1875) and at Berlin University (1875 — 1887). From 1863 he was a corresponding member of the Petersberg Academy of Sciences, and from 1870 he was a member of the Berlin Academy of Sciences. He was the author of many investigations on mathematical physics, and particularly on elasticity theory.

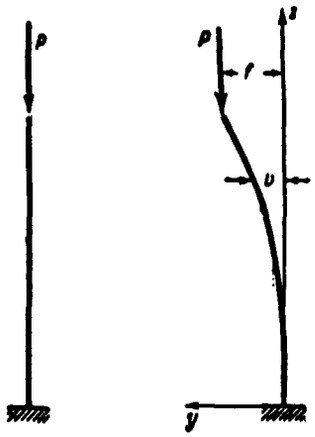

Fig. 3.1. Longitudinal deflection of a cantilever column.

1850 and was applied to problems of the theory of elasticity by Brown (1891) and S. P. Timoshenko (1906). The energy method is based on the Lagrange — Dirichlet theorem for conservative systems subject to holonomic, steady-state, and ideal constraints: if the system's potential energy at the equilibrium position has a minimum, the equilibrium position is stable. The paradox which arises in one of the versions of this method's application is described below.

We will recall the main idea of the energy method, following S. T. Timoshenko's book "The Stability of Elastic Systems" (Moscow, 1955, p. 91), in which the cantilever illustrated in Figure 3,1 (a) is discussed:

"Let us assume that a buckling has occurred, as shown in Figure 3.1 (b); then the deformation energy increases due to the fact that the energy of the bar's deflection is added to the energy of compression. At the same time the potential energy of the load decreases in conformity with a lowering of the point of application. This decrease of the potential energy is simply the work performed by the load as a result of the lowering of the bar's top. If ΔV denotes the deformation energy of the bar's deflection and ΔT denotes the work performed by the load due to the deflection, it is possible to draw the conclusion that an exact shape of the compressed bar is stable if

$$\Delta V - \Delta T > 0;$$

It will be unstable if

$$\Delta V - \Delta T < 0.$$

The critical value of the load at which the straight equilibrium shape changes from a stable state to an unstable one is determined from the equation $\Delta V = \Delta T$". /25

In agreement with the basic idea of the energy method for calculating ΔV and ΔT, it is necessary to proceed from the definite ideas adopted earlier regarding the deflected configuration of a bar: a "suitable" shape of the bent axis should be planned with the actual boundary conditions taken into account.

It is assumed in S. P. Timoshenko's solution that the bent axis is described by the equation

$$v = f\left(1 - \cos \frac{\pi z}{2l}\right), \tag{3.1}$$

where f is the bending deflection of the bar's upper end.

One can convince oneself by a direct substitution that Equation (3.1) satisfies all the boundary conditions of the problem:

$$\begin{aligned} v &= 0 \text{ and } v' = 0 \quad \text{when} \quad z = 0, \\ v &= f \text{ and } v'' = 0 \quad \text{when} \quad z = l. \end{aligned}$$

The bending moment in the transverse cross-section is equal to

$$M = P(f - v) = Pf \cos \frac{\pi z}{2l}, \tag{3.2}$$

and the corresponding energy of the deflection is

$$\Delta V = \int_0^l \frac{M^2 dz}{2EJ} = \frac{P^2 f^2 l}{4EJ}. \tag{3.3}$$

The vertical displacement of the bar's upper end is

$$\lambda = \frac{1}{2} \int_0^l \left(\frac{dv}{dz}\right)^2 dz = \frac{\pi^2 f^2}{16l}, \tag{3.4}$$

and the corresponding work done by the force P is

$$\Delta T = \frac{\pi^2 P f^2}{16l}. \tag{3.5}$$

Equating ΔV and ΔT:

$$\frac{P^2 f^2 l}{4EJ} = \frac{\pi^2 P f^2}{16l}, \tag{3.6}$$

S. P. Timoshenko finds that the critical force is equal to /26

$$P_{crit} = \frac{\pi^2 EJ}{4l^2}. \tag{3.7}$$

This result is completely exact; such success in the application of, in essence, an approximate method is explained by the fact that the function (3.1) represents the exact equation of the bent axis. Upon solving other problems in which the equation of the bent axis is not known in advance, this method leads to approximate results which are more exact as the approximating function describes more accurately the actual shape of the bent axis.

In 1951, P. F. Drozdov turned his attention to an unexpected result which is obtained if one compares the values of ΔV and ΔT found above first for $P < P_{crit}$ and then for $P > P_{crit}$.

We will denote the dimensionless load parameter by

$$\alpha = \frac{P}{P_{crit}}; \tag{3.8}$$

thereupon $\alpha < 1$ if $P < P_{crit}$, and $\alpha > 1$ if $P > P_{crit}$. Using the dimensionless parameter α, we will rewrite Equations (3.3) and (3.5) in the following form:

$$\Delta V = \alpha^2 \frac{\pi^2 EJf^2}{64l^3}, \tag{3.9}$$

$$\Delta T = \alpha \frac{\pi^2 EJf^2}{64l^3}. \tag{3.10}$$

It is thus clear that when $\alpha < 1$ we have $\Delta V - \Delta T < 0$, and when $\alpha > 1$ we will find $\Delta V - \Delta T > 0$. It is found that when $\alpha < 1$ (when $P < P_{crit}$) the straight equilibrium shape should be recognized as being unstable, and when $\alpha > 1$ (when $P > P_{crit}$), it should be recognized as being stable. In other words, S. P. Timoshenko's solution gives the value of the critical force as the force which when exceeded makes the supposedly unstable straight equilibrium shape stable.

This conclusion is an evident contradiction with common sense. What is the reason for this unexpected result? P. S. Drozdov correctly noted that it is associated with Equation (3.3). The problem is that in the expression /27

$$\Delta V = \int_0^l \frac{M^2 dz}{2EJ} \tag{3.11}$$

the bending moment M can be introduced not only as the moment of the external load in the form of Equation (3.2), but as the moment of the internal forces in the form

$$M = EJ\frac{d^2w}{dz^2}. \tag{3.12}$$

If one uses this expression and substitutes the function (3.1) in it, one obtains in place of Equation (3.3) the following equation,

$$\Delta V = \int_0^l \frac{M^2 dz}{2EJ} = \frac{\pi^4 EJf^2}{64l^3}. \tag{3.13}$$

This result, in contrast to Equation (3.9), does not contain the force P.

The final expressions (3.3) and (3.13) in the problem under discussion are not equivalent in their very basic nature. The first of them expresses the potential energy of the deflection for a bent equilibrium shape, while the expression (3.13) defines the potential energy of the deflection for an arbitrary deflected state which is possibly not an equilibrium state.

P. F. Drozdov wrote in his article: "With respect to the idea of the start of possible displacements and the principle of the minimum of the potential energy, the work of the internal forces in a virtual deflection does not depend on the size of the load P and is wholly determined by the arbitrarily specified shape of the deflection. Thereupon in the deflected state under discussion there can be equilibrium which is not maintained, and the moment of the internal forces, which is determined by the deflection's shape, may differ from the moment of the external forces."

If we now compare the correct expressions (3.10) and (3.13), the true

result is obtained:

$$\Delta V > \Delta T \text{ when } \alpha < 1 \text{ i.e., when } P < P_{crit}),$$

$$\Delta V < \Delta T \text{ when } \alpha > 1 \text{ i.e., when } P > P_{crit}).$$

Thus, S. P. Timoshenko's calculations are based on consideration of an adjacent equilibrium shape for which the expressions (3.2) and (3.12) agree. /28 But in such a case a system's potential energy is clearly identical for the initial and for the deflected shapes. Therefore, S. P. Timoshenko's calculations have led to the correct result for the critical force; at the same time the attempt to explain with this method what happens when the force P reaches the value $P = P_{crit}$ (whether it is a transition from a stable state to an unstable state or vice versa) was doomed from the start. Fortunately, intuition prompts the correct answer in similar cases.

At the same time it is necessary to recognize that, by assigning an approximate shape of the deflection and then using Timoshenko's method, we will obtain a more accurate value of the critical force, since the differentiation operation indicated in Equation (3.12) always increases the solution's error.

P. F. Drozdov's article was published in the journal "Vestnik inzhenerov i tekhnikov" (No. 2, 1951). References are given in this article to other publications in which the same error is repeated. An analysis of the paradox under discussion is also contained in S. D. Leytes' book "The Stability of Compresssed Steel Bars" (Moscow, Section 8, 1954).

§ 4. Loads Whose Values Depend on the Displacements

In order to establish the characteristics of the problems under discussion here, it is necessary to discard at once certain ideas for which a habit has

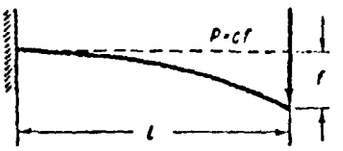

Fig. 4.1. The load P is proportional to the deflection f.

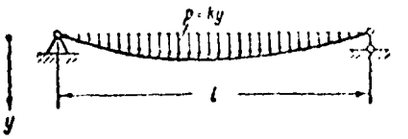

Fig. 4.2. The intensity of the distributed load p = p(z) is proportional to the deflections y = y(z).

been cultivated by the usual statement of the problems of elasticity theory and the strength of materials. In the majority of the latter problems the external load is specified in this or the other way: as a function of the coordinates of the loaded object's points in static problems, and in addition as a function of time in dynamical problems. Thereupon it is assumed that all elastic effects (displacement, deformation, tension) depend on the load but cannot themselves affect the load.

However, there exists an extensive class of problems for which the interference of external loads and displacements is typical: not only do the displacements depend on the load, but the loads themselves vary as a function of the displacement. Such loads do not remain indifferent to variations in the shape or position of the system as if they were "tracking" these variations.

In this section we will dwell on those problems in which the bar's displacements cause variations only in the size of the load(*). /29

Such are the following problems, for example, which are posed in a problem book on strength of materials.

(*) The cases in which the displacements affect the direction of the loads do not relate to the theme of this chapter, since the Eulerian kind of stability loss cannot represent them; see Chapter IV for such cases.

1. A beam of constant cross-section is fastened at one end; a force proportional to the deflection, P = cf, begins to act at the free end in the event of a deflection arising. The problem is to determine the minimum value of the coefficient c for which a straight shape of the beam will be unstable. The beam's stiffness is EJ and its length is l (Figure 4.1).

2. A beam having a constant stiffness EJ and length l is supported by hinges at the ends. Upon a deflection arising, a load proportional to the deflection, $p = ky^{(*)}$, distributed along the entire length of the beam begins to act. The problem is to determine the minimum value of the coefficient k for which a straight shape of the bar will become unstable (Figure 4.2).

The loads in these problems respond to linear displacements and are proportional to the latter. Such loads develop, for example, upon displacements of elastic systems located in a magnetic field; such systems are called /30 magnetoelastic.

However, depending on the physical nature of the generating forces, they may be proportional to nonlinear displacements of the points of the bar's axis, as in the cases just described, and to angular displacements (i.e., to the first derivative of the linear displacement with respect to the spatial coordinate) or to the curvature of the bar's axis (i.e., to the second derivative of the linear displacement with respect to the spatial coordinate). Such loads are in particular of aerodynamic or hydrodynamic origin; the corresponding systems are called aeroelastic or hydroelastic.

All these cases are successively discussed in this section; the possibility of stability loss is clarified each time. Here the reader will be able to convince himself that stability loss in Euler's sense is not necessarily associated everywhere with the traditional concept of buckling of a compressed column.

(*) It would be inconvenient in this section to denote the displacement by the letter v (it will denote the velocity).

a) Loss of stability of a bar located in a magnetic field. The forces of magnetic attraction change their magnitude as a function of the distance between the magnet and the armature; therefore, if the latter is fastened elastically, these forces constitute a load which "tracks" the elastic deflection.

First we will discuss an elastically suspended armature located in a stationary magnetic field which is symmetric with respect to the average position. Such a field can be produced by two magnets, as is illustrated in Figure 4.3.

We will assume the static characteristics of the elastic system of the armature to be linear and the stiffness coefficient to be equal to c; therefore, if y is the deflection of the armature from its equilibrium position, an elastic restoring force arises in the case of deflections of the armature which is equal to cy and is directed opposite to the deflection.

The attractive forces of the magnets are balanced only when the armature is in its average position (y = 0). Upon a displacement of the armature the attractive forces of the magnets change, but in different proportions. One can assume in the case of small deflections that the magnitude of the attractive force of each of the magnets depends on the displacement y in the following manner: /31

$$P_1 = \frac{K}{(a+y)^2}, \quad P_2 = \frac{K}{(a-y)^2},$$

where a and K are constants (a is the initial distance between the magnet and the armature); the result of these forces is equal to

$$R = \frac{K}{(a-y)^2} - \frac{K}{(a+y)^2} = \frac{4aKy}{(a^2-y^2)^2}$$

and is in the same direction as the displacement. In the case of very small deflections $y < a$, it is possible to assume approximately that

$$R \approx \frac{4Ky}{a^3}. \tag{4.1}$$

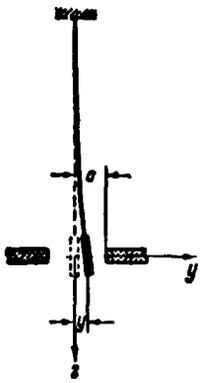

Fig. 4.3. Elastically mounted armature in a symmetrical magnetic field.

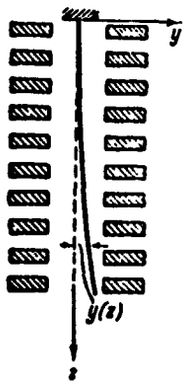

Fig. 4.4. The magnetic field is uniform with respect to the z coordinate.

According to this expression, the result of the attractive forces of the magnets is proportional to the displacement y.

Let us imagine that due to some accidental cause the armature is disturbed from its average position. According to the Eulerian statement of the problem it is necessary to ascertain whether or not the deflected state is an equilibrium state. The equilibrium condition of the armature in the deflected state,

$$-cy+\frac{4Ky}{a^3}=0$$

permits one to conclude that stability loss occurs when the stiffness coefficient c is equal to

$$c=\frac{4K}{a^3}. \qquad (4.2)$$

This value of the stiffness coefficient is the critical value. In the case of such a value for the coefficient the rescoring force of the elastic bar on a deflection of the armature by an amount y is $-cy=-\frac{4Ky}{a^3}$, i.e., it balances the force $R=\frac{4Ky}{a^3}$ exactly. If $c>\frac{4K}{a^3}$, the armature's original equilibrium state is stable. If $c<\frac{4K}{a^3}$, this equilibrium state is unstable. /32

In the case of any small deflection the restoring force of the magnet's attraction proves to be greater than the restoring force of the elastic bar, and after the initial disturbance the armature will steadily move away from its original position until its complete "sticking" to one of the magnets; however, these phenomena are outside the framework of the Eulerian statement of the problem, and a nonlinear expression for the force R would have to be used for a complete analysis of them.

We will complicate the problem and discuss a system with distributed parameters. Let us picture to ourselves that a cantilever elastic bar (Figure 4.4) experiences along its entire length a load whose intensity is determined by an expression similar to Equation (4.1):

$$r = \frac{4ky}{a^3} \tag{4.3}$$

(y is the instantaneous deflection). Such a load can be produced by two kinds of magnets, often positioned along the bar on each side of it. We will rewrite the differential equation of the bar's deflection

$$EJ\frac{d^2y}{dz^2} = \frac{4ky}{a^3}$$

in the form

$$\frac{d^4y}{dz^4} - \alpha^4 y = 0, \tag{4.4}$$

where

$$\alpha = \sqrt[4]{\frac{4k}{EJa^3}}. \tag{4.5}$$

The general solution of Equation (4.4) contains four constants and has the form

$$y = A_1 \operatorname{sh} \alpha z + A_2 \operatorname{ch} \alpha z + A_3 \sin \alpha z + A_4 \cos \alpha z. \tag{4.6}$$

This solution should satisfy the boundary conditions:

$$y = 0, \quad \frac{dy}{dz} = 0 \quad \text{when} \quad z = 0,$$

$$\frac{d^2y}{dz^2} = 0, \quad \frac{d^3y}{dz^3} = 0 \quad \text{when} \quad z = l.$$

Substituting the solution (4.6) here, we find /33

$$\left.\begin{aligned} A_2 + A_4 &= 0, \\ A_1 + A_3 &= 0, \\ A_1 \operatorname{sh} \alpha l + A_2 \operatorname{ch} \alpha l - A_3 \sin \alpha l - A_4 \cos \alpha l &= 0, \\ A_1 \operatorname{ch} \alpha l + A_2 \operatorname{sh} \alpha l - A_3 \cos \alpha l + A_4 \sin \alpha l &= 0. \end{aligned}\right\} \tag{4.7}$$

The derived system of Equations (4.7) is uniform with respect to the constants, and therefore it is satisfied by the trivial solution·

$$A_1 = A_2 = A_3 = A_4 = 0.$$

But the function $y \equiv 0$ corresponds to such a solution, which confirms an evident fact, namely, that a straight shape is the equilibrium shape. In order to find a curved equilibrium shape, one must assume that not all the constants A_1 are equal to zero; the system of Equations (4.7) has nonzero solutions only on the condition that the determinant composed of the system's coefficient is equal to zero:

$$\begin{vmatrix} 0 & 1 & 0 & 1 \\ 1 & 0 & 1 & 0 \\ \operatorname{sh} \alpha l & \operatorname{ch} \alpha l & -\sin \alpha l & -\cos \alpha l \\ \operatorname{ch} \alpha l & \operatorname{sh} \alpha l & -\cos \alpha l & \sin \alpha l \end{vmatrix} = 0.$$

Having expanded the determinant, we arrive at the following transcendental equation:

$$\cos \alpha l \cdot \operatorname{ch} \alpha l = -1. \tag{4.8}$$

A graphical solution of this equation is given in Figure 4.5; its smallest root is equal to

$$\alpha l = 1{,}873. \tag{4.9}$$

Substituting Equation (4.5) in here, we obtain the critical ratio between the system's parameters

$$\frac{kl^4}{EJa^3} = 3{,}09, \tag{4.10}$$

for which stability loss occurs.

With the value of αl found it is possible to derive from Equation (4.6) the following equation of a curved axis:

$$y = A \frac{\operatorname{sh} 1{,}873 \frac{z}{l} \cos 1{,}873 \frac{z}{l} - \sin 1{,}873 \frac{z}{l} \operatorname{ch} 1{,}873 \frac{z}{l}}{\operatorname{ch} 1{,}873 \frac{z}{l} + \cos 1{,}873 \frac{z}{l}}, \tag{4.11}$$

which contains a unique indeterminant parameter which we will denote by the letter A, which characterizes only the scale of the deflection's curve.

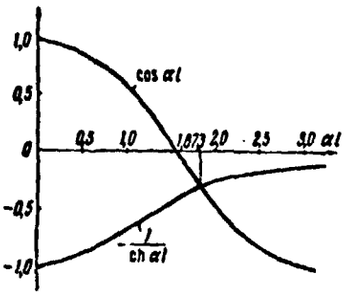

Fig. 4.5. Graphical solution of the transcendental equation (4.8).

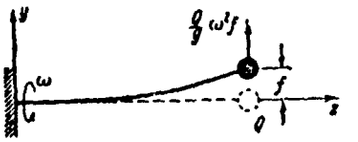

Fig. 4.6. A centrifugal force is proportional to the deflection f of the end of the beam.

One can treat the system being investigated as a beam line on a solid elastic foundation having a negative imbedding coefficient. In general, the usual elastic foundation can also be assumed to be the reason why forces of the type under discussion arise, since the reaction r of the elastic foundation is proportional to the displacement y; however, such a reaction cannot serve as the cause of stability loss, since it is directed opposite to the deflection. In our problem the attractive forces of the magnets cause a destabilizing effect, since they are always opposite in direction to the deflection. These forces represent only one of the versions of the physical realization of loads illustrated in Figure 4.1 and 4.2. Centrifugal forces are also loads of this type.

Let the cantilever bar be rotated around its axis with a specified angular velocity ω. If for some accidental reason, the bar is found to be curved, centrifugal loads arise, namely, a concentrated force in the case of a weightless bar with a point mass at its end (Figure 4.6) or a distributed load if /35 the bar's mass is continuously distributed along its length (Figure 4.7).

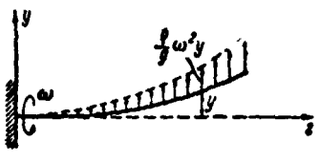

Fig. 4.7. The intensity of the load from centrifugal forces is proportional to the deflection y.

In the first case, the centrifugal force is proportional to the deflection f of the bar's end:

$$R = \frac{Q}{g}\omega^2 f, \qquad (4.12)$$

where Q is the weight of the end load; correspondingly in the second case, the intensity of the centrifugal load amounts to:

$$r = \frac{q}{g}\omega^2 y, \tag{4.13}$$

where q is the intensity due to the weight of the bar.

Equations (4.12) and (4.13) are similar to Equations (4.1) and (4.3); therefore, the stability analysis will result in the following critical ratios for the parameters of the systems, which are similar to the results (4.2) and (4.10):

$$c = \frac{Q}{g}\omega^2 \tag{4.14}$$

(for a bar with a concentrated mass) and

$$\frac{q}{g}\omega^2 \frac{l^4}{EJ} = 12{,}36 \tag{4.15}$$

(for a bar with a uniformily distributed mass). One can find from these relationships the well-known critical values for the angular velocity ω:

$$\omega_{crit} = \sqrt{\frac{cg}{Q}}, \quad \omega_{crit} = \frac{3{,}51}{l^2}\sqrt{\frac{gEJ}{q}}. \tag{4.16}$$

Thus, the case in which the attractive forces of magnets are acting is similar in a certain sense to the case in which centrifugal forces due to the bar's rotation are acting. However, this analogy refers only to the critical state; it is well-known that if Equations (4.14) and (4.15) are violated, the rotating bar is stable regardless of whether or not the inequality $\omega < \omega_{crit}$ or the inequality $\omega > \omega_{crit}$ holds.

b) <u>Aeroelastic static instability.</u> Aerodynamic loads (for example, loads on an airplane's wing), which respond to variations of the position and shape of streamlined construction, belong to the category of loads under discussion.

While the <u>direct</u> effect (of loads on elastic displacements) belongsto the field of elasticity theory or strength of materials, the <u>reverse</u> effect

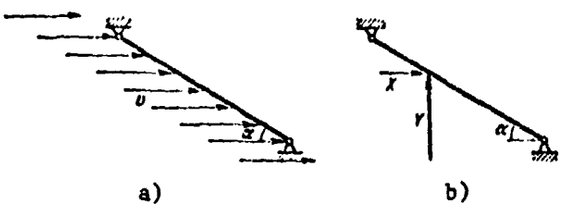

a) b)

Fig. 4.8. Layout of the way in which an airstream acts on an inclined plate.

(of the displacements on the load) is determined by the laws of aerodynamics. Therefore, problems regarding the behavior of deformable elements in a stream of air (gas) cannot possibly be solved just by the methods of elasticity theory or just by the methods of aerodynamics; such problems lie at the boundary of both sciences and now belong to an independent scientific discipline, namely, aeroelasticity theory. Of course, the more flexible the element is, the greater is the distinctness with which the characteristics of the aeroelastic phenomena stand out.

Among the various aeroelastic phenomena, the different kinds of stability loss of aviation structures are of importance. Some of the problems of this class permit a purely static statement of the problem in the spirit of Euler's conception; here we will dwell precisely on such problems, which belong to the problem of the divergence of the lifting surfaces of aircraft.

We will begin from the elementary data of the field of applied aerodynamics, and we will discuss the simplest set-up, namely, the flow of an airstream around a completely rigid, very long rectangular plate. The z-axis is coincident with the plate's long side and the x-axis lies along the direction of the air flow; the plate's cross-section perpendicular to the z-axis is illustrated in Figure 4.8 (a).

The angle α between the direction of flow and the plate's plane is called /37 the angle of attack. The direction of the resultant aerodynamic load on the plate does not coincide with the flow direction: in addition to the X component in the direction of the stream velocity, a Y component arises which is perpendicular to the stream velocity. The first component is called the drag and the second component is called the lift force (Figure 4.8, b). They

depend on the plate's area S which is subject to the effect of the load, the air density ρ, the stream velocity v, and the angle of attack α.

It has been established that at moderate speeds (not exceeding 0.6 — 0.7 times the speed of sound in air) the lift force is defined by the expression

$$Y = c_y \frac{\rho v^2}{2} S. \tag{4.17}$$

The fraction $\frac{\rho v^2}{2}$ appearing in this equation is called the dynamic pressure and represents the kinetic energy of a unit volume of air. The lift force coefficient c_y at small angles of attack is proportional to the angle of attack α:

$$c_y = \frac{dc_y}{d\alpha} \alpha,$$

where $\frac{dc_y}{d\alpha}$ is the angular coefficient of the straight line characterizing the variation of the coefficient c_y. Thus, the lift force Y is also proportional to the angle of attack α.

Let us now turn to the simplest problem of aeroelasticity theory, namely, the flow around a rigid plate elastically supported along its left edge, and we will assume that the horizontal position of the plate is undisturbed (Figure 4.9, a). In this position it is not loaded in general, since $\alpha = 0$ and along with this $X = Y = 0$(*). However, this equilibrium state may turn out to be unstable in the case of a large stream velocity v, since a lift force possibly capable of holding the plate in a deflected position arises upon deflections of the plate (Figure 4.9, b).

If b is the plate's width and l is its length, then $S = bl$ and the lift force Y which develops upon a deflection of the plate by the angle α is equal to /38

$$Y = \frac{dc_y}{d\alpha} \frac{\rho v^2}{2} bl\alpha. \tag{4.18}$$

(*) If we ignore the very small frictional force of the flow over the plate's surface.

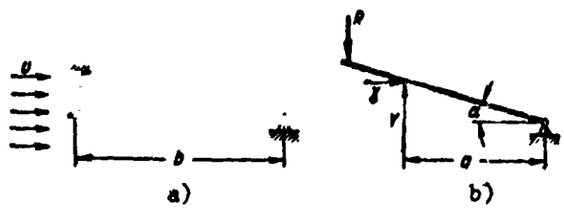

Fig. 4.9. Layout of the way in which an airstream acts on an elastically mounted plate; the initial angle of attack is equal to zero.

The reaction of the elastic support in the case of a small angle α amounts to

$$R = cabl, \tag{4.19}$$

where c is the support's stiffness coefficient computed per unit length of the plate.

We will explain under what conditions equilibrium of the plate is possible in a deflected position. The equilibrium condition of the plate in a deflected position (Figure 4.9, b) has the form

$$cab^2l - \frac{dc_y}{d\alpha}\frac{\rho v^2}{2}bla \cdot a = 0, \tag{4.20}$$

where a is the moment arm of the lift force. The moment of the drag force X is not included in this equation, since its moment arm is aα, a quantity which is small with respect to the moment arm of the force Y. Thus,

$$ab^2l\left(c - \frac{a}{b}\frac{\rho v^2}{2}\frac{dc_y}{d\alpha}\right) = 0. \tag{4.21}$$

The structure of the last expression confirms the possibility of a deflected equilibrium state when $\alpha \neq 0$. In order for this to occur, it is necessary that the expression in parentheses appearing in Equation (4.21) be equated to zero:

$$c - \frac{a}{b}\frac{\rho v^2}{2}\frac{dc_y}{d\alpha} = 0. \tag{4.22}$$

If the value of c is specified, it is possible to find from Equation (4.22) the critical stream velocity

$$v_{crit} = \sqrt{\frac{2cb}{\rho \frac{dc_y}{d\alpha} a}}, \tag{4.23}$$

and if the velocity v is specified, then the critical value of the stiffness is defined by the equation

/39

Fig. 4.10. The aerodynamic moment increases when the wing is twisted.

$$c_{crit} = \frac{\rho v^2}{2} \frac{a}{b} \frac{dc_y}{d\alpha}. \qquad (4.24)$$

The condition $v < v_{crit}$ must be fulfilled in order for the plate to be stable. When $v = v_{crit}$, the undisturbed horizontal position of the plate ceases to be stable; the aerodynamic forces become sufficiently great to overcome the resistance of the elastic couplings and to hold the plate in a deflected position.

One can say that the system's effective rigidity (against rotation around its hinged axis) decreases as the stream velocity v increases; when $v = v_{crit}$, this rigidity becomes zero. It is easy to notice here the analogy with the properties of a compressed flexible bar: its rigidity in the transverse direction decreases as the compressive force P increases, and it becomes zero when $P = P_{crit}$.

A similar situation can arise in the case of the flow around an airplane wing having some finite torsional rigidity. Just as for the plate discussed above, an increase in the wing's angle of attack (Figure 4.10) results in the appearance of an additional aerodynamic moment tending to twist the wing and, consequently, to increase still more the angle of attack. Therefore, as the flight speed increases due to the effect of the aerodynamic forces, the wing's effective torsional rigidity <u>decreases</u>. The wing's total loss of torsional rigidity results in catastrophic consequences; the state in which this rigidity vanishes is called <u>divergence</u> of the wing, and the corresponding flight speed /40 is referred to as the <u>critical divergence speed</u>.

Of course, it is impossible to apply directly the Equation (4.23) cited above to the more complicated layout of the problem of a wing's twisting, but the principle of determining the critical velocity remains the same for a wing. It follows from the theory of wing divergence (the foundations of this theory were laid by G. Reissner in 1926) that the critical velocity decreases

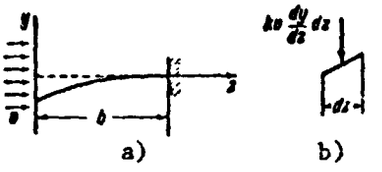

a) b)

Fig. 4.11. Layout of the way in which an airstream acts on an ela tic plate.

as the wing's torsional rigidity decreases, which is analcgous • the result obtained for our simplified layout.

The critical divergence velocity is practically unattainable since already at slower speeds structural breakdown is unavoidable due to the finite but sufficiently large deformations(*). It may be that precisely such a "pre-divergence" state was the cause of the accident of Langley's monoplane (1903); due to this accident aviation designers for many years feared the monoplane design of airplanes.

Let us pause now on another phenomenon of aeroelastic static instability which we can call panel divergence. In contrast to the layout imagined in Figure 4.9, in which the plate itself was assumed to be rigid and its pliability was distributed along one edge (the elastic support), here we will discuss an elastic plate which is rigidly supported along one of its long edges and free along the other edge.

Let the flow be directed parallel to the undisturbed middle surface of the plate, as illustrated in Figure 4.11, a. Here the curved middle surface, which can be assumed to be cylindrical in the case of a sufficiently large length of the plate (measured perpendicularly to the plane of the drawing) is illustrated by a sketch. Just as in the preceding problems, we will attempt to clarify /41 the conditions under which a curved equilibrium shape is possible along with the undisturbed equilibrium shape (the uncurved plate), when the plate's deflection is caused by aerodynamic loads corresponding to this deflection.

In general, the flow around a given curved surface of the plate constitutes a complicated problem of aerodynamics; this problem is complicated still further

(*) Or due to stability loss for other reasons (see Chapter VII about this).

in the case being discussed here when the shape of the plate's deflection is not specified but depends on the distribution of the aerodynamic load. However, in the case of supersonic stream velocities the solution can be greatly simplified if one uses the so-called "piston theory." According to this theory(*), the local pressure on the curved surface is proportional to the local angle of attack and the stream velocity v. Thus, if we stick to the piston theory, the pressure on the plate's curved cylindrical surface is determined by the expression

$$q = -kv\frac{dy}{dz}, \tag{4.25}$$

where k is a constant, y = y(z) is the plate's deflection, and $\frac{dy}{dz}$ is the local angle of attack (Figure 4.11, b).

We will write the differential equation of the plate's cylindrical deflection as

$$D\frac{d^4y}{dz^4} = q, \tag{4.26}$$

in which

$$D = \frac{Eh^3}{12(1-\mu^2)} \tag{4.27}$$

is the cylindrical rigidity (E is the material's modulus of elasticity, h is the plate's thickness, and μ is Poisson's coefficient). Substituting Equation (4.25) into the differential equation (4.26), we obtain the basic differential equation of the problem in the form

$$\frac{d^4y}{dz^4} + s^3\frac{dy}{dz} = 0, \tag{4.28}$$

in which /42

$$s = \sqrt[3]{\frac{kv}{D}} \tag{4.29}$$

represents a quantity dependent on the flow velocity v (and also, of course, on the plate's parameters).

(*) Its validity is now being disputed by some authors; we will not delve into the nature of this controversial problem, which is far removed from the framework of our topic.

Then the usual question for Euler's theory is posed: whether values of the parameter s exist for which, in addition to the trivial solution

$$y = 0 \tag{4.30}$$

the differential equation (4.28) has other solutions corresponding to a curved equilibrium shape, and at what stream velocity does this become possible? Upon reaching such a velocity the undisturbed shape ceases to be stable, and divergence arises.

Just as in the solution of the usual stability problems, it is necessary to find the general solution of the differential equation (4.26), and have it satisfy the boundary conditions:

$$\left.\begin{aligned} y''=0, \quad y'''=0 \quad \text{when} \quad z=0, \\ y=0, \quad y'=0 \quad \text{when} \quad z=b, \end{aligned}\right\} \tag{4.31}$$

and, finally, establish the values of the parameter s for which nonzero solutions differing from the solution (4.30) are possible.

The particular solution of the differential equation (4.28) will be taken in the form

$$y=Ae^{\lambda z}. \tag{4.32}$$

Having substituted it into the differential equation (4.28) we obtain the characteristic equation

$$\lambda(\lambda^3+s^2)=0. \tag{4.33}$$

This algebraic equation of the fourth degree has four roots which can be found most simply by putting Equation (4.33) in the form

$$\lambda(\lambda+s)(\lambda^2-\lambda s+s^2)=0. \tag{4.34}$$

Equating each of the factors to zero in order, we find the following roots:

$$\left.\begin{aligned} &\lambda_1=0; \quad \lambda_2=-s; \quad \lambda_3=\frac{s}{2}\left(1+\sqrt{3}i\right); \\ &\lambda_4=\frac{s}{2}\left(1-\sqrt{3}i\right). \end{aligned}\right\} \tag{4.35}$$

According to Equation (4.32), the general solution to the differential equation (4.28) has the form

$$y=A_1+A_2e^{-sz}+A_3e^{(1+\sqrt{3}i)\frac{sz}{2}}+A_4e^{(1-\sqrt{3}i)\frac{sz}{2}}$$

or, if we change over to trigonometric functions.

$$y = A_1 + A_2 e^{-sz} + e^{\frac{sz}{2}}\left(A_3' \sin \frac{\sqrt{3}}{2} sz + A_4' \cos \frac{\sqrt{3}}{2} sz\right), \tag{4.36}$$

where

$$A_3' = l(A_3 - A_4), \quad A_4' = A_3 + A_4.$$

Now it is necessary to subject the solution (4.36) to the boundary conditions (4.31); thereupon we obtain four equations which are homogeneous with respect to the constants A_1, A_2, A_3, and A_4:

$$\left.\begin{aligned} &A_2 - \frac{1}{2} A_3' + \frac{\sqrt{3}}{2} A_4' = 0, \quad A_2 + A_3' = 0, \\ &A_1 + A_2 e^{-sb} + A_3' e^{\frac{sb}{2}} \cos \frac{\sqrt{3}}{2} sb + A_4' e^{\frac{sb}{2}} \sin \frac{\sqrt{3}}{2} sb = 0, \\ &-A_2 e^{-sb} + \frac{1}{2} e^{\frac{sb}{2}}\left(\cos \frac{\sqrt{3}}{2} sb - \sqrt{3} \sin \frac{\sqrt{3}}{2} sb\right) A_3' + \\ &\quad + \frac{1}{2} e^{\frac{sb}{2}}\left(\sqrt{3} \cos \frac{\sqrt{3}}{2} sb + \sin \frac{\sqrt{3}}{2} sb\right) A_4' = 0. \end{aligned}\right\} \tag{4.37}$$

Of course, this system is satisfied by zero values of the constants

$$A_1 = A_2 = A_3' = A_4' = 0,$$

which corresponds to the trivial solution (4.30) In order that the constants A_1, A_2, A_3, and A_4 not vanish, it is necessary that the determinant composed of the coefficients of the system of equations (4.37) be equated to zero:

$$\begin{vmatrix} 0 & 1 & -\frac{1}{2} & \frac{\sqrt{3}}{2} \\ 0 & 1 & 1 & 0 \\ 1 & e^{-sb} & e^{\frac{sb}{2}} \cos \frac{\sqrt{3}}{2} sb & e^{\frac{sb}{2}} \sin \frac{\sqrt{3}}{2} sb \\ 0 & -e^{-sb} & \frac{e^{\frac{sb}{2}}}{2}\left(\cos \frac{\sqrt{3}}{2} sb - \sqrt{3} \sin \frac{\sqrt{3}}{2} sb\right) & \frac{e^{\frac{sb}{2}}}{2}\left(\sqrt{3} \cos \frac{\sqrt{3}}{2} sb + \sin \frac{\sqrt{3}}{2} sb\right) \end{vmatrix} = 0.$$

Expanding this determinant, we obtain the following transcendental equation /44 for the parameter sb:

$$\cos \frac{\sqrt{3}}{2} sb = -0{,}5 e^{-\frac{3}{2} sb}. \tag{4.38}$$

A graphical solution (Figure 4.12) gives a unique root of the equation (4.38):

$$sb = 1{,}854. \tag{4.39}$$

Now it is possible to find from Equation (4.29) the critical stream velocity:

$$v = 6{,}38\frac{D}{kb^2}. \qquad (4.40)$$

At this velocity the plate's undisturbed equilibrium shape ceases to be stable, and a state of divergence arises.

c) The static instability of a tube. We have already seen in the preceding problems that the forces can respond to a linear displacement (in the case of a magnetic field) or to an angle of rotation (in the case in which aerodynamic forces are acting). The case in which the resulting forces are associated with the curvature of a system's deformed axis is discussed below.

We will discuss the possibility of stability loss of a vertical section of tubing through which a liquid is flowing with velocity v (Figure 4.13, a).

It is obvious that the state illustrated in the figure, in which the tubing's axis is rectilinear, is an equilibrium state for any flow velocity v of the liquid. We have to clarify whether or not a distorted equilibrium shape can exist when a deflection of the tubing is produced (or perhaps it is better to say, when a deflection is maintained) by centrifugal forces of /45 the fluid particles; these forces arise due to the curvature of the trajectories. Such a possibility is a natural one, since upon a deflection of the tubing, for example, to the right (Figure 4.13, b) the centrifugal forces are also directed to the right, and the problem lies only in whether or not the size of these forces is sufficient to maintain the deflection. We will take the coordinate axes according to Figure 4.13, b and we will denote: $y = y(z)$ — the deflection of the tubing's axis, v — the liquid's flow velocity, EJ — the rigidity of a transverse cross-section of the tubing, q — the weight of the liquid per unit length of the tubing, and g — the gravitational acceleration.

The element of the load occupying a segment of length dz generates an inertial force $\frac{q}{g}dz\frac{v^2}{\rho}$; here ρ is the trajectory's radius of curvature,

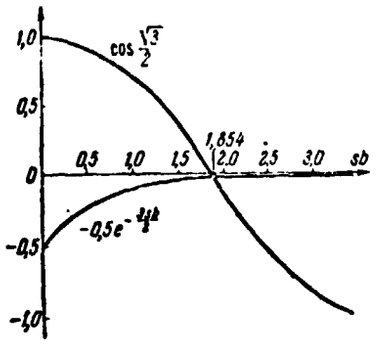

Fig. 4.12. Graphical solution of the transcendental equation (4.38).

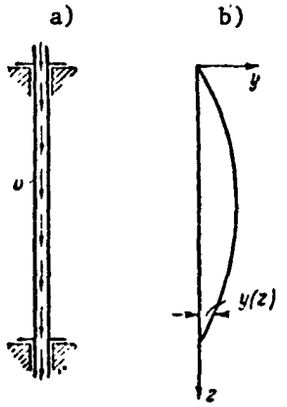

Fig. 4.13. Layout of a pipe duct; the liquid's rate of flow is equal to v.

i.e., the radius of curvature of the tubing's curved axis. In the case of small deflections one can take

$$\frac{1}{\rho}=\frac{d^2y}{dz^2}. \tag{4.41}$$

Consequently, the strength of the distributed inertial load is $\frac{qv^2}{g}\frac{d^2y}{dz^2}$. Thus the transverse load on the tubing "tracks", the second derivative of the function which describes the deflections of the tubing's axis; it is useful to note that the strength of this load depends on the flow velocity.

The differential equation of the deflection of the tubing's axis should be written in the form

$$EJ\frac{d^4y}{dz^4}=-\frac{qv^2}{g}\frac{d^2y}{dz^2} \tag{4.42}$$

or

$$\frac{d^4y}{dz^4}+s^2\frac{d^2y}{dz^2}=0, \tag{4.43}$$

where the parameter s has the value /46

$$s=v\sqrt{\frac{q}{gEJ}}. \tag{4.44}$$

The general solution of equation (4.43) can be found in the form

$$y=A_1+A_2z+A_3\sin sz+A_4\cos sz. \tag{4.45}$$

The constants A_1, A_2, A_3 and A_4 should be determined so that the boundary conditions are satisfied: if the ends of the tubing are hinged, then

$$\left.\begin{aligned} y=0, \quad y''=0 \quad \text{at } z=0, \\ y=0, \quad y''=0 \quad \text{at } z=l. \end{aligned}\right\} \tag{4.46}$$

Using these conditions, we arrive at the equation

$$\sin sl=0. \tag{4.47}$$

(If sin sl $\neq$ 0, all the constants A_i vanish, i.e., a trivial solution corresponding to the unbent equilibrium shape is derived).

We find from equation (4.47) the first non-zero root (it is uniquely important, just as in Euler's ordinary problem on the buckling of a compressed rod):

$$s=\frac{\pi}{l}. \tag{4.48}$$

Substituting equation (4.44) here, we arrive at an equation which determines the condition for the existence of a bent equilibrium shape:

$$\frac{\pi}{l}=v\sqrt{\frac{q}{gEJ}}. \tag{4.49}$$

From this we obtain the value of <u>critical velocity</u> as

$$v_{crit}=\frac{\pi}{l}\sqrt{\frac{gEJ}{q}}. \tag{4.50}$$

Thus, when $v = v_{crit}$, stability loss of the rectilinear equilibrium shape begins, and the effective transverse rigidity of the tubing just disappears.

The first two problems (see Figure 4.1 and 4.2) are cited in the book by A.A. Umanskiy, A.M. Afanas'yev, A.S. Vol'mir, Yu.P. Grigor'yev, A.I. Kodanev, V.A. Mar'in, and N.I. Prigorovskiy entitled "Collection of Problems on the Strength of Materials" (Gostekhizdat, Moscow, 1954) (problems 766 to 767). The expressions preceding equations (4.1) are given, for example, in R.A. Mozniker's book "The Effect of a Constant Magnetic Field on the Free Oscillations of a Mechanical System" (Izvestiya AN USSR, 1959).

The literature devoted to the problems of aeroelasticity will be mentioned at the end of Chapter VIII.

The solution cited above for the problem of the stability of tubing was essentially given by Bresse(*), who, it is true, had a different construction in mind, namely, a bridge, along which is moving the infinite band of a uniformily distributed load.

(*) John Anton Charles Bresse(1822 - 1883) was a French scientist and a student of Clapeyron. He introduced the concept of the kernel of a cross section, began to apply the curves of bending moments, and stated in a general form the problem of calculating statically indeterminant systems by the method of forces.

CHAPTER II

LOSS OF STABILITY UPON THE APPEARANCE OF NON-SIMILAR EQUILIBRIUM SHAPES

It was pointed out in the introduction that the loss of stability of some systems can be expressed in terms of sudden transitions of a system from one state to another, also an equilibrium state but not similar to the first state (stability loss in the form of jumps).

Some examples of such systems are gathered together in this chapter. The discussion of the behavior of the systems begins with a solution of the simplest problem, namely, the problem of the deformation of a bar system, the so-called "Mises' truss" (*). The investigation of this simple system permits us to explain many essential features of systems of the type being discussed.

§ 5. The Mises' Truss

We will find the relation between the load P and the vertical displacement v of the junction of a symmetrical two-bar system (Figure 5.1, a). We will assume the bars to be linearly deformed and the material to be indefinitely strong.

Let us assume that the displacements v are not small; in order to imagine this possibility, one can assume, for example, that each of the bars is a twisted spring (Figure 5.1, b); in this case sufficiently large shortening /49
of the springs, and consequently, noticeable rotations of their axes, can

(*) Richard Mises (1883 - 1960) was a professor at Strausberg and Berlin during 1909 - 1933; after his emigration from Germany, he was a professor at Istambul (1933 - 1939) and then at Harvard University (1939 - 1960). He was the author of a number of investigations on the theory of probabilities, aerodynamics, and the applied theory of elasticity. He was the founder of the scientific journal "Zeitschrift für angewandte Mathematik und Mechanik".

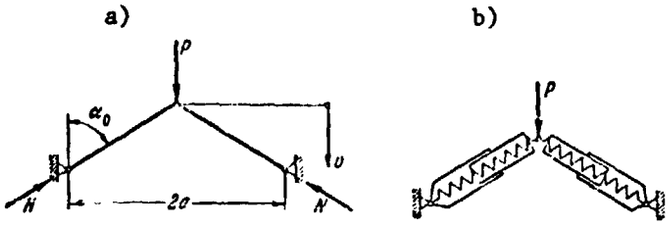

Fig. 5.1. a) A two-bar junction (Mises' truss);
b) the springs are located in telescoping guides.

correspond to small deformations and strains.

Since the displacement v is not small and the system's shape actually varies in the process of the loading, one should set up the equilibrium equations for the deformed set-up and take into account in writing these equations that elastic equilibrium corresponds to a configuration noticeably different from that specified. The equilibrium equation of the junction gives

$$N=\frac{P}{2\cos\alpha}, \tag{5.1}$$

where N are the stresses in the bars and α is the angle between the direction of the axis of the deformed bar and the vertical. Thus, upon a calculation of the deformations the system under discussion becomes statically indeterminate, since the unknown angle α, which differs from the initial value α_0, enters into equation (5.1).

We will set up one more (deformation) relationship between the stresses N and the displacement v. Since the shortening of each bar is equal to

$$\Delta l=\frac{a}{\sin\alpha_0}-\frac{a}{\sin\alpha}, \tag{5.2}$$

the stresses in the bars amount to (*) (l_0 is the initial length)

$$N=\frac{EF\,\Delta l}{l_0}=EF\left(1-\frac{\sin\alpha_0}{\sin\alpha}\right). \tag{5.3}$$

(*) If instead of bars the system contains springs, the rigidity EF in equation (5.3) should be replaced by the equivalent rigidity of the spring.

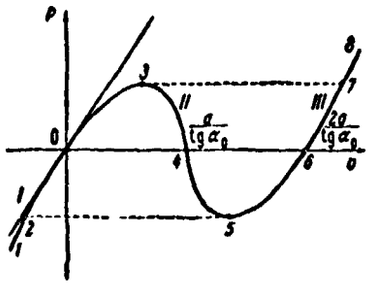

Fig. 5.2. Curve of the equilibrium states; the tangent at the point 0 corresponds to the solution based on the linear theory.

Now equating the right-hand sides of equations (5.1) and (5.3), it is possible to find a relation between the load P and the angle α: /50

$$P = 2EF\left(1 - \frac{\sin\alpha_0}{\sin\alpha}\right)\cos\alpha. \qquad (5.4)$$

Furthermore, it is possible to transform from the angle α to the linear displacement v of the junction with the help of the relationship

$$v = a\frac{\operatorname{tg}\alpha - \operatorname{tg}\alpha_0}{\operatorname{tg}\alpha \cdot \operatorname{tg}\alpha_0}. \qquad (5.5)$$

After some rearrangement one obtains in place of equation (5.4)

$$P = 2EF\left(1 - \frac{v}{a}\operatorname{tg}\alpha_0\right)\left[\frac{1}{\sqrt{\operatorname{tg}^2\alpha_0 + \left(1 - \frac{v}{a}\operatorname{tg}\alpha_0\right)^2}} - \cos\alpha_0\right]. \qquad (5.6)$$

Equation (5.6) is graphically illustrated in Figure 5.2 in the form of the curve 1 - 2 - 0 - 3 - 4 - 5 - 6 - 7 - 8. Some equilibrium state of the system characterized by the quantities P and v corresponds to each of the points of this curve. The straight line which passes through the origin of the coordinates along the tangent to the P - v curve corresponds to the solution obtained according to the linear theory. The curve of equilibrium states has the shape of the graph illustrated in the introduction in Figure 0.2; it has two extrema, namely, a maximum at the point 3 and a minimum at the point 5. These points divide the curve into three characteristic sections I, II and III; within the limits of each of these sections the relationship between P and v is of a monotonic nature.

The part of section I situated to the left of the point 0 corresponds to negative forces P, i.e., forces which are directed upwards, whereby for $|P| \to \infty$, the junction is displaced upward without limit.

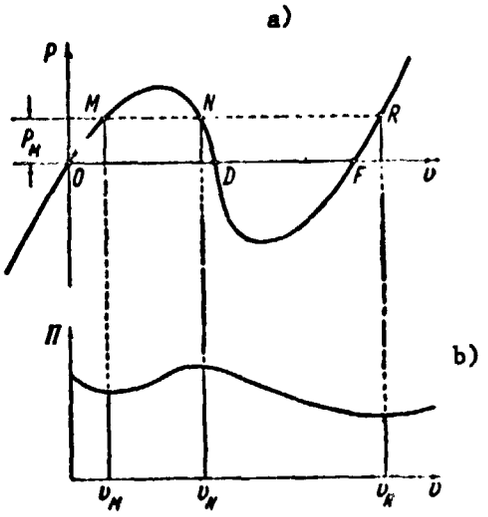

Fig. 5.3. Stable equilibrium states correspond to the points M and R; the potential energy has a minimum at these points. The equilibrium is unstable at the point N.

Let us suppose that the loading process occurs monotonically from zero (the point 0). It is evident that after the system achieves the state characterized by the point 3, the system should execute a jump immediately to the section III (point 7). Two different configurations of the system correspond to one and the same load $P_3 = P_7$, i.e., immediately prior to the jump and immediately after it. Upon further increasing the force P, still higher points of the section III will correspond to equilibrium states of the system (Figure 5.3). /51

The process of unloading the system, which starts from some point 8 located on the third section above the point 7, is described by the section III, and the system's equilibrium states will be characterized successively by the points 8 - 7 - 6 - 5. We note that upon passing through the point 7 a reverse jump to the point 3 does not occur.

A load $P_6 = 0$ and a displacement $P_6 \neq 0$ correspond to the point 6. Thus if at first we load the system up to the level of the force P_8 and then completely unload the system to the point 6, it will not return to its original state. Furthermore, negative (i.e., directed upward) loads P are necessary for the transition from the state 6 to the state 5. With a further decrease in the force P (i.e., upon an increase in the load directed upward) the system completes its reverse jump to the first section (point 2), and then a monotonic process of deformation is established downward along the section I (Figure 5.2). /52

The equilibrium states characterized by the points of section II and Figure 5.2 are not realized in the entire process described. We are convinced that unstable equilibrium states correspond to these points. In order to establish this contention, we will investigate the potential energy of all possible deviations of the system's states if it is loaded by some specified force P_M plotted in Figure 5.3, a. As is evident, three equilibrium states characterized by the points M, N and R are possible in the case of such loading. In order to analyze the stability of each of these states, it is necessary to consider the dependence of the total potential energy of the system on the displacements v, assuming the force P to be constant; in other words, it is necessary to discuss the states of the system described by all the points of the horizontal straight line $P = P_M$, i.e., not only the equilibrium states but also the nonequilibrium states.

The total potential energy of the system in the deformed state consists of two parts: the potential energy of the deformation, which we will specify by the equation

$$\Pi_1 = 2\frac{N^2 l_0}{2EF} = EFl_0\left[1 - \cos\alpha_0\sqrt{\operatorname{tg}^2\alpha_0 + \left(1 - \frac{v}{a}\operatorname{tg}\alpha_0\right)^2}\right]^2, \tag{5.7}$$

and the loading potential

$$\Pi_2 = -Pv \tag{5.8}$$

(if one supposes that a load P is suspended from the truss junction, upon a displacement v its potential energy changes by the amount $-Pv$). Consequently, the system's total potential energy is

$$\Pi = \Pi_1 + \Pi_2 = EFl_0\left[1 - \cos\alpha_0\sqrt{\operatorname{tg}^2\alpha_0 + \left(1 - \frac{v}{a}\operatorname{tg}\alpha_0\right)^2}\right]^2 - Pv. \tag{5.9}$$

The relationship $\Pi = \Pi(v)$ is illustrated in Figure 5.3, b; it is important to notice that the abscissas of the extrema coincide with the abscissas of the points M, N and R, in Figure 5.3, a. Thereupon, at the points with the abscissas v_M and v_R the potential energy is a minimum, i.e., the equilibrium is stable; at the point with the abscissa v_N, the potential energy has a maximum, and the corresponding equilibrium state is unstable. /53

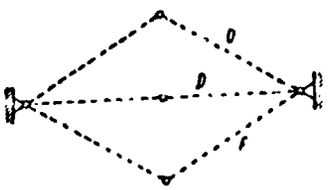

Fig. 5.4. Three equilibrium states are possible in the absence of a load. The state D is unstable.

We should note that nonidentical quantities are in essence denoted by one and the same letter v in Figures 5.3, a and 5.3, b: in the first case the true displacements corresponding to the variable force P are understood by v, and in the second case this same letter is taken to denote the possible displacements of the system in the case of the specified force P (including the displacements corresponding to the nonequilibrium states of the system).

The instability of the states described by the points of the branch II can be easily understood by discussing, for example, one of the characteristic points of this branch, namely, the point D, which corresponds to a null load P = 0 (also see Figure 5.4). Thereupon, the bars are compressed and, naturally, will tend to one of the unloaded states indicated by the dashed line in Figure 5.4; these states are characterized by the points 0 and 6 in Figure 5.2.

Thus, the ascending sections of the P — v curve correspond to stable equilibrium states, and the descending sections correspond to unstable equilibrium states. If the system is "wound up" in some artificial way into the unstable section II and then left to itself, the system will execute a jump to one of the stable equilibrium states after any small perturbation: either to the section I or to the section III. These two possibilities are shown in Figure 5.3, a, in which the direction of the jump from the point N (to the point M or R) depends on the sign of the random perturbation.

It is interesting that after the loading and the complete unloading a residual change in shape appears; therefore, it would be possible to call the system under consideration an inelastic one. Of course, in the case of a properly made up program of variation of the load, the original shape of such an "inelastic" system would, of course, be completely restored (for example, /54

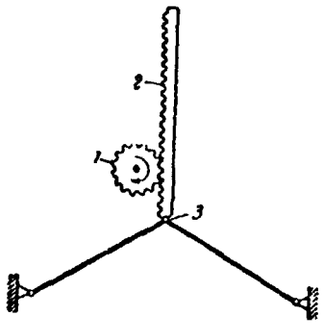

Fig. 5.5. The toothed rack is connected with the junction and transmits to it a monotonic displacement downward.

upon a variation of the load according to the cycle 0 - 3 - 7 - 8 - 7 - 6 - 5 - 2 - 0, Figure 5.2).

In the case of a jump from an unstable equilibrium state to a stable state the potential energy of the system is instantaneously decreased, since a lower energy level corresponds to the latter state. The energy which is freed upon this jump changes into the form of kinetic energy, and therefore oscillations arise which damp out in the course of time due to the dissipation of mechanical energy.

We note in conclusion that it is possible to conduct a system along the entire curve of equilibrium states, including the section II, if one creates special artificial conditions of deformation and a compulsory method of gradually displacing the junction downward, excluding the possibility of jumps.

Such a process of kinematically defined loading can be constructively accomplished, for example, according to the scheme indicated in Figure 5.5. A gradual lowering of the toothed rack 2, which is hinged at the junction 3, is achieved by the smooth rotation of the gear 1. Jumps are excluded, and the stresses transmitted by the rack to the junction will vary exactly along the curve 1 - 2 - 0 - 3 - 4 - 5 - 6 - 7 - 8, since a gradual increase of the junction's displacement, but not the loads on it, is provided by a uniform rotation of the gear.

It is possible to discuss a somewhat more complicated system, namely, a Mises' girder equipped with an additional elastic support (Figure 5.6, a). The relation between the load P and the vertical displacment v for such a system has the form

$$P = 2EF\left(1 - \frac{v}{a}\operatorname{tg}\alpha_0\right)\left[\frac{1}{\sqrt{\operatorname{tg}^2\alpha_0 + \left(1 - \frac{v}{a}\operatorname{tg}\alpha_0\right)^2}} - \cos\alpha_0\right] + cv, \qquad (5.10)$$

where c is the rigidity coefficient of the elastic support.

The relation (5.10) differs from the relation (5.6) only by the term cv on the right-hand side. But it is precisely this term which determines the distinctive nature of the curve (5.10). If the rigidity c is small, the P — v curve maintains its previous appearance with respect to the main features. If the value of c is large enough, the plot of the relation (5.10) can have a shape like that in Figure 5.6, b. The system characterized by such a P — v relation returns to its original position upon complete unloading (a decrease of the load to zero), since upon unloading a jump occurs in the case of a positive value of the force P. /55

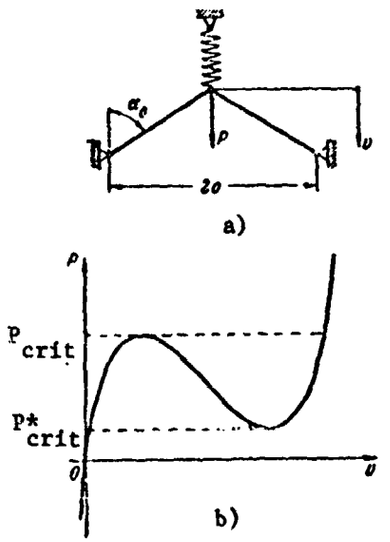

Fig. 5.6. a) Mises' truss with an additional elastic support; b) a reverse jump (upon unloading) occurs at a positive value of the force $P = P^*_{crit}$.

One can point out two characteristic values of the load P_{crit} and P^*_{crit}, which are usually called the upper and lower critical loads, on the P — v curves (Figures 5.2 and 5.6, b). Depending on the rigidity c of the additional support, the lower critical load P^*_{crit} can turn out to be negative (according to the model of Figure 5.2) or positive (according to the model of Figure 5.6, b).

The two-bar junction discussed above represents the simplest system capable of jumps and can in this sense serve as a characteristic example of a whole category of structural elements.

The uniqueness of the behavior of this system and its capacity for jumps were first noted by Mises (see R. Mises "Über die Stabilitätsprobleme der Elastizitätstheorie" (The Stability Problem of Elasticity Theory), Zeitschr. angew. Math. Mech., 1923, pp. 406 - 462; R. Mises, J. Ratzersdorfer "Die Knicksicherheit von Fachwerken" (Protection Against Cracking of Framework), Zeitschr. angew. Math. Mech., 1925, pp. 218 - 231). We note that Mises investigated a somewhat more general problem, having assumed that the junction can be displaced not only vertically but also horizontally. Striving /56 for the utmost simplification of the layout, we intentionally excluded the possibility of the appearance of horizontal displacements.

§ 6. The Stability of a Fluted Strip

The capacity of some systems for jumps sometimes finds a useful application. Thus, flexible elements are used in instrument manufacture, the curves of whose equilibrium states possess a characteristic maximum; after this maximum is reached, the system executes a jump to a new equilibrium state corresponding to the second ascending branch of the curve. These properties are possessed, for example, by flapping membranes, electrical spring switches, ribbed springs and so on.

The properties of fluted strips upon bending (Figure 6.1, a) are interesting. Such strips are used as the elastic element of spring motors; the tapes of metallic tape measures are also sometimes made in the form of fluted strips. When such a tape is unwound, it has the shape of a shallow trough and possesses appreciable bending regidity, at any rate sufficient for the strip's longitudinal axis to remain practically straight under the action of its own weight. But if we apply to the tape a more substantial bending load, the fluted shape can lose its stability: the most loaded /57 transverse cross-section suddenly straightens, and the tape's rigidity to bending almost completely disappears.

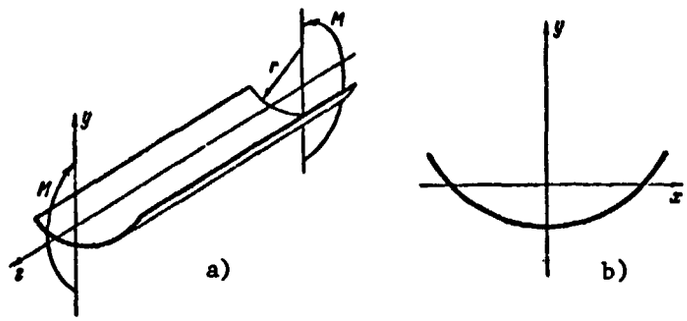

Fig. 6.1. Pure bending of a fluted strip:
a) layout of the loading, b) transverse cross-section.

We will investigate in detail the properties of a fluted strip in the case of pure bending. We will assume that in the unloaded state the generatrices of the strip are parallel to the z-axis and the average curve of any transverse cross-section is an arc of a circle of radius r. We will denote the main central axes of the cross-section by x and y.

In the case of the action of moments M the generatrices will be bent, remaining in planes parallel to the yz plane. The generatrices will be shortened in the upper part of the cross-section (above the x-axis, see Figure 6.1, b), and they will be lengthened in the lower part of the cross-section. We will assume that the cross-sections of the strip perpendicular to the z-axis are planes before the loading and remain planes after the loading. This assumption is exactly fulfilled if each of the end moments M is realized in the form of a system of normal stresses which coincides with the system of normal stresses in any transverse cross section of the strip; otherwise, according to the Saint-Venant principle the method of applying the end moments cannot have a noticeable effect on the strains and deformations at a sufficient distance from the strip's ends. If the strip's cross-sections remain flat, the lengthening of any generatrix is determined by the expression

$$\varepsilon_z = -\frac{y}{\rho}, \qquad (6.1)$$

where ρ is the radius of curvature of the generatrix and y is the coordinate of the point of intersection of the generatrix with the plane of the cross-section (Figure 6.1, b). The variation of the shape of the strip's transverse

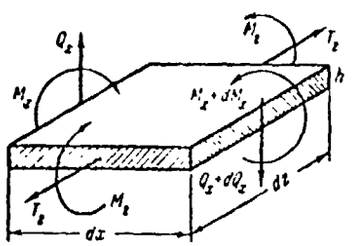

Fig. 6.2. Layout of the loading of an element of the bar. The stresses T_z and M_z do not depend on the coordinate z.

cross-section plays an important role in the problem under discussion; therefore, one should understand by y a coordinate referred to the deformed condition of the cross-section.

According to Equation (6.1) one can find from Hooke's law that the longitudinal stress T_z (i.e., the stress computed per unit length of arc of the transverse cross-section) is equal to

$$T_z = -\frac{Ehy}{\rho}, \tag{6.2}$$

where E is the modulus of elasticity of the strip's material and h is its thickness.

The stress T_z found in this way corresponds to a beam model of the strip's bending; along with this there arise the moments M_x, M_z and the transverse force Q_x, which corresponds to the deflection of the strip in the manner of a plate (or a mildly sloping shell). In Figure 6.2 is illustrated an infinitely small element of the strip dx·dz·h and the stresses acting on it. In view of the pure bending of the strip its transverse cross-sections are free from shear stresses (parallel to the medium surface) and from the distributed torques; due to the pairing of the shear stresses, there are no stresses in the shell's longitudinal cross-sections.

The following two relationships between the stresses derive from the equilibrium conditions of the element:

$$T_z = \rho \frac{dQ_x}{dx}, \tag{6.3}$$

$$Q_x = \frac{dM_x}{dx}. \tag{6.4}$$

Equation (6.3) is derived from the equation of the projections on to the normal to the median surface, written with account taken of the bending of the corresponding generatrix; equation (6.4) agrees with the analogous relationship

for beams. Consequently, the longitudinal stress T_z and the bending moment M_x are related to one another by the expression

$$T_z = \rho \frac{d^2 M_x}{dx^2}. \tag{6.5}$$

As is well known, the bending moments M_x, M_z are associated with the increases in the corresponding curvatures x_{xy} and x_{yz} in the xy and yz planes by the following relationships:

$$\left.\begin{aligned} M_x &= D(x_{xy} + \mu x_{yz}), \\ M_z &= D(x_{yz} + \mu x_{xy}), \end{aligned}\right\} \tag{6.6}$$

where μ is the Poisson coefficient and $D = \frac{Eh^3}{12(1-\mu^2)}$ is the cylindrical rigidity. /59

One can take the curvature in the xy plane to be equal to $\frac{d^2y}{dx^2}$; since the initial curvature in this plane is equal to $1/r$, the increase in curvature amounts to

$$x_{xy} = \frac{d^2y}{dx^2} - \frac{1}{r}. \tag{6.7}$$

The curvature in the yz plane is equal to

$$x_{yz} = \frac{1}{\rho}. \tag{6.8}$$

Therefore, we obtain from equations (6.5) and (6.6) the following expressions for the bending moments:

$$M_x = D\left(\frac{d^2y}{dx^2} - \frac{1}{r} + \frac{\mu}{\rho}\right), \tag{6.9}$$

$$M_z = D\left(\frac{1}{\rho} + \mu\frac{d^2y}{dx^2} - \frac{\mu}{r}\right). \tag{6.10}$$

Let us now turn to the relation (6.5) and substitute equation (6.2) into its left-hand side and equation (6.9) into its right-hand side; these substitutions lead to the equation

$$\frac{d^4y}{dx^4} + \frac{12(1-\mu^2)}{\rho^2 h^2} y = 0. \tag{6.11}$$

The solution of this equation has the form

$$y = C_1 \operatorname{ch}\frac{nx}{\rho}\cos\frac{nx}{\rho} + C_2 \operatorname{sh}\frac{nx}{\rho}\sin\frac{nx}{\rho} + \\ + C_3 \operatorname{ch}\frac{nx}{\rho}\sin\frac{nx}{\rho} + C_4 \operatorname{sh}\frac{nx}{\rho}\cos\frac{nx}{\rho}, \tag{6.12}$$

where

$$n = \sqrt[4]{\frac{3(1-\mu^2)\rho^2}{h^2}}. \tag{6.13}$$

Four boundary conditions expressing the absence of loads on the longitudinal edges of the strip serve to determine the constants C_1, C_2, C_3, and C_4:

$$Q_x = 0, \quad M_x = 0 \text{ at } x = \pm\frac{b}{2} \tag{6.14}$$

(b is the strip's width). On taking into account equations (6.4) and (6.9), we find from these conditions

$$C_{1,3} = \frac{\rho^2}{2n^2}\left(\frac{1}{r} - \frac{M}{\rho}\right)\frac{\operatorname{sh}\frac{nb}{2\rho}\cos\frac{nb}{2\rho} + \operatorname{ch}\frac{nb}{2\rho}\sin\frac{nb}{2\rho}}{\operatorname{sh}\frac{nb}{2\rho}\operatorname{ch}\frac{nb}{2\rho} + \sin\frac{nb}{2\rho}\cos\frac{nb}{2\rho}}, \tag{6.15}$$

$$C_{2,4} = 0.$$

Thus we have found a curve y(x) which describes the shape of the bent transverse cross-section of the strip and which depends on the radius of curvature ρ in the longitudinal direction. Now it is possible to associate the external moment M with the curvature $\frac{1}{\rho}$, if we present it in the form (Figure 6.3)

$$M = \int_{-\frac{b}{2}}^{\frac{b}{2}} (M_x - T_x y)\,dx. \tag{6.16}$$

With the help of equations (6.5), (6.10) and (6.12) and taking equations (6.15) into account, we find

$$M = \frac{bD}{r}\left[\left(\frac{r}{\rho} - \mu\right) + \mu\left(1 - \frac{\mu r}{\rho}\right)F_1 - \left(1 - \mu\frac{r}{\rho}\right)^2 \frac{\rho}{r}F_2\right], \tag{6.17}$$

where

$$F_1 = \frac{2}{\lambda}\frac{\operatorname{ch}\lambda - \cos\lambda}{\operatorname{sh}\lambda + \sin\lambda}, \\ F_2 = \frac{1}{2\lambda}\frac{\operatorname{ch}\lambda - \cos\lambda}{\operatorname{sh}\lambda + \sin\lambda} - \frac{\operatorname{sh}\lambda\sin\lambda}{(\operatorname{sh}\lambda + \sin\lambda)^2}. \tag{6.18}$$

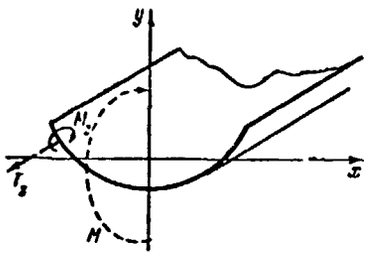

Fig. 6.3. The sum of the moments of the stresses T_z and M_z with respect to the x-axis is equal to M.

and /61

$$\lambda = \frac{nb}{\rho} = \sqrt[4]{3(1-\mu^2)}\,\frac{b}{\rho h}. \qquad (6.19)$$

Equation (6.17) describes the relation sought between the load M and the corresponding curvature $1/\rho$.

An analysis of this relation in its general form is difficult; let us dwell for an example on the particular case in which the spring's parameters have the values:

$b = 20$ mm, $r = 20$ mm, $h = 0.2$ mm, $\mu = 0.25$ mm, $E = 2.1 \cdot 10^4$ kg/mm^2

Specifying a series of values of r/ρ, let us find the corresponding values of λ, and then the values of F_1 and F_2; after this we will determine from equation (6.17) the corresponding values of the moment M.

TABLE OF THE VALUES OF $M = M\left(\frac{r}{\rho}\right)$ *

$\frac{r}{\rho}$	M, kg·mm	$\frac{r}{\rho}$	M, kg·mm	$\frac{r}{\rho}$	M, kg·mm
−5,00	−77,9	−0,06	−46,5	0,07	36,0
−4,00	−63,0	−0,05	−50,9	0,08	30,4
−3,00	−48,1	−0,04	−63,0	0,09	25,8
−2,00	−33,4	−0,03	−49,7	0,10	21,8
−1,00	−18,8	−0,02	−39,4	0,20	7,1
−0,50	−12,4	−0,01	−22,2	0,30	4,6
−0,40	−11,3	0	0	0,40	4,8
−0,30	−11,0	0,01	22,4	0,50	5,7
−0,20	−12,5	0,02	38,4	1,00	11,9
−0,10	−27,0	0,03	47,5	2,00	20,3
−0,09	−31,7	0,04	49,0	3,00	41,2
−0,08	−36,2	0,05	46,5	4,00	56,1
−0,07	−41,4	0,06	41,5	5,00	71,0

* Commas represent decimal points.

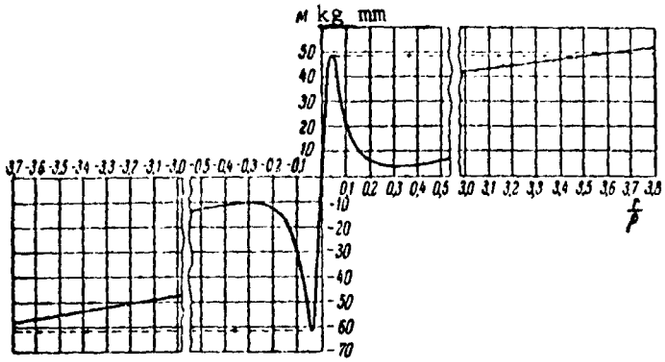

Fig. 6.4. Characteristic curve of the bar. Part of the abscissa is not shown.

The results of these calculations are given in the table above and are presented graphically in Figure 6.4; they refer both to the case of the loading represented in Figure 6.3 ($1/\rho > 0$) as well as to the case of loading by a negative moment ($1/\rho < 0$).

It is evident in Figure 6.4 that the stability of an elastic strip is expressed in jumps upon its bending both by positive and by negative moments (at $M = 49.0$ kg·mm if $M > 0$, and at $M = -63.0$ kg·mm if $M < 0$). We note that in the latter case (in which the signs of the curvature $1/\rho$ and $1/r$ are opposite) the jump occurs more sharply.

After the jump the rigidity of the fluted strip decreases sharply; this decrease is explained by the fact that almost a complete disappearance of the curvature in the transverse direction corresponds to the jump. The behavior of the strip after the jump, i.e., for large values of r/ρ, can be estimated approximately by setting $y'' = 0$ in equation (6.10), assuming that the transverse cross-section has completely straightened:

$$\mathring{M}_z = \frac{D}{r}\left(\frac{r}{\rho} - \mu\right), \tag{6.20}$$

and the total moment turns out to be equal to

$$M = \frac{6D}{r}\left(\frac{r}{\rho} - \mu\right). \tag{6.21}$$

Fig. 7.1. Cross-section of the membrane.

In the supercritical region the strip becomes practically linearly deformed, but its rigidity is ten times less than its initial rigidity.

The stability of a fluted strip was first investigated by V.P. Vepchinkin and Ya.I. Sekerzh-Zen'kovich in the paper "The Stability of Cylindrical Plates Upon Deflection," Trudy Ts AGI (Transactions of the Central Aero-Hydrodynamics Institute), No. 76, Moscow, 1931; (also see the book of S.V. Serensen, /63 "Principles of the Engineering Theory of Elasticity," Gostekhizdat Ukrainy, Kiev, 1934). In our own exposition we have followed the more recent book of W. Wuest "Einige Anwendungen der Theorie der Zylinderschale" (Some Applications of the Theory of Cylindrical Shells), Zeitschr. angew. Math. Mech., No. 12, 1954.

§ 7. More Examples of Systems with Jumps; Discussion of the Results

We will discuss another series of systems which possess the capacity for jumps. In contrast to the preceding two sections, we will not be delayed by calculations but we will cite prepared curves of the equilibrium states and turn immediately to a discussion of the properties of the corresponding elastic systems.

The flapping membrane is a mildly sloping thin-walled dome (Figure 7.1). If one gradually increases the pressure p on the membrane's surface, it reaches a certain value at which a "popping through" occurs, and the membrane takes on a new equilibrium shape. Versions of the P — v curves are illustrated in Figure 7.2 for various types of membranes, which are characterized by the H:h ratio (H is the rise of the arch and h is the thickness of the membrane), with the values $v = w_0:h$, where w_0 is the deflection of the membrane's center. In Figure 7.1, r denotes the radius of the reference contour.

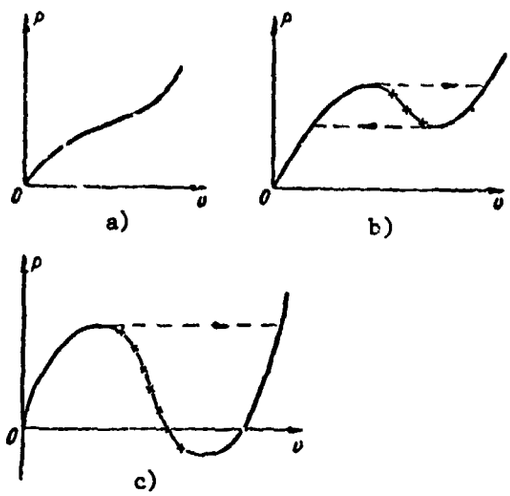

Fig. 7.2. Characteristic curves of the membranes: a) a membrane which is deformed without flapping; b) a flapping membrane which returns to its original position after unloading; and c) a flapping membrane which has residual bending after unloading.

Very mildly sloping membranes ($H < 1.5\ h$) do not in general possess the capacity for jumps (see Figure 7.2, a).

In the case of average values of the arch height ($1.5\ h < H < 3.4\ h$), the membrane returns to its original state after the popping through and the subsequent unloading to zero (see Figure 7.2, b). The ordinary oil can for lubricating sewing machines is constructed on the principle of a flapping membrane of this type; the energy which is freed upon the popping through of the bottom is expended on the expulsion of the oil. The construction of powder sprayers is based on this same principle.

In the case of large values of the arch height ($H > 3.4\ h$), the membrane does not return to its original speed after popping through and the subsequent complete unloading; in order to establish the original state, it is necessary /64 to apply negative pressure during the unloading (see Figure 7.2, c). The so-called "popouts", i.e., the local bulges on the steel plates which remain after welding the bodies of railroad cars, ships, and so on, may possess similar properties. Each "popout" is considered a defect of the construction, but "popouts" with a negative low critical pressure are considered particularly undesirable.

Among the $P - v$ curves discussed above, there were none which had vertical sections. However, systems with such $P - v$ curves are possible and are of specific practical interest. Such systems are, for example, spring-loaded electrical contact devices.

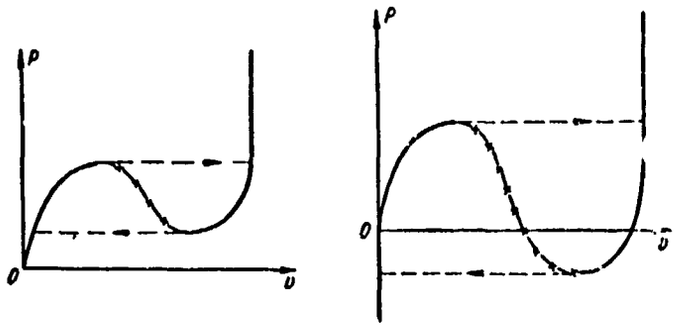

a) b)

Fig. 7.3. Characteristic curves of switches:
a) pressure, b) toggle.

It is necessary in these devices that upon the attainment of a specified load a movable contact jump from one fixed contact to another fixed contact. /65
Depending on the purpose of the design, two versions are possible for carrying it out: 1) after removal of the load the movable contact returns to its previous position, and 2) after removal of the load the moveable contact remains in its new position.

In the first case (pressure switch) the P — v curve has the shape illustrated in Figure 7.3, a, i.e., the lower critical load is positive; in the second case (a toggle switch which one often sees on the wall of a room) the P — v curve has the shape shown in Figure 7.3, b, i.e., the lower critical load is negative. The stiffness of these devices after the jump is far greater than the initial stiffness, so that there are almost vertical sections on the P — v curves.

In all the cases which have been discussed above (including those which are discussed in §§ 5 and 6) the jumps occur only upon reaching the appropriate "force barrier". If the load P is less than the upper critical load, a jump is impossible, since it is impossible to alter the quantity v in the case of a specified value of P.

At the same time there exist systems of a different type in which jumps are possible for any value of the load P lying within the interval

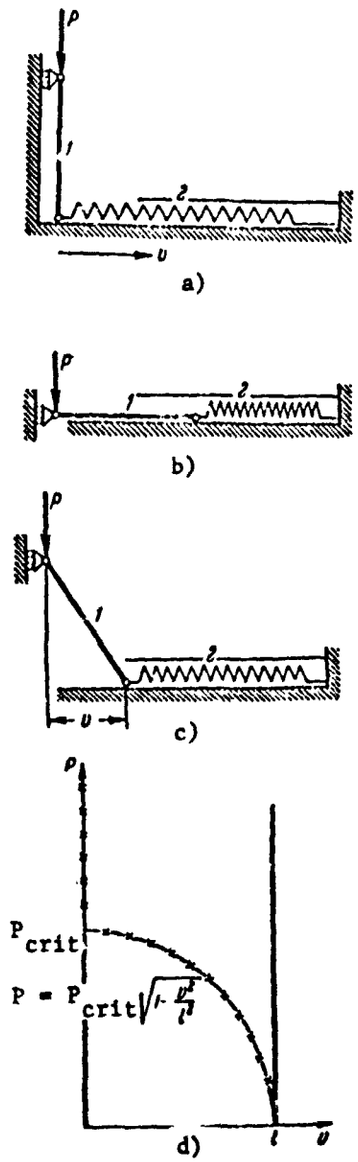

Fig. 7.4. Three equilibrium states of the system are possible for any force ($0 < P < P_{crit}$). When $P > P_{crit}$, two equilibrium states are possible (a and b). d) Curve of the system's equilibrium states.

$P^*_{crit} < P < P_{crit}$ (here, just as everywhere below, we will denote by P_{crit} the upper critical load and by P^*_{crit} the lower critical load). /66

These are systems into which a deformation perturbation can be introduced "indirectly" without changing the main load P.

Let us discuss, for example, the simple system illustrated in Figure 7.4, a. It consists of a rigid rod 1 and a spring 2 which is located in a rigid tube and cannot protrude. The equilibrium state presented in Figure 7.4, a is stable in the case of forces P which do not exceed the value

$$P_{crit} = cl \qquad (7.1)$$

(here c is the spring's compressional rigidity coefficient and l is the rod's length). When $P = P_{crit}$, this equilibrium state ceases to be stable and the system moves discontinuously to the position illustrated in Figure 7.4, b (the rod axis is horizontal); this equilibrium state is stable for any value of the force P greater than zero. /67

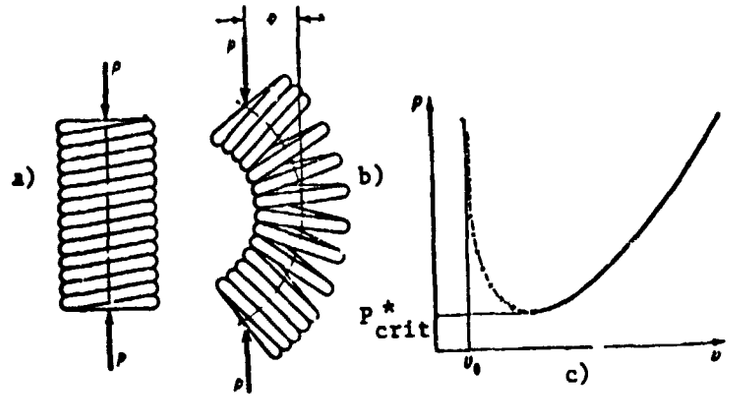

Fig. 7.5. Spring with contiguous coils (a, b). c) Curve of the equilibrium states of the spring. The branch corresponding to tensile stresses is not shown.

In addition to these two equilibrium states, there corresponds one more equilibrium configuration of the system (Figure 7.4, c) for each value of the force P lying in the interval $P^*_{crit} < P < P_{crit}$, which is determined by the lower hinge's shifting by an amount

$$v = l\sqrt{1 - P : P_{crit}}. \qquad (7.2)$$

However, this configuration is unstable. The overall curve of the equilibrium states is presented in the form illustrated in Figure 7.4, d. Here the upper critical load is defined by equation (7.1), and the lower critical load is equal to zero. The main distinctive feature of this system consists of the fact that jumps are possible for forces P less than the value P_{crit}.

For example, let the load on the vertical rod be equal to $P_1 < P_{crit}$. We will introduce a certain deformation perturbation by the application of a horizontal force to the lower hinge, and then we will remove the latter. If the perturbation v_1 applied to the system satisfies the inequality

$$v_1 < l\sqrt{1 - P_1 : P_{crit}} \qquad (7.3)$$

the rod will return to the vertical position. Otherwise case the system will move discontinuously to the equilibrium state corresponding to Figure 7.4, b.

A centrally compressed spring with contiguous coils (Figure 7.5, a) possesses similar features. The curve of equilibrium states corresponding to it is given in Figure 7.5, c. A curious peculiarity of this system is the infinitely large value of the upper critical force. However, this fact does not indicate that the equilibrium states characterized by the right-hand ascending branch of the curve are unattainable. In order for a jump to these states to occur (Figure 7.5, b) it is necessary that the compressive force exceed the value P^*_{crit} and, in addition, that a sufficient perturbation be transmitted to the spring in the form of a lateral deflection (not less than v_0); of course, the latter condition requires the application of some additional lateral load.

Thus systems exist which allow an "indirect" method of changing the configuration in the case of a constant main load. It can be said that in /68
such systems the jump requires surmounting not a force barrier (in the form of an upper critical load) but a deformation barrier (of course, on the condition that the specified load exceeds the lower critical value).

These considerations have played a significant role in the discussion of the problem of the stability of a circular cylindrical shell uniformly compressed along its generating lines (Figure 7.6). We will pause in detail on this problem, which already for more than half a century has served as the cause of lively discussions.

The first solution of this problem was proposed in 1908 by R. Lorenz. He used Euler's method and significantly simplified the problem having assumed that upon stability loss all the generating lines are deflected exactly the same (the axisymmetrical form of stability loss). Lorenz found that the critical compressive stress is equal to

$$\sigma_{crit} = \frac{Eh}{R\sqrt{3(1-\mu^2)}} \approx 0{,}6\frac{Eh}{R}. \qquad (7.4)$$

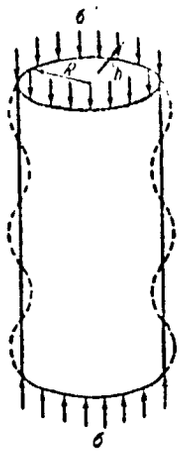

Fig. 7.6. Axisymmetrical shape of the stability loss of a cylindrical shell.

Here E is the modulus of elasticity of the shell material, μ — the Poisson coefficient, h — the shell's thickness, and R — the generating circle's radius.

The subsequent experimental verifications did not confirm this theoretical result. It was constantly discovered in the experiments that the critical stress is significantly less than is derived from equation (7.4); in some experiments a critical stress three times smaller than that predicted by Lorenz's equation was observed. /69

In 1939 - 1941 T. Karman(*) and Ch'ien Hsueh-sen investigated this problem, but they rejected the Eulerian formulation of the problem and set themselves the goal of constructing the p — v curve on the basis of nonlinear relationships taking into account the finiteness of the displacements. The results obtained by these authors are presented in Figure 7.7, a, in the form of a relation between the longitudinal load and the convergence of the shell's ends. The values of the relative longitudinal contraction ε increased by a factor of R:h, are plotted along the abscissa, and the values of the dimensionless stress $p = \sigma R/Eh$ are plotted along the ordinate. A replotted graph is illustrated in Figure 7.7, b; here the values of the dimensionless deflection $v = w_0:h$ are plotted along the abscissa (w_0 is the largest deflection of the shell).

As is evident, there are for the shell under discussion two critical values of the compressive stress: an upper critical stress p_{crit}, whose

(*) Theodore Karman (1881 - 1963) was born in Hungary. From 1909 - 1929 he worked in Germany, and from 1929 - 1963 in the USA. He is well-known for many papers in the area of the applied theory of elasticity and in particular in the area of hydroaerodynamics.

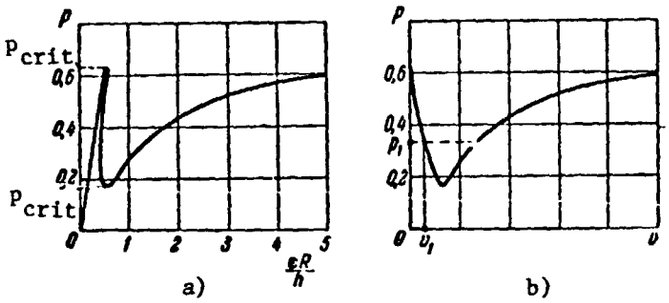

Fig. 7.7. a) Curve of the equilibrium states of a compressed cylindrical shell. The relative approach of the faces multiplied by R:h is plotted along the abscissa. b) The curve of the equilibrium states of a cylindrical shell. The dimensionless maximum deflection of the shell is plotted along the abscissa.

value coincides with the result of Lorenz's calculations, and a lower critical stress p^*_{crit}, which is approximately three times smaller than p_{crit}.

The close agreement of the calculated value p^*_{crit} with the experimental results found earlier is deserving of attention. Karman and Ch'ien Hsueh-sen concluded from this agreement that in the experimental investigations stability loss occurs in the form of a jump for stresses close to the lower critical stress p^*_{crit}.

For example, let the shell experience a compressive stress p_1 lying in /70 the interval $p^*_{crit} < p_1 < p_{crit}$ (Figure 7.7, b). In order to have a jump of a representative point from the ordinate axis to the ascending branch of the $p - v$ curve, it is necessary that the perturbation of the coordinate v exceed the value v_1.

Karman and Ch'ien Hsueh-sen proceeded on the basis of the fact that the unavoidable imperfections of the experimental set-up are equivalent to the indicated perturbation and, consequently, a jump becomes very probable already upon reaching the lower critical stress p^*_{crit}. On the basis of the

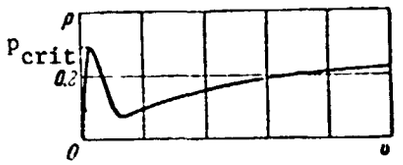

Fig. 7.8. Curve of the equilibrium states of a shell with initial imperfections of the shape.

fact that the energy of a system corresponding to a displaced equilibrium shape is less than the energy of a system in an unperturbed state, Ch'ien Hsueh-sen introduced the following energy principle: under actual "non-ideal" conditions the most probable equilibrium state of a system is the state with the minimum energy level. Thereupon it is assumed that the problem of creating the perturbations necessary for the corresponding jumps of the system is taken care of.

The lower critical stress takes on a special significance in such a conception; it serves as the upper limit of unconditionally stable states, and if the actual stress is greater than p^*_{crit}, it is impossible to consider the original equilibrium state unconditionally stable.

Similar arguments have been extensively used in other theories of the stability of shells (for example, spher[illegible] shells). Nevertheless, very critical remarks have been expressed concerning the energy principle, along the lines of the following: "This principle does not have a logical basis and by its very nature is simply an empirical principle" Y.G. Fung and E.E. Sechler, 1960).

We will lend an ear to this comment and consider what kind of perturbations are being spoken of in the Ch'ien Hsueh-sen principle and what kind of perturbations were actually unavoidable in the experimental investigations which were spoken of above; as we will see immediately, these perturbations are of a completely different nature.

A jump is assumed [illegible] the energy principle in the case of compressive stresses less than p_{crit}; but in order for this to occur it is necessary to overcome a deformation barrier, i.e., the perturbation of the exact cylindrical shape of the shell by the application of an additional transverse force

or impulse, whereby the force should be applied "opportunely" when the main compressive stress has reached the value p^*_{crit}.

Of course, there were no such loads in the experimental investigations.

Another question is whether or not the shell's deviations from an exact cylindrical shape due to causes of an engineering nature were unavoidable; these deviations also could have been called perturbations, but they are not at all equal to the perturbations spoken of in the energy principle. Due to the initial imperfection in the shell's shape, it is deformed somewhat differently from the very onset of loading than a shell of a rigorously cylindrical shape; for a shell with initial imperfections the curve of the equilibrium states looks approximately like what is presented in Figure 7.8. If additional transverse perturbations are excluded, the shell under discussion loses its stability no earlier than when the upper critical stress p_{crit} for this non-cylindrical shell is attained. It is natural to think that precisely the value /72 p_{crit} was observed in the experiments which due to the imperfections in the shell's shape could have been much lower than p_{crit} for an ideal cylindrical shell. In other words, the jumps in the experimental investigations being discussed require overcoming a force barrier.

These ideas have been clearly formulated only quite recently. They undermine the confidence in the energy principle, in which two different concepts have been mistakenly identified: the perturbations applied to the shell in the form of additional transverse forces (or impulses) and the initial disturbances of the shell's exact cylindrical shape.

Investigators at the present time are tending more and more to the opinion that the loss of stability in experimental investigations is associated not with a jump at the lower critical stress of an ideal shell but with the attainment of the upper critical stress of the actual (non-ideal) shell. Confirmation for this point of view can be found in the recent experimental investigations of Tennyson (1963 - 1964), in which stability loss of very carefully

prepared cylindrical shells was observed in the case of stresses close to the value of equation (7.4). As Tennyson remarks, the jump could be caused at lower stresses, but in order for this to occur it would be necessary to apply great lateral perturbations.

Evidently, it is necessary in the interpretation of the results of experimental stability investigations to orient oneself to the upper critical stress, but calculated of course, not for a hypothetical shell of a rigorously cylindrical shape, but for a real shell of real material.

One should not conclude from what has been said above that the concept of the lower critical stress is not of practical significance. The question is whether or not lateral perturbations, which are usually absent under laboratory conditions, may prove to be completely likely and even unavoidable in the operation of an actual design. It is clear that under these conditions the danger arises of jumps at stresses less than p_{crit} and, possibly, not exceeding p^*_{crit} by much. However, this does not indicate a revision of the Ch'ien Hsueh-sen concept for two reasons. In the first place, the value of p^*_{crit}, just as the value of p_{crit}, should be determined for the real and not for an ideal shell; and in the second place, the jump at p^*_{crit} should /73 not be considered fatally unavoidable — it is necessary for such a jump to exceed a specified level of lateral perturbations, and strong arguments are necessary in order to consider that this level is actually attainable.

A detailed investigation of flapping membranes is given in the papers of V.I. Feodos'yev (see his book "Elastic Elements in Precision Instrument Making", Moscow, Oborongiz, 1949). The jumps in spring contacts have been investigated in a paper by Ye.P. Popov entitled "The Phenomenon of a Large Jump in Elastic Systems and a Calculation of Spring Contact Devices" (Inzh. sb., Vol. 5, No. 1, 1948). Jumps due to a temperature variation in systems containing bimetalic elastic elements are discussed in an article by

E.I. Grigolyuk entitled "The Equilibrium and Stability of Bimetallic Strips" (Inzh. sb., Vol. 7, 1950).

Regarding the properties of P — v curves, see V.V. Bolotin's article "Nonlinear Elasticity Theory and Stability in the Large" (Coll: "Strength Calculations in Machine Design", No. 3, 1958), and also see § 94 of A.S. Vol'mir's book "Thick Plates and Shells" (Gostekhizdat, Moscow, 1956).

A system similar to that illustrated in Figure 7.4 was investigated by R. Grammel (see his article "Scissor Problems" in the journal "Ingenieur-Archiv", Vol. 17, No. 1 - 2, 1949). See a bibliographical citation to Lorenz's paper at the end of § 14. Tennyson's papers have been published in the journal "Rocket Technology and Astronautics" (AIAA Journal), No. 2, 1963, pp. 234 - 235; No. 7, 1964, pp. 239 - 241. The papers of Karman and Ch'ien Hsueh-sen are in "Journal of the Aeronautical Sciences", Vol. 7, No. 2, 1939; Vol. 8, No. 8, 1941.

The problems of the stability loss of shells are covered in A.S. Vol'mir's book "The Stability of Elastic Systems" (Fizmatgiz, Moscow, 1963). Also see the book "Elastic Shells" (the bibliography of the book "Mechanics", IL, Moscow, 1962; the article by Fung and Sechler entitled "The Instability of Thin Elastic Shells").

For a summary of the theoretical and experimental results referring to stability loss of cylindrical shells compressed along their generating lines see the paper: Madsen W.A., Hoff N.J., The Snap-Through and Postbuckling Behavior of Circular Cylindrical Shells under Axial Load. Department of Aeronautics and Astronautics, Stanford University (SUDAER), No. 227, 1965.

CHAPTER III
STABILITY LOSS UPON THE DISAPPEARANCE OF STABLE EQUILIBRIUM SHAPES

In this chapter a special kind of stability loss is discussed in which /74
at a certain load the elastic system ceases on the whole to possess stable equilibrium shapes and changes from a state of rest to motion. This kind of stability loss was illustrated in Figure 0.3 in the Introduction and is associated, in particular, with the problem of the action of "tracking" loads whose direction varies as a function of the change in the system's configuration.

§ 8. Tracking Loads. Static Statement of the Problem

In Figure 8.1, a, is shown an elastic cantilever, loaded by a compressive force P. What is the critical value of the force equal to? It seems that the equation

$$P_e = \frac{\pi^2 EJ}{4l^2} \tag{8.1}$$

gives an exhaustive reply to this question. The situation is actually more complicated. Let us recall that in the derivation of equation (8.1) it is assumed that the force P remains upon stability loss parallel to its own original direction (Figure 8.1, b). However, such a nature for the behavior of the load cannot be assumed to be uniquely possible. Depending on the structural layout of the loading device, countless versions of the load's behavior are possible; two of them are shown in Figure 8.1, c, d. In the case illustrated in Figure 8.1, c, the force acting on the cantilever constantly passes through one fixed point. In Figure 8.1, d is illustrated /75
a cantilever loaded by a tracking force; the direction of the force upon buckling coincides with the tangent to the axis at the upper cross section.

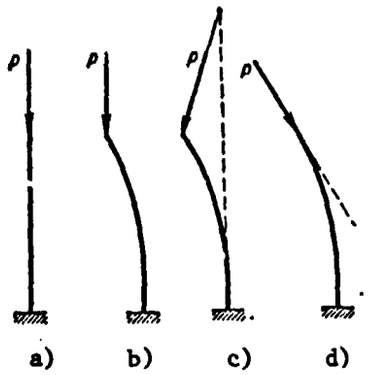

Fig. 8.1. Versions of the behavior of a compressive force P in the case of buckling of a column.

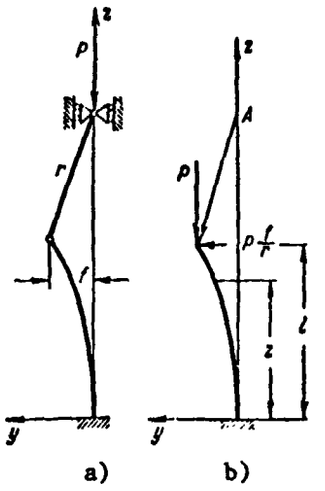

Fig. 8.2. The effect of a force passing through a fixed point A.

As we see, the value of the critical force differs in both the latter cases from that determined from equation (8.1).

First let us discuss the bar illustrated in Figure 8.1, c. The nature of the loading assumed here can be carried out, for example, just as illustrated in Figure 8.2, a, in which the compressive force is transmitted to the bar through an absolutely rigid element of length r. In contrast to the layout in Figure 8.1, b, a horizontal component of the load arises here in the case of stability loss (Figure 8.2, b).

Let us determine the critical force, using Euler's method. According to Figure 8.2, b, the bending moment at the bar's instantaneous cross section is equal to

$$M = P\frac{f}{r}(l - z) + P(f - v), \tag{8.2}$$

where z is the coordinate of the cross section, v — its deflection, l — the bar's length, f — the deflection of its end, and r — the length of the rigid element. Substituting

$$M = EJv'' \tag{8.3}$$

/76

into equation (8.2) and differentiating once more, we obtain the differential equation

$$v''' + \alpha^2 v' = -\frac{\alpha^2 f}{r}, \tag{8.4}$$

in which

$$\alpha^2 = \frac{P}{EJ}. \tag{8.5}$$

The general solution of this differential equation has the form

$$v = A \sin \alpha z + B \cos \alpha z + C - \frac{fz}{r} \tag{8.6}$$

and should be subject to the four boundary conditions:

$$\left.\begin{array}{llll} v = 0 \text{ and} & v' = 0 & \text{at } z = 0, \\ v = f \text{ and} & v'' = 0 & \text{at } z = l. \end{array}\right\} \tag{8.7}$$

Thereupon a system of equations is derived which is uniform with respect to the constants A, B, C, f:

$$\left.\begin{array}{l} B + C = 0, \\ A\alpha - \frac{f}{r} = 0, \\ f = A \sin \alpha l + B \cos \alpha l + C - \frac{fl}{r}, \\ A \sin \alpha l + B \cos \alpha l = 0. \end{array}\right\} \tag{8.8}$$

This system is satisfied by the trivial solution:

$$A = B = C = f = 0, \tag{8.9}$$

which indicates that the original shape is an equilibrium shape for any values of the compressive force. Another solution to the system (8.8) which is different from zero is possible if the determinant composed of the coefficients of the unknowns is equal to zero: /77

$$\begin{vmatrix} 0 & 1 & 1 & 0 \\ \alpha & 0 & 0 & -\frac{1}{r} \\ \sin \alpha l & \cos \alpha l & 1 & -\left(\frac{l}{r} + 1\right) \\ \sin \alpha l & \cos \alpha l & 0 & 0 \end{vmatrix} = 0. \tag{8.10}$$

Expanding this determinant, we obtain the characteristic equation

$$\frac{\operatorname{tg} \alpha l}{\alpha l} = 1 + \frac{r}{l}, \tag{8.11}$$

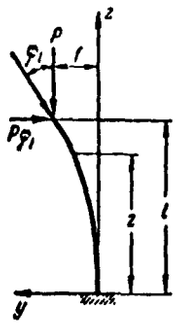

Fig. 8.3. Layout for setting up the differential equation of the elastic equilibrium of a bar.

from which the critical value of the parameter αl can be found.

It is evident from a consideration of Figure 8.2 that the larger the ratio r:l is, the weaker will be the effect of that component of the compressive force which is perpendicular to the original direction of the bar's axis. Actually, when $r:l \to \infty$, equation (8.11) takes the form

$$\operatorname{tg} \alpha l = \infty,$$

from which follows the usual value (8.1) of the critical force for a cantilever bar.

When the values of the ratio r:l are finite, the critical force turns out to be <u>smaller</u> than that determined from equation (8.1). Thus, for example, if r:l = 1, the characteristic equation takes the form

$$\operatorname{tg} \alpha l = 2\alpha l;$$

The smallest root of this equation which differs from zero is

$$\alpha l = 1{,}16,$$

i.e., the critical force is equal to

$$P_{crit} = \frac{1{,}84EJ}{l^2},$$

which is 1.84 times less than the force determined from equation (8.1). One could in the same way trace out in detail the change in the critical force for any other ratios r:l. We will not do this, assuming that the effect of a turning of the compressive force is sufficiently clarified without such a discussion. /78

Thus it is clear that the behavior of the load upon stability loss seriously affects the value of the critical force.

As an example of the second problem of this type we will investigate the possibility of the stability loss of a cantilever bar loaded at the end by a tracking force (see Figure 8.1, d). Considering the deflected position (Figure 8.3), we can notice that the component of the compressive force perpendicular to the original direction of the bar's axis tends to decrease the bar's deflection. Therefore, one can expect that the critical value of the compressive force will turn out to be larger than according to equation (8.1). We will see immediately to what an unexpected extent this assumption is born out.

The bending moment at the instantaneous cross section of the bent column is

$$M = P(f - v) - P\varphi_1(l - z),$$

where f and φ_1 are, respectively, the deflection and turn angle of the column's upper cross section, z is the coordinate of the cross section, and l is the column's length. Consequently,

$$EJv'' = P[(f - v) - \varphi_1(l - z)]. \tag{8.12}$$

In order to eliminate the deflection f, we will differentiate this equation with respect to the coordinate z:

$$v''' + \alpha^2 v' = \alpha^2 \varphi_1, \tag{8.13}$$

where $\alpha = \sqrt{\frac{P}{EJ}}$. The solution of equation (8.3) is of the form

$$v = A \sin \alpha z + B \cos \alpha z + C + \varphi_1 z. \tag{8.14}$$

The first three terms represent the solution of the corresponding uniform equation, and the last term represents the particular solution of the non-uniform equation (8.12).

The four constants A, B, C, φ_1, which appear in the solution (8.14) are associated with each other by the boundary conditions: /79

$$\left.\begin{aligned} v = 0, \quad v' = 0 \quad &\text{at } z = 0, \\ v' = \varphi_1 \quad v'' = 0 \quad &\text{at } z = l. \end{aligned}\right\} \tag{8.15}$$

As a result we obtain a uniform system of equations

$$\left.\begin{aligned} B + C = 0, \quad \alpha A + \varphi_1 = 0, \\ A \cos \alpha l - B \sin \alpha l = 0, \\ -A \sin \alpha l - B \cos \alpha l = 0. \end{aligned}\right\} \tag{8.16}$$

First let us turn our attention to the last two equations; only two constants, A and B, appear in them. A system of these two equations has the solution A = B = 0 (which is a trivial solution and corresponds to the original equilibrium shape); another solution of this system which differs from zero is possible if the determinant composed of the coefficients of the unknowns is equal to zero.

But in our case the determinant does not equal zero; actually,

$$\begin{vmatrix} \cos \alpha l & -\sin \alpha l \\ -\sin \alpha l & -\cos \alpha l \end{vmatrix} = -1,$$

and, consequently, the system of the last two equations of (8.16) has the unique solution

$$A = B = 0.$$

Thereupon it also follows from the first two equations of (8.16) that

$$C = \varphi_l = 0.$$

This result should be interpreted in the following way: bent equilibrium shapes of the bar do not exist for any values of the tracking load. In other words, the rectilinear equilibrium shape is the only equilibrium shape.

Based on this correct conclusion, Pflüger put forward the following incorrect statement in 1950: since bent equilibrium shapes are impossible, the rectilinear shape is stable for any values of the compressive force; consequently, the column illustrated in Figure 8.1, d, was called the column /80 which does not lose its stability. An error is committed in this conclusion which in logic is called substitution of the thesis.

Actually, one should distinguish the following two situations:

1) The absence of displaced equilibrium shapes, i.e., the uniqueness of the rectilinear equilibrium shapes; 2) the stability of this rectilinear equilibrium shape.

Only the customary formulation of the Euler problem hides the difference between these situations. Although the rectilinear shape is the only equilibrium shape, and other equilibrium shapes do not exist, nevertheless it may be unstable.

One should not assume that stability loss is expressed only in the form of a transition of the system to a displaced equilibrium shape. For example, one can imagine that after the perturbation of the rectilinear equilibrium shape the bar will oscillate about it with increasing amplitudes. An aperiodic departure from this equilibrium shape is also possible. In these cases, it is impossible to designate the original equilibrium shape as stable, although other equilibrium shapes are in general absent.

Thus it follows that the futility of searching for adjacent equilibrium shapes still does not give one the right to designate the original rectilinear equilibrium shape as stable. In order to get a certain estimate of a system's stability, it is necessary in general to discard the static approach to the solution and turn to a dynamic analysis. In the next section it will be explained in what cases a dynamic investigation can result in conclusions differing from the results of a static investigation; as we will see, the problem just discussed regarding the compression of a bar by a tracking force will be one of these cases.

However, here we will not depart from the framework of static stability analysis and we will explain what Euler's method can give for a system of a somewhat more general nature — a cantilever column under the influence of a force tracking the tangent to the elastic line with a certain lead or lag. Just as before let φ_1 be the turn angle of the tangent at the column's end and $\eta\varphi_1$ be the angle which the force makes with the vertical, while η is a constant coefficient (Figure 8.4, a). If $\eta = 0$, the force P is constantly vertical and P_{crit} is determined by equation (8.1); if $\eta = 1$, we return to /81 the preceding problem.

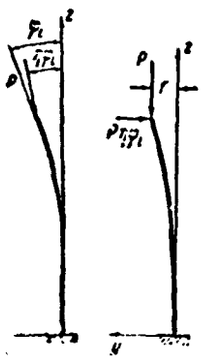

a) b)

Fig. 8.4. Buckling of a column under the action of a force which follows the deflection of the column's end with a certain lag.

If we resolve the force into vertical and horizontal components (Figure 8.4, b), the bending moment at the cross section with coordinate z is equal to

$$M = P[f - v - \eta\varphi_1(l - z)]. \tag{8.17}$$

and the differential equation of the bent axis, similar to equation (8.1), is written in the form

$$EJv'' = P[f - v - \eta\varphi_1(l - z)]. \tag{8.18}$$

Its solution is similar to the solution of equation (8.4) and is of the form

$$v = A\sin\alpha z + B\cos\alpha z + C + \eta\varphi_1 z. \tag{8.19}$$

Using the boundary conditions (8.15) which are valid in this case, we arrive at a system of equations with respect to the constants A, B, C and φ_1:

$$\left.\begin{aligned} B + C = 0, \quad \alpha A + \eta\varphi_1 = 0, \\ \alpha A\cos\alpha l - \alpha B\sin\alpha l + \varphi_1(\eta - 1) = 0, \\ A\sin\alpha l + B\cos\alpha l = 0. \end{aligned}\right\} \tag{8.20}$$

Of course, for any value α, i.e., for any compressive force, the trivial $A = B = C = \varphi_1 = 0$ is possible, which corresponds to the original equilibrium shape. We will check whether or not a non-trivial solution is possible.

The system of uniform equations (8.20) has a solution different from zero if the determinant made up of the coefficients of the unknowns is equal to zero. Therefore the condition for the existence of a displaced equilibrium shape of the column consists in equating to zero the determinant

$$\begin{vmatrix} 0 & 1 & 1 & 0 \\ \alpha & 0 & 0 & \eta \\ \alpha\cos\alpha l & -\alpha\sin\alpha l & 0 & \eta - 1 \\ \sin\alpha l & \cos\alpha l & 0 & 0 \end{vmatrix} = 0. \tag{8.21}$$

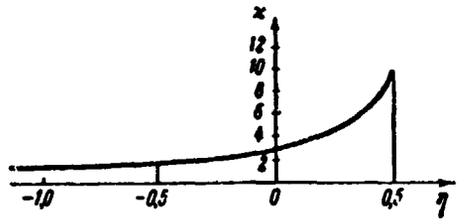

Fig. 8.5. Dependence of the parameter χ of the critical force on the parameter η of the lag. When η > 1/2, displaced equilibrium states do not exist.

If we expand this determinant, the following transcendental equation is obtained: /82

$$\cos \alpha l = \frac{\eta}{\eta - 1}, \qquad (8.22)$$

which associates the value of the critical force (concealed by the symbol α) with the parameter η, which characterizes the lag of the compressive force's direction from the direction of the tangent.

Having assumed in particular η = 0, i.e., returning to Euler's problem, we find that

$$\cos \alpha l = 0,$$

i.e., $\alpha l = \frac{\pi}{2}$ and the critical force is actually determined by equation (8.1). When η = 1 (when the force's direction coincides with the direction of the tangent), equation (8.22) has no solution, and we arrive at the result already obtained: there is no such force which is capable of maintaining the column's equilibrium in a displaced position.

In general, equation (8.22) determines the critical force only on the condition that two inequalities are fulfilled:

$$-1 \leqslant \frac{\eta}{\eta - 1} \leqslant 1, \qquad (8.23)$$

i.e., when $\eta \leq \frac{1}{2}$. If $\eta > \frac{1}{2}$, there are no bent equilibrium shapes for any compressive forces. In particular, Pflüger's result obtained for η = 1 is explained by this.

Let us discuss the case in which the parameter η satisfies the inequality (8.23); then

$$\sqrt{\frac{P}{EJ}}\, l = \arccos \frac{\eta}{\eta - 1},$$

i.e.,

$$P_{crit} = \chi \frac{EJ}{l^2}, \qquad (8.24)$$

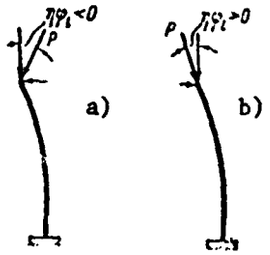

Fig. 8.6. When $\eta < 0$ (case a), both components of the load contribute to the buckling. When $\eta > 0$ (case b), the horizontal component of the load acts against the buckling.

where

$$\varkappa = \left(\arccos\frac{\eta}{\eta - 1}\right)^2. \qquad (8.25)$$

A plot is given in Figure 8.5 of the /83 variation of the coefficient χ as a function of the parameter η. It is curious that the critical load is very small for negative values of η. This situation is explained by the fact that in this case ($\eta < 0$) the horizontal component of the force P contributes to the bar's bending (Figure 8.6, a), while when $\eta > 0$, the horizontal component (Figure 8.6, b) plays the role of a force acting against the bending. Thus as the parameter increases right up to the value $\eta = 0.5$, the critical force increases and finally, at $\eta = 0.5$, reaches the value $\frac{\pi^2 EJ}{l^2}$.

Comprehensive estimates of the column's stability for various values of η can be obtained, as has already been stated, only by discarding the static criterion; this approach is made in the following section.

Pflüger's erroneous conclusion of the unlimited stability of a column compressed by a tracking force is cited in his book "Stability Problems of Static Elasticity" (Springer-Verlag, Berlin, 1950). The case of a tracking force is discussed in A.R. Rzhanitsyn's book, "The Stability of Elastic /84 Systems" (Moscow, 1955) under the heading "The Impossible Case of Limiting Conditions". On page 162 an unexpected conclusion is drawn from a true statement of the nonconservative nature of the tracking force: "Therefore, it is practically impossible to realize such conditions." Here the realizability of these or the other boundary conditions is tied up completely uselessly with the conservative nature of the system. In particular, one can realize the load in the form of a tracking force, for example, with the help of a reactive jet, as is shown in Figure 8.7, a. The tracking force acting

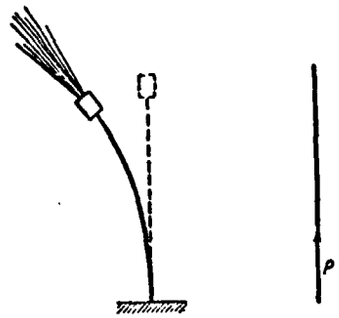

Fig. 8.7. The tracking force can be produced by a reactive jet: a) cantilever column under the effect of the jet's reaction; b) the rocket's reactive thrust is a tracking force and can cause stability loss.

on the end of a bar lacking supporting attachments (Figure 8.7, b) may be of this same nature; see the end of § 11 concerning the results of the solution of the last problem.

Further references will be pointed out at the end of each of the next two sections.

§ 9. Tracking Loads. Dynamic Statement of the Problem

In some cases stability loss appears not as the change of the system to a different equilibrium state (adjacent or nonadjacent) but as a change of the system to a motion regime. In order to clarify this possibility, a change is necessary to a dynamic investigation essentially amounting to the following. We shall study the motion of the bar starting after some initial perturbation; according to the properties of this motion one can judge as to the stability or instability of the bar's rectilinear shape. If it turns out that the perturbed motion occurs in the form of oscillations with increasing amplitudes or represents an aperiodic departure from the equilibrium state, the latter is unstable.

We will apply this method to the system discussed in § 8; as we will see, stability loss is possible not only when $n < 0,5$ (as has been discovered with the help of Euler's method) but also when $n > 0.5$.

In order to solve the problem in its dynamic formulation, it is necessary to proceed from specified assumptions with regard to mass distribution (the latter point is unimportant in the static solution). The simplest version is illustrated in Figure 9.1, where it has been assumed that a /85

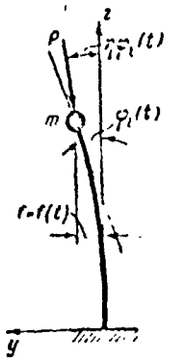

Fig. 9.1. Dynamical layout of a column.

concentrated load of mass m occurs at the end of a weightless column. In the case of small displacements under discussion, the motion of the load occurs only parallel to the y-axis, the system being investigated has a single degree of freedom, and its shape at any instant of time is determined by the deflection f = f(t) of the column's upper end. When the system is moving, the inertial force of the load

$$R = -m\ddot{f}. \tag{9.1}$$

is acting on the column's upper end in addition to the tracking force P. Consequently, the bending moment at the instantaneous cross section with coordinate z is

$$M = EJv'' = P(f - v) - (P\eta\varphi_1 - R)(l - z), \tag{9.2}$$

where v = v(z, t) is the deflection at the bar's instantaneous cross section and $\varphi_1 = \varphi_1(t)$ is the deflection angle of the end cross section; the operation of differentiation with respect to the z coordinate is denoted by primes. It is assumed in writing (9.2) that the compressive force mg produced by the load is small in comparison with the vertical component of the force P (or is included in this component).

Introducing the former notation

$$\alpha^2 = \frac{P}{EJ}, \tag{9.3}$$

we arrive at the differential equation

$$v'' + \alpha^2 v = \alpha^2 f - \left(\alpha^2 \eta\varphi_1 - \frac{R}{EJ}\right)(l - z). \tag{9.4}$$

Having integrated this equation with respect to the z coordinate (i.e., assuming the quantities f, φ_1 and R to be constant) and having subjected the solution to the boundary conditions

$$v = 0, \quad v' = 0 \quad \text{at} \quad z = 0, \tag{9.5}$$

we obtain /86

$$v = \frac{1}{\alpha}\left(\eta\varphi_1 - \frac{R}{\alpha^2 EJ}\right)(\alpha l \cos\alpha z - \sin\alpha z - \alpha l + \alpha z) + f(1 - \cos\alpha z). \tag{9.6}$$

At the column's upper end the boundary condition should be

$$v=f, \quad v'=\varphi_l \text{ at } \gamma=z \tag{9.7}$$

Therefore, two equations follow from equation (9.6):

$$\left(\eta\varphi_l-\frac{R}{a^2EJ}\right)(\alpha l\cos\alpha l-\sin\alpha l)-\alpha f\cos\alpha l=0, \tag{9.8}$$

$$\left(\eta\varphi_l-\frac{R}{a^2EJ}\right)(1-\alpha l\sin\alpha l-\cos\alpha l)+\alpha f\sin\alpha l-\varphi_l=0. \tag{9.9}$$

Having eliminated the angle φ_1 and having substituted equation (9.1) for the inertial force, we arrive at the fundamental differential equation of our problem:

$$\ddot{f}+\omega^2 f=0, \tag{9.10}$$

in which we denote

$$\omega^2=\frac{a^2EJ(\eta+\cos\alpha l-\eta\cos\alpha l)}{m(\sin\alpha l-\alpha l\cos\alpha l)}. \tag{9.11}$$

Depending on the sign of ω^2, the solution of equation (9.10) is of the form

$$f=C_1\sin\omega t+C_2\cos\omega t, \quad \text{if} \quad \omega^2>0, \tag{9.12}$$

$$f=D_1\operatorname{sh}|\omega|t+D_2\operatorname{ch}|\omega|t, \quad \text{if} \quad \omega^2<0. \tag{9.13}$$

In the first case motion of the column's end consists of harmonic oscillations with a frequency ω and a constant amplitude (which depends on the initial conditions) and in the second case there occurs an aperiodic increase in the deflections. Thus the sign of the expression (9.11) determines the stability of the column's rectilinear equilibrium shape.

For small values of the parameter αl the quantity ω^2 is positive, but as αl increases (i.e., as the force P increases), the numerator of the expression (9.11) may become zero and then negative. Therefore, the critical state is determined by the equation

$$\eta+\cos\alpha l-\eta\cos\alpha l=0. \tag{9.14}$$

We note that the latter relationship agrees with the condition (8.21) investigated earlier and, consequently, returns us to the results presented in /87
Figure 8.6; we recall that when $\eta > 0.5$, equation (9.14) is in general not satisfied, since its left-hand side is always greater than zero.

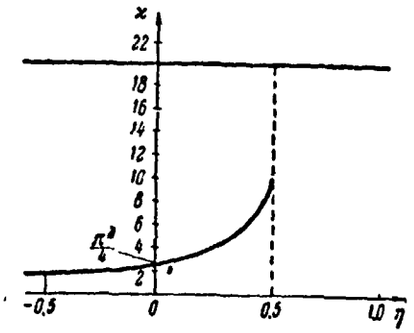

Fig. 9.2. Dependence of the parameter X of the critical force on the parameter η of the lag.

However, it is necessary to verify whether or not the quantity ω^2 can become negative because of a change in the sign of the denominator of equation (9.11) (in the case of a positive value of the numerator of the same expression). Considering equation (9.11), we see immediately that when $\sin \alpha l \cos \alpha l$, the denominator is positive, and when $\sin \alpha l < \alpha l \cos \alpha l$, it is negative. Thus, a change in the sign of ω^2 occurs not only when equation (9.14) is satisfied but also upon the condition that

$$\sin \alpha l - \alpha l \cos \alpha l = 0. \tag{9.15}$$

The value thus determined for the parameter

$$\alpha l = 4{,}493 \tag{9.16}$$

also corresponds to the critical state of the column. According to (9.16), the critical force is

$$P_{crit} = 20{,}19 \frac{EJ}{l^2}. \tag{9.17}$$

At this value of the tracking force, a loss of stability occurs which is expressed in an unlimited increase in the column's deflections.

This result is presented in Figure 9.2, in which $X = (\alpha l)^2$ is designated; as is evident, the stability loss can arise at any values of the parameter η. /88 If $\eta < 0.5$, the critical state may be determined by Euler's method (the curve). If $\eta > 0.5$, Euler's method becomes unsuitable, and the critical force is determined with the help of the dynamic method (horizontal straight line).

Thus when $\eta > 0.5$, a rectilinear shape of the column's rectilinear axis is the only equilibrium shape. However, for forces P which exceed the value given by (9.17), this shape becomes unstable; these properties of the system correspond to Figure 0.3 in the Introduction (see p. 3).

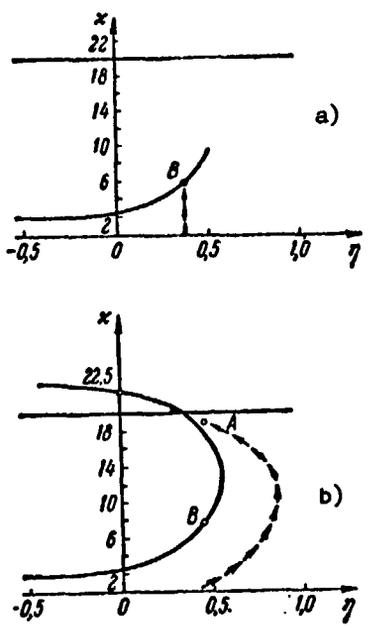

Fig. 9.3. The loading cycle is shown by arrows: a) in the case of a constant value of η, b) upon a uniform variation of the parameters χ and η.

Everything that has been expounded above is based on the assumption that the lag parameter η remains constant in the case of a gradual increase in the load. Due to this assumption, the process of gradual loading is described graphically as shown by the vertical arrows in Figure 9.3, a; the first intersection of the curve at the point B determines the stability loss.

Furthermore, it is necessary to take into account the fact that in Figure 9.3, a, only the lower branch is illustrated of the curve $\chi = \chi(\eta)$, which corresponds to equation (8.25), since the complete curve has the shape illustrated by the solid curve in Figure 9.3, b. The points located to the right of this curve and simultaneously lying below the horizontal straight line $\chi = 20.19$ (for example, the point A) correspond to stable states of the system. Let us imagine a more complicated history of the loading in which the process of increase of the loading is accompanied by a change in the parameter η, as is shown in the same Figure 9.3, /89 b by arrows. Here it is possible by means of a "round-about maneuver" to avoid stability loss right up to the completion of the loading process (point A), although a compressive force significantly exceeding the Eulerian load (point B) corresponds to this state(*).

The necessity of turning to the dynamic method for investigating stability is usually associated with the nonconservative nature of the problem

(*) The possibility of stable equilibrium states of the system under discussion in the case of loads exceeding the Eulerian value was pointed out by A.D. Myshkis in a personal letter to the authors.

(in particular, systems with tracking loads are, as a rule, nonconservative systems). In one of the reviews of the theory of elastic stability it is correctly pointed out: "Regardless of the fact that in elementary physics analysis of stability is always based on the theory of slightly perturbed motions, the theory of elastic stability, following Euler, Lagrange, and Bryan, is almost exclusively based on the ideas of statics. The fact that an analogous purely static theory is completely satisfactory for the theory of linear elastic systems loaded by conservative forces is rather curious." In a word, we should be amazed not at the fact that the static method of investigating stability may prove to be inadequate,but rather at the fact that it is very effective for a broad class of problems.

Discussing the possibilities of a static solution, it is necessary to bear the following in mind. If by "static method" is understood the energy method of investigating stability, its usefulness for conservative systems is established by the Lagrange-Dirichlet theorem. But, unfortunately, this theorem is more often called Euler's method. However, these two methods are not completely equivalent to each other, not only with respect to the computational procedure but, what is most important, with respect to the essence of the matter, since, using these methods, we obtain answers to different questions:

The energy method: what is the value of the load at which the potential energy of the system ceases to be positive definite?

Euler's method: what is the value of the load at which adjacent equilibrium configurations of the system arise?

Therefore, Euler's method may prove to be insufficient for the analysis

of the stability of equilibrium shapes even in conservative cases(*). On the other hand, the possibility is not excluded that with the help of Euler's method true estimates can be derived for the stability in some nonconservative problems. One can say that the limit of the range of applicability of Euler's method does not coincide with the limit separating the region of conservative and nonconservative systems. /90

The problem of the stability of a cantilever bar loaded by a tracking force was first solved in the dynamic formulation by M. Beck (see his article "The Buckling Load of a Singly Clamped, Tangentially Compressed Column" (Zeitscher. angew. Math. Phys., Vol. 3, No. 3, 1952). The case of tracking with a lag ($\eta \neq 1$) has been investigated by G.Yu. Dzhanelidze in his paper "The Stability of a Bar under the Action of a Tracking Force" (Transactions of the Leningrad Polytechnic Institute, No. 192, 1958); similar results were obtained by König (see the journal "Stahlbau", No. 5, 1960).

The article cited above is taken from an article of Sechler and Fung entitled "The Instability of Inelastic Shells" (see the bibliography of the book "Mechanics", the issue on "Elastic Shells", IL, Moscow, 1962, p. 67). See § 11 for similar literature citations.

(*) L.I. Balabukh turned attention to the fact that the system illustrated in Figure 9.1 is conservative, although the load is a tracking one; one can convince oneself of this by considering equation (9.10): an energy integral can be derived for it. As we have seen in § 8, Euler's method proves to be inadequate for this system when $r > 0.5$. The inertia of the load's turning makes the system nonconservative and the results derived not only on the basis of Euler's method but also with the help of the energy method become doubtful.

§ 10. Tracking Loads. A System with Two Degrees of Freedom

Due to the limiting simplification of the dynamic scheme (Figure 9.1) the solution expounded in § 9 contains one curious peculiarity to which we have still not turned our attention(*).

Let us assume that the condition (9.15) is exactly satisfied, i.e., the column is situated in the critical state. But, having glanced at equation (9.8), we notice with amazement that the deflection f of the column's upper end is identically equal to zero. Of course, this situation is not tied up with what has been stated above and becomes incomprehensible, as it is possible to speak of an aperiodic departure of the system from an equilibrium position if the column's end remains fixed (and, consequently, a rectilinear shape of /91 the column's axis is maintained).

In order to clarify the cause for what has been said, let us turn to the differential equation (9.10) and notice that it is possible to arrive at this same equation by considering the problem of the free transverse oscillations of the column in the absence of the force P if we set

$$\omega^2 = c : m, \tag{10.1}$$

where c is the stiffness coefficient. Thus a change in ω^2, which occurs according to equation (9.11) upon an increase in the parameter αl can be explained as a change in the effective stiffness coefficient of the column $c = m\omega^2$. Let us now trace the variation in the latter upon a gradual transition through zero of the difference

$$\Delta = \sin \alpha l - \alpha l \cos \alpha l, \tag{10.2}$$

which appears in the denominator of equation (9.11). As the positive values of Δ decrease, the coefficient c increases, and when $\Delta = 0$, it turns out to be infinitely large. Displacements of the column's upper end become impossible for precisely this reason. Furthermore, when $\Delta < 0$, the coefficient c

(*) This peculiarity was noticed by E.A. Beylin.

becomes negative; the solution takes the form (9.13), and the perturbed motion of the column acquires the nature of an aperiodic departure from the equilibrium state. We notice that the smaller the absolute value of the negative difference (10.2) is, the larger the velocity of this motion turns out to be.

It is thus evident that an arbitrarily small excess over the critical value of the force given by (9.17) is sufficient in order that the aperiodic process pointed out above begin. In this sense the solution which has been expounded does not contain a paradox.

At the same time a change in the effective transverse stiffness of the column must be recognized as unusual: as the force P increases, the stiffness first increases to infinity and then (at the critical value of the force P_{crit}) suddenly becomes negative. This peculiarity of the solution does not derive from the essence of the problem and is associated with the extreme idealization of the system being considered which was adopted above. One can convince oneself of this if one takes into account, for example, the inertia of the end load's rotation.

Let us do this, having assumed $\eta = 1$ to simplify the calculations. Besides the force P and the horizontal force of the load's inertia (9.1), an /92 inertial moment

$$M_{\text{inertia}} = -m\rho^2\ddot{\psi}_l \tag{10.3}$$

also acts at the column's end (ρ is the load's radius of inertia). Therefore, we obtain in place of equation (9.2)

$$M = EJv'' = P[f - v - \varphi_l(l-z)] + R(l-z) + M_{\text{inertia}} \tag{10.4}$$

Hence, after integration and subjection of the solution to the boundary conditions (9.5), we will find in place of (9.6)

$$v = \frac{R - \varphi_l \alpha^2 EJ}{\alpha^3 EJ}\sin \alpha z + \frac{\varphi_l l\alpha^2 EJ - f\alpha^2 EJ - Rl - M_{\text{inertia}}}{\alpha^2 EJ}\cos \alpha z + f - \varphi_l(l-z) + \frac{R(l-z) + M_{\text{inertia}}}{\alpha^2 EJ}. \tag{10.5}$$

Using the boundary conditions (9.7), taking equations (9.1) and (10.3) into account, a system of differential equations with respect to the

time functions f(t) and $\varphi_1(t)$ is obtained:

$$\left.\begin{aligned} a_{11}\ddot{f} + a_{12}f + b_{11}\ddot{\varphi}_1 + b_{12}\varphi_1 = 0, \\ a_{21}\ddot{f} + a_{22}f + b_{21}\ddot{\varphi}_1 + b_{22}\varphi_1 = 0. \end{aligned}\right\} \tag{10.6}$$

Here we have designated:

$$\left.\begin{aligned} a_{11} &= \frac{m}{a^2EJ}(\alpha l\cos\alpha l - \sin\alpha l); \\ b_{11} &= \frac{mp^2}{a^2EJ}(\cos\alpha l - 1); \\ a_{12} &= -\cos\alpha l \quad b_{12} = \frac{1}{a}(\alpha l\cos\alpha l - \sin\alpha l), \\ a_{21} &= \frac{m}{a^2EJ}(\alpha l\sin\alpha l + \cos\alpha l - 1); \\ b_{21} &= \frac{mp^2}{aEJ}\sin\alpha l; \\ a_{22} &= -a\sin\alpha l; \quad b_{22} = \alpha l\sin\alpha l + \cos\alpha l. \end{aligned}\right\} \tag{10.7}$$

The particular solution of the system (10.6) has the form

$$f = Ae^{i\omega t}, \quad \varphi_1 = Be^{i\omega t}. \tag{10.8}$$

Substituting (10.8) into equation (10.6), we obtain

$$\left.\begin{aligned} A(-a_{11}\omega^2 + a_{12}) + B(-b_{11}\omega^2 + b_{12}) = 0, \\ A(-a_{21}\omega^2 + a_{22}) + B(-b_{21}\omega^2 + b_{22}) = 0. \end{aligned}\right\} \tag{10.9}$$

Thus follows the frequency equation /93

$$\omega^4 - 2a\omega^2 + b = 0, \tag{10.10}$$

where to shorten the writing we have introduced the notations

$$a = \frac{a_{11}b_{22} + a_{12}b_{21} - a_{22}b_{11} - a_{21}b_{12}}{2(a_{11}b_{21} - b_{11}a_{21})}, \quad b = \frac{a_{12}b_{22} - b_{12}a_{22}}{a_{11}b_{21} - b_{11}a_{21}}. \tag{10.11}$$

If the expressions (10.7) are substituted in here, we obtain

$$a = \frac{aEJ}{2mp^2}\frac{(1 + a^2p^2)\sin\alpha l - \alpha l\cos\alpha l}{-2\cos\alpha l - \alpha l\sin\alpha l}, \tag{10.12}$$

$$b = \left(\frac{a^2EJ}{mp}\right)^2\frac{1}{2 - 2\cos\alpha l - \alpha l\sin\alpha l}. \tag{10.13}$$

The properties of the perturbed motion described by the solutions (10.8) depend on the kind of roots of the bi-quadratic equation (10.10).

If the roots ω^2 prove to be complex, the corresponding motion will consist of oscillations with unlimited increasing amplitudes (oscillatory instability); if just one of the roots turns out to be negative, the motion

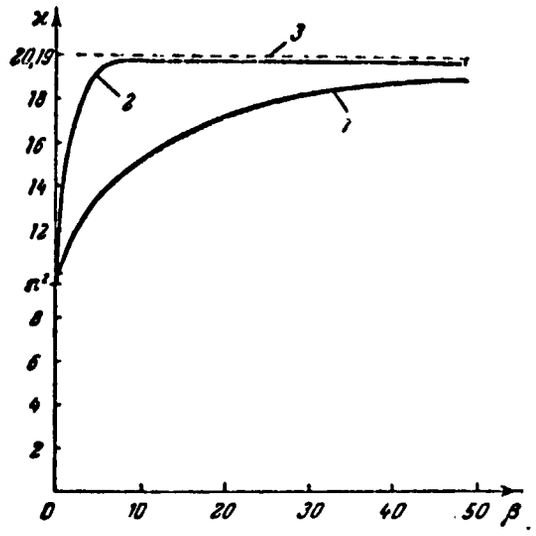

Fig. 10.1. Dependence of the parameter χ of the critical force on the parameter β. Curve 1 is plotted according to the condition (10.17), curve 2 according to the condition (10.18), and curve 3 is the asymptote corresponding to ρ = 0.

will take place in the form of an aperiodic departure of the system from its equilibrium position (aperiodic instability).

Therefore, it is necessary, in order to have stability of the rectilinear shape of the column's axis, that both roots ω^2 of the biquadratic equation (10.10) be real and positive(*). Only if these conditions are observed will the perturbed motion consist of oscillations with a constant amplitude.

We note first of all that according to the expression (10.13) the coefficient b is positive for values of the parameter αl which lie within the wide interval $0 < \alpha l < 2\pi$; as we will see, the critical value of αl does not lie beyond the limits of this interval, and therefore, analyzing the kind of roots ω^2 of equation (10.10):

$$\omega^2 = a \pm \sqrt{a^2 - b}, \tag{10.14}$$

we have a right to assume that $b > 0$. In such a case the inequality /94

$$a^2 \geq b, \tag{10.15}$$

should be fulfilled in order for ω^2 to be real, and the condition for both roots ω^2 to be positive is of the form

$$a > 0. \tag{10.16}$$

The inequalities (10.15) and (10.16) solve the problem of the stability of the system under discussion.

(*) For more detail on this see page 290.

Substituting the expressions (10.12) and (10.13) into the inequalities (10.15) and (10.16), we obtain the stability conditions in the form

$$\left[\frac{\beta}{\alpha l}(\sin \alpha l - \alpha l \cos \alpha l) + \frac{\alpha l}{\beta} \sin \alpha l\right]^2 + 4(\alpha l \sin \alpha l + 2\cos \alpha l - 2) \leqslant 0, \tag{10.17}$$

$$\frac{\beta}{\alpha l}(\sin \alpha l - \alpha l \cos \alpha l) + \frac{\alpha l}{\beta} \sin \alpha l \geqslant 0; \tag{10.18}$$

Here the ratio $l:\rho$ is denoted by β.

The critical states correspond to the equality sign in the relationships (10.7) and (10.18). Having calculated the roots of the transcendental equations thus obtained, one can plot graphs of the variation of the parameter $\chi = (\alpha l)^2$ as a function of the value of β; these graphs are presented in Figure 10.1. It is evident here that for any value $\beta > 0$ the condition (10.17) is determinant, since smaller values of the critical parameter χ correspond to it. This indicates that stability loss is expressed in the development of oscillations with increasing amplitudes. /95

According to Figure 10.1, as the load's radius of inertia decreases, i.e., as the parameter β increases, the critical force monotonically increases and asymptotically tends to the value (9.17). It is curious that the load's turning inertia decreases the value of the critical force, i.e., it exerts a destabilizing effect.

§ 11. The History of the Problem

In 1927 - 1929 Ye.L.Nikolai investigated with the help of Euler's method the stability of a cantilever compressed and twisted bar and thereupon arrived at an unexpected result: if the torsional moment is not equal to zero, the rectilinear equilibrium shape is the only equilibrium shape. It turned out that a bent equilibrium shape is possible only in the absence of the torsional moment (if the compressive force attains the Eulerian value). Understanding clearly that the absence of bent equilibrium shapes does not at all indicate the stability of the original shape, Ye.L.Nikolai continued his investigation of the stability with the help of the dynamic method

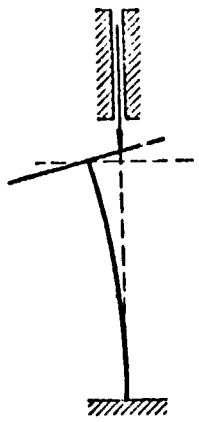

Fig. 11.1. Compressive force with a fixed line of action.

(thereupon some paradoxical properties of the system were also discovered on which we will not dwell here).

A check of the stability of the equilibrium shape of elastic systems by means of an analysis of the solutions of the equations of motion was recently proposed. However, for a long time the dynamic approach has been assumed to be only a version of a computational procedure; it has been assumed that the estimates derived with the help of the dynamic criterion should agree with the estimates derived by the static method. In Ye.L. Nikolai's solution the inadequacy of the static approach and the non-equivalency of it to the dynamic investigation were first discovered.

The investigations carried out by Ye.L. Nikolai were the theme of two of his lectures at the Leningrad Mechanical Society (1927). Having commented during the discussion, P.F. Papkovich(*) expressed the notion that the failure of the application of Euler's method to a compressed and twisted bar is evidently associated with the nonconservative nature of the problem. /96

In 1939 V.I. Reut attempted to apply Euler's method to an investigation of the stability of a bar loaded by a force with a fixed line of action (Figure 11.1); here also it was found that the rectilinear shape of the column's axis is the only equilibrium shape. In the same year B.L. Nikolai solved the same problem by means of an investigation of the properties of the system's motion and found a finite value for the critical force. In an article B.L. Nikolai correctly remarks: "... for conservative systems the

(*) Peter Fedorovich Papkovich (1887 - 1946) was a professor at the Army-Navy Academy and the author of many papers on the theory of stability of elastic systems and the structural mechanics of a ship. He was an Associate Member of the USSR Academy of Sciences from 1933 on.

frequencies of the oscillations decrease as the load increases, and a transition of the values of the frequency λ occurs from real to imaginary values at $\lambda = 0$; in these cases the "static" method of determining the critical load is completely valid. However ... in the case of engineer Reut's scheme the transition of the values of λ from real to imaginary values occurs without any transition through zero, which deprives the "static" method of any meaning."

The validity of these arguments was not realized for a long time. In § 8 we have also written about the error of Pflüger, who assumed that a static investigation can give a reliable estimate of the stability in a problem concerning the effect of a tracking force. The true solution of the latter problem was only given in 1952 by Beck (for the case of a uniform distribution of mass along the column's entire length).

Since that time (to a significant extent due to the interesting papers of H. Ziegler) the dynamic method of investigating the stability of elastic /97 systems has had general recognition, and a large number of problems on the effect of tracking loads have already been solved up to the present time with the help of this method.

In particular, the problems of the effect of a tracking force on a free bar are of serious practical interest (see Figure 8.7, b above); the static formulation of these problems is in general devoid of meaning. The first solution was proposed in 1960 by K.N. Gopak; having replaced the bar's distributed mass by fixed concentrated masses, K.N. Gopak found the following approximate value of the critical force:

$$P_{crit} = 90 \frac{EJ}{l^2}. \qquad (11.1)$$

Subsequently the coefficient appearing in this equation was refined by a number of investigators; the following values were obtained:

V.D. Babanskiy (1962)	100;
König (1964)	110.19;
Beal (1965)	109.9;

V.I. Feodos'yev (1965) 109.69;
O.A. Goroshko (1965) 115.

The result calculated by V.I. Feodos'yev deserves complete confidence; this result was obtained on an electronic computer taking into account 60 terms in the series expansion of the solution (other authors took into account no more than 5 terms).

The dynamic approach was successfully applied to investigations of the stability of the two-dimensional shape of a strip's deflection. An extensive cycle of investigations has been completed by V.V. Bolotin, the author of the only monograph especially devoted to the problems of the theory of the elastic stability of nonconservative systems (1961). We will also point out the papers of M.Ya. Leonov and his co-workers (the effect of the methods of the distribution of masses along a bar's length on its stability, the effect of inelastic strength, the case of tracking loads which assume the application of Euler's method, and so on) and also Z. Kordas, who has solved G. Yu. Dzhanelidze's problem in its most general formulation.

The investigations of Ye.L. Nikolai are included in a book of his papers (Ye.L. Nikolai "Trudy po mekhanike" (Works on Mechanics), Gostekhizdat, 1955, pp. 357 - 406). The subsequent development of these investigations is given by G.Yu. Dzhanelidze ["The Problem of the Equilibrium of a Compressed and Twisted Bar", "Trudy Leningradskogo industrial'nogo instituta" (Transactions of the Leningrad Industrial Institute) No. 3, 1939] and I.Ye. Shashkov "Prikladnaya matematika i mekhanika" Vol. 3, No. 2, 1939; Inzh. Sb., Vol. 1, No. 1, 1941; Inzh. Sb., Vol. 7, 1950). An attempt was made in S.P. Vyaz'- /98
menskiy's paper to take into account the effect of the finite torsional rigidity of a bar (Inzh. Sb., Vol. 25, 1959).

The papers of V.I. Reut and B.L. Nikolai were published in Issue 1 of the "Trudy Odesskogo instituta inzh. grazhd. i kommun. st-va" (Transactions

of the Odessa Institutute of Civil Engineering and Communal Construction) (1939). One can read through H. Ziegler's paper entitled "The Stability of Elastic Systems" in a Russian translation (see the book of articles "Problems of Mechanics," No. 2, IL Moscow, 1959). For subsequent literature see V.V. Bolotin's monograph "Nekonservativnyye zadachi teorii uprugoy ustoychivosti" (Nonconservative Problems on the Theory of Elastic Stability) (Fizmatgiz, Moscow, 1961). Among the most recent publications we note the articles of M.Ya. Leonov and M.L. Zoriy (Scientific Notes of the Ukrainian SSR Academy of Sciences Institute of Machine Control and Automation, Vol. 7, 1961). See the book by A.I. Lur'ye entitled "Analiticheskaya mekhanika" (Analytic Mechanics) (Fizmatgiz, Moscow, 1961, pp. 196, 197) regarding the possibility of the nonconservative nature of positional forces. Z. Kordas' article has been published in the journal "Bulletin de L'Academie Polonaise des Sciences techniques", Vol. 11, No. 12, 1963.

The following have been devoted to the problem of the stability of a free bar subjected to the action of a tracking force: Gopak K.N. "The Loss of Stability by a Free Bar Moving in an Accelerated Manner under the Effect of a Tracking Force" (Izvestiya AN SSSR, OTN, Mekhanika i mashinostroyeniye, No. 4, 1960); Beal, T.R. "The Dynamic Stability of a Fixed Rocket under the Action of a Constant and Pulsating Thrust Force" (Raketnaya tekhnika i kosmonavtika, No. 3, 1965); König, H. "Raumfahrtforschung" (Space Flight Research), Vol. 8, No. 1, 1964; V.I. Feodos'yev " Concerning a Problem of Stability" (Prikladnaya matematika i mekhanika, Vol. 29, No. 2, 1965). See the results of V.D. Babanskiy and O.A. Goroshko in the book by the latter entitled "Dinamika uprugoy konstruktsii v usloviyakh svobodnogo poleta" (The Dynamics of an Elastic Structure Under the Conditions of Free Flight) ("Naukova Dumka" Press, Kiev, 1965).

CHAPTER IV
STABILITY LOSSES WHEN ANY FORMS OF EQUILIBRIUM DISAPPEAR

In this chapter we shall examine mechanical systems in which a load maximum is reached in the deformation process, as is shown in Figure 0.4 in the Introduction. Sometimes, in reference to these cases, we are talking about stability loss of the second kind.

For a correct estimate of the properties of such systems, it is necessary to determine what method may be used to carry the system through a state of equilibrium, as described by the graph P — v. Two methods of loading are possible:

1) Monotonic increase in the load, i.e., a load in the direct meaning of this word. After the load reaches a maximum, the system begins to move with an unlimited increase in displacements;

2) Monotonic increase in displacement. In the majority of tensile testing machines which we tested, the load is achieved by this method.

The interpretation of the graph P — v is different in these two cases. It must be noted that the discussion in the Introduction of instability in the right branch of the graph pertains only to the first case of loading. For the second loading regime, when forces are not given, but rather the displacements, a spontaneous increase in the displacements is impossible. Nevertheless, in this case unusual phenomena occur, which also may be called stability losses.

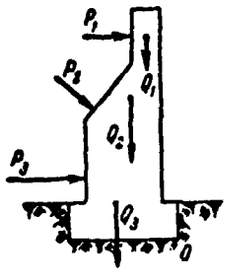

Fig. 12.1. Forces Q_i produce the holding moment, forces P_i — the tilting moment; the letter 0 designates the tilting edge.

§ 12. General Stability of High Buildings

When designing high buildings, such as factories and plants, water towers, television towers, supports for high-voltage communication lines, bulkheads, etc., the problem of /100 the general stability of the structure is given a great deal of attention. Very frequently, the stability of a structure is designated by the ratio of the holding moment M_h to the tilting moment M_t:

$$k_t = \frac{M_h}{M_t}, \qquad (12.1)$$

which is called the stability coefficient. Both moments are calculated with respect to the tilting edge 0 (Figure 12.1), while when determining M_t the forces P_1, P_2, are calculated (wind pressure, soil, water, inertia forces during earthquakes, etc.), and when determining M_h — the forces Q_1, Q_2 (weight). There are standard requirements which determine the minimum value of the stability coefficient k_t, depending on the type of construction (for example, for metallic radio masts $k_t \geq 2.5$). It would appear that such a method must provide the general stability of a structure, since formulating the holding and tilting moments should completely correspond to the problem at hand.

In actuality, the problem is more complex than appears at first glance, and the relatively high standard values of the minimum stability coefficient are in essence used to compensate for the lack of validity in the computational method. The problem is not simply that the calculated loads are not determined with sufficient precision (although this does occur for such loads as, for example, wind pressure) — we shall not discuss this important aspect of the

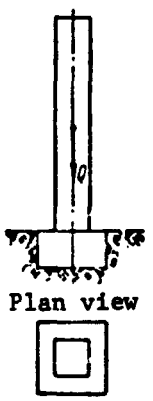

Fig. 12.2. Rigid column on elastic base.

problem here(*). The main disadvantage of using this formula (12.1) for the calculation consists of completely ignoring the deformation of the system, particularly of a base located under the bottom of the construction.

For example, let us consider the overall stability /101 of a rigid column, which passes through the base and rests on the ground, and is subjected to the action of only its own weight (Figure 12.2). Since there are no horizontal forces, the tilting moment equals zero, and according to formula (12.1) it is found that the stability coefficient equals infinity no matter how high the column is. Naturally, it is impossible to agree with such an estimate of stability.

In 1935 - 1936 H. Kramer and N.P. Pavlyuk greatly improved the computational scheme of the problem, and studied the Euler stability of a rigid column on an elastic base (Figure 12.3, a). Their solution is as follows. Let us assume that the physical properties of the base are described by the Winkler model(*) (which has been widely used in designing beams on a solid elastic base) i.e., we assume that the reaction of the base at a given point is proportional to the strength of the base at this point:

$$r = -cy; \qquad (12.2)$$

Here c is the coefficient of proportionality (bed coefficient). In the unperturbed state of equilibrium, the diagram for the reaction of the base has the form of a rectangle (Figure 12.3, b), and in the deflected (perturbed) state of equilibrium — the form of a trapezoid (Figure 12.3, c). In the

(*) The problem of determining the calculated loads is an independent problem, and in many cases it is necessary to reject a deterministic analysis in favor of an analysis based on the methods of the theory of probability.

(**) E. Winkler (1835 - 1888) — Professor of the theory of structures and bridges in Dresden, Prague, Vienna and Berlin. The author of the technical theory of a curved beam, and several works on designing beams of an elastic base, as well as solid beams and arches.

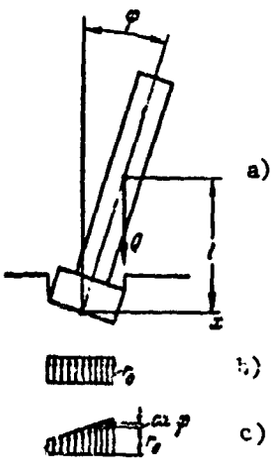

Fig. 12.3. a) Scheme for compiling the equation of equilibrium of a rigid column in the deflected position; b) diagram of the reaction of the base in a non-deflected position; c) diagram of reaction of the base in deflected position.

first case, we have

$$r = r_0 = \frac{Q}{F} \tag{12.3}$$

(F — area of the base), and in the second case

$$r = r_0 + cx\varphi. \tag{12.4}$$

Here φ is the angle of deflection of the stand, x — distance of the running point from the axis passing perpendicularly to the plane of the drawing through the center of gravity of the foundation. In the deflected state of equilibrium, the equation of moments with respect to this axis must be satisfied: $-Ql\varphi + \int_{(F)} rbx\,dx = 0$

/102

(b = b(x) — size of the base which is perpendicular to the plane of the drawing). Here the first term expresses the moment of the weight Q, and the second term — the moment of the distributed forces of reaction for the base. After substituting (12.4) and integrating, we obtain

$$-Ql\varphi + c\varphi J = 0, \tag{12.5}$$

where J is the moment of inertia of the area of the base with respect to this axis. Naturally, equation (12.5) is satisfied for any values of Q, if φ = 0. This trivial solution points to the possibility of equilibrium of the column in the undeflected position. However, the same equation is satisfied for φ ≠ 0, if the force satisfies the condition

$$Q = Q_{cr} = \frac{cJ}{l} \tag{12.6}$$

The value obtained for the force Q is the Euler load for the column under consideration.

Using this expression, N.P. Pavlyuk and H. Kramer used the following as the stability coefficient

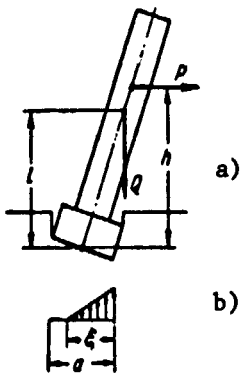

Fig. 12.4. a) Scheme for compiling the equation of equilibrium of a rigid column under the action of the forces Q and P; b) with a large rotation of the base, a portion of it separates from the foundation.

$$k = \frac{Q_{cr}}{Q} = \frac{cJ}{Ql} \qquad (12.7)$$

The value of this approach is undisputed: the stability of a rigid column can be determined quantitatively even in the case when there are no horizontal forces.

However, if we reject criterion (12.1), /103 then how are we going to establish the column stability when there are horizontal loads? To answer this question, we must examine the entire set of possible states of equilibrium when there is a gradual increase in the horizontal forces. Naturally, the study may be done with allowance for the base compliance.

Figure 12.4, a shows the same column, but subjected to the additional horizontal force P. To determine the angle of column deflection, we must use the equation of moments, which has the following form in contrast to (12.5)(*)

$$-Ph - Ql\varphi + c\varphi J = 0, \qquad (12.8)$$

where h is the ordinate of the point at which the force P is applied. From equation (12.8) we find the linear dependence

$$P = \frac{cJ - Ql}{h}\varphi. \qquad (12.9)$$

This relationship is valid only until the diagram of the reaction of the base has the form of the trapezoid, which is shown in Figure 12.3, c. However, with an increase in the angle φ in the last analysis a state occurs in which the reaction on the left edge of the base vanishes, and then — with a further increase in the angle φ — the diagram of the reaction of the base assumes the form shown in Figure 12.4, b (the left side of the base separates from the foundation).

(*) To simplify the computations, we shall not consider the differences between the angle φ and its functions sin φ and tg φ (in this case, we are discussing the finite angles φ and this does indeed exist).

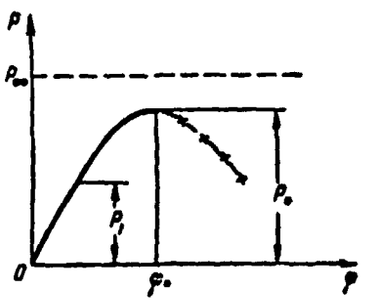

Fig. 12.5. Curve of equilibrium states; P_1 — force at which separation of the base begins and the relationship $P(\varphi)$ becomes nonlinear; P_* — greatest value of the force P, at which equilibrium of the column is possible; P_∞ — value of P_* for an infinitely large rigidity of the base.

Omitting the elementary calculations, we shall give the final expressions for the case when the base is a rectangle with the sides a and b so that $J = ba^3/12$. The angle φ, at which there is a change from a trapezoid diagram to a triangular diagram, is determined by the formula /104

$$\varphi_1 = \frac{2Q}{ca^2b}, \tag{12.10}$$

and the corresponding value of the force equals zero

$$P_1 = \frac{Qa}{6l}\left(1 - \frac{Ql}{cJ}\right). \tag{12.11}$$

With a further increase in the angle φ, the moment of reaction for the base may be determined by expression

$$M_r = Q\left(\frac{a}{2} - \frac{\xi}{3}\right), \tag{12.12}$$

where ξ is the width of the zone where the base contacts the foundation:

$$\xi = \sqrt{\frac{2Q}{\varphi bc}}. \tag{12.13}$$

Thus, instead of equation (12.8) we obtain

$$-Ph - Ql\varphi + Q\left(\frac{a}{2} - \frac{1}{3}\sqrt{\frac{2Q}{\varphi bc}}\right) = 0. \tag{12.14}$$

This equation nonlinearly connects the horizontal force P with the angle φ

$$P = \frac{Q}{h}\left(\frac{a}{2} - \frac{1}{3}\sqrt{\frac{2Q}{\varphi bc}} - l\varphi\right). \tag{12.15}$$

Figure 12.5 graphically shows the linear dependence (12.9) and the nonlinear dependence (12.15), forming a curve for the states of equilibrium of the column under consideration.

We should first of all note that the nonlinear nature of the second part of the curve is a direct consequence of the physical conditions of the interaction between the bed and the base — when the foundation separates from

the base, the moment of distributed forces of the reaction becomes proportional to the angle of inclination of the column.

The curve $P - \varphi$ has a maximum which determines the greatest value of the force $P = P_*$, at which equilibrium of the column is possible. For $P > P_*$ there are no equilibrium states. The decreasing section (indicated by crosses) expresses the unstable states of equilibrium, and is of no practical importance.

In the same Figure 12.5, the horizontal dashed line shows the level characterizing the tilting force P_∞, calculated under the assumption of absolute base rigidity, i.e., /105

$$P_\infty = \frac{Qa}{2h}. \tag{12.16}$$

This value may be found from formula (12.1), if we set $k = 1$. We may establish that the maximum of the curve in Figure 12.5 is always located below the line (12.16). In actuality, the maximum of (12.15) is achieved with the following value of the angle of inclination for the column:

$$\varphi_* = \left(\frac{1}{2l}\sqrt{\frac{2Q}{bc}}\right)^{2/3}, \tag{12.17}$$

to which the critical load corresponds

$$P_* = \frac{Qa}{2h}\left[1 - \sqrt[3]{\frac{Ql}{cJ}}\right], \tag{12.18}$$

which is always less than the force given by expression (12.16).

Let us assume a certain force $P < P_*$ is given. The ratio $P_*:P$, which shows how much larger the limiting force is than the force which is actually in operation, is assumed to be the coefficient of stability of the system. However, if we use the expressions (12.1) and (12.16), then for the stability coefficient we obtain a larger value of $P_\infty:P$. It thus follows that formula (12.1) exaggerates the actual stability reserve.

This exaggeration may be very great. It depends on the characteristic ratio $cJ:Ql$. Thus, for example, even for a column characterized by a very high value of the ratio $cJ:Ql = 6$, the use of formula (12.1) would produce a two-fold error. /106

The curve of the equilibrium states (Figure 12.5) is typical for all systems examined in this ch ter. Striving to obtain the greatest classification possible of the role of the base deformation, we have deliberately disregarded the following four factors:

1. When writing the equation of equilibrium, we replace the trigonometric functions sin φ and tg φ with the values of the angle φ. When solving the Euler problem, i.e., when deriving the formula (12.6), such a substitution is not only permissible but natural, since by definition infinitely small angles of φ are being examined. However, when compiling the curve of equilibrium states, pertaining to the action of a horizontal force P, this substitution generally speaking entails certain quantitative errors.

2. The natural rigidity of the column is assumed to be infinitely large. In determining the deformation of the column, the entire curve of equilibrium states is located below the curve shown in Figure 12.5.

3. When the base sags to a great extent, the Winkler relationship poorly describes the real properties of the base. The elastic-plastic properties of the base reaction will tend to decrease the ordinate of part of the curve of equilibrium states.

4. The force P may change its direction, following the rotation of the column (this is particularly apparent, for example, in the case of water pressure). This interesting problem was studied by Ya.B. L'vin in 1950.

These factors must be taken into account in practical computations, but they will be refinements of a quantitative, and not a qualitative, nature.

The work of N.F. Pavlyuk was published in the collection "Trudy Leningradskogo instituta inzhenerov kommunal'nogo stroitel'stva" (Transactions of the Leningrad Institute of Communal Construction Engineers), No. II, ONTI, Leningrad, 1935.

For the article by H. Kramer, see the journal "Zement", No. 4, 1936, p. 52. The article by Ya.B. L'vin "The Stability of Rigid Walls and Massive Structures on an Elastic Base under the Action of Forces Which Have an Arbitrary Direction Including Rotating Forces", was published in the collection "Trudy Voronoezhskogo inzhenerno-stroitel'nogo instituta" (Transactions of the Voronezh Engineering-Structural Institute), No. 2, 1950.

The stability of high buildings on an elastic-plastic base was studied in a dissertation by B.P. Garmus (Kaunas Polytechnic Institute, 1958).

§ 13. Characteristics of "Deformation Calculations"

In his work "Stability of Elastic Systems", H. Ziegler, characterizing different methods of studying instability, wrote: "Certain problems of stability may be solved by the 'method of non-ideality'. This method is characterized by the following question: What is the magnitude of the force at which the deflection of a non-ideal system becomes infinitely large?" Non-ideality here designates different deviations from idealized conditions, which are characteristic for the Euler formulation of the stability problem. Thus, initial experiments on the compressive force, initial deflection of an axis, asymmetry of physical properties (which arises, for example, due to residual stresses from welding, rolling, or straightening), etc. pertain to the imperfection of a compressed rod.

One essential feature of the solution using the imperfection method lies in the fact that deviations from the initial configuration of the system (for example, bending of a compressed rod axis) arise from the very beginning of the loading. In contrast to the Euler method, the occurrence of such deviations cannot be a sign of stability loss.

Some authors clearly prefer the imperfection method, and include in the analysis certain initial non-idealities, even in those cases which in principle are assumed in the Euler formulation of the problem. Thus, in the

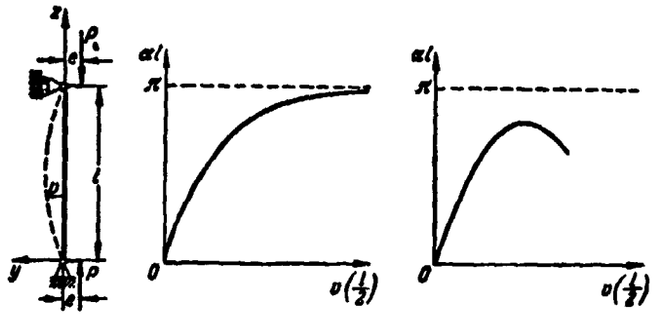

a) b) c)

Fig. 13.1. a) Diagram of a rod loaded off center; b) curve of equilibrium states, corresponding to equation (13.4); c) form of the curve of equilibrium states reflecting the nonlinearity of the system.

book "Ustoychivost' uprugikh sistem" (Stability of Elastic Systems), S.P. Timoshenko systematically avoided the Euler formulation, and determined, for example, the critical force for a bent rod by solving the problem of off-center compression. The computations basically proceed as follows (for a rod with hinge supported ends, Figure 13.1, a).

Instead of a homogeneous differential equation, pertaining to the Euler formulation of the problem

$$\frac{d^2v}{dz^2}+\alpha^2v=0 \qquad (13.1)$$

($v = v(z)$ — deflection of points on the rod axis, $\alpha^2 = P:EJ$, P — compressive force, EJ — rigidity during bending), the nonhomogeneous differential equation is examined

$$\frac{d^2v}{dz^2}+\alpha^2v=\alpha^2e, \qquad (13.2)$$

in which e is the eccentricity of the compressive force. The solution of /108 (13.2), which is satisfied by the boundary conditions of the problem, has the form

$$v=e\left[\frac{\cos\alpha\left(\frac{l}{2}-z\right)}{\cos\frac{\alpha l}{2}}-1\right], \qquad (13.3)$$

where l is the rod length. We may follow the sequential development of bending, for example, with the values of the deflection in the middle of the span, i.e., $z = 0.5l$

$$v\left(\frac{l}{2}\right)=e\left(\frac{1}{\cos\frac{\alpha l}{2}}-1\right). \tag{13.4}$$

It may be seen from this expression that, with an increase in the dimensionless parameter αl (and a corresponding increase in the compressive force) the deflection increases monotonically and for

$$\alpha l=\pi \tag{13.5}$$

becomes infinitely large. A graph illustrating (13.4) is shown in Figure 13.1, b. Substituting α in (13.5), we find the critical state of the force corresponding to this: /109

$$P=\frac{\pi^2 EJ}{l^2}, \tag{13.6}$$

which, as may be seen, coincides with the smallest Euler force. We should note that the result (13.6) does not depend on the initial eccentricity.

In support of this method (sometimes called the deformation calculation), it is usually stated that ideal conditions cannot exist in practice, and allowance for imperfections makes the problem formulation approximate real conditions.

However, in order that the solution approximate reality, the following conditions must be assumed (which are not taken into account in the solution just given):

a) Deviations from the Hooke law unavoidably arise during a gradual increase in the load, and the equations such as (13.2) become invalid. Therefore, on a certain level of the loading it becomes necessary to take into account the physical nonlinearity of the system.

b) For large displacements, the complete expression must be used for the curvature of a bent axis, i.e., the geometric nonlinearity must be taken into account (we should note that this is not necessary when studying

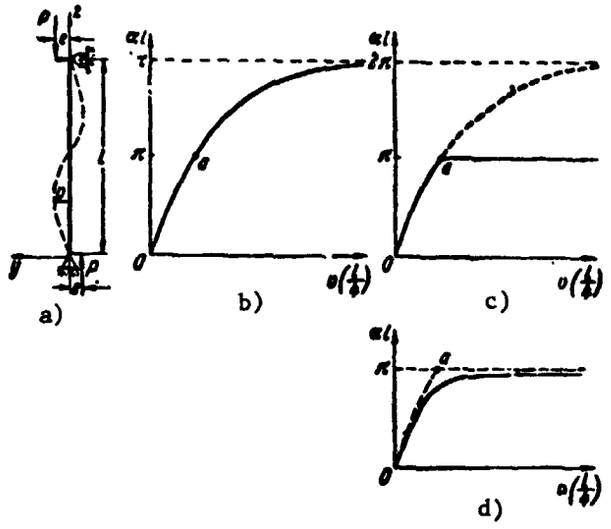

Fig. 13.2. a) Diagram of a rod loaded off center; b) curve of equilibrium states corresponding to equation (13.9); c) curve of equilibrium states reflecting bifurcation of equilibrium forms at the point a; d) curve of equilibrium states of a system with "secondary" imperfections.

stability by means of the differential equation (13.1), where by definition the deflections v(z) are infinitely small).

If we do not take these factors into account (particularly the first one), then a deformation calculation acquires a somewhat arbitrary nature, and cannot pretend to closely approximate real conditions. Thus, if we take into account real nonlinearities of the off-center compression of a hinge-supported rod, then instead of the curve characterizing the connection P — v, shown in Figure 13.1, b, we obtain the curve shown in Figure 13.1, c. In principle, it coincides with the curve in Figure 12.5 of the preceding section, where the deformation calculation was solved with allowance for physical nonlinearity. Therefore, as a rule, a deformation calculation only has meaning in the nonlinear (at least, physically nonlinear) formulation.

However, a deformation calculation has still another characteristic, which /110 is clearly apparent when analyzing the following case.

In the first volume of the book by Burgermeister and Steup "Theory of Elastic Stability" (1957), by way of an example they solved the problem of off-center compression of a rod shown in Figure 13.2, a. In the notation assumed above, the differential equation for the bent rod axis may be written as:

$$\frac{d^2v}{dz^2}+\alpha^2v=\alpha^2e\left(\frac{2z}{l}-1\right). \tag{13.7}$$

The solution of equation (13.7) which is satisfied by the boundary conditions of the problem has the form

$$v=e\left[\cos\alpha z-(1+\cos\alpha l)\frac{\sin\alpha z}{\sin\alpha l}+\frac{2z}{l}-1\right] \tag{13.8}$$

and describes the antisymmetric (with respect to the middle of the span) form /111 of the bent axis. Thus, for example, for $z = 0.25l$, i.e., in a quarter of the span, the deflection is

$$v\left(\frac{l}{4}\right)=\frac{e}{2}\left(\frac{1}{\cos\frac{\alpha l}{4}}-1\right). \tag{13.9}$$

Figure 13.2, b shows a graph corresponding to this relationship.

Naturally, the criticisms given above concerning disregarding the nonlinear effects may be repeated for this solution — but we shall not discuss this at this time. The graph in 13.2, b leads to the unexpected — and suspicious — conclusion that instability occurs only for $\alpha l = 2\pi$, i.e., for the force

$$P=\frac{4\pi^2EJ}{l^2}, \tag{13.10}$$

which is four times greater than the least Euler value. Judging from the graph, when $\alpha l = \pi$, i.e., for the first Euler force, the system under consideration has no dangerous tendencies and the state of equilibrium which is noted on the graph is very ordinary and, from the qualitative viewpoint, differs in no way from other states of equilibrium characterized by other points on the curve.

It is worth mentioning the fact that, due to the action of antisymmetric end couples $\pm$ Pe, the rod appears to be able to escape satisfactorily the danger of stability loss during the first Euler force. How can this be?

To answer this question, we must examine the deformation calculation in greater detail. This method establishes a set of equilibrium states, which correspond to different loading levels. But it does not enable us to determine the stability of these states. Therefore, it may happen that any of these states (any shown on the graph in Figure 13.2, b) may be unstable. For example, we have in mind the possibility that, along with the state of equilibrium, /112 there is a mixed form of equilibrium for the same load(*).

To control the stability of a certain state of equilibrium, we must determine whether there is a function which differs from (13.8), but satisfies the same differential equation (13.7). Let us designate this function by $v(z) + \delta v(z)$, where $\delta v(z)$ — variation of the function $v(z)$. If it is found that, for a given load, there is no function $\delta v(z)$ which identically equals zero, then the form of equilibrium $v(z)$ must be designated as unstable. If $\delta v(z) \equiv 0$, then the function $v(z)$, which uniquely satisfies the differential equation (13.7), describes the stable state of equilibrium. Let us substitute the sume $v + \delta v$ in the differential equation (13.7):

$$\frac{d^2(v+\delta v)}{dz^2}+\alpha^2(v+\delta v)=\alpha^2 e\left(\frac{2z}{l}-1\right). \tag{13.11}$$

If we now subtract (13.7) from equation (13.11), we obtain the following differential equation for the variation δv:

$$\frac{d^2(\delta v)}{dz^2}+\alpha^2(\delta v)=0. \tag{13.12}$$

We should note that the equation obtained completely coincides with equation (13.1), which we would reach by omitting the eccentricities and studying the stability of the rectilinear form of equilibrium of a rod which is loaded in the center using the method of Euler. With a gradual increase in the load (the parameter αl) equation (13.12) has the trivial solution

$$\delta v \equiv 0 \tag{13.13}$$

(*) It may also be assumed that there is dynamic instability, i.e., the system tends to change from the state of equilibrium to oscillatory motion with increasing amplitudes. In this problem it is sufficient to examine the conditions of static instability expressed in the appearance of mixed forms of equilibrium.

only until $\alpha l < \pi$. For $\alpha l = \pi$, a nontrivial solution of the differential equation (13.12) appears, which satisfies the boundary conditions of the problem:

$$\delta v = C \sin \frac{\pi z}{l}. \qquad (13.14)$$

Consequently, as only the level of the load $\alpha l = \pi$ will be reached (for $P = \frac{\pi^2 EJ}{l^2}$), the form of equilibrium (13.8) being studied becomes unstable. /113

Correspondingly, the curve P — v in actuality must be similar to that shown in Figure 13.2, c (nonlinearities are not taken into account !)

Although the solution just presented is outwardly similar to the solution of the Euler problem [see the differential equations (13.1) and (13.12], it must be kept in mind that the stability of the bent form [determined by expression (13.8)] is determined by our solution, and not the stability of the rectilinear form of equilibrium.

This example shows that, by using the deformation calculation and ignoring a study of stability in the direct meaning of the word, we may erroneously estimate the real properties of the system.

If we introduce a "secondary" imperfection into this investigation in the form of a small difference in the eccentricities at the ends of the rod, we then obtain the curve P — v shown in Figure 13.2, d, which is very similar to the curve shown in the preceding Figure 13.2, c.

It is interesting to note that Burgermeister and Steup, obtaining the solution in the form (13.8), could not correctly interpret this result. Assuming that for $\alpha l = \pi$ the rod must necessarily lose instability, when analyzing the stability of solution (13.8), they tried to determine this from the structure of the expression (13.8). It was found by these authors that the second term in the brackets in (13.8) becomes indeterminate when $\alpha l = \pi$, and on this basis they concluded that for $\alpha l = \pi$ stability loss occurs. Burgermeister and Steup did not note that, after expanding the indeterminacy , this term equals

zero, and the solution assumes the form

$$v = e\left(\cos\frac{\pi z}{l} + \frac{2z}{l} - 1\right). \tag{13.15}$$

In particular, for z = 0.25l the deflection equals

$$v\left(\frac{l}{4}\right) = 0{,}207e. \tag{13.16}$$

As we have seen above, this final solution is unstable. However, in order to observe this, it is sufficient to examine the expression (13.8) without reference to the differential equation (13.7). /114

All of the statements made above are valid not only for problems of buckling of rods. Let us recall, for example, the problems solved in § 4. They were all specially formulated so that it would be possible to determine the stability loss in the Euler meaning. However, frequently the same systems have a certain non-ideality, and then the analysis of the systems requires the solution of nonhomogeneous equations.

Let us examine an example with a pipeline (Figure 4.13), and in this case we can see that the method of imperfections reveals its own weakness. Let us assume that the pipeline axis in the initial state is S-shaped:

$$y_0 = f\sin\frac{2\pi z}{l}. \tag{13.7}$$

If we use y = y(z) to designate the deflection arising during the pipeline deformation, then the bent axis may be described by the sum $y_0 + y$. Correspondingly, the strength of the inertial rigidity forces may be determined by the expression

$$-\frac{qv^2}{g}\frac{d^2(y+y_0)}{dz^2} = \frac{qv^2}{g}f\frac{4\pi^2}{l^2}\sin\frac{2\pi z}{l} - \frac{qv^2}{g}\frac{d^2y}{dz^2} \tag{13.8}$$

and, instead of the homogeneous differential equation (4.43), we obtain the nonhomogeneous equation

$$\frac{d^4y}{dz^4} + s^2\frac{d^2y}{dz^2} = f\left(\frac{2\pi s}{l}\right)^2\sin\frac{2\pi z}{l}. \tag{13.19}$$

We should recall that the parameter s is determined by formula (4.44), and is proportional to the liquid flow rate. The following solution satisfies the boundary conditions being considered and the differential equation (13.19)

$$y = \frac{f}{\left(\frac{2\pi}{sl}\right)^2 - 1} \sin \frac{2\pi z}{l}. \qquad (13.20)$$

We may now conclude that the critical state occurs when

$$sl = 2\pi, \qquad (13.21)$$

i.e., when the liquid flow rate is two times greater than was found in § 4 [see formula (4.49)].

Naturally, it is impossible to represent the fact that the preliminary /115 (and arbitrarily small) deflection of the pipeline be two times greater than its stability margin. The solution itself (13.20) when $sl = \pi$ becomes unstable, and we may establish this by studying the variations of the differential equation.

For this, let us assume that the differential equation (13.19) is satisfied not only by this solution (13.20), but also by the similar solution $y(z) + \delta y(z)$. Substituting this sum in (13.19) and subtracting (13.19) from the result obtained, we have

$$\frac{d^4(\delta y)}{dz^4} + s^2 \frac{d^2(\delta y)}{dz^2} = 0. \qquad (13.22)$$

According to the statements made in § 4, it follows that for $sl = \pi$ there is a non-zero solution for the function $\delta y(z)$. This points to the instability of the solution (13.20) for $sl = \pi$.

Thus, using the deformation calculations (by the method of imperfections), we cannot observe certain critical states.

We should recall this characteristic of deformation calculations (the present section must serve as such a reminder), but at the same time it would be incorrect to overestimate its importance. Deformation calculations, as a rule, provide completely unreliable results (the examples given above are naturally exception), particularly if the real non-linearities and imperfections of the system are properly accounted for.

For the work of H. Ziegler, see the collection "Problems of Mechanics",

No. II (Foreign Literature Press, Moscow, 1959, p. 119). Regarding the error made in the book by Burgermeister and Steup "Stabilitätstheorie" (Stability Theory) (Vol. 1, Berlin, 1957, p. 583), see A.A. Pikovskiy "Statika sterzhevykh sistem so szhatymi elementami" (Statics of Rod Systems with Compressed Elements) (Fizmatgiz, Moscow, 1961, pp. 361 - 362). See also the report by V.V. Bolotin "The Stability Concept in Structural Mechanics" (Collection: "Problemy ustoychivosti v stroitel'noy mekhanike" (Problems of Stability in Structural Mechanics), (Stroyizdat, Moscow, 1965, pp. 23 - 24).

§ 14. Two Discussions (Solutions of R. Lorenz and V. Z. Vlasov)

In this section, we shall discuss the formulation of problems on the stability of two different objects — A cylindrical casing uniformly compressed along the axis (under the assumption of small axisymmetric displacements) and a thin-walled rod with an open profile, which is subjected to off-center compressions (Figure 14.1). Both problems were solved long ago (the first in 1908, and the second in 1940). Subsequently, they gave rise to controversies which have still not been resolved up to the present. As we shall see below, in the last analysis imperfections are organically inherent in both systems, and a "pure" Euler formulation of the problem, based on the assumption that there is no imperfection, is simply impossible. Nevertheless, the solutions of R. Lorenz and V.Z. Vlasov (the first researchers on these problems) ignored the imperfection and regarded the system as an Euler system. This is a controversial element in both solutions. /116

Axisymmetric swelling of a circular, cylindrical casing, uniformly compressed along the generatrices. Historically, it has been shown that in the first solution which R. Lorenz gave, this problem was simplified. In particular, it was assumed that all generatrices are bent in the same manner during stability loss. With this arbitrary (but not absurd) assumption, Lorenz excluded from the examination other variations of development of deformation in the casing. Only much later was the enormous influence of

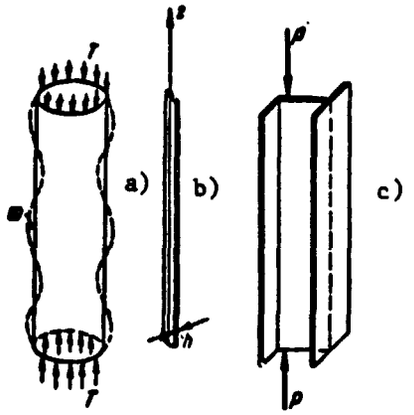

Fig. 14.1. a) Diagram of cylindrical, circular casing; b) elementary beam strip; c) thin-walled rod of an open profile, which is subjected to off-center compression.

non-axisymmetric forms of stability loss revealed. Such an assumption — just like every a priori statement regarding the shape of a deformed surface — introduced an error of a definite sign, which exaggerated the critical value of the load. However, we are interested in another /117 aspect of the Lorenz solution, which is essentially not connected with the assumption just made. First of all, let us recall the basic elements of the solution.

Let us examine an elementary beam strip separated by two mixed sections passing through the axis of the casing (Figure 14.1, b). Due to the assumed axial symmetry of the deformed state (Figure 14.1, a), the bending of all such beam strips is identical, and each one represents a beam lying on a solid elastic base. For any given beam strip, the role of the elastic base is played by the remaining part of the casing.

Let us set: z — coordinate of the section measured along the casing axis, $w = w(z)$ — deflection of points on the middle surface, T — compressive force pertaining to a unit of length of the transverse section, $D = Eh^3$: $12(1-\mu^2)$ — cylindrical rigidity, h — wall thickness, μ — Poisson coefficient, $k = Eh:R^2$, R — radius of the transverse section of the middle surface. With this notation, the differential equation of arbitrary bending of a beam strip may be written in the form

$$\frac{d^4w}{dz^4} + \frac{T}{D}\frac{d^2w}{dz^2} + \frac{k}{D}w = 0. \qquad (14.1)$$

The boundary conditions which depend on the form of the support devices at the ends of the casing must be related to this differential equation. Lorenz studied the case of hinged support of the end sections and assumed

$$w=0, \qquad \frac{d^2w}{dz^2}=0 \text{ for } z=0 \text{ and } z=l. \tag{14.2}$$

In this case, the solution of the differential equation (14.1) has the form

$$w=C\sin\frac{n\pi z}{l}. \tag{14.3}$$

Here n is an arbitrary whole number, equal to the number of half-waves, into which the casing generatrices are divided in the case of stability loss. Substituting (14.3) into (14.1), we obtain the equation

$$\left(\frac{n\pi}{l}\right)^4-\frac{T}{D}\left(\frac{n\pi}{l}\right)^2+\frac{k}{D}=0, \tag{14.4}$$

from which we have the following expression for the critical compressive force /118

$$T=D\left(\frac{n\pi}{l}\right)^2+k\left(\frac{l}{n\pi}\right)^2. \tag{14.5}$$

As may be seen, the result depends on the number n. The latter may be found, based on the condition that the smallest value of the load is of practical importance, which may be found from the formula (14.5). Assuming that $n \gg 1$ (this is valid for sufficiently long casings), we may write the equation for the minimum of T in the form

$$\frac{dT}{dn}=0. \tag{14.6}$$

This yields

$$n=\frac{l\sqrt[4]{12(1-\mu^2)}}{\pi\sqrt{Rh}}, \tag{14.7}$$

and, instead of (14.5), we obtain

$$T_{crit}=\frac{Eh}{R\sqrt{3(1-\mu^2)}}. \tag{14.8}$$

This yields the expression (7.4), which has already been discussed (in another connection of course) in § 7. Immediately after Lorenz, S.P. Timoshenko reached the same result (14.8), using the energy method. The expression (14.3) was at the basis of the solution.

In 1926 L. Foppl turned his attention to the particular role which is played by the limiting condition $w = 0$ in the problem under consideration.

Due to the Poisson effect, a tendency toward transverse expansion of the casing arises from the very beginning of the load. Therefore, if the ends

are fastened in the manner assumed by Lorenz, i.e., $w = 0$ when $z = 0$ and $z = l$, then even for small loads the middle surface must assume a bell-shaped form. Consequently, the bending of the generatrices constantly accompanies the longitudinal loading, and may serve as an indicator of stability loss. Was the Euler formulation, which was used by Lorenz, valid for this problem?

This problem was clarified by J. Geckeler in 1928. His line of reasoning is as follows. For an isolated hinge-supported beam strip on an elastic base, /119 the Lorenz solution is valid, but the equation for the problem must be written somewhat differently for a casing. The total displacement w must be represented in form of the sum of two components

$$w = w_0 + w_1, \tag{14.9}$$

where

$$w_0 = \frac{\mu RT}{Eh} \tag{14.10}$$

is a displacement which is identical for all points on the middle surface and is caused by axial compression of the casing, and $w_1(z)$ — displacement arising due to the bending of the generatrices and satisfying the differential equation

$$\frac{d^4w_1}{dz^4} + \frac{T}{D}\frac{d^2w_1}{dz^2} + \frac{k}{D}w_1 = 0. \tag{14.11}$$

If the boundary conditions at the ends of the casing for the function w have the form (14.2), then for the function w_1 the boundary conditions must be written in the form

$$w_1 = -\frac{\mu RT}{Eh}, \quad \frac{d^2w_1}{dz^2} = 0 \text{ for } z = 0 \text{ and } z = l. \tag{14.12}$$

Thus, the problem reduces to integrating the homogeneous differential equation (14.11), but for nonhomogeneous boundary conditions (14.12).

There is also another equivalent variation for writing the equations of the problem. Let us substitute the following in (14.11)

$$w_1 = w - w_0, \tag{14.13}$$

as follows from (14.9). We then obtain a nonhomogeneous differential equation

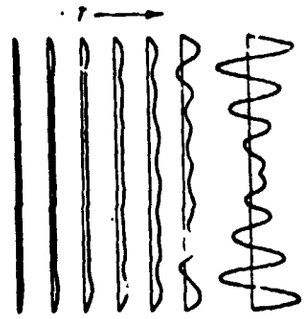

Fig. 14.2. Successive development of bending of generatrix with an increase in the compressive load.

$$\frac{d^4w}{dz^4} + \frac{T}{D}\frac{d^2w}{dz^2} + \frac{k}{D}w = \frac{\mu T}{RD} \qquad (14.14)$$

for homogeneous boundary conditions (14.2).

Consequently, with a correct formulation the problem is nonhomogeneous as a whole. Using any variant — (14.11), (14.12) or (14.14), (14.2) — we may determine how the casing buckling develops gradually with an increase in the load. Figure 14.2 shows consecutively /120 developing forms of bending of the generatrices with different increasing values of the compressive force.

As may be seen, for small loads the bending is primarily localized close to the ends of the casing, and is local in nature. With an increase in the load, the bending gradually encompasses a much larger region, and attenuation of the edge effect becomes weaker. As is shown, with a load determined by the Lorenz-Timoshenko formula, the displacements become infinitely large. Therefore, we may attribute a specific formal value to formula (14.8) — it determines the critical load in the sense of the imperfection method (see the beginning of § 13).

Thus, for a correct analysis the Euler formulation of the problem is impossible, and we may speak about a deformation calculation, i.e., a study of the gradually increasing bending. However, with this formulation we must take into account nonlinear phenomena. As the bending develops, these phenomena will become much more apparent, and long before the compressive force reaches the value (14.8). Thus, plastic deformations unavoidably arise (primarily at the ends of the casing, where the bending is the greatest), after which it is impossible to use purely elastic relationships in general. For this reason, the Lorenz-Timoshenko formula cannot correctly provide an answer to the problem of the critical force used in the sense of the imperfection method. The only value which can be given to this formula is a

rather rough upper estimate of the critical load.

For other boundary conditions, the factors may change sharply, and the Euler formulation of the problem may become appropriate. For example, let us assume there are no bending moments at the ends of the casing, or constraints preventing radial displacements of points on the middle surface. Then the boundary conditions must be written in the form /121

$$\frac{d^2w}{dz^2}=0,\quad \frac{d^2w_1}{dz^2}+\frac{T}{D}\frac{dw}{dz}=0 \quad \text{for} \quad z=0 \quad \text{and} \quad z=l. \tag{14.15}$$

According to (14.9), the same boundary conditions pertain to the function w_1

$$\frac{d^2w_1}{dz^2}=0,\quad \frac{d^2w_1}{dz^2}+\frac{T}{D}\frac{dw_1}{dz}=0 \quad \text{for} \quad z=0 \quad \text{and} \quad z=l. \tag{14.16}$$

Thus, the problem reduces to integrating the homogeneous differential equation (14.11) for homogeneous boundary conditions (14.16). We shall not discuss the solution of this Euler problem (it was studied by N.A. Kil'chevskiy in 1942, and then by him together with S.N. Nikulinskaya in 1965).

Stability losses of a thin-walled rod which is subjected to off-center compression. In 1929 H. Wagner first studied the torsional form of stability loss of a thin-walled rod with an open profile subjected to off-center compression. Wagner assumed that the transition to the twisted form of equilibrium occurs in the form of rotations of the sections around the bending centers. It was later noted that the assumption of Wagner was not valid, and as a rule did not correspond to reality. In 1937 Lundquist and Fligg determined the coordinates of the section rotation centers from the condition of a minimum of the critical compressive force.

There is a particular case for which the Wagner theory is valid: if the center of bending and the center of gravity of the section coincide (for example, in cases of an I-shaped or Z-shaped section), then the center of rotation is located at the same point for a torsional form of stability loss. We shall dwell on this particular case for a moment, which has one interesting feature. In this case the critical force is determined by the

expression (we are assuming the ends are hinged)

$$P_* = \frac{1}{r_p^2}\left(\frac{\pi^2 EJ_\omega}{l^2} + GJ_k\right). \tag{14.17}$$

Here l is the rod length, EJ_ω — sectorial rigidity, GJ_k — rigidity of free torsion, r_p — polar radius of inertia of the cross section. In order to calculate this value, it is necessary that it be less than the critical force, corresponding to the bending form of stability loss /122

$$P_e = \frac{\pi^2 EJ_{min}}{l^2} \tag{14.18}$$

(EJ_{min} — least rigidity during bending). If the cross section has a zero sectorial rigidity (for example, a cross-shaped section, a section in the form of an angle, etc.), then formula (14.18) assumes the form

$$P_* = \frac{GJ_k}{r_p^2}. \tag{14.19}$$

We thus reach the unexpected conclusion that in these cases the critical force corresponding to the torsional form of stability loss does not depend on the rod length.

For very long rods, the critical force is determined by the formula (14.18). With a decrease in the length, the critical force (14.18), which determines the bending form of stability loss, will gradually increase, and finally will be comparable with the critical force (14.19). Such a rod has equal stability with respect to bending and with respect to twisting. Its length is determined from the equality of expressions (14.18) and (14.19):

$$l_* = \pi r_p \sqrt{\frac{EJ_{min}}{GJ_k}}. \tag{14.20}$$

For all rods having the length $l < l_*$ one and the same value of (14.19) is the calculated value, and decreasing the length of the rod further, we find no increase in the critical value of the compressive force. We shall not go into the reasons for this conclusion which seems to be physically invalid: they fall outside of the framework of this section. We shall only note that in view of the similarity of the technical theory of thin-walled rods and, in particular, the hypothesis of a nondeformable contour, it is understandable

that the shorter the rod, the less tenable is this hypothesis(*). We shall now turn to the basic theme.

V.Z. Vlasov(**) developed the general theory of the stability of thin-walled rods with an open profile. His results were published in 1940. Let us discuss the problem which he solved regarding a thin-walled rod subjected to off-center compression, and let us set: z — coordinate of the section, measured along the axis of the rod, x, y — coordinates of the section points in a system of the main central axes of inertia, a_x, a_y — coordinates of the bending center, $\xi(z)$ and $\eta(z)$ — displacements of the bending center, $\theta(z)$ — section angle of rotation /123

$$\left.\begin{aligned}\beta_x &= \frac{1}{2J_y}\left(\int_{(F)} x^3\,dF + \int_{(F)} xy^2\,dF\right) - a_x,\\ \beta_y &= \frac{1}{2J_x}\left(\int_{(F)} y^3\,dF + \int_{(F)} x^2 y\,dF\right) - a_y\end{aligned}\right\} \tag{14.21}$$

— special geometric characteristics of the section, N, M_x and M_y — longitudinal force and bending moments in the section. Then the system of differential equations which determine the bending and torsion of the rod assume the form

$$\left.\begin{aligned}&EJ_y\xi'' + N\xi + (a_yN + M_x)\theta = M_y,\\ &EJ_x\eta'' + N\eta - (a_xN - M_y)\theta = -M_x,\\ &(a_yN + M_x)\xi - (a_xN - M_y)\eta + EJ_\omega\theta'' +\\ &\qquad + (r^2N + 2\beta_xM_y - 2\beta_yM_x - GJ_k)\theta = 0\end{aligned}\right\} \tag{14.22}$$

As may be seen, these equations are nonhomogeneous, and in the general case at the same time not only compression and bending of the rod occurs, but also its twisting occurs in the case of off-center compression. We shall note

(*) This feature was pointed out in the second volume of the book by S.P. Timoshenko "Soprotivleniye materialov" (Strength of Materials), Izdatel'stvo "Nauka", Moscow, 1966, p. 226.

(**) Vasiliy Zakharovich Vlasov (1906 - 1958) — from 1936 until the war Professor of the Moscow Engineering-Construction Institute. From 1953 — Associate Member of the Academy of Sciences of the USSR. Author of many studies in the field of the theory of thin-walled structures and shells.

two exceptions to this general rule.

a) Compressive force is applied in the bending centers of the end sections. In this case (Figure 14.3, a)

$$M_x = -a_y P, \quad M_y = a_x P \tag{14.23}$$

and the differential equations (14.22) assume the form

$$\left.\begin{aligned} EJ_y\xi'' + P\xi &= a_x P, \\ EJ_x\eta'' + P\eta &= a_y P, \\ EJ_\omega\theta'' + (r^2 P + 2\beta_x a_x P + 2\beta_y a_y P - GJ_k)\theta &= 0. \end{aligned}\right\} \tag{14.24}$$

The structure of these equations is such that each of them includes only one /124 of the functions ξ, η and θ. The first two equations are thus nonhomogeneous, and describe the longitudinal-transverse bending of a rod in the two main planes. The third equation determines the rod twisting. At the same time it is satisfied by the trivial solution $\theta = 0$. However, for specific — critical — values of the force $P = P_{crit}$ the equation has a solution which also differs from zero and describes twisting of the rod during stability loss. The problem of determining P_{crit} is apparently the Euler problem.

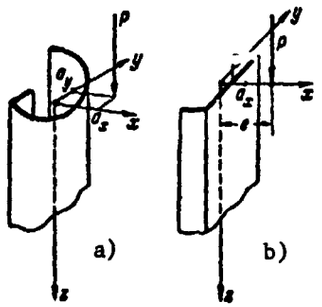

Fig. 14.3. a) Compressive force applied at the center of bending of an end cross section; b) compressive force applied at a point on the symmetry axis of the end cross section.

b) The section has an axis of symmetry (for example, the x axis — see Figure 14.3, b), and the compressive forces lie in the plane of symmetry xz. Using e to designate the eccentricity of the compressive force, we have

$$a_y = \beta_y = 0, \quad M_x = 0, \quad M_y = Pe, \tag{14.25}$$

and the differential equations (14.22) may be written as

$$\left.\begin{aligned} EJ_y\xi'' + P\xi &= Pe, \\ EJ_x\eta'' + P\eta - P(a_x - e)\theta &= 0, \\ -P(a_x - e)\eta + EJ_\omega\theta'' + (Pr^2 + & \\ + 2P\beta_x e - GJ_k)\theta &= 0. \end{aligned}\right\} \tag{14.26}$$

In this case, the main form of equilibrium represents bending in the plane of symmetry yz, and is determined by the first (nonhomogeneous) differential equation (14.26). The last two equations are homogeneous and are satisfied by the trivial solution

$$\eta = 0, \quad \theta = 0. \tag{14.27}$$

For certain values of the compressive force P these equations can have nonzero solutions which describe bending in the yz plane and twisting. Determining the condition for the development of the critical state is also the Euler problem. /125

There are disagreements in the literature on the characteristics of the particular cases. The general case is controversial, which is described by the differential equations (14.22) forming a nonhomogeneous system. Due to the nonhomogeneity of the problem, the Euler formulation is not used, since a definite form of bending and twisting of a rod corresponds to each level of loading (up to a certain limit). If we trace the development of rod deformation with a gradual increase in the load, it is found that at a certain loading level displacements ξ, η and θ formally become infinitely large. This corresponds to stability loss in the sense of the imperfection method.

If we are not interested in the process of a gradual development in the deflections ξ and η and the angles of twisting θ, but concentrate all of our attention only on determining the critical load, then it is sufficient to examine a homogeneous system corresponding to the nonhomogeneous system (14.22)

$$\left.\begin{aligned} &EJ_y\xi'' + N\xi + (a_yN + M_x)\theta = 0,\\ &EJ_x\eta'' + N\eta - (a_xN - M_y)\theta = 0,\\ &(a_yN + M_x)\xi - (a_xN - M_y)\eta + EJ_\omega\theta'' +\\ &\quad + (r^2N + 2\beta_xM_y - 2\beta_yM_x - GJ_k)\theta = 0, \end{aligned}\right\} \tag{14.28}$$

and to find the condition for the development of nontrivial solutions. V.Z. Vlasov used this method.

If the reader returns to the beginning of § 13 in this book, he will note that the critical force may be determined in the same way (i.e., the

force producing unlimited buckling) for a system with eccentricity (Figure 13.1). To do this, it is necessary to omit the right-hand side of the differential equation (13.2), and to find the condition for which the nontrivial solution of the corresponding homogeneous equation becomes possible. Thus, the level of the asymptote in Figure 13.1, b is determined. However, as we saw in § 13, the original differential equations are based on the assumption of infinite linearity of the problem. Since nonlinear effects become more pronounced gradually with an increase in the load, the actual curve P-v is as is shown in Figure 13.1, c.

These considerations are general in nature, and pertain to an equal degree /126 to the solution of any nonhomogeneous problem, in particular, problems of off-center compression of a thin-walled rod in the general case. If the loading process of such a rod were infinitely linear, then it would be impossible to raise any objections to the method of V.Z. Vlasov. Only a clearer understanding would be required of the fact that the appearance of the Euler solution for a homogeneous problem in actuality means determining the load maximum in the corresponding nonhomogeneous problem.

However, with a gradual increase in the load (and corresponding deformations of bending and twisting), an unavoidable state of the rod would occur, in which it would be impossible to ignore the nonlinearity (primarily of a physical nature). Therefore, the real critical load is less than is obtained from an analysis of the homogeneous system (14.28). In essence, this is one of the criticisms directed against the solution of V.Z. Vlasov.

Another critical comment is related to the fact that in real structures the problem of strength is a more pressing problem than that of stability: due to the right-hand sides of the system (14.22) the stresses become impermissibly large long before the load approximates the critical value. Therefore, the analysis of a homogeneous system (14.28) hides the true problem arising in the calculation of thin-walled rods.

The first study of Lorenz was published in the journal "Zeitschrift des Vereines Deutscher Ingenieure", Vol. 52, 1908, p. 1706. For the article by S.P. Timoshenko, see "Izvestiya elektrotekhnicheskogo instituta", No. II, 1914. The work of L. Foppl "Achsensymmetrisches Ausknicken zylindrischer Schalen" (Axisymmetric Buckling of Cylindrical Shells) was published in the journal "Münchener Berichte," 1926. For the article by J. Geckeler see "Zeitschrift für angewandte Mathematik und Mechanik," Vol. 8, 1928, p. 341 (see also the translation of his book "Statika uprugogo tela" (Statics of an Elastic Body), GTTI, Moscow, 1934, pp. 271 - 276). We borrowed Figure 14.2 from the book by W. Flugge "Statika i dinamika obolochek" (Statics and Dynamics of Shells) (Gosstroyizdat, Moscow, 1961).

The book by H. Wagner was published in the anniversary collection "Festschrift 25-Jahre Technische Hochschule Danzig" (Anniversary of the 25th Year of the Danzig Technical Academy), 1929. For the article by Lundquist and Fligg see N.A.C.A. Tech. Rep., 1937, p. 582. The article by N.A. Kil'chevskiy and S.N. Nikulinskiy was published in the journal "Prikladnaya mekhanika" AN USSR, No. 11, 1965. The book by V.Z. Vlasov "Tonkostennyye uprugiye sterzhni" (Thin-Walled Elastic Rods) was published twice: first edition — Stoyizdat, Moscow, 1940; second edition — Fizmatgiz, Moscow, 1959. For critical notes on the solution of V.Z. Vlasov for the problem of stability of /127
a thin-walled rod subjected to off-center compression, see: "Deformation Calculation and Stability of Thin-Walled Rods of an Open Profile" (Trudy Novocherkasskogo politekhnicheskogo instituta) (Transactions of the Novocherkassk Polytechnic Institute), Vol. 79 - 83, 1958; B.M. Broude "Linearization of Stability Equations for the Equilibrium of a Rod Subjected to Off-Center Compression" [Collection: "Issledovaniya po teorii sooruzheniy" (Studies on the Theory of Structures), No. VIII, 1959]; A.A. Pikovskiy "Statika sterzhnevykh sistem so szhatymi elementami" (Statics of Rod Systems with Compression Elements) (Fizmatgiz, Moscow, 1961, Chap. V).

§ 15. Stability Losses of a Rod Under Tension

We would like to preface the main portion of this section with a somewhat detailed introduction, devoted to large deformations.

A linear deformation may be represented in the form

$$\varepsilon = \frac{\Delta l}{l_0} \tag{15.1}$$

(l_0 — initial length of the segment, Δl — its absolute extension) and is one of the basic concepts of the strength of materials and calssical (linear) theory of elasticity. Expression (15.1) may always be used for small values of ε. However, recently, particularly in connection with the appearance of new synthetic materials which can withstand very great extensions without being destroyed, several different methods of determining large deformations have been proposed.

The quantity ε determined by expression (15.1) may be used as a measure of deformation in those cases when the extensions are commensurate with the initial length l_0. However, such a determination will have certain drawbacks. Let us assume the loading is done in steps, and l_{k-1} and l_k are the lengths of the segment at the beginning and end of the k^{th} step. An increase in the length by one step of the process equals $l_k - l_{k-1}$, and the increase of the deformation according to expression (15.1) is

$$\Delta\varepsilon_k = \frac{l_k - l_{k-1}}{l_{k-1}}. \tag{15.2}$$

It is natural to assume the sum of the increases $\Delta\varepsilon_k$, which are produced at each step of the entire process, represents the complete deformation. However, this sum

$$\varepsilon = \sum \Delta\varepsilon_k = \sum \frac{l_k - l_{k-1}}{l_{k-1}} \tag{15.3}$$

does not coincide with the quantity /128

$$\varepsilon = \frac{l - l_0}{l_0}, \tag{15.4}$$

which is determined all at once for the entire loading process. Thus, the

deformation determined by (15.1) does not enable us to use the summation operation.

Another method of determining a large deformation is free of this drawback.

Let us study the process of a monotonic increase in the segment length from the value l_0 up to a much larger value l. Let us assume that at the current moment the segment length is z, and $l_0 < z < l$. There is also an infinitely small extension in an infinitely small interval of the process under consideration, and we shall designate this extension by dz. The increase with respect to the extension may naturally be determined by equation $\frac{dz}{z}$, i.e., we set $d\varepsilon = \frac{dz}{z}$. The total relative extension, which accumulates throughout the entire process, may be logically determined by integration:

$$\varepsilon = \int_{l_0}^{l} \frac{dz}{z} = \ln \frac{l}{l_0} = \ln \left(1 + \frac{\Delta l}{l_0}\right). \tag{15.5}$$

This total result differs from (15.1), and the difference is more significant, the greater the ratio $\frac{\Delta l}{l_0}$.

Naturally, for small ratios $\frac{\Delta l}{l_0}$ the result (15.5) changes into (15.1), since

$$\ln \left(1 + \frac{\Delta l}{l_0}\right) = \frac{\Delta l}{l_0} - \frac{1}{2}\left(\frac{\Delta l}{l_0}\right)^2 + \cdots,$$

and both estimates coincide within an accuracy of the second order of smallness.

Thus, the <u>logarithmic deformation</u> (15.5) may be used in the summation operation. However, this is not the only advantage of this method. It may be found that the know expression for the volumetric deformation in the form /129 $\varepsilon_1 + \varepsilon_2 + \varepsilon_3$ remains in force for large deformations, if the logarithmic method is used.

The representation of deformation in the form (15.1) was proposed by

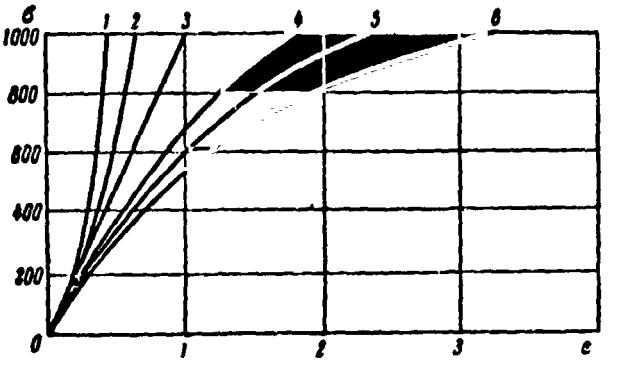

Fig. 15.1. Dependence of the stress σ on deformation ε, obtained from an analysis of identical experimental results by different methods: 1 — Almansi; 2 — Koerber and Swainger; 3 — Hencky; 4 — Cauchy; 5 — Kuhn; 6 — Green.

Cauchy(*), and in the form (15.5) — by Hencky. Along with these expressions, there are other expressions for determining the deformation, which are given by different authors.

There is the assumption of Almansi:

$$\varepsilon = \frac{1}{2}\left(1 - \frac{1}{\lambda^2}\right); \tag{15.6}$$

the assumption of Koerber-Swainger:

$$\varepsilon = 1 - \frac{1}{\lambda}; \tag{15.7}$$

the assumption of Kuhn:

$$\varepsilon = \frac{1}{3}\left(\lambda^3 - \frac{1}{\lambda}\right), \tag{15.8}$$

the assumption of Green:

$$\varepsilon = \frac{1}{2}(\lambda^2 - 1). \tag{15.9}$$

(*) Augustine Louis Cauchy (1789 - 1857) — French Mathematician, Member of the Paris Academy of Sciences from 1816. One of the founders of the theory of elasticity.

In these expressions

$$\lambda = \frac{l}{l_0} = \frac{l_0 + \Delta l}{l_0} \tag{15.10}$$

is a quantity which is called the multiplicity (or degree) of extension. If we use this notation, the Cauchy deformation may be written in the form

$$\varepsilon = \lambda - 1, \tag{15.11}$$

and the logarithmic deformation (15.5) — in the form

$$\varepsilon = \ln \lambda. \tag{15.12}$$

The magnitude of the difference between the scales of ε may be determined from the following hypothetical example. Let us assume that the following /130 pairs of experimental data were recorded when checking a rod for extension:

Stress, kg/cm^2(*)	0	200	400	600	800	1000
Multiplicity	1	1.22	1.49	1.82	2.23	2.72

Let us assume that we must obtain the dependence between the stress σ and the deformation ε. Here the question arises of recalculating the experimental values of λ for the deformation ε. It is clear that the results are not identical and will depend on the deformation method used.

Figure 15.1 shows curves obtained when using the formulas in expressions (15.6) — (15.9), (15.11), (15.12). As may be seen, the curves differ greatly at the first degree of loading, and then diverge more and more. If we use the Cauchy, Green, and Kuhn relationships, then the material under consideration will be called soft, since the derivative $\frac{d\sigma}{d\varepsilon}$ gradually decreases with an increase in the deformation ε. Using the formulas of Almansi and Koerber- /131 Swainger, we must conclude that the material being studied is rigid. If we use the Hencky method, it is found that deformation of the material precisely obeys the Hooke law. Other sets of experimental data lead to different curves, which also greatly differ from each other.

(*) Calculated with allowance for decrease in rod transverse cross section.

Thus, the concept of the physical linearity or nonlinearity of the material is not completely definite, but depends on the selection of the magnitude of ε (naturally, nonlinearity or linearity of a mechanical system is a completely objective concept, since it is related to the behavior of the load-displacement curve).

It is not surprising that there are several deformation magnitudes which do not coincide. The concept of the deformation magnitude pertains to the category of "design values", and therefore is arbitrary to a certain extent. The basis of any deformation magnitude may be regarded as artificial or not fully logical (as, for example, the Cauchy method), but all the variations given above are inter-related by unique relationships, and they all may serve as the measure of deformation. For this reason, there is no basis for assigning the name "real" to any deformation measure(*). In essence, each of the deformation measures gives only its particular scale: Reiner correctly indicated that the deformation measure may be assumed to be any dimensionless function of λ, if for $\lambda \to 1$ it degenerates into the deformation measure of Cauchy (15.11). Of course this requirement is met by schemes other than those presented here.

Let us now turn to our basic subject — stability loss of a rod under tension.

An arbitrarily loaded rod may lose stability not only in the case of a compressive load. Under certain conditions, an unexpected (but only on first glance) stability loss of an ideally elastic rod is possible in the case of tension.

Let us represent the process of monotonically loading a rod with a tensile stress (Figure 15.2), and we shall assume that the force increases so slowly that we can disregard the inertial effects. Let also assume that /132

(*) Sometimes the most frequently used logarithmic measure of deformation, proposed by Hencky, is given this name.

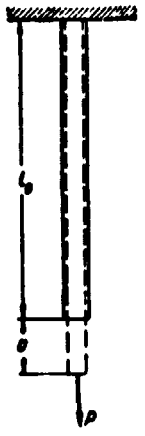

Fig. 15.2. Stretching of an ideally elastic rod.

the rod material is infinitely strong and obeys the Hooke law:

$$\sigma = E\varepsilon, \tag{15.13}$$

where E is the modulus of elasticity. We shall not limit the examination to small deformations, and therefore we shall use σ to designate the true stress

$$\sigma = \frac{P}{F} \tag{15.14}$$

(P — load, F — true area of the transverse section, differing due to transverse deformation from the initial area of the section F_0), and ε — the logarithmic deformation.

In order to determine the true area of the transverse section, we shall use the method corresponding to the assumptions of Hencky. The square element of the section in an infinitely small interval of the deformation process changes its size a so that the relative transverse deformation is

$$\frac{da}{a} = -\mu\, d\varepsilon = -\mu \frac{dl}{l}, \tag{15.15}$$

where μ is the Poisson coefficient which is invariable and equals 0.5.

Integrating the left-hand side of equation (15.5) in the limits from a_0 (initial size) to a, and the right-hand side from l_0 to l, we obtain

$$\ln \frac{a}{a_0} = -0{,}5 \ln \frac{l}{l_0}, \tag{15.16}$$

i.e.,

$$\frac{a}{a_0} = \sqrt{\frac{l_0}{l}}. \tag{15.17}$$

It is apparent that for any form of the section the ratio of the area F to the initial area F_0 equals the square of the ratio of the size a to the initial size a_0:

$$\frac{F}{F_0} = \left(\frac{a}{a_0}\right)^2 = \frac{l_0}{l}. \tag{15.18}$$

Finally, we have the following connection between the section area and the length of the rod l: /133

$$F = F_0 \frac{l_0}{l}. \tag{15.19}$$

This relationship expresses the invariability of the rod volume throughout the entire deformation process.

The formulas (15.14), (15.15) and (15.19) are the initial formulas. Using them, we can now find the relationship which we need between the complete extension of the rod

$$\Delta l = l - l_0 \tag{15.20}$$

and the load.

Let us examine an infinitely small interval of the loading process, during which the force P increases by the quantity dP, and the stress — by the quantity dσ. We may find the increase dσ from (15.14):

$$d\sigma = \frac{F\,dP - P\,dF}{F^2}. \tag{15.21}$$

It may be stated that the right-hand side expresses the stress increase due to the load increase, and the second term — the change in the section area. According to (15.19), we have

$$dF = -\frac{F_0 l_0}{l^2}\,dl. \tag{15.22}$$

Therefore, expression (15.21) assumes the form

$$d\sigma = \frac{dP + \frac{P}{l}\,dl}{F_0 \frac{l_0}{l}}. \tag{15.23}$$

On the other hand, from (15.13) we obtain the increase in the stress dσ in the form

$$d\sigma = E\,d\varepsilon = E\frac{dl}{l}. \tag{15.24}$$

The basic differential equation ot the problem follows from expressions (15.23) and (15.24)

$$\frac{dP}{dl} + \frac{P}{l} - \frac{EF_0 l_0}{l^2} = 0. \tag{15.25}$$

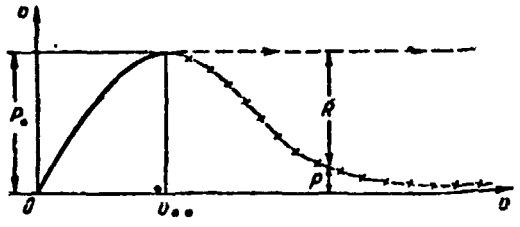

Fig. 15.3. Curve for the equilibrium states of an elongated rod. The points on the ascending branch are stable states; points on the descending branch are unstable states.

The solution of this equation which satisfies the initial condition /134

$$l=l_0 \quad \text{for} \quad P=0,$$

has the form

$$P=\frac{EF_0 l_0}{l}\ln\frac{l}{l_0}. \tag{15.26}$$

Let us transform this expression so as to establish the dependence of the force P on the displacement of the rod end

$$v=l-l_0. \tag{15.27}$$

Then instead of (15.26) we obtain

$$P=\frac{EF_0}{1+\frac{v}{l_0}}\ln\left(1+\frac{v}{l_0}\right). \tag{15.28}$$

Figure 15.3 shows a curve describing the dependence (15.28). As may be seen it corresponds to the graph in Figure 0.4.

If we assign the monotonic increase in the force P, for example, by consecutively increasing the number of tensile loads, then states of equilibrium are only possible up to the value of the force P_*. For larger values of the force P, equilibrium becomes impossible. In practice, this means that when $P = P_*$ the rod length increases infinitely, as is shown by the dashed line in Figure 15.3 (the points on this line correspond to non-equilibrium states). The descending branch of the curve cannot be realized in general with this method of loading.

The value of the force P_* at which the critical state occurs may be obtained from the condition $\frac{dP}{dv} = 0$ in the form

$$P_*=\frac{EF_0}{e}; \tag{15.29}$$

The following extension corresponds to it

$$v_*=l_0(e-1)\approx 1{,}72l_0. \tag{15.30}$$

at which, when it is reached, the displacements increase infinitely. The force P_* is naturally called the critical force, and the value of v_* is the critical extension.

It may be readily shown what the motion will be, if, for example, the rod axis is vertical, its upper end is fixed, and a load with the weight P_* is attached to the lower end. During the motion, when $v > v_*$, two forces, which are not equal to each other, act at the same time upon the load: a) the weight of the load P_* (downwards), b) the reaction of the rod P which is determined by expression (15.28) (upwards). These forces are determined by the ordinates in Figure 15.3: a) the horizontal dashed line passing at the level $P = P_*$, b) the descending branch of the curve shown by the solid line. The resultant direction of these two forces is downwards, and equals the difference

$$R = P_* - P = \frac{EF_0}{e} - EF_0 \frac{1}{1+\frac{v}{l_0}} \ln\left(1+\frac{v}{l_0}\right). \tag{15.31}$$

The equation of motion for the load has the form

$$R = \frac{EF_0}{eg}\frac{d^2v}{dt^2}, \tag{15.32}$$

where according to (15.29) $\frac{EF_0}{eg}$ is the mass of the load. Substituting (15.31), we obtain the nonlinear differential equation for the function $v = v(t)$:

$$\frac{d^2v}{dt^2} + \frac{ge}{1+\frac{v}{l_0}} \ln\left(1+\frac{v}{l_0}\right) = g. \tag{15.33}$$

This differential equation must be integrated for the initial conditions /136

$$v = \Delta l_*, \quad \frac{dv}{dt} = 0 \quad \text{for } t = 0, \tag{15.34}$$

which correspond to motion with the initial velocity equal to zero.

We shall not integrate the differential equation (15.21), but we would like to note that the motion will take place with increasing acceleration, since the unbalanced force R increases with time (and an increase in deformation), as may be seen in Figure 15.3.

All of our computations have dealt with the case when the material of the rod is not only infinitely strong, but also linearly deformable. Qualitatively, these same phenomena may be observed in the more complex case, when the physical law of deformation is determined by the nonlinear function

$$\sigma = \sigma(\varepsilon), \tag{15.35}$$

and also when $\mu \neq 0.5$.

The same graph $P - v$ (Figure 15.3) must be interpreted in a different manner, if we are given a monotonic increase in the displacement v, as, for example, occurs in tensile testing machines with lever force meters. Here the external influence is introduced into the system not along the "force" channel, but along the "deformation" channel, and the change in the force P is determined by the properties of the system. In this case, all points of the curve $P - v$ will first be on the ascending, and then on the descending branch.

It would appear that under such loading conditions we cannot speak about stability loss in general. However, this is not completely valid, although naturally stability loss, which is expressed in an infinite increase in deformation and displacements, is impossible. Under these conditions the stability of the cylindrical form of the rod is lost, as soon as the point of the maximum is reached on the curve $P - v$.

In order to clarify this type of stability loss, let us return to the assumption made above regarding the rigorous cylindrical nature of the initial form of the rod, and let us assume that — within the limits of a small portion of the length of the unloaded rod — the transverse sections have a somewhat smaller area $F_0 - \Delta F_0$ than on the remaining length. It may be seen from /137 formula (15.29) that the greatest force which may arise with a gradual extension of the rod is

$$P_* = \frac{E(F_0 - \Delta F_0)}{e}. \tag{15.36}$$

With a further extension of the rod, the force decreases, and consequently the critical value of the force will not be reached in the main portion. Therefore, whereas on the weakened section the deformation will progressively

increase, on the remaining part of the rod there will be a decrease in deformation (due to a decrease in the load). The extension of the entire rod will be determined primarily by the behavior of this section, whose cross section will continuously decrease.

Thus, any small disturbance of the initial cylindrical form for the rod is sufficient to initiate intensive local contraction, within the limits of a small section of the length, in a definite state of the loading process. This comprises the stability loss of the cylindrical form of the rod.

It must not be assumed that these phenomena are only of theoretical interest. On the other hand, using the statements made above, we may determine the reason for the formation and development of a neck which is formed when samples made of plastic materials are extended.

Concerning different measures of great deformation, see the article by N.N. Malinin (Zhurnal prikladnoy mekhaniki i tekhnicheskoy fiziki, No. 3, 1961). See also: M. Reiner "Rheology" (Izdatel'stvo "Nauka", Moscow, 1965); Yu.N. Rabotnov "Soprotivleniye materialov" (Strength of Materials) (Fizmatgiz, Moscow, 1961, § 81).

In the majority of monographs devoted to the problem of the stability of elastic systems, the stability loss during extension is not considered. One exception is the book by A.R. Rzhanitsyn "Ustoychivost' ravnovesiya uprugikh sistem" (Stability of Elastic System Equilibrium) (Goztekhizdat, Moscow, 1955, § 23). Regarding the formation of a neck, as the state of equilibrium instability, see the book by A. Nadai "Strength and Destruction of Solid Bodies" (Foreign Literature Press, Moscow, 1954, Chapt. VIII, § 1 and 2).

An unusual phenomenon has been observed when polymer samples are stretched: immediately after the formation of the neck, its cross section is stabilized, after which local tapering of the rod gradually develops along its length. For information on this subject, see the work by G.I. Barenblatt "The Development of a Neck during stretching of Polymer Samples" (Prikladnaya Matematika i mekhanika, Vol. 28, 1964, pp. 1048 - 1060).

§ 16. Critical Internal Pressure for a Spherical Shell

The phenomenon of the stability loss of a stretched rod, which was discussed in the preceding section, may bring to mind the possible stability loss of a spherical shell under the action of internal pressure. Let us write the solution of this problem, given in the cited book by A.R. Rzhanitsyn, and then let us make certain comments on this solution. For purposes of simplicity, we shall assume that $\mu = 0.5$.

Let us assume that R is the radius of the shell, h — thickness of the wall depending on the internal pressure p; their initial values (when p = 0) may be designated by R_0 and h_0, respectively. By analogy with (15.19), A.R. Rzhanitsyn assumes the following for the shell thickness

$$h = h_0 \frac{R_0}{R} \tag{16.1}$$

and finds the following expression for the stress

$$\sigma = \frac{pR}{2h} = \frac{pR^2}{2h_0R_0}. \tag{16.2}$$

Assuming that the material obeys the Hooke law, for the conditions studied here of a plane stress state, we have the following relationship between the stress σ and the deformation ε:

$$\varepsilon = \frac{\sigma}{E}\left(1 - \mu\right) = \frac{\sigma}{2E}. \tag{16.3}$$

The logarithmic deformation of the shell meridian equals the natural logarithm of the ratio between the meridian length $2\pi R$ and the initial meridian length $2\pi R_0$:

$$\varepsilon = \ln \frac{R}{R_0}. \tag{16.4}$$

Substituting the expressions (16.2) and (16.3), we obtain

$$p = \frac{4Eh_0R_0}{R^2} \ln \frac{R}{R_0}. \tag{16.5}$$

Figure 16.1 gives a graph of the dependence of p on v, where p is the pressure, $v = R - R_0$ — increase in the shell radius when it is deformed, which is a characteristic kinematic parameter of our problem. If we now use the condition /139

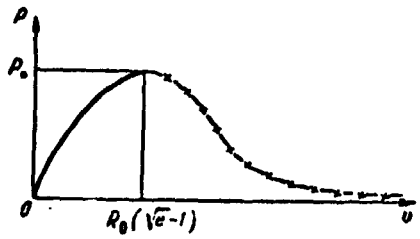

Fig. 16.1. Curve of the equilibrium states of an extended shell.

$$\frac{dp}{dR}=0, \tag{16.6}$$

we find that for

$$R=R_0\sqrt{e}\approx 1{,}65R_0 \tag{16.7}$$

the pressure has a maximum value equal to

$$p_*=\frac{2Eh_0}{eR_0}. \tag{16.8}$$

We would like to make two remarks regarding this solution which are of differing importance.

The first comment is related to expression (16.1) for the thickness h which changes during the loading process. Figure 16.2 shows a diagram of the loading of a shell element. For an infinitely small interval of the loading process, the following relationships are valid, and follow from Hooke's law (when $\mu = 0.5$):

$$d\varepsilon_1=\frac{d\sigma_1}{E}-\frac{1}{2}\frac{d\sigma_2}{E},$$
$$d\varepsilon_2=\frac{d\sigma_2}{E}-\frac{1}{2}\frac{d\sigma_1}{E},$$
$$d\varepsilon_3=-\frac{1}{2}\frac{d\sigma_1}{E}-\frac{1}{2}\frac{d\sigma_2}{E}.$$

Since $\sigma_1 = \sigma_2$ and $\varepsilon_1 = \varepsilon_2$, the first two relationships may be written more simply, similarly to (16.3);

$$d\varepsilon=\frac{d\sigma}{2E}, \tag{16.9}$$

and this equation may be written in the form /140

$$\frac{dh}{h}=-\frac{d\sigma}{E}, \tag{16.10}$$

i.e., with allowance for (16.9)

$$\frac{dh}{h}=-2d\varepsilon. \tag{16.11}$$

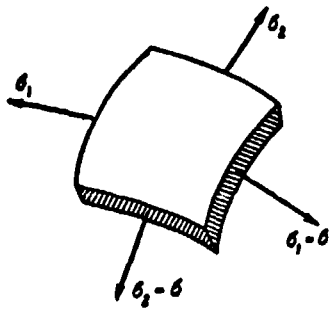

Fig. 16.2. Stresses acting on the edges of the shell element.

Integrating, we obtain

$$\ln \frac{h}{h_0} = -2\varepsilon,$$

i.e., according to (16.4)

$$\ln \frac{h}{h_0} = -2 \ln \frac{R}{R_0};$$

from which we finally obtain

$$h = h_0 \left(\frac{R_0}{R}\right)^2. \qquad (16.12)$$

In contrast to (16.1), this relationship satisfies the condition that the shell volume does not change when it is loaded.

If we continue the computations in the manner used above, then we do not use expression (16.1), but the correct expression (16.12). We then obtain a result which greatly differs from (16.8), namely:

$$p_* = \frac{4h_0 E}{3R_0 e}. \qquad (16.13)$$

The second comment is of theoretical importance, and has the meaning which follows from the term "critical pressure" in this case.

As we have already seen above, it is impossible to predict the behavior of the system, if the method of loading is not clearly established. Two variations of loading may be used for the rod: by assigning the load and by assigning the displacements. For the shell we are considering, two cases also may be distinguished: /141

1) The shell is connected to a very large tank, in which the pressure is given and barely changes when the shell dimensions increase;

2) Newer and newer portions of gas (or liquid) are delivered to the shell by means of a pump.

In the first case, when the pressure in the tank is greater than p_*, the

process will develop as follows: at first there will be a rapid increase in the pressure in the shell from zero (at the moment it is connected to the tank) up to the value p_*. This stage of the process represents a continuous sequence of equilibrium states (the ascending branch of the curve in Figure 16.1)(*). Since only the pressure in the shell reaches the value p_*, elastic equilibrium of the shell becomes impossible. With a further increase in the pressure, the shell will gradually increase in size, passing through a sequence of non-equilibrium states. Therefore (16.3) determines the pressure at which the shell diameter increases indefinitely.

The situation is different in the second case. With an increase in the amount of liquid being delivered, the shell radius will continuously increase. If the change in the pressure is followed (by a manometer), then — in complete agreement with the graph in Figure 16.1 — at first there is an increase, and then a decrease in the pressure. It is not inconceivable that the shell spontaneously becomes "inflated" with a fixed amount of gas (liquid). Therefore, although the curve $p - v$ has a maximum in Figure 16.1, when the gas (liquid) is delivered, the system must pass through all the states described by the graph in Figure 16.1.

In the case we are considering, the independent variable is apparently not the pressure, but the amount of gas (liquid) delivered. The value of the pressure p (just like the displacement v corresponding to it) is determined by the same amount. With an increase in the amount of gas (liquid), the shell radius will increase monotonically, and the pressure — first increases, and then decreases.

In this case of loading, at a maximum pressure stability loss of the form of the shell like that described at the end of § 15, occurs: the thinnest place on the shell becomes thinner and thinner (this phenomenon may be observed, for example, when a volleyball is inflated). However, there will not be a spontaneous increase in the shell diameter. /142

(*) If we do not take into account the forces of inertia for the shell.

§ 17. Rotation of a Flexible Shaft in a Rigid Tube-Shell

There are two meanings of the term "flexible shaft".

Shafts are called flexible whose angular velocity of rotation is greater than the critical velocity. The word "flexible" is here connected with a low natural frequency and with rotation of the shaft in the supercritical region, when the shaft strives to be self-centered.

The same term describes the special construction of shafts which are flexible in the direct meaning of the word. Such shafts are widely used as the drive for vibrating instruments, automobile parts, etc. Structurally, they represent several layers of coils which are wound one on top of another, so that the direction of the winding layers alternate. Such a multi-layered unit is placed in a tube-shell. This shaft construction provides relatively high torsional rigidity and very slight bending rigidity. A tube-shell device like this makes it possible to curve its axis and to assign to it arbitrary forms which also determine the form of the shaft axis. However, the tube bending rigidity is incomparably greater than the shaft bending rigidity.

Based on its construction, a flexible shaft must not have great resistance to rotation for any given form of its axis. For this purpose, the entire tube cavity is filled with a viscous lubricant, due to which there is practically no friction of the shaft on the tube-shell. Nevertheless, sometimes there is a considerable resistance of the shaft to rotation. This resistance changes in one rotation of the shaft, which leads to nonuniform rotation of the driven end of the shaft even for rigorous uniformity of the driving end rotation. Oscillations in the angular velocity of the driven end of the shaft are revealed in vibrations of the pointers on the instruments, which is a very great drawback of this construction. The periodically changing resistance of the shaft to rotation may be the result of <u>initial bending</u> of the shaft, i.e., curvature of its axis before being placed in the tube. As we can see, the rotation of such a shaft is accompanied by periodically repeated stability losses. /143

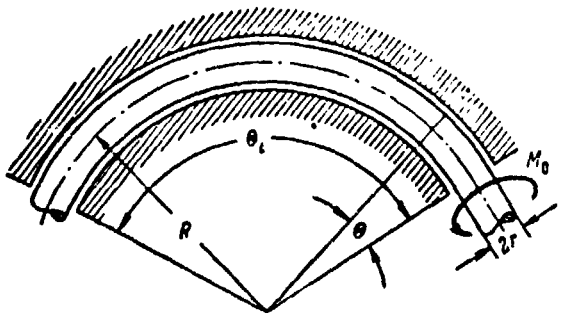

Fig. 17.1. Curvilinear elastic rod in a rigid tube-shell.

The characteristics of a flexible shaft may be clarified by using a simplified model of a curvilinear rod in a rigid tube-shell, whose axis is a circular arc with the radius R. The rod axis has this form after it is placed in the tube-shell. We shall assume that the rod axis also is a circular arc, but with a different radius k_0, before being placed in the shell. In particular, the rod initially may be rectilinear.

The position of the cross section over the rod length will be determined by the central angle Θ, determined from one of the tube ends (Figure 17.1).

In an arbitrary cross section of the rod, we use a system of coordinates whose origin coincides with the center of gravity for the section, and the x axis is directed along the external normal to the rod axis (Figure 17.2).

We first find the initial normal stresses σ^0 developing when the system is installed, i.e., when introducing the rod into the tube-shell. We shall assume that the planes containing the curvilinear axes of both elements coincide directly before the installation. Then, after the rod is placed in the shell, its axis changes its curvature from $\frac{1}{R_0}$ to $\frac{1}{R}$, and in every case identical bending moments occur, which equal /144

$$M_y^0 = -\frac{EJ}{R} + \frac{EJ}{R_0} \tag{17.1}$$

(EJ — bending rigidity of the rod). The normal stresses in the transverse sections of the rod correspond to them

$$\sigma^0 = -\frac{M_y^0}{J} x = Ex\left(\frac{1}{R} - \frac{1}{R_0}\right). \tag{17.2}$$

Let us now study the displacements, deformation, and stresses arising under the action of the torque M_0 which is applied to one of the ends of the shaft, when each section of the shaft turns in its own plane (there is no slipping of the shaft along the tube). We shall disregard the friction forces between the rod and the tube-shell, which may develop when the sections rotate. Thus, the reaction of the shell will represent only a system of distributed normal pressures.

Based on the conditions of the problem, each transverse section has only one degree of freedom — the possibility of rotating around the tangent to the geometric axis of the rod. These angles of rotation will be designated by ψ, and $\psi = \psi(\Theta)$.

Let us determine the extension of any circular wire, whose image in the plane of the transverse section is designated by the point A in Figure 17.2. If the polar coordinates of this point before deformation are ρ and α, then the Cartesian coordinates are

$$x = \rho \cos \alpha, \quad y = \rho \sin \alpha.$$

When the section turns at the angle ψ, this point assumes a new position A', determined by the coordinates /145

$$x' = \rho \cos (\alpha + \psi) = x \cos \psi - y \sin \psi, \tag{17.3}$$

$$y' = \rho \sin (\alpha + \psi) = y \cos \psi + x \sin \psi; \tag{17.4}$$

and the relative extension of the wire is

$$\varepsilon = \frac{(R + x') - (R + x)}{R + x}.$$

The numerator represents the difference in the wire radius of curvature after rotation and before it. Substituting expression (17.3) and omitting the component x in the denominator, we have

$$\varepsilon = \frac{1}{R} [x (\cos \psi - 1) - y \sin \psi]; \tag{17.5}$$

and the corresponding normal stress is determined by

$$\sigma' = E\varepsilon = \frac{E}{R} [x (\cos \psi - 1) - y \sin \psi]. \tag{17.6}$$

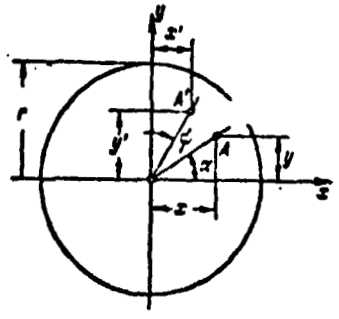

Fig. 17.2. Transverse cross section of a rod: α — angular coordinate of point A; ψ — angle of rotation for the cross section.

Summing expressions (17.2) and (17.6), we obtain the total normal stress

$$\sigma = \sigma^0 + \sigma' = -\frac{E}{R_0}x + \frac{E}{R}x\cos\psi - \frac{E}{R}y\sin\psi. \tag{17.7}$$

This system of stresses reduces to the bending moments whose positive directions are shown in Figure 17.3:

$$M_x = \int_F \sigma y'\,dF = -\frac{EJ}{R_0}\sin\psi, \tag{17.8}$$

$$M_y = -\int_F \sigma x'\,dF = EJ\left(\frac{1}{R}\cos\psi - \frac{1}{R}\right). \tag{17.9}$$

The analysis of the normal stresses and the bending moments corresponding to them ends at this point. We shall now determine the displacements, shearing stress, and torques.

To find the displacement, let us consider Figure 17.4, which shows the rotations of two mixed transverse sections of a rod. As may be seen, the displacement angle equals the ratio of the differences in the lengths of the arcs BB' and AA' to the length of the arc OO': /146

$$\gamma = \frac{\rho}{R}\frac{d\psi}{d\theta}. \tag{17.10}$$

The shearing stress according to Hooke's law is

$$\tau = \frac{G\rho}{R}\frac{d\psi}{d\theta}, \tag{17.11}$$

and the torque is

$$M_z = -\int_F \tau\rho\,dF = -\frac{G}{R}\frac{d\psi}{d\theta}\int_F \rho^2\,dF = -\frac{GJ_p}{R}\frac{d\psi}{d\theta}. \tag{17.12}$$

Let us investigate the equilibrium of a rod element with the length $Rd\theta = ds$, shown in Figure 17.5. We also show the transverse forces Q_x and Q_y.

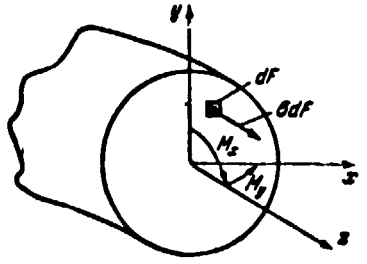

Fig. 17.3. Bending moments in a rod transverse section

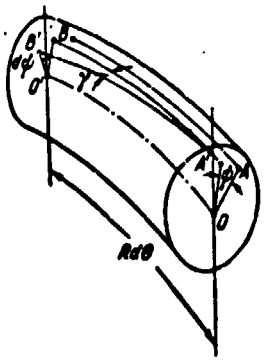

Fig. 17.4. Shift of γ occurs due to the difference dψ in the angles of rotation of two adjecent rod sections.

The reaction of a supporting surface (reaction of the shell) is shown in the form of stresses passing through the axial line and the normals to it. This reaction consists of the components $q_y ds$ and $q_x ds$ in an infinitely small section of the rod. The center of the coordinate system x'y'z' is combined with the center of gravity of the middle section of an element.

The six equations of equilibrium reduce to the following relationships after simple transformations: /147

$$Q_x = 0, \tag{17.13}$$

$$q_x = 0, \tag{17.14}$$

$$q_y = \frac{1}{R}\frac{\partial Q_y}{\partial \theta}, \tag{17.15}$$

$$\frac{\partial M_z}{\partial \theta} - M_x = 0, \tag{17.16}$$

$$Q_y = -\frac{1}{R}\left(M_z + \frac{\partial M_x}{\partial \theta}\right), \tag{17.17}$$

$$\frac{\partial M_y}{\partial \theta} = 0. \tag{17.18}$$

Now substituting (17.8) and (17.12) in the equation of moments (17.16), we obtain the basic differential equation of the problem:

$$\psi''' - a^3 \sin\psi = 0, \tag{17.19}$$

in which the primes designate differentiation with respect to the coordinate θ, and the following abbreviated notation is introduced /148

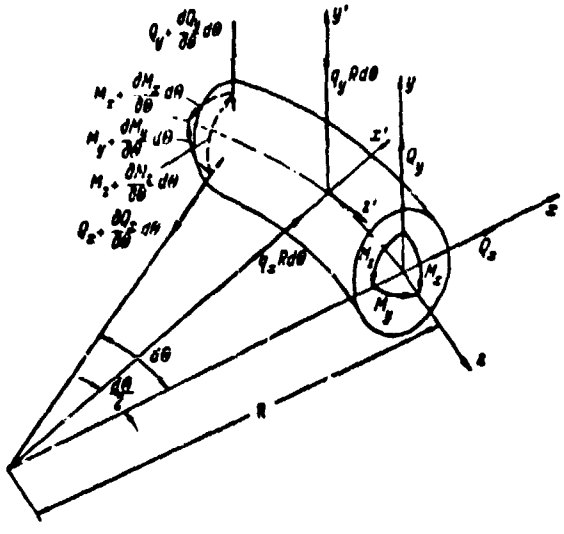

Fig. 17.5. Diagram of forces acting on a rod element.

$$a = \sqrt{\frac{EJ}{GJ_k}\frac{R}{R_0}}. \qquad (17.20)$$

The solution of the second order differential equation (17.19) must satisfy the two boundary conditions

$$\left.\begin{aligned} \psi &= \psi_0 \text{ for } \theta = 0, \\ \psi' &= 0 \text{ for } \theta = \theta_l. \end{aligned}\right\}. \qquad (17.21)$$

By means of the first condition, we shall introduce the angle of rotation of the torqued end of the shaft ($\theta = 0$) into the solution. The second condition expresses the action of a torque on the driven end ($\theta = \theta_l$).

To solve the differential equation (17.19), let us represent it in the form

$$\psi'' = a^2 \sin\psi.$$

Multiplying both parts of this equation by

$$2\psi' d\theta = \frac{2d\psi}{d\theta} d\theta = 2d\psi$$

and then integrating, we obtain

$$(\psi')^2 = -2a^2\cos\psi + C, \qquad (17.22)$$

where C is the integration constant which must equal the following, according to the second condition (17.21)

$$C = 2a^2\cos\psi_l.$$

We may find the first derivative from (17.22)

$$\psi' = \pm\sqrt{2a^2(\cos\psi_l - \cos\psi)}. \qquad (17.23)$$

After transformations, we obtain

$$d\theta = \pm \frac{d\psi}{2a\sqrt{\cos^2\frac{\psi_l}{2} - \cos^2\frac{\psi}{2}}}. \tag{17.24}$$

Let us integrate this expression within the limits of a section of the rod length, located between the sections with coordinates θ, θ_l. Within these limits, the section angle of rotation changes from the value ψ to the value ψ_l /149 at the driven end. The result of integration has the form

$$a(\theta_l - \theta) = \pm\frac{1}{2}\int_{\psi}^{\psi_l} \frac{d\psi}{\sqrt{\cos^2\frac{\psi_l}{2} - \cos^2\frac{\psi}{2}}}. \tag{17.25}$$

In addition we introduce the substitutions

$$\left.\begin{aligned} \cos\frac{\psi_l}{2} &= k, \\ \cos\frac{\psi}{2} &= k\sin\varphi, \end{aligned}\right\} \tag{17.26}$$

and

$$d\psi = -\frac{2k\cos\psi}{\sqrt{1 - k^2\sin^2\varphi}}\,d\varphi. \tag{17.27}$$

After substituting (17.26) and (17.27) in (17.25), and after changing the integration limits, we obtain

$$a(\theta_l - \theta) = \mp\int_{\varphi}^{\frac{\pi}{2}} \frac{d\varphi}{\sqrt{1 - k^2\sin^2\varphi}} \tag{17.28}$$

or, representing the integral obtained in the form of the difference between two elliptical integrals of the first kind, we have

$$a(\theta_l - \theta) = \mp\left[\int_0^{\frac{\pi}{2}} \frac{d\varphi}{\sqrt{1 - k^2\sin^2\varphi}} - \int_0^{\varphi} \frac{d\varphi}{\sqrt{1 - k^2\sin^2\varphi}}\right]. \tag{17.29}$$

Equation (17.29) determines the dependence between the coordinates θ and θ_l, on the one hand, and the angles of rotation of the corresponding sections ψ and ψ_l, on the other hand. If we set $\theta = 0$ and $\psi = \psi_0$, equation (17.29) will express the relationship between the angle of rotation of the driving

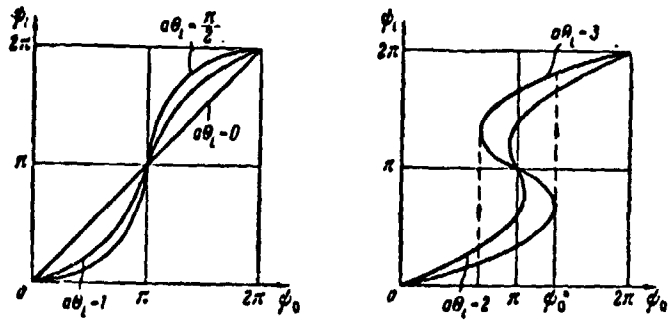

Fig. 17.6. Dependence of the angle of rotation ψ_l of the end section on the angle of rotation ψ_0 of the initial section: a) for values of the parameter $a\theta_l \leqslant \frac{\pi}{2}$; b) for values of the parameter $a\theta_l > \frac{\pi}{2}$.

end of the rod ψ_0, the angle of rotation of the torqued end ψ_l, and the parameter of the system $a\theta_l$.

Using the tables of elliptical integrals of the first kind, we may obtain the relationships which we need in numerical form. These results are shown in Figure 17.6 in the form of the graphs $\psi_l = \psi_l(\psi_0)$. Figure 17.6, a shows /150 typical graphs for values of the parameter $a\theta_l \leq \frac{\pi}{2}$, and Figure 17.6, b — values of the parameter $a\theta_l > \frac{\pi}{2}$.

The dependence of ψ_l on ψ_0 is characteristic for the curves shown in Figure 17.6, a. When $a\theta_l = 0$ the angles ψ_0 and ψ_l are identically equal, and the corresponding graph represents a line passing through the origin at the angle 45°. With an increase in the parameter $a\theta_l$, the curves branch out from this line more and more. As a whole, the law governing the motion of the driven end is nonlinear, but smooth in nature.

Figure 17.6, b shows curves corresponding to $a\theta_l = 2$ and $a\theta_l = 3$. A new quality of the curves is very apparent here — the indeterminacy of $\psi_l = \psi_l(\psi_0)$. If ψ_0 increases continuously (as usually occurs, since the uniform rotation of the driven end is given), then for a value of $\psi_0 = \psi_0^*$ there is a jump — an instantaneous increase in the value ψ_l, as is shown in Figure 17.6, b by

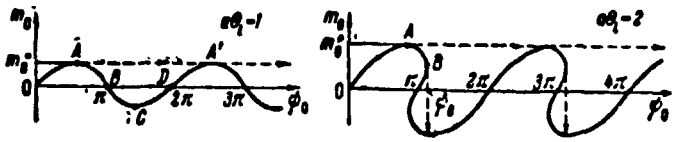

a) b)

Fig. 17.7. Curves of equilibrium states of a curvilinear rod; for $m_0 = m_0^*$ there is continuous rotation of the rod.

the arrow. A further increase in ψ_0 involves a smooth increase in ψ_l in a certain section, and then a new jump, etc. Consequently, a discontinuous law governing motion of the driven end corresponds to a continuous motion of the driving end of the rod.

By examining the curve for the equilibrium states of the system, we may see a close connection between the phenomena discussed here and the subject of this section. For this purpose, we must find the law governing the change in the external torque with a monotonic increase in the angle of rotation ψ_0. /151

According to (17.12), we have

$$M_0 = -\frac{GJ_k}{l}\psi_0'\theta_l.$$

where $l = R\theta_l$. From expression (17.23), we have

$$\psi_0' = \pm\sqrt{2a^3(\cos\psi_l - \cos\psi_0)}.$$

In addition we find

$$M_0 = \mp\frac{GJ_k a\theta_l}{l}\sqrt{2(\cos\psi_l - \cos\psi_0)}. \qquad (17.30)$$

In order to perform calculations with this formula, we must substitute the values of ψ_l in it, which are determined as a function of ψ_0, as was shown above. In this way we will determine the relationship, in which we are interested, between the angle of rotation ψ_0, and the corresponding moment M_0.

Let us determine what sign must be used in formula (17.30).

1. When $\psi_0 > \psi_l$ the function $\psi = \psi(\theta)$ is a decreasing function, and

consequently $\psi' < 0$. According to (17.12), in this case $M_z > 0$, and therefore for M_0 a plus sign must be used.

2. When $\psi_0 < \psi_l$ the function $\psi = \psi(\Theta)$ is an increasing function, and consequently $\psi' > 0$. Proceeding as above, we find that a minus sign must be used in formula (17.30).

Figure 17.7, a shows a curve described by the equation (17.30) and corresponding to the case when $a\Theta_l = 1$. The values of the dimensionless moment $m_0 = \frac{M_0 l}{GJ_k}$ are plotted along the ordinate axis; this moment must be interpreted /152 as the twisting angle of a circular-cylindrical cantilever rod with the length l, which has torsional rigidity GJ_k under the action of the moment applied to its free end. The state when a further increase in the moment is impossible without disturbing the equilibrium corresponds to point A. For a gradual increase in ψ_0, not an increase in the moment is necessary, but — on the contrary — a decrease (section AB). The state of unstable equilibrium without an external load corresponds to the point $B(\psi_0 = \pi)$. For a gradual further increase in ψ_0 the moment must have the opposite sign (section BCD).

The dimensionless moment m_0^* which corresponds to the maximum of the curve determines the greatest resistance to rotation. It is the <u>critical value of the load</u>, at which elastic stability is lost, i.e., there is a jump — an instantaneous increase in the angle ψ_0, as is shown in Figure 17.7, a by the dashed arrows. However, after the jump the system does not return to the state of stable equilibrium, but immediately performs the next jump, etc., i.e., <u>a continuous series of jumps</u> begins, which will be observed as non-uniform rotation of the torqued end of the rod. The value of m_0^* is <u>the minimum value of the dimensionless moment providing a continuous rotation of the rod</u>. Since in general there are no equilibrium states for larger loads, the system discussed here is more similar to the systems discussed in this ch[illegible] than to the systems with jumps, which were discussed in the second chapter.

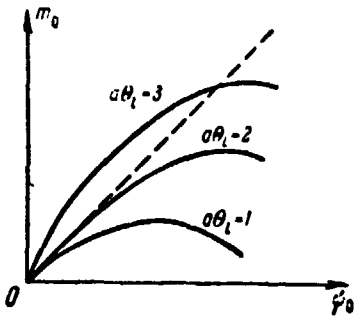

Fig. 17.8. Initial rigidity of a curvilinear rod depends on the parameter $a\theta_l$.

Figure 17.7, b, shows one curve drawn on the basis of equation (17.30) and describing the rod resistance to rotation when $a\theta_l = 2$. This graph is interesting since it represents the relationship with is multi-valued not only with respect to ψ_0, but also with respect to the moment m_0. However, with a gradually increasing moment, when $m_0 = m_0^*$ stability loss occurs and, as in the preceding case, a continuous sequence of jumps begins.

Figure 17.8 shows the initial sections of the curves of equilibrium states for rods with different values of $a\theta_l$. The dashed line shows the dependence $m_0 = m_0(\psi)$ for a cantilever rod with a rectilinear axis. We may readily see /153 for certain values of the parameter $a\theta_l$ it is more difficult to turn a curved rod, which lies freely in a shell, than a straight rod of the same length which is rigidly fixed. This is the extent to which a flexible shaft may lose the properties of its mechanical action!

The phenomena occurring when the torqued end of a flexible shaft is rotated are in many respects similar to the phenomena occurring when a ring is loaded with tilting moments (Figure 17.9). A graph showing the dependence between the load and the angle of rotation for the section has the same form as the graph shown above in Figure 17.7, a. For small values of the moment the ring has elastic resistance to being turned over. However, there is a certain critical value of the moment, after which the ring loses stability and a continuous series of jumps begins. The ring turns into an unusual mechanism.

Among other things, the basic tenets of the theory presented above may /154 find an unexpected application in the analysis of the structure shown in Figure 17.10. In this structure (which is used in certain electric vibrating machines) monolithic stoppers are inserted at the ends of a cylindrical spring.

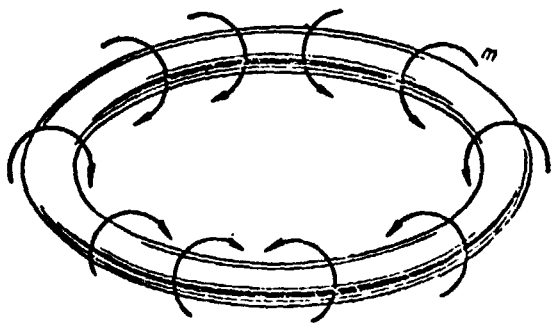

Fig. 17.9. For a critical value of the load m "inverting" of the ring occurs.

These stoppers transmit longitudinal forces which are primarily tensile stresses to the spring. There is a spiral groove with a semi-circular cross section on the surface of the stopper. Although it is usually assumed that the windings of the spring do not slip with respect to the stopper at the place where the spring is connected with the stopper, it is valid to formulate the problem of stresses and deformations of the spring in the region where it contacts the stopper.

It may be assumed that the spring windings lying in the spiral groove are subjected to conditions which are similar to the computational scheme shown in Figure 17.1 (it is assumed that the spring has a small pitch). The initial section of this portion is loaded with the torque

$$M = PR, \tag{17.31}$$

where P is the longitudinal force, R — radius of the spring. The angles of the section twisting are determined by the differential equation (17.19), in which the parameter a is calculated according to the formula

$$a = \sqrt{\frac{EJ}{GJ_p}} \approx 1{,}12,$$

which follows from expression (17.20). The subsequent solution is greatly simplified due to the fact that, in contrast to a flexible shaft, the angles ψ are very small. Therefore, instead of the differential equation (17.19), we shall solve the linearized equation

$$\psi'' - a^2\psi = 0. \tag{17.32}$$

Its solution has the form /155

$$\psi = C_1 e^{a\theta} + C_2 e^{-a\theta}. \tag{17.33}$$

Since the angle ψ must remain finite for an infinite increase in θ, the constant C_1 must equal zero. The constant C_2 is determined from the condition

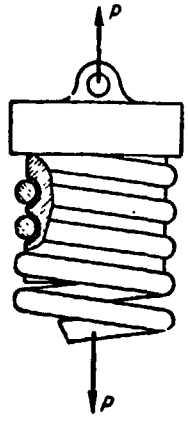

Fig. 17.10. Connection of a twisted cylindrical spring with an end stopper.

$$\frac{d\psi}{Rd\theta}=\frac{M}{GJ_p} \text{ for } \theta=0,$$

which corresponds to the initial section. We thus find

$$C_1=\frac{MR}{aGJ_p}, \tag{17.34}$$

and the solution acquires the form

$$\psi=\frac{MR}{aGJ_p}e^{-a\theta}. \tag{17.35}$$

The greatest twisting angle corresponds to the initial section, i.e., $\theta = 0$:

$$\psi_0=\frac{MR}{aGJ_p}.$$

Thus, the torsional compliance of a section of a spring winding, which is in complete contact with the stopper, is equivalent to the torsional compliance of a free section of the winding with the length R:a $\approx$ 0.9R.

Such an analysis is useful, not only for determining the compliance of the structure, but also for determining the friction forces between the surfaces of the windings on the stopper. In their turn, these forces determine the structural deformation in this connection, which is usually assumed to be non-deformable.

For more details on the behavior of a flexible shaft when it rotates, see the article by I.I. Gubanov "Rotation of a Curvilinear Elastic Rod in a Non-Deformable Curvilinear Shell" (Izvestiya AN Latv. SSSR, No. 10, 1966) and "Complex Cases of the Rotation of a Curvilinear Elastic Rod in a Curvilinear Tube" (Collection: Voprosy dinamiki i prochnosti [Problems of Dynamics and Strength], No. V, Riga, 1958).

The solution of the problem of inverting a ring was given by R. Grammel (see C.B. Biezeno and R. Grammel "Technical Dynamics", Vol. 1, Gostekhizdat, 1950). The problem pertaining to Figure 17.10 was investigated in 1965 by G.I. Ninoshvili.

CHAPTER V

BUCKLING OF NOT FULLY ELASTIC RODS

In the preceding four chapters, we discussed the stability loss of systems made of fully elastic material. In this chapter, we examine the problems of elastic-plastic buckling and buckling with allowance for creep.

§ 18. Elastic-Plastic Buckling; Classical Concept

Discussions have continued up to the present regarding the theory of buckling in the case of stresses exceeding the proportionality limit; this theory was developed by F. Engesser, Ya.S. Yasinskiy and T. Karman. In this section, we shall recall the basic features of the classical concept of elastic-plastic buckling, and in the next section we shall turn to the new ideas which have been advanced in this field.

It is well-known that calculations of the critical force using the Euler formula may provide both valid and invalid results. If the critical state arises during stresses which are less than the proportionality limit, the Euler theory gives the correct value of the critical force. This corresponds to loading of flexible long beams. Larger compressive forces are necessary for buckling of relatively short beams, and stability losses occur with stresses exceeding the proportionality limit. In these cases we cannot use the Euler formula.

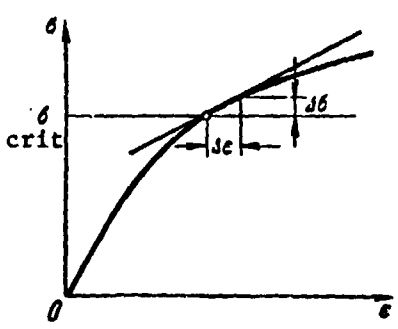

Fig. 18.1. Diagram of compression of beam material.

In 1845 Lamarle first calculated the value of rod flexibility, which provided a lower limit for the region of applicability of the Euler formula. It was found that

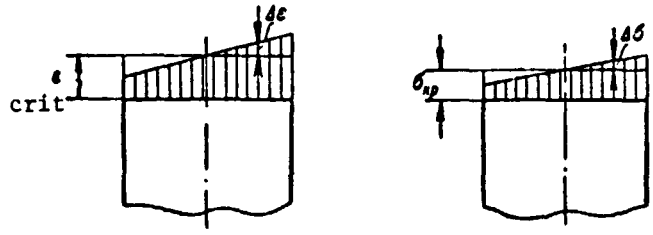

Fig. 18.2. Change in deformation (a) and stress (b) with Engesser buckling.

the flexibility of rods which are most frequently used in engineering lie below the given limit. A somewhat paradoxical situation arose: the Eular theory could provide information which only pertained to regions which are of little interest in technology, while the phenomenon of the stability loss had not been theoretically studied at all in the most important region in practice (with relatively short columns). /157

Only at the end of the XIX century was the first attempt made to provide a theoretical basis for calculating the critical forces for short rods. In 1889 Engesser(*) proposed using the actual diagram of compression of material $\sigma = \sigma(\varepsilon)$ (see Figure 18.1), and calculating the critical force from the Euler formula, but replacing the elasticity modulus E by the tangent modulus E_*:

$$P_* = \frac{\pi^2 E_* J}{l^2}. \tag{18.1}$$

The tangent modulus is determined by the angle of inclination of the tangent to the stress-deformation curve

$$E_* = \frac{d\sigma}{d\varepsilon}, \tag{18.2}$$

and is a variable, which depends on the stress σ, at which stability loss occurs.

(*) Friedrich Engesser (1848 - 1931) wrote a practical study on the construction of railroad tracks, and made numerous studies in the field of structural mechanics. In 1885 1915 he was Professor of the theory of structures at Karlsruhe.

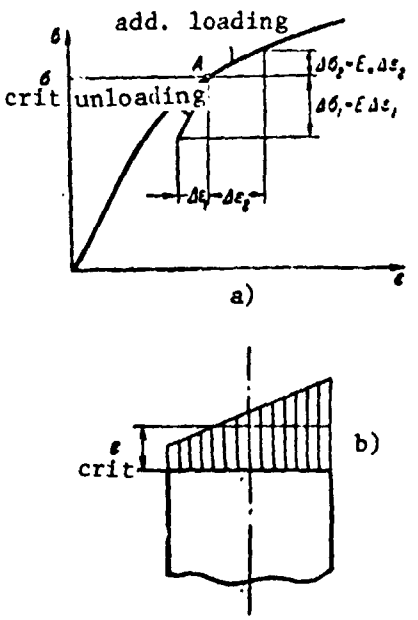

Fig. 18.3. In the case of buckling, unloading occurs in a cross section: a) dependence of stress σ on deformation ε; b) deformation diagram; c) diagram of normal stresses.

Engesser used the diagrams of deformation and stress shown in Figure 18.2. Due to the rod bending, the compression deformations in one section increased, while in the other they decreased. On the whole, the change in the deformation Δε follows a plane law (Figure 18.2, a), and increases in the stress Δσ are proportional to the corresponding increases in deformation Δε (Figure 18.2, b). The tangent modulus serves as the proportionality coefficient /158

$$\Delta\sigma = E_*\Delta\varepsilon. \qquad (18.3)$$

Figure 18.2, b shows the distribution of the total stresses over the beam cross section. These concepts regarding the distribution of the stresses σ lead to the necessity of replacing the modulus of elasticity E by the tangent modulus E_*.

However, Engesser overlooked the fact that the relationship (18.3) is only valid for the right-hand side of the cross section, where a portion of the section has an additional loading (the compressive stresses increase). The compressive stresses decrease in the left-hand side of the section, and the law governing the unloading (the left-hand side of the section) is determined by the relationship

$$\Delta\sigma = E\Delta\varepsilon, \qquad (18.4)$$

which was first experimentally established by Gerstner(*) and has been

(*) F.I. Gerstner (1756 - 1832) — Professor of the Paris University in 1789 - 1806. In 1806 he organized in Prague the "Czech Technical Institute", and until the end of his life was a Director, while at the same time fulfilling the duties of Professor of Mechanics. This relationship was first published in 1831.

repeatedly confirmed since. According to the Gerstner law, the additional loading and unloading processes are different from that shown in Figure 18.1, and in actuality resemble that shown in Figure 18.3, a. The diagrams of ε and σ must have the form shown in Figure 18.3, b and c.

This omission of Engesser was noted by F.S. Yasinskiy(*) in 1895. /159
F.S. Yasinskiy published critical comments on the article by Engesser. Immediately afterwards, he responded to the criticism of F.S. Yasinskiy, and in 1895 he gave a corrected general formula for the critical force

$$P_{**} = \frac{\pi^2 E_{**} J}{l^2}, \tag{18.5}$$

in which E_{**} is a quantity (which shall later be called the reduced modulus of elasticity) which depends on the moduli E and E_*, as well as the form of the rod transverse cross section. However, the discussion between Engesser and Yasinskiy did not at first attract a great deal of attention, and formula (18.5) was again obtained by T. Karman in 1909. In particular, T. Karman also provided a closed expression for the reduced modulus for a rectangular cross section: /160

$$E_{**} = \frac{4EE_*}{(\sqrt{E} + \sqrt{E_*})^2}. \tag{18.6}$$

Since that time, the theory of the reduced modulus(**) has received universal recognition, has been included in the scientific and technical literature, and has retained a monopolistic importance for a long time. Later, the theory of the reduced modulus was used to study the stability of several structures which are more complex than a simple beam.

To illustrate the different approaches to determining the critical force, let us use the simplified model of a beam, shown in Figure 18.4. This model represents an absolutely rigid body, supported on two deformable supporting rods.

(*) Felix Stanislavovich Yasinskiy was born in Warsaw in 1856. After finishing the St. Petersburg Institute of Engineers (1877), he performed a great deal of practical and research studies. He was a Professor of the same Institute from 1895 up until his death (1899).

(**) It is interesting to note that the Engesser-Karman formula was published in 1912 independently of these authors by Southwell.

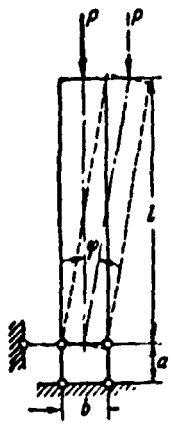

Fig. 18.4. Model of a beam.

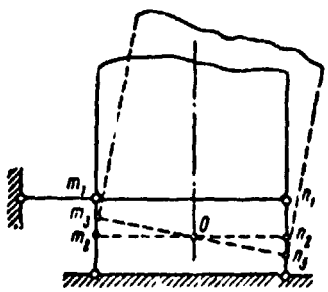

Fig. 18.5. One and the same compressive force P corresponds to the states m_2n_2 and m_3n_3.

We must first determine the critical Euler force for our beam, assuming that the material of both supporting rods obeys the Hooke law. Let us use a to designate the initial length of each of the rods, and F — the cross sectional area of each of the rods. Let us study the three states of the system shown in Figure 18.5. The first of them (points m_1, n_2) applies to the case when there is no external load on the beam. The second state (points m_2, n_2) and the third state (points m_3, n_3) correspond to the loading of the beams by one and the same force — the critical load P. We use φ to designate an infinitely small angle of rotation for the beam in the case of stability loss. The additional contractions of the supporting rods (with the transition from the section m_2n_2 to the position m_3n_3) equal

/161

$$\Delta l_1 = -\frac{\varphi b}{2}, \quad \Delta l_2 = \frac{\varphi b}{2} \tag{18.7}$$

(contractions of the rods from the total contraction $\overline{m_1m_2} = \overline{n_1n_2}$ are not included). Using the Hooke law, we may find the additional stresses in both rods (we shall assume the compressive forces are positive):

$$\left.\begin{aligned} \Delta P_1 &= EF\frac{\Delta l_1}{a} = -\frac{EF}{a}\frac{\varphi b}{2}, \\ \Delta P_2 &= EF\frac{\Delta l_2}{a} = \frac{EF}{a}\frac{\varphi b}{2}. \end{aligned}\right\} \tag{18.8}$$

The sum of the moments of these forces with respect to point O must equal the moment of the external force $Pl\varphi$ (see Figure 18.4). Substituting expression (18.8), we obtain the equation

$$\frac{EFb^2}{2a}\varphi = Pl\varphi. \tag{18.9}$$

The inequality $\varphi \neq 0$ is the condition for the existence of the deflected form of equilibrium. Then from (18.9) we obtain the Euler critical force

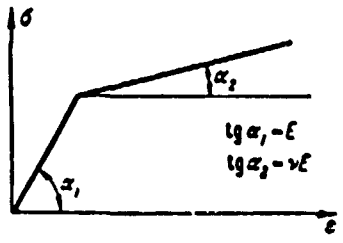

Fig. 18.6. Diagram of material compression with linear strengthening.

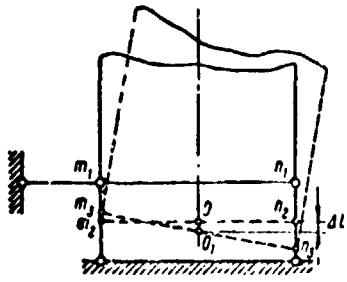

Fig. 18.7. One and the same value of the compressive force P_{**} corresponds to the states m_2m_2 and m_3n_3; the points O and O_1 do not coincide.

$$P = \frac{EFb^2}{2al}. \tag{18.10}$$

We now assume that the properties of the rod material are characterized by the compression diagram shown in Figure 18.6 (case of material with linear contraction). Below the proportionality limit the modulus of elasticity equals E, and in the second section the tangent modulus is constant and equals νE (it is assumed that ν is given).

Let us assume that stability losses occur with stresses which correspond /162 to the second section of the diagram. For a short time we shall forget the Gerstner law, and use the earlier viewpoint of Engesser. To determine the critical force, we may use the scheme shown in Figure 18.5. All of the discussions and calculations remain the same, if everywhere — beginning with expressions (18.8) — instead of the modulus of elasticity E we write the tangent modulus νE. In the last analysis, we obtain for the tangent-modulus critical force the formula

$$P_* = \frac{\nu EFb^2}{2al}. \tag{18.11}$$

We need this formula for several following computations.

Let us now turn to the derivation of the formula for the critical force using the theory of the reduced modulus. For this purpose, let us examine

Figure 18.7, which differs somewhat from Figure 18.5 given above.

Just as above, points m_2, n_2 and m_3, n_3 characterize two different states of equilibrium for the beam ; these states correspond to one and the same compressive force P_{**}. Therefore, a decrease in the compressive force of the left rod must exactly equal the increase in the compressive force of the right rod. However, these increases in the forces (negative on the left and positive on the right) are determined by different moduli of elasticity (E — on the left and νE — on the right). Consequently, the additional deformations of the rod cannot be the same. It thus follows that the segment m_3n_3 does not pass through the middle of m_2n_2 (in contrast to the diagram shown in Figure 18.5). In the case of the beam stability loss (change of the points m_2, n_2 to the position m_3, n_3) additional contractions of the supporting rods are

$$\Delta l_1 = -\frac{\varphi b}{2} + \Delta l, \quad \Delta l_2 = \frac{\varphi b}{2} + \Delta l, \tag{18.12}$$

where Δl is the drop in the middle point O. Naturally, this does not include the contractions $\overline{m_1m_2}$ and $\overline{n_1n_2}$ which develop when the beam is loaded until the force reaches the value P_{**}. The additional compressive stresses in the rods are

$$\left.\begin{aligned} \Delta P_1 &= EF\frac{\Delta l_1}{a} = -\frac{EF}{a}\left(\frac{\varphi b}{2} - \Delta l\right), \\ \Delta P_2 &= \nu EF\frac{\Delta l_2}{a} = \frac{\nu EF}{a}\left(\frac{\varphi b}{2} + \Delta l\right). \end{aligned}\right\} \tag{18.13}$$

The sum of these increases must equal zero, since the total compressive force P does not change. We thus first find the connection between Δl and φ :

$$\Delta l = \frac{\varphi b}{2}\frac{1-\nu}{1+\nu}, \tag{18.14}$$

and then the increase in the forces

$$-\Delta P_1 = \Delta P_2 = \frac{EFb}{a}\cdot\frac{\nu}{1+\nu}\varphi. \tag{18.15}$$

The sum of the moments of the additional forces ΔP_1 and ΔP_2 with respect to the point O_1 must equal the moment of the external load

$$2\frac{EFb}{a}\frac{\nu}{1+\nu}\varphi\frac{b}{2} = P_{**}l\varphi. \tag{18.16}$$

In the case of the stability loss $\varphi \neq 0$; we thus have

$$P_{**}=\frac{\nu EFb^3}{(1+\nu)\,al}. \qquad (18.17)$$

This formula determines the critical force according to the Engesser-Karman theory, and

$$E_{**}=\frac{\nu E}{1+\nu} \qquad (18.18)$$

represents the reduced modulus. Comparing this result with formula (18.11), we see that $P_{**} > P_{*}$ always, since $\nu < 1$. When $\nu = 1$ (linearly deformable material) all three formulas (18.10), (18.11) and (18.17) give the same results.

These solutions are given only as an illustration of the "classical" concept of elastic-plastic bending. Without this, it would be difficult to discuss the new concept, which is the theme of the following section.

§ 19. Elastic-Plastic Buckling; Present-Day Concept /164

After the study of Karman, for several years there were no new ideas in this field.

A new turning point in the history of the problem was reached with the publication in 1946 - 1947 of two articles by F.R. Shanley, the first of which was called "Paradox of Buckling". F.R. Shanley wrote: "A doubtful assumption was made in the derivation of the theory of the reduced modulus. It was assumed, at least by definition, that the beam remains a straight line with an increase in the axial load up until a previously determined critical value, after which the beam bends or may curve". Here the term "previously determined value" designates the Engesser-Karman critical force, expressed by formula (18.5) for the reduced modulus E_{**}. Later Shanley proposed establishing whether or not bent forms of the beam equilibrium exist for loads less than P_{**}. Certain qualitative considerations led him to the opinion that these forms are possible with loads which exceed P_{*}, given above in formula (18.1). We shall not dwell on these considerations, but shall immediately turn to an analytical determination of this relationship for the model examined above (we should note that Shanley also used a similar diagram of the beam.)

Let us turn to Figure 18.7, but we shall interpret it somewhat differently. As previously, let us assume that m_1n_1 is the position of the base when there is no load. Following Shanley, we also assumed that when the beam is loaded deflected states of equilibrium are possible, beginning with a certain specific position m_2n_2, and the load P_+ which is less than P_{**} (the value of P_+ is previously unknown; it has only been calculated that $P_+ = P_*$) corresponds to the position m_2n_2. Let us also assume that the external load continues to grow beyond the value of P_+, and let us study the possibility of deflections of the beam positions with loads $P_+ + \Delta P < P_{**}$ (ΔP — final increase in the load).

Let us assume the segment m_3n_3 corresponds to the position of the beam base for a certain load $P = P_+ + \Delta P$. Using Δl to designate the average contraction of the rod from the additional force ΔP and φ to designate the beam angle of rotation (angle of inclination of the segment m_3n_3), we find the contraction of the rods caused by the additional force: /165

$$\left.\begin{aligned}\Delta l_1 &= -\frac{\varphi b}{2} + \Delta l,\\ \Delta l_2 &= \frac{\varphi b}{2} + \Delta l\end{aligned}\right\} \qquad (19.1)$$

and the corresponding increases in the compressive forces:

$$\left.\begin{aligned}\Delta P_1 &= -\frac{EF}{a}\left(\frac{\varphi b}{2} - \Delta l\right),\\ \Delta P_2 &= \frac{EF}{a}\left(\frac{\varphi b}{2} + \Delta l\right).\end{aligned}\right\} \qquad (19.2)$$

In contrast to § 18, the displacements φ and Δl are small but finite values. The formulas (19.2) are written under the assumption that at this stage in the gradual increase of the load from the value of P_+ to the value $P_+ + \Delta P$ (i.e., with a change from the state m_2n_2 to state m_3n_3), the point m always rises upwards, and the point n always drops down. In other words, the left rod is continuously unloaded, and the right rod is continuously additionally loaded.

The sum of the increases (19.2) must equal the additional force ΔP:

$$\frac{EF}{a}\Delta l(1+\nu) - \frac{EFb}{2a}\varphi(1-\nu) = \Delta P, \qquad (19.3)$$

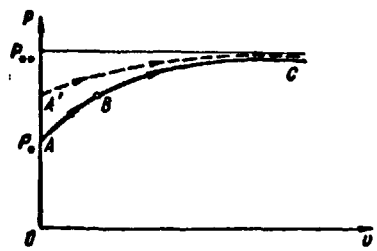

Fig. 19.1. Curves of the equilibrium states of a compressed beam; P_* — least force at which a deflected equilibrium state is possible; P_{**} — critical force according to the theory of the reduced modulus.

and the moments of these increases with respect to the point O_1 must equal the external load $P = P_+ + \Delta P$:

$$-\frac{EFb}{2a}\Delta l(1-\nu)+\frac{EFb^2}{4a}\varphi(1+\nu)=(P_++\Delta P)l\varphi. \tag{19.4}$$

We may use equations (19.3) and (19.4) to find both kinematic parameters φ and Δl:

$$\varphi=\frac{b(1-\nu)\Delta P}{2l(1+\nu)(P_{**}-P)}, \tag{19.5}$$

$$\Delta l=\frac{b^2\left(1+\nu-2\nu\frac{P}{P_*}\right)\Delta P}{4l(1+\nu)(P_{**}-P)}. \tag{19.6}$$

Here we introduce the notation

$$P_*=\frac{\nu EFb^2}{2al}, \tag{19.7}$$

$$P_{**}=\frac{\nu EFb^2}{(1+\nu)al}, \tag{19.8}$$

which correspond to the formulas (18.11) and (18.17) obtained previously.

Expressions (19.5) and (19.6) were derived under the assumption that unloading occurs in the left rod, whose force is analytically written in the form

$$\frac{\varphi b}{2}\geqslant\Delta l. \tag{19.9}$$

Substituting the expressions φ and Δl which have been found, we obtain this condition in the form

$$P\geqslant P_*, \tag{19.10}$$

Thus, the deflected equilibrium state of the beam assumed above is only possible when condition (19.9) is satisfied, i.e., if the load increases beginning at the level P_*. Consequently, the force, which we designated by P_+ above, coincides with the tangent-modulus load P_*.

Let us follow the change in the deflection of the upper end $v = \varphi l$ of the beam with an increase in the load P from the value P_* up to the value

P_{**}, writing the following instead of (19.5)

$$\varphi = \frac{b(1-\nu)(P-P_*)}{2l(1+\nu)(P_{**}-P)}. \tag{19.11}$$

This change is shown by the solid line in Figure 19.1. As may be seen, beginning with a value of the load P_*, the bending of the upper end of the beam monotonically increases and becomes infinite when $P = P_{**}$. Each point of this curve represents a definite position of equilibrium for the beam, and the curve as a whole designates the curve of equilibrium states. It must be noted that the /167 curve may only be realized continuously in the direction of increasing bending ($A \to B \to C$). If when $P = P_*$ (point A) we keep the beam from turning artificially and assume the possibility of rotation, let us say only at the point A', then the beam "does not jump" into the equilibrium state corresponding to point B, and the process will develop as shown by the dashed line. Thus, depending on the situation, any point of the region between the line $P = P_{**}$ and the curve ABC may represent the state of equilibrium.

What is the critical force for the beam under consideration — the force P_* or the force P_{**}? The answer to this question depends on what we mean by the term "critical force". In a certain sense, it is more natural to call the critical force P_*, since immediately after this force is reached deflected states of equilibrium become possible(*).

The new formulation of the problem compelled Shanley to characterize an equation with the form of (19.11) only as "the equation of equilibrium states of the beam" in order to avoid any problems pertaining to the determination of stability loss.

(*) Independently of Shanley's concepts, W. Koiter assumed that the critical states (determined by the point of bifurcation on the axis P) be divided into stable and unstable, depending on the sign of the derivative $\frac{dP}{dv}$; for $\frac{dP}{dv} > 0$ (as, for example, in the Shanley solution) the critical state is stable, and when $\frac{dP}{dv} < 0$ (see, for example, Figure 7.3) the critical state is unstable.

The following characteristic idea of Shanley, which was given by T. Karman in 1947 is interesting: "In the last thirty years many authors have discussed the theory of the stability loss of a beam compressed by an axial load which exceeds the elasticity limit. However, many objections were unavoidable. At the present time, Shanley has raised an objection which deserves some attention. The studies performed by Engesser and myself were based on the assumption that the equilibrium of a straight line beam becomes unstable when equilibrium forms appear which are infinitely close to the equilibrium form of a straight line beam under the same axial load. The correct answer to this problem can be obtained by substituting the so-called reduced modulus in the Euler formula for the elasticity m[illegible] The studies of Shanley represent a generalization of the problem". It is advantageous to turn our attention to the words "under the same axial load". The fact that the load does not change during the transition to the deflected state of equilibrium is a basic assumption of the Euler theory. In essence, this assumption imposes a definite limitation on the behavior of the new branch of the curve of equilibrium states, namely:

$$\frac{dP}{dv}=0 \text{ for } v=0. \tag{19.12}$$

The same limitation applies to the solution of Karman. Therefore, this solution cannot detect the possibility of bifurcation, which was promoted by Shanley. The initial assumption of Engesser has the same drawbacks.

Using the concept of Shanley, and prescribing the stability reserve with respect to the "tangent-modulus" load, we always arrive at simpler calculations than by using the formula of Engesser-Karman (the reduced modulus in the latter depends sometimes on the form of the cross section in a complex manner). Thus, in the concept of Shanley, fortunately depth of analysis is combined with simplicity of the final computational formulas. This concept rapidly gained in popularity. The curves for the equilibrium states were compiled by other authors for beams of a real form with continuously distributed deformability.

In order to reliably determine the practical importance of this concept,

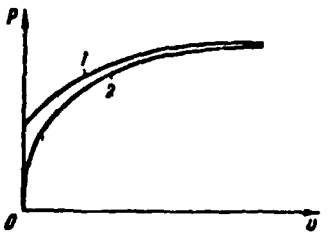

Fig. 19.2. Shanley curve 1 is the limiting curve for a set of curves (type 2) for cases of eccentric loading of a beam.

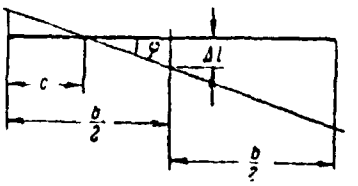

Fig. 19.3. With Shanley buckling, the unloading region determined by the section c continuously increases.

it is useful to use the beam loading process, assuming that the compressive force is proportional to the initial eccentricity. The result of this study is shown schematically by curve 2 in Figure 19.2. It is important to note that /169 with an increase in the initial eccentricity the curve will pass closer and closer to the Shanley curve 1: the latter is the limit to which the lower curve strives with an unlimited decrease in the initial eccentricity.

It thus follows that the region above the curve 1 cannot be realized in general, as a small eccentricity is always unavoidable. The bending begins to increase vigorously not at the critical force determined by the theory of the reduced modulus, but at the force calculated from the tangent modulus(*).

It is important to note that the concept of Shanley is not always properly understood. Sometimes the matter is treated as though Shanley found the possibility for the development of longitudinal bending without unloading on the convex side of the beam. In actuality, this is not the case.

Let us follow the change in the parameter c which determines the extent

(*) In the last analysis, the value of each idealized scheme lies primarily in the fact that the solution obtained with it is the limiting solution with respect to the solution of nonidealized schemes (for non-idealities which strive to zero). The schemes of Euler and Shanley have these limiting characteristics. The solution of Karman does not have this property.

of the unloading zones. According to Figure 19.3 we have

$$c = \frac{b}{2} - \frac{\Delta l}{\varphi}. \tag{19.13}$$

Substituting the expressions (19.5) and (19.6), we find

$$c = \frac{\nu b}{1-\nu}\left(\frac{P}{P_*} - 1\right). \tag{19.14}$$

With a gradual increase in the force P above the value P_* the size of c also increases, beginning with the value c = 0. When $P = P_{**}$, i.e., when the force P reaches the value of the critical force given by the theory of the reduced modulus, the magnitude of c reaches the value $c = \frac{\nu}{1+\nu} b$.

Thus, the process studied by Shanley takes place with a continuous increase /170 in the unloading zone, and the agreement between the final formula of Shanley and the formula proposed by Engesser does not indicate that the two concepts are completely identical.

Although our calculations pertain to the model of a column with linear strength increase, the qualitative conclusions remain valid for a rod with a continuously distributed elasticity with an arbitrary form of the relationship $\sigma = \sigma(\varepsilon)$.

In an exact study, the fact must be taken into account that the unloading modulus cannot remain constant infinitely, since the unloading follows Figure 19.4, a in its general outlines. Therefore, when the unloading process reaches the point A, the total rigidity of the system sharply decreases, and the Shanley curve acquires the descending section, as shown in Figure 19.4, b.

The article by F.R. Shanley was translated into Russian and used as the appendix in a book by Shanley "Analysis of the Weight and Strength of Aircraft Structures" (Oborongiz, 1957, Chapt. 18). A dynamic analysis of the phenomena studied above was given by V.D. Klyushnikov in the article "Stability of Compression of an Idealized Elastic-Plastic Rod" (Izvestiya AN SSSR, OTN, Mekhanika i Mashinostroyeniye, No. 6, 1964). For an analysis of the role of the decreasing unloading modulus, see the article by Ya.G. Panovko "The

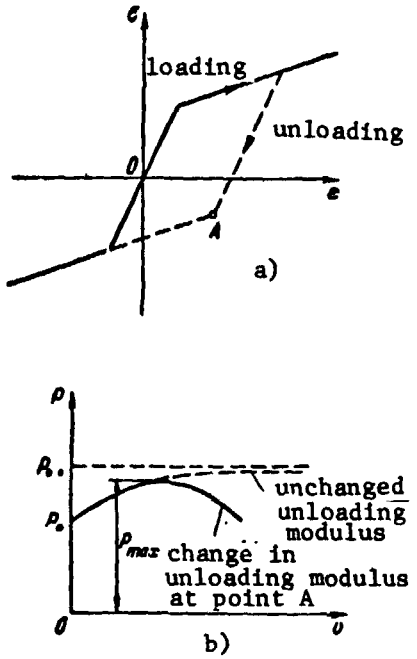

Fig. 19.4. a) Unloading modulus at point A changes its value; b) when $P = P_{max}$ the descending section of the curve for equilibrium states begins.

Critical Force of a Compressed Rod in the Inelastic Region" (Inzh. Sb., Vol. XX, Izdatel'stvo SSSR, 1954).

§ 20. Buckling of a Rod in a Statically Indeterminate System /171

Differences between the properties of statically determinate and statically indeterminate systems are well-known. In this section, the fact that the distribution of forces in rods of a statically indeterminate system depends on the rigidity of its elements is of importance for us.

Let us assume that the critical state is reached during the increase of the external load in any superfluous element of a statically indeterminate hinged-rod system, and that the rod bulges(*). Due to this, the effective longitudinal rigidity of this element naturally decreases, and it would not be absurd to assume that the force on this element also decreases. If this is the case, then the decreasing force is inadequate to maintain a curved form of equilibrium. Thus, such an unexpected situation may be conceived as follows: the critical state would produce conditions for restoring the stability of the rectilinear form of equilibrium, i.e., the rod "escapes" from the stability loss. Is this really the case?

(*) We should emphasize that we are only discussing superfluous rods. If the force is statically determinate (these rods are called necessary) in any rod of a statically indeterminate system, then the condition for stability loss of this rod differs in no way trom the conditions for an isolated rod.

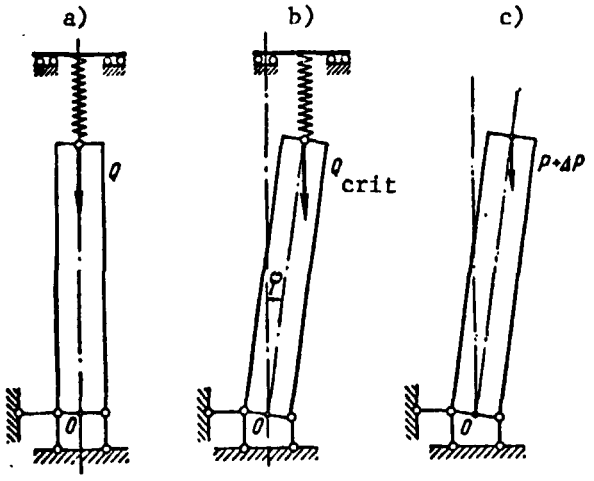

Fig. 20.1. Case when compressive force is statically indeterminate; a) pre-critical state; b) deflected state of system; c) deflected state of beam .

This problem was formulated in 1932 by I.M. Rabinovich, who first solved the problem of determining the critical force for a superfluous rod included in an elastic statically indeterminate system. In this case it was found that the situation, the development of which we suspected, is impossible in actuality, and the critical value of the stress in a rod included in a statically indeterminate elastic system is the same as for an isolated rod.

The problem of the elastic-plastic buckling of superfluous rods was studied by A.A. Il'yushin in 1960. The problem which he solved pertains to problems of the Euler type in the sense that the stability loss is investigated in the case of unchanged loading. We will /172 discuss the connection between this problem and the concept of Shanley at the end of this section.

As has been shown, in this case a situation actually exists about which we wrote earlier. Naturally, the rod "cannot" completely avoid stability losses, but the critical state occurs at forces which differ from the critical force P_{**} of Engesser-Karman for an isolated rod.

Thus, the static indeterminacy of a system has no influence on the critical force of an elastic rod, wheras it is important when determining the critical force for an elastic-plastic rod. How can we explain this principal difference?

The reason for this difference lies in the following important, although sometimes unnoted fact: the convergence of the ends of an elastic rod in the

case of stability loss has a second order of smallness as compared with buckling, whereas in the case of an elastic-plastic rod this convergence has the order of smallness of the buckling (due to the compression of the axis — see, for example, Figure 18.7).

Let us treat the solution of A.A. Il'yushin on the simplified model shown /173 above in Figure 18.4, but we shall assume that the upper end of the beam is connected with an elastic structure, which may be schematically represented in the form of a spring (Figure 20.1, a). Let us use Q to designate the load on a system. Then the corresponding force which compresses the beam will be

$$P = -\frac{Q}{1+\frac{ca}{2EF}}, \tag{20.1}$$

where c is the spring rigidity. Let us assume that for a certain value of the external load $Q = Q_{crit}$ stability losses of the beam occur (20.1, b) in the Euler sense, i.e., a deflected form of the beam equilibrium occurs, which is infinitely close to the basic form. The supporting rods are deformed as is shown in Figure 18.7 when deriving the Engesser-Karman formula.

It is important to note the sag of the central point 0. Due to this sag, the spring is extended, and consequently is subjected to the additional force $c\Delta l$. The force transmitted to the beam is changed by the quantity

$$\Delta P = -c\,\Delta l. \tag{20.2}$$

Let us clarify how a deflected state of equilibrium for the beam (Figure 20.1, c) is possible for any force P. Additional contractions of the supporting rods are determined by the previous formulas (18.12), and the additional compressive forces in the rods — by the formulas (18.13). The equation of moments with respect to point 0 has the form

$$-\Delta P_1 \frac{b}{2} + \Delta P_2 \frac{b}{2} = (P + \Delta P) l\varphi. \tag{20.3}$$

Based on the definition of the problem being solved, we are discussing an infinitely small deflection of the beam , so that the displacements φ and

Δl and also the additional forces ΔP_1, ΔP_2 and ΔP are infinitely small quantities. Therefore, we must omit the term ΔP in equation (20.3), after which the equation of moments assumes the form

$$-\Delta P_1 \frac{b}{2} + \Delta P_2 \frac{b}{2} = Pl\varphi. \tag{20.4}$$

The equation for the projection onto the vertical axis may be written in the form /174

$$\Delta P_1 + \Delta P_2 = \Delta P. \tag{20.5}$$

Substituting expressions (19.2) and (20.2) in these equations, we arrive at the system which is homogeneous with respect to the displacements φ and Δl:

$$\left.\begin{aligned} \left[\frac{EFb^2}{4a}(\nu+1) - Pl\right]\varphi + \frac{EFb}{2a}(\nu-1)\Delta l = 0, \\ \frac{EFb}{2a}(\nu-1)\varphi + \left[\frac{EF}{a}(\nu+1) + c\right]\Delta l = 0. \end{aligned}\right\} \tag{20.6}$$

The deflected state of equilibrium is only possible under the condition that the determinant of this system equals zero. Expanding the determinant, we obtain an equation which contains the single unknown — the critical force which we shall designate by P_{***}. From this equation, we obtain

$$P_{***} = \frac{EFb^2}{4al}\left[1 + \nu - \frac{(1-\nu)^2}{1+\nu+\alpha}\right], \tag{20.7}$$

where the dimensionless parameter

$$\alpha = \frac{ca}{EF} \tag{20.8}$$

characterizes the relative rigidity of the elastic system, which was shown schematically in the form of a spring.

Naturally, the following well-known cases follow from the formula (20.7):

1. The case $\nu = 1$ (elastic stability loss). The Euler formula is obtained from formula (20.7).

2. The case $\alpha = 0$ (isolated rod). In this case, formula (20.7) reduces to formula (18.17) which determines the critical force P_{**} according to the Engesser-Karman theory.

To determine the critical external load Q_{crit}, it is necessary to use

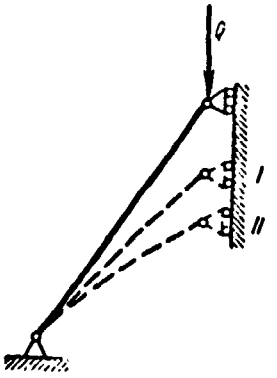

Fig. 20.2. A compressive force in the rod arises with stability loss (transition from state I to state II).

formula (20.1). We thus obtain

$$Q_{crit} = \frac{EFb^2}{4al}\left[1 + \nu - \frac{(1-\nu)^2}{1+\nu+\alpha}\right](1 + 0{,}5\,\alpha). \qquad (20.9)$$

It must not be assumed that $\alpha \geq 0$ always. A.A. Il'yushin pointed out the existence of a class of additionally loaded structures, for which $\alpha < 0$. These structures are such that in the case of buckling the sag of the rod does not entail a decrease, but an increase in the force P_{***} acting on the rod, i.e., the quantity ΔP is greater than zero. In formal terms, the additionally loaded systems may /175 have the form shown in Figure 20.1, but a negative rigidity must be attributed to the spring.

The additionally loaded systems may be encountered more frequently than is assumed. Thus, for example, this is the case for the interesting system shown in Figure 20.2. We shall assume that, with an increase in the load Q, the rod reaches the critical state I. In the case of buckling, there is a decrease in the length of the axis, and the junction point will move from position I to position II. As the junction point falls, the stress in the rod increases, i.e., the system belongs to the category of additionally loaded systems. In such cases, we obtain $P_{***} < P_{**}$ according to formula (20.7).

As was indicated above, this solution was based on the concept of Euler-Karman. The study of stability was made on the assumption that the load Q is the same in the basic state of equilibrium and in the deflected state. In § 19 we noted that this approach imposes the additional relationship $\frac{dP}{dv} = 0$ on the solution, which in actuality does not exist. Let us renounce this condition, and show that for any load deflected states of equilibrium may occur in the process of an increasing load, i.e., under the conditions studied by Shanley.

Let us verify the possibility of the following process. Let us assume that, beginning with a certain load Q_+, when the force compressing the beam equals P_+, a gradually increasing deflection of the beam occurs, and a definite deflected state of equilibrium corresponds to each value of $Q > Q_+$.

The extension of the spring and the sag Δl equal to it will be determined from the position corresponding to the load Q_+. During the loading process, /176 the total load is $Q_+ + \Delta Q$, and the force compressing the beam is $P_+ + \Delta P$. Consequently, the additional force acting on the spring equals the difference $Q - \Delta P$, and the corresponding extension of the spring may be written in the form

$$\Delta l = \frac{\Delta Q - \Delta P}{c}. \tag{20.10}$$

Thus, instead of (20.2), we obtain

$$\Delta P = -c\,\Delta l + \Delta Q. \tag{20.11}$$

In this case, the equation of moments must be given in the form (20.3), and we must substitute P_+ instead of P, and (20.11) instead of ΔP (this increase is small, but finite). Thus, we obtain

$$-\Delta P_1 \frac{b}{2} + \Delta P_2 \frac{b}{2} = (P_+ - c\,\Delta l + \Delta Q)\,\varphi l. \tag{20.12}$$

The equation for the projection is similar to the equation (20.5) and may be written in the form

$$\Delta P_1 + \Delta P_2 = -c\,\Delta l + \Delta Q. \tag{20.13}$$

In the last equations ΔP_1 and ΔP_2 are determined by the previous formulas (18.13). Equations (20.12) and (20.13) differ from equations (20.4) and (20.5) as follows:

1. In the equation for the projection, the fact is taken into account that the change of the load on the rod is not only connected with the contraction of the beam by Δl, but also with an increase in the external load by ΔQ.

2. Deflections Δl and φ (and the increases ΔP_1, ΔP_2, ΔP along with this) are regarded as small but finite quantities. It is assumed that specific numerical values correspond to each value of the load $Q > Q_+$.

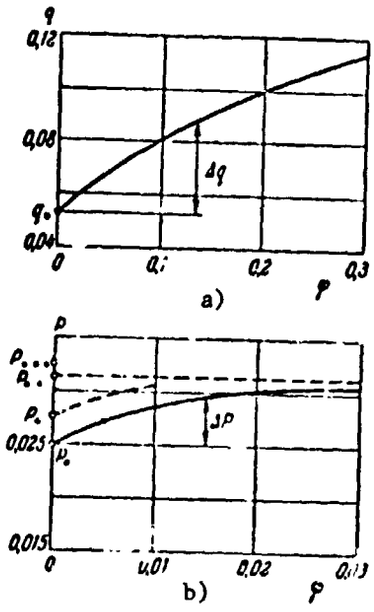

Fig. 20.3. Curves for equilibrium states; a) connection between dimensionless parameter of the load and the beam angle of deflection; b) connection between dimensionless compressive force and the beam angle of deflection.

Let us first find the force P_+, beginning with which the process described above may occur. For this purpose, it is sufficient to study the equation (20.12) in the case of the infinitesimal quantities φ, Δl and ΔQ. We find the following from this equation

$$\Delta l : \frac{\varphi b}{2} = \frac{1+\nu}{1-\nu} - \frac{4P_+ la}{(1-\nu)EFb^2}. \qquad (20.14)$$

In order that the assumed scheme for the deformation of supporting rods may hold (i.e., in order that the increase ΔP_1 is less than zero), expression (20.14) must be less than unity. We thus obtain the inequality /177

$$P_+ > \frac{\nu EFb^2}{2al}. \qquad (20.15)$$

Thus, the least value of the force P_+ at which the process under consideration is possible

$$P_+ = \frac{\nu EFb^2}{2al}, \qquad (20.16)$$

precisely coincides with the tangent-modulus critical force (18.11).

We can now find the connection between the increase in the load ΔQ and the angle of deflection φ from equations (20.12) and (20.13)

$$\Delta Q = \frac{EF}{2} \frac{b\varphi\,[2b\nu + a\,(b + 2\varphi l)]}{a\,[b + 2\varphi l\,(1+\nu) : (1-\nu)]} \qquad (20.17)$$

This relationship is illustrated in Figure 20.3, a, and the dimensionless quantities are plotted along the ordinate axis

$$q = \frac{Q}{\quad}. \qquad (20.18)$$

When the graph was drawn, it was assumed that $\nu = 0.5$, $a = 1$, $b =$ [illegible]. We use

q_* to designate the dimensionless load $Q_*:cb$, at which the beam compression force equals P_*. If we trace the corresponding change in the force in the beam , we obtain the graph shown in Figure 20.3, b. The following dimensionless quantities are plotted along the ordinate axis

$$p=\frac{P}{cb}. \tag{20.19}$$

Thus, the deflections begin with the load Q_*, i.e., before the force P_{**} or the force P_{***} occur in the beam .

If we investigate the phenomenon of buckling from the position advanced by Shanley, it is found that the critical force (i.e., the force at which buckling begins) is determined by the value P_* not only for isolated rods, but also for superfluous rods included in statically indeterminate systems.

Naturally, this does not mean that there is an identical character of reaching the critical state in superfluous rods and rods in which the compressive force is statically indeterminate. Let us note the following words of I.M. Rabinovich: "The critical load of statically determinate rods may be validly called 'catastrophic'. The critical load of 'a superfluous' rod is not catastrophic, since generally speaking a girder would remain unchanged after the complete failure of this rod. It stands to reason that it would remain unchanged with partial failure due to bulging as a result of buckling." /178

The study of I.M. Rabinovich was given in his work "Ob ustoychivosti sterzhney v staticheski neopredelimykh sistemakh" (Stability of Rods in Statically Indeterminate Systems) (Gostransizdat, Moscow-Leningrad, 1932). The work of A.A. Il'yushin "Elastic-Plastic Stability of a Structure Including Rod Elements" was given in "Inzhenerniy sbornik", Vol. XXVII, 1960; for the solution of A.A. Il'yushin see the article by V.G. Zubchaninov "Stability of Rods Beyond the Elasticity Limit in Certain Structures" (Inznenerniy sbornik, Vol. XXVIII, 1960).

An investigation of these problems under the conditions of additional loads is given in the article by Ya.G. Panovko "Elastic-Plastic Buckling of

Rods in Statically Indeterminate Systems" (Izvestiya AN SSSR, OTN, Mekhanika i mashinostroyeniye, No. 2, 1962).

§ 21. Stability Loss in the Case of Material Creep

/179

Beginning in 1946, the problem of the stability of structures in the case of material creep was discussed in the scientific technical literature. The influence of creep has such unusual effects that the concept "stability loss" has taken on a new meaning, which does not agree with even one of the variations given in the preceding sections.

The phenomenon of a deformation increase in time, which occurs even with unchanged loads, is called material creep(*). For steel this phenomenon is only important at rather high temperatures. However, in many non-ferrous metals, light alloys, and high-polymer materials it may be observed at room temperature.

It has been established that creep of polymer materials becomes much more intense if, in addition to the basic static load, the material is subjected to the action of an additional vibration load (even if the latter is small). Apparently, this phenomenon of vibration creep is connected with a decrease in the material elasticity modulus due to warming up in the case of vibrations. Due to a decrease in the elasticity modulus, the amplitudes of the oscillations increase, and consequently the material heats up very greatly, there is a further decrease in the elasticity modulus, etc. Thus, the accompanying vibration leads to a continuous decrease in the material elasticity modulus, which is manifested in an accelerated increase in deformations caused by the main static load.

The ability of materials to undergo creep may have a significant influence on the state of the structure when it is in operation. Recently, due to the

(*) Sometimes this process is called the aftereffect, and the term "creep" is given a broader meaning, with creep designating the aftereffect, and relaxation.

development of tube construction, the problems of the creep of turbine disks and blades operating at high temperatures have become particularly important. There are several cases when due to creep the clearances between the ends of the blades and the turbine housing have overlapped, and a breakdown has occurred.

In addition, creep leads to a gradual redistribution of stresses in statically indeterminate systems. This must be taken into account in the design stage, keeping the fact in mind that such structures (for example, railroad bridges) may last tens and even hundreds of years. /180

For a theoretical solution of each problem of the loading of a structure, with allowance for creep, we must know the law governing creep — the relationship between the acting stress σ and the creep rate ε_c. Experimental data enable us to give this law in the form of a power relationship:

$$\dot{\varepsilon}_c = \left(\frac{\sigma}{\lambda}\right)^m. \tag{21.1}$$

In addition, when the stresses themselves change in time, also the elastic deformation rate must be taken into account, which is determined from the Hooke law:

$$\dot{\varepsilon}_e = \frac{\dot{\sigma}}{E}. \tag{21.2}$$

Thus, the total deformation rate depends both on the stress and on the rate at which it changes:

$$\dot{\varepsilon} = \left(\frac{\sigma}{\lambda}\right)^m + \frac{\dot{\sigma}}{E}, \tag{21.3}$$

where λ and m are the material constants (at a fixed temperature). Such simplified concepts are adequate for clarifying all the characteristics of stability loss in the case of creep. We shall adhere to these concepts, although the experimental data also provide other variations for describing the creep process.

There are two approaches toward analyzing stability loss in the case of creep. The first assumes ideal conditions (absence of initial bending and eccentricity of the compressive force). Bulging occurs after certain initial perturbations (impact or initial displacement). The second approach is based

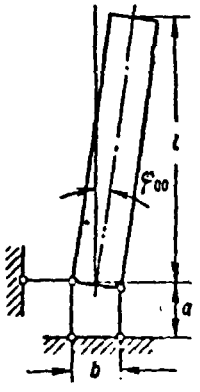

Fig. 21.1. In the beginning state the beam axis forms an angle φ_{00} with the vertical.

on certain given disturbances of the ideal conditions (for example, initial bending). We shall examine the problem in this way.

In the preceding sections of this chapter, we used the model of the beam shown in Figure 21.1, assuming that the creep of the material in the supporting rods was described by equation (21.3). Let us assume that /181 the beam is loaded by the compressive force P which is less than the Euler force

$$P < P_e = \frac{EFb^2}{2al}, \tag{21.4}$$

and the stresses in the supporting rods do not exceed the proportionality limit.

We shall assume that before the loading the beam axis has an initial small deflection from the vertical by the angle φ_{00}. Immediately after applying the load P, the angle of deflection will be

$$\varphi_0 = \frac{\varphi_{00}}{1 - \frac{P}{P_e}}. \tag{21.5}$$

Fig. 21.2. Deflected state of the beam at instantaneous time.

For the further creep process, it is important that, due to asymmetry of the system, the stress in the right rod be greater than the stress developing in the left rod from the very beginning. Due to the different stress level, the creep of both rods will behave differently. According to (21.3), deformations of the right rod will increase more rapidly than deformations of the left rod. It is important to note that due to this the system asymmetry will be increased. Consequently, the difference in the deformation rates of both rods will increase. This means that the deflection of the beam axis from the vertical will occur at a constantly increasing rate.

Strictly speaking, the processes studied here are dynamic. However, since they are comparatively slow, the inertial effects may be assumed not to exist, and we may write and study the equation of equilibrium, instead of the differential equations of motion.

An interesting feature of this phenomenon is that the changing stresses in the rods correspond to a constant load, and due to this the beam deflection rate is variable. As a quantitative study shows, for certain conditions the /182
deformation rate can strive to infinity in a certain period of time. This represents the phenomenon of stability loss of the beam being considered.

Let us assume that φ is the beam angle of deflection at the moment of time t, P_1 and P_2 — compressive forces in the left and right rods. Then the equations of the beam equilibrium have the form (Figure 21.2)

$$\left.\begin{aligned} P_1 + P_2 &= P, \\ -P_1\frac{b}{2} + P_2\frac{b}{2} &= Pl\varphi. \end{aligned}\right\} \tag{21.6}$$

Just as before, b is the distance between the supporting rods, l — height of the beam. Using these equations, we find the compressive forces in both rods:

$$\left.\begin{aligned} P_1 &= \frac{P}{2}\left(1 - 2\varphi\frac{l}{b}\right), \\ P_2 &= \frac{P}{2}\left(1 + 2\varphi\frac{l}{b}\right). \end{aligned}\right\} \tag{21.7}$$

On the other hand, these forces are connected with the deformation rates of the rod by the relation (21.3):

$$\frac{d\varepsilon_1}{dt} = \left(\frac{P_1}{\lambda F}\right)^m + \frac{\dot{P}_1}{EF}, \quad \frac{d\varepsilon_2}{dt} = \left(\frac{P_2}{\lambda F}\right)^m + \frac{\dot{P}_2}{EF}. \tag{21.8}$$

(Just as above, F is the cross section area of each of the rods).

Let us substitute $\varepsilon_1 = \frac{\Delta a_1}{a}$ and $\varepsilon_2 = \frac{\Delta a_2}{a}$ in the left-hand sides of these equations (a is the length of the supporting rods), and in the right-hand

sides — the expressions (21.7). We then obtain

$$\left.\begin{aligned}\frac{d\Delta a_1}{dt} &= a\left[\frac{P}{2\lambda F}\left(1-\frac{2\varphi l}{b}\right)\right]^m - \frac{P\dot{\varphi}al}{bEF},\\ \frac{d\Delta a_2}{dt} &= a\left[\frac{P}{2\lambda F}\left(1+\frac{2\varphi l}{b}\right)\right]^m + \frac{P\dot{\varphi}al}{bEF}.\end{aligned}\right\} \tag{21.9}$$

By means of these relationships, the contraction rates of both supporting rods are connected with the angle of deflection of the beam. However, there is a kinematic relationship between the contractions themselves and this angle /183

$$\varphi = \varphi_0 + \frac{\Delta a_2 - \Delta a_1}{b}, \tag{21.10}$$

Differentiating this equation with respect to time, we obtain

$$\dot{\varphi} = \frac{1}{b}\left(\frac{d\Delta a_2}{dt} - \frac{d\Delta a_1}{dt}\right). \tag{21.11}$$

With allowance for expressions (21.9), we obtain the differential equation for the angle φ of the beam deflection

$$\dot{\varphi} = \frac{a}{b}\left[\left(1+\frac{2\varphi l}{b}\right)^m - \left(1-\frac{2\varphi l}{b}\right)^m\right]\left(\frac{P}{2\lambda F}\right)^m + \frac{2P\dot{\varphi}al}{b^2EF}; \tag{21.12}$$

It assumes separation of the variables, and thus leads to a quadrature. Let us set, for example, m = 3(*). Then, instead of (21.12), we obtain

$$\dot{\varphi} = \varphi\left[1.5\left(\frac{b}{l}\right)^3 + 2\varphi^3\right]k, \tag{21.13}$$

where

$$k = \left(\frac{P}{P_e}\right)^3\left(\frac{E}{2\lambda}\right)^3\left(\frac{b}{a}\right)^3 : \left(1-\frac{P}{P_e}\right). \tag{21.14}$$

Separating the variables and integrating, we obtain

$$t = \frac{1}{k}\int \frac{d\varphi}{\varphi\left[2\varphi^3 + 1.5\left(\frac{b}{l}\right)^3\right]} + C. \tag{21.15}$$

We thus have

$$t = \frac{l^3}{3kb^3}\ln\frac{\varphi^3}{2\varphi^3 + 1.5\left(\frac{b}{l}\right)^3} + C. \tag{21.16}$$

(*) Naturally, for real materials m cannot be a whole number. We assume that m is whole to simplify the solution. Assuming that m is odd, we obtain a single description for the process of both compression and extension.

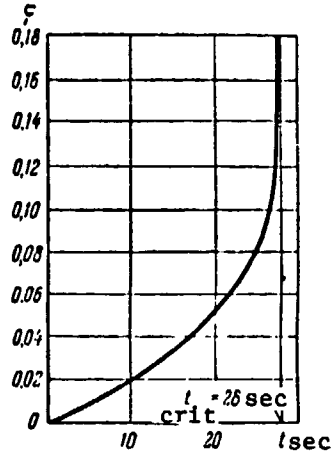

Fig. 21.3. Dependence of the angle φ on time t. When $t = t_{crit}$ the angle φ increases infinitely.

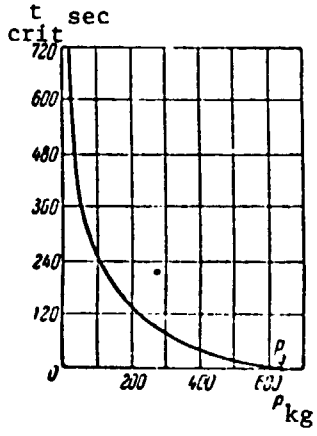

Fig. 21.4. Critical time decreases with increase in the compressive force P. When $P = P_{crit}$ the critical time equals zero.

In order to determine the constant C we must use the initial condition

$$\varphi = \varphi_0 \text{ for } t = 0, \tag{21.17}$$

which yields /184

$$C = -\frac{l^3}{3kb^3} \ln \frac{\varphi_0^2}{2\varphi_0^2 + 1.5\left(\frac{b}{l}\right)^3}. \tag{21.18}$$

Now returning to expression (21.16), we finally have the angle φ as a function of time:

$$\varphi = \sqrt{\frac{1.5\left(\frac{b}{l}\right)^3 \varphi_0^2 e^{3kt\left(\frac{b}{l}\right)^3}}{1.5\left(\frac{b}{l}\right)^3 + 2\varphi_0^2\left[1 - e^{3kt\left(\frac{b}{l}\right)^3}\right]}}. \tag{21.19}$$

We should note that for a certain value of the time t the denominator of the radicand becomes equal to zero, i.e., the beam angle of deflection φ strives to infinity. The time t, in which there is an infinite increase in the deflections, may be said to represent the lifetime of the beam . This time is called the critical time. We find from expression (21.19) that the critical time equals

$$t_{crit} = \frac{1}{3}\left(\frac{P_э}{P}\right)^3 \left(\frac{2\lambda}{E}\right)^3 \left(\frac{al}{b^2}\right)^3 \ln\left[1 + \frac{3}{4}\left(\frac{b}{\varphi_0 l}\right)^3\right]\left(1 - \frac{P}{P_э}\right). \qquad (21.20)$$

For illustration, let us use the following values of the constants:

$$E = 5 \cdot 10^5 \text{ kg/cm}^2,\ \lambda = 17\,100 \text{ kg} \cdot \text{cm}^{-2} \text{sec}^{1/3},\ \frac{l}{b} = 100,$$

$$\frac{a}{b} = 4,\ \varphi_{00} = 2 \cdot 10^{-4},\ F = 1 \text{ cm}^2,\ P = 500 \text{ kg}$$

With these values, we obtain the following according to formula (16.3):

$$P_e = 625 \text{ kg}$$

i.e., the condition $P < P_e$ is satisfied.

Using formula (21.5) we calculate $\varphi_0 = 10^{-3}$. Figure 21.3 shows the relationship $\varphi = \varphi(t)$ [calculated by means of expression (21.19)]. The critical time according to formula (21.21) equals $t_{crit} = 28$ sec.

As may be seen from formula (21.20), the critical time depends not only on the parameters of the beam itself, but also on the value of the compressive force P $\left(\text{more precisely, on the } \frac{P}{P_e} \text{ ratio}\right)$. When $P = P_e$, the beam immediately loses stability, since according to (21.20) the critical time /185
equals zero independently of the creep characteristics. When $P < P_e$ the critical time is greater, the smaller is the ratio $\frac{P}{P_e}$. Figure 21.4 shows the dependence of the critical time on the force P for the conditions of the example solved above. It is apparent that for any force $P > 0$ in the last analysis stability loss occurs, and therefore it is difficult to speak about the critical force; the concept of the critical time has much greater determinacy.

It is interesting to note that with a linear connection between the steady creep rate and the acting stress [i.e., when $m = 1$ in 21.3)] the stability loss is impossible in the sense given above. Assuming $m = 1$ in the differential equation (21.12), we obtain

$$\frac{d\varphi}{dt} = \frac{EP}{\lambda(P_e - P)}\varphi. \qquad (21.21)$$

Using the initial condition (21.17) given previously, integrating we obtain /186

$$\varphi = \varphi_0 e^{\frac{EP}{\lambda(P_e - P)}t}. \qquad (21.22)$$

This relation is much "more smooth" than relationship (21.19), since — although the angle φ increases with increasing velocity — it remains limited for any finite t. In this case, we may arbitrarily assume that stability loss corresponds to the moment when the rate of increase in the angle φ reaches a certain limiting value.

The first research in this field belongs to A.R. Rzhanitsyn (see his article "Deformation Processes in Structures Made of Elastic-Viscous Elements", Doklady AN SSSR, Vol. 52, No. 1, 1946; A.D. Ross (see the journal "The Struct. Eng.", No. 8 in 1946, and No. 5 in 1947), A.M. Freudental (Report to the Sixth International Congress on Applied Mechanics, Paris, 1946) and J. Marin (see the journal "Journal of Applied Physics", No. 1 in 1947). Up to the present, there has been a very great number of theoretical and experimental studies. These studies were collected together in 1958 by N. Hoff (see the periodical collection of foreign translations "Mekhanika", No. 1 (59) in 1960). Here, in particular, the interesting paradox is discussed which was found by Yu.N. Rabotnov and S.A. Shesterikov (see their article "Stability of a Rod Under Creep Conditions", Prikladnaya Matematika i Mekhanika, No. 6, 1956.

Some of the problems of stability loss in the case of creep were examined in the book by N. Hoff "Buckling and Stability" (Foreign Literature Press, Moscow, 1955). See also the article by V.I. Rosenblyum "Stability of a Compressed Rod in the Case of Creep" (Inzh. Sbornik, Izdatel'stvo AN SSSR, Vol. 18. 1954) and the work by A.R. Rzhanitsyn "Stability in the Case of Creep" (Collection: "Problemy ustoychivosti v stroitel'noy mekhanike" [Problems of Stability in Structural Mechanics], Stroyizdat, Moscow, 1955, pp. 104 - 118.

The general problems of creep were studied in the book by N.N. Malinin (Osnovy raschetov na polzuchest' [Fundamentals of Creep Calculations], Mashgiz,

1948), N.Kh. Arutyunyan ("Nekotoryye voprosy teorii polzuchesti" [Problems in the Theory of Creep], Gostekhizdat, 1955) and L.M. Kachanov ("Teoriya polzuchesti" [Theory of Creep], Fizmatgiz, 1960).

For the phenomenon of vibration creep, see the article by G.I. Barenblatt in the journal "Prikladnaya matematika i mekhanika", Vol. 30, No. 1, 1966.

PART 2

OSCILLATIONS OF ELASTIC SYSTEMS

INTRODUCTION

The theory of mechanical oscillations has very diverse and multi-faceted applications in almost every field of technology. Irrespective of the structural appearance of different mechanical systems, their oscillations obey the same physical laws, whose study is the purpose of general theory. /187

The linear theory of oscillations has been developed most extensively. Even in the XVIII century, in the "Analytical Mechanics" of Lagrange, it was developed for systems with several degrees of freedom. The bases of the linear theory of oscillations of systems of an infinite number of degrees of freedom (i.e., with a continuous distribution of mass over the entire volume of a deformable system) were developed in the studies of several authors in the XIX century (especially Rayleigh). In the XX century, the linear theory was completed. Today, the complexity of studies of oscillatory processes in linear systems is only connected with the validity of determining the essential degrees of freedom and determining the external disturbances, i.e., selecting a computational scheme. Some problems of linear theory are examined below in Chapter VI.

Many problems of the oscillations of mechanical systems as a function of specific relationships between parameters assume both a linear and a nonlinear formulation. For example, these are the problems of the action of a mobile load, which arose more than a hundred years ago when building large railway bridges. Later, other applications of this theory were determined (for example, oscillations of pipelines). The specifics of these problems have

N74-14628

been expressed so clearly that we have devoted a separate chapter to them (Chapter VII). We have been guided by the same considerations in discussing in a special chapter (Chapter VIII) the unusual problems of dynamic aeroelasticity, which are very important not only for the theory of aircraft, but also for structures to be used "on the earth". /188

The last two chapters (Chapters IX and X) are devoted to purely nonlinear problems. Many physical phenomena which are observed during the oscillations of mechanical systems cannot be explained merely by linear theory. Therefore, the nonlinear theory of oscillations, which has been extensively developed recently, can be used to apply small corrections to the results obtained from linear theory. The role of nonlinear theory is much more important — it can be used to describe phenomena which disappear from view in a linear examination. It must be noted that these phenomena are related to nonlinear (even very small!) terms of differential equations of motion.

Unfortunately, as a rule these equations cannot be solved in closed form. Therefore, the efforts of the formulators of nonlinear theory, beginning with Poincaré(*) and Lyapunov (**) were directed toward compiling rational algorithms making it possible to obtain approximate results with a certain level of accuracy. Some of the methods of nonlinear theory make it possible to compile successive approximations of greater and greater accuracy (the methods of Poincaré and Lyapunov, the method of Krylov(***) — Bogolyubov); other methods

(*) Henri Poincaré (1854 - 1912) was a French mathematician, a member of the Paris Academy of Sciences from 1887. His main works are devoted to a qualitative theory of differential equations, mathematical physics, and celestial mechanics.

(**) Aleksandr Mikhaylovich Lyapunov (1857 - 1918), mathematician and mechanician, from 1900 an associate member of the Russian Academy of Sciences; from 1901, an academician. The founder of the contemporary theory of stability of motion, the author of several works on mathematical analysis and mathematical physics.

(***) Nikolay Mitrofanovich Krylov (1879 - 1955), author of several works on mathematical physics and mechanics. From 1922, member of the UkSSR Academy of Sciences; from 1928 — associate member of the USSR Academy of Sciences; from 1929 — academician.

(for example, the method of Van der Pol) make it possible to obtain only the first approximation (if it is assumed that the linear theory gives a zero approximation).

The particular practical importance of the first approximation must be acknowledged. A description of all specific nonlinear phenomena is most frequently included in the first approximation. At the same time, the amount of /189
computations necessary to compile higher approximations sharply increases with each subsequent approximation step. However, there is one consideration which frequently casts in doubt the advantage of compiling higher approximations: the parameters in the equations of motion of specific mechanical systems are only known with a certain limited accuracy. Therefore, it is logical to compile an approximation only up to the level of accuracy which corresponds to the accuracy of specifying the parameters. In many nonlinear problems, it is reasonable to deal with the first approximation — compiling higher approximations can only give the illusion of increased accuracy. The literature contains examples of "refined" solutions of specific nonlinear problems with thoroughly determined initial values of the parameters. Such solutions appear to be quite simple. In this connection, the problems examined in chapters IX and X are only solved in the first nonlinear approximation. Such a simplified formulation is particularly valid in a book such as this.

CHAPTER VI

CERTAIN PROBLEMS OF OSCILLATIONS OF LINEAR SYSTEMS

This chapter discusses simple problems involved in the theory of oscillations of linear mechanical systems, but in selecting certain aspects of the examination we have discarded the traditions in the scientific literature. Part of Sections 22 - 26 is devoted to free oscillations; Sections 27 - 31 are devoted to forced oscillations. Section 32 examines parametric excitation of oscillations. The last sections 33 - 36 discuss certain special problems of the action of friction forces. /190

§ 22. System with a Fractional Number of Degrees of Freedom

A certain amount of care must be taken when discussing results derived from studying idealized systems.

Let us present a well-known example. Friction forces very frequently be ignored when determining the eigenfrequencies of oscillations of mechanical systems. However, if we do not take into account the friction forces when analyzing free oscillations as a whole, a conclusion is reached which explicitly contradicts the experimental facts — oscillations are not damped and continue always. A correct determination of the development of free oscillations must take into account friction forces.

The lack of validity in individual results of schematized theories is unavoidable. Therefore, when encountering partial inconsistencies, it is necessary to establish the applicability limits of the theory, and not hurry with a complete discussion of it. The following problem is discussed in this way.

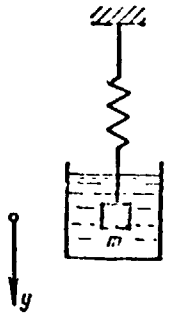

Fig. 22.1. Elastic-viscous system with 1 degree of freedom.

Let us study the motion of a simple system with one degree of freedom (Figure 22.1). We shall assume that a load suspended in an elastic manner is disturbed from a state of equilibrium, and after this is left to itself. We shall assume that, when the load moves, in addition to the elastic resistance cy, the force of viscous resistance arrises — $k\dot{y}$ (y — displacement of the load from the equilibrium position, $\dot{y}$ — its velocity, c — rigidity of the elastic connection, and k — viscosity coefficient). We shall also assume that the mass m of the load is very small. If we assume that m = 0, the inertia term will not be included in the differential equation of motion /191

$$k\dot{y} + cy = 0 \tag{22.1}$$

The solution of this equation

$$y = Ae^{-\frac{ct}{k}} \tag{22.2}$$

contains only one constant A, and therefore cannot satisfy simultaneously both initial conditions

$$y(0) = y_0, \quad \dot{y}(0) = v_0.$$

If, for example, it is necessary to satisfy the first condition, then we obtain $A = y_0$ and the solution assumes the form

$$y = y_0 e^{-\frac{ct}{k}}, \tag{22.3}$$

and

$$v = \dot{y} = -\frac{cy_0}{k} e^{-\frac{ct}{k}}. \tag{22.4}$$

It is interesting that this solution "imposes" the following value on the initial velocity

$$\dot{y}(0) = -\frac{cy_0}{k}, \tag{22.5}$$

which may differ as much as desired from the value of v_0 which is given independently. Relationship (22.5) follows directly from Equation (22.1). It implies that the displacement and velocity are always proportional to each other:

$$\dot{y} = -\frac{cy}{k}. \tag{22.6}$$

For example, the following conditions for the beginning of motion indisputably hold: the load is displaced from the equilibrium position at the distance y_0, and then is released with zero initial velocity. However, the possibility of this is contradicted by Expression (22.5), and it may be concluded that, if at the beginning of motion the displacement is $y(0) = y_0$, the velocity must equal $\frac{cy_0}{k}$. In exactly the same way, if the initial velocity v_0 is given, then this completely determines the initial displacement /192

$$y_0 = -\frac{kv_0}{c}. \tag{22.7}$$

It is found that the solution of the degenerate problem under consideration cannot simply reflect the given initial conditions, and it is impossible "to include" all the factors of the beginning of motion in the solution which is found.

In order to clarify the nature of this conflict, we must turn to the complete equation and examine its solution in the case of finite values of the mass m. The complete differential equation of motion of the mass m:

$$m\ddot{y} + k\dot{y} + cy = 0 \tag{22.8}$$

has the following solution for large values of k

$$y = e^{-\frac{kt}{2m}}\left(y_0 \operatorname{ch}\sqrt{\frac{k^2}{4m^2} - \frac{c}{m}}\,t + \right.$$
$$\left. + \frac{v_0 + \frac{ky_0}{2m}}{\sqrt{\frac{k^2}{4m^2} - \frac{c}{m}}} \operatorname{sh}\sqrt{\frac{k^2}{4m^2} - \frac{c}{m}}\,t\right). \tag{22.9}$$

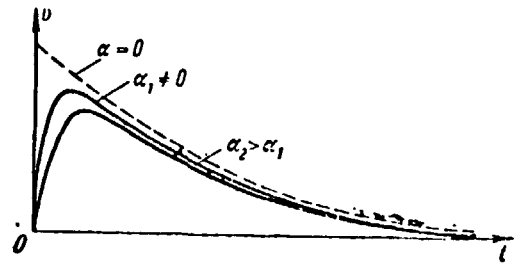

Fig. 22.2. Velocity at the beginning of motion increases with a decrease in the dimensionless parameter α.

This solution describes the aperiodic damping motion of a mass in the equilibrium position. The role of the initial conditions, which may be represented by two values (which are given independently) of the initial displacement y_0 and the initial velocity v_0, may be clearly seen in the solution of (22.9). Correspondingly, the velocity at any moment of time equals

$$v = \dot{y}(t) = e^{-\frac{kt}{2m}}\left(v_0 \operatorname{ch}\sqrt{\frac{k^2}{4m^2}-\frac{c}{m}}\,t - \frac{kv_0+2cy_0}{2m\sqrt{\frac{k^2}{4m^2}-\frac{c}{m}}}\operatorname{sh}\sqrt{\frac{k^2}{4m^2}-\frac{c}{m}}\,t\right), \tag{22.10}$$

and in the particular case, when $v_0 = 0$, we have: /193

$$v = \dot{y}(t) = -y_0\frac{c}{m\sqrt{\frac{k^2}{4m^2}-\frac{c}{m}}}e^{-\frac{kt}{2m}}\operatorname{sh}\sqrt{\frac{k^2}{4m^2}-\frac{c}{m}}\,t. \tag{22.11}$$

This dependence is shown in Figure 22.2 by the solid lines for different values of the dimensionless parameter $\alpha = \frac{mc}{k^2}$. The smaller the value of α, the closer the curves approximate the graph of the function (22.4) which is expressed by the dashed line in the same figure. As may be seen, the degenerate system behaves differently than real systems only at the beginning of motion. In a small period of time, the velocity of the degenerate and the real system are practically the same. Completely ignoring the mass of the system leads to the formal possibility of simultaneously changing the velocity from the given initial value v_0 to "the value imposed" by the equation $-cy_0/k$. Such a velocity discontinuity indicates infinite accelerations.

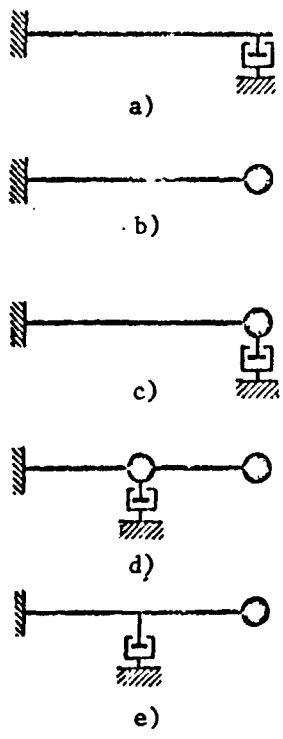

Fig. 22.3. Similar systems with different degrees of freedom: a) 1/2 degree of freedom; b) and c) 1 degree of freedom; c) 2 degrees of freedom; and d) 1 and 1/2 degrees of freedom.

For finite forces, this is only possible to the extent that the mass of the system is assumed to equal zero. In actuality, the initial elasticity force cy_0 acting on a very small mass produces very large accelerations, i.e., a very rapid, although not instantaneous increase in velocity.

Thus, the lack of agreement between the number of constants and the number of initial conditions has only a local (in time) value. Those conflicts arising in the theory of degenerate systems represent a forced contribution to idealization. L.I. Mandel'shtam(*) wrote that "idealization builds on itself". Any discrepancies usually are only local in nature, and their zones of action cannot be extended very far (in space or in time). /194

This degenerate case was examined in the book by A.A. Andronova, A.A. White, and S.E. Whiking "The Theory of Oscillations". This system was called "a system with 1/2 degree of freedom", since the equation of motion for a system with one degree of freedom is of second order, and the equation obtained here is of the first order.

Let us continue the discussion of the problem using an example of five systems shown in Figure 22.3, assuming in every case a cantilever rod which

(*) Leonid Isaakovich Mandel'shtam (1879 - 1944) was an academician (since 1929), and professor of Moscow University. His works are well-known in the field of optics, radio engineering, and the theory of oscillations. He is one of the founders of the theory of nonlinear oscillations.

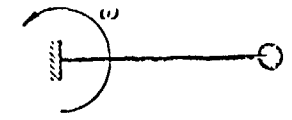

Fig. 23.1. Elastic cantilever rotating with a constant angular velocity ω.

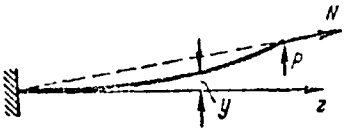

a)

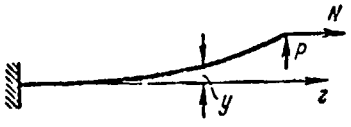

b)

Fig. 23.2. Two noncoinciding diagrams for a stretched and bent rod.

is ideally elastic and weightless. System a has 1/2 degree of freedom, while system b has only 1 degree of freedom. It is apparent that system c has only 1 degree of freedom. System d has 2 degrees of freedom. But how many degrees of freedom does system e have? In order to answer this question, this system must be regarded as a degenerate variation of the preceding system, when one of the masses equals zero. Therefore, system e has one and a half degrees of freedom. The book by A.A. Andronova, A.A. White, and S.E. Whiking was published twice (first edition, Joint Scientific and Technical Publishing House, Moscow, 1937; second edition, enlarged by N.A. Zheleztsov, Fizmatgiz Press, Moscow, 1959).

§ 23. Free Oscillations of a Cantilever in the Field of Centrifugal Forces

/195

Let us discuss the problem of free bending oscillations of an elastic cantilever, which is shown in Figure 23.1, if a rigid insert rotates uniformly in the plane of the drawing. Such a system represents an extremely simplified system for a turbineblade. The general rotation of the system produces a centrifugal force, which stretches the cantilever. Due to this, its bending rigidity becomes greater than when there is no rotation. According to this, the eigenfrequencies of the oscillations will be greater than the eigenfrequency of oscillations of a nonrotating cantilever(*).

(*) The unfortunate term "static frequency" is sometimes used for the eigenfrequencies of nonrotating turbine blades.

Will this effect be quantitatively identical in the case of oscillations in the plane of the drawing and in the case of oscillations out of the plane of the drawing? This problem is the subject of the present section. An answer necessitates the solution of two auxillary static problems, whose systems are shown in Figure 23.2.

In both cases, there is transverse bending with the force P applied with the accompanying action of the longitudinal force N. However, in case a the force N turns during bending and passes through the initial cantilever section. In case b, the force N does not change direction. Let us find the value of the effective rigidity coefficient c for both systems:

$$c=\frac{P}{f}, \tag{23.1}$$ /196

where f is the bending of the cantilever end.

Let us solve both problems, describing in parallel the corresponding computations for each case.

The bending moment in the running cross-section:

a) $$M=\left(P+N\frac{f}{l}\right)(l-z)-N(f-y); \tag{23.2}$$

b) $$M=P(l-z)-N(f-y), \tag{23.3}$$

where y is the bending of the running cross-section of the cantilever. The differential equation of the curved axis:

a) $$y''-\alpha^2y=\frac{Nf+Pl}{lEJ}(l-z)-\alpha^2f; \tag{23.4}$$

b) $$y''-\alpha^2y=\frac{P}{EJ}(l-z)-\alpha^2f; \tag{23.5}$$

Here

$$\alpha=\sqrt{\frac{N}{EJ}}. \tag{23.6}$$

The general solution of the differential equation:

a) $$y = C_1 \operatorname{sh} \alpha z + C_2 \operatorname{ch} \alpha z - \left(\frac{P}{N} + \frac{f}{l}\right)(l - z) + f; \tag{23.7}$$

b) $$y = C_1 \operatorname{sh} \alpha z + C_2 \operatorname{ch} \alpha z - \frac{P}{N}(l - z) + f. \tag{23.8}$$

The boundary conditions are:

$$\text{a) and b) } y = 0,\ y' = 0 \text{ for } z = 0. \tag{23.9}$$

The expressions for the integration constants:

a) $$C_1 = -\frac{1}{\alpha}\left(\frac{f}{l} + \frac{P}{N}\right),\quad C_2 = \frac{Pl}{N}; \tag{23.10}$$

b) $$C_1 = -\frac{P}{\alpha N},\qquad C_2 = \frac{Pl}{N} - f. \tag{23.11}$$

The equation for the curved axis: /197

a) $$y = -\frac{1}{\alpha}\left(\frac{f}{l} + \frac{P}{N}\right)\operatorname{sh} \alpha z + \frac{Pl}{N}\operatorname{ch} \alpha z - \left(\frac{P}{N} + \frac{f}{l}\right) \times (l - z) + f; \tag{23.12}$$

b) $$y = -\frac{P}{\alpha N}\operatorname{sh} \alpha z + \left(\frac{Pl}{N} - f\right)\operatorname{ch} \alpha z - \frac{P}{N}(l - z) + f. \tag{23.13}$$

Substituting z = l and y = f, we obtain

a) $$f = \frac{Pl^3}{EJ}\,\frac{\alpha l \operatorname{ch} \alpha l - \operatorname{sh} \alpha l}{(\alpha l)^2 \operatorname{sh} \alpha l}; \tag{23.14}$$

b) $$f = \frac{Pl^3}{EJ}\,\frac{\alpha l \operatorname{ch} \alpha l - \operatorname{sh} \alpha l}{(\alpha l)^2 \operatorname{ch} \alpha l}. \tag{23.15}$$

It may be shown that, when there is no longitudinal force ($\alpha = 0$), in both cases the following is obtained after the limiting transition

$$f = \frac{Pl^3}{3EJ}. \tag{23.16}$$

Corresponding to (23.1), we find from (23.14) and (23.15) the rigidity coefficient:

a) $$c = \frac{(\alpha l)^2 \operatorname{sh} \alpha l}{3(\alpha l \operatorname{ch} \alpha l - \operatorname{sh} \alpha l)}\, c_0; \tag{23.17}$$

b) $$c = \frac{(\alpha l)^2 \operatorname{ch} \alpha l}{3(\alpha l \operatorname{ch} \alpha l - \operatorname{sh} \alpha l)}\, c_0. \tag{23.18}$$

where

$$c_0 = \frac{3EJ}{l^3} \tag{23.19}$$

is the rigidity coefficient for N = 0 (and for $\alpha = 0$, respectively). For large values of αl, we may assume $\operatorname{sh} \alpha l \approx \operatorname{ch} \alpha l$ and expressions (23.17) and (23.18) assume the following form:

a) $$c \approx \frac{(\alpha l)^3}{3(\alpha l - 1)} c_0; \tag{23.20}$$

b) $$c \approx \frac{(\alpha l)^3}{3(\alpha l - 1)} c_0. \tag{23.21}$$

Figure 23.3 shows the ratio $c:c_0$ as a function of the dimensionless product αl. It may be seen from the graphs that the rigidity coefficients differ substantially, and consequently both of the cases under consideration cannot be combined.

Let us now return to the problem of bending oscillations of a canteliver. /198 If these oscillations occur in the rotation plane, then the translational inertial force has the direction shown in Figure 23.2, a; if the oscillations come from the rotation plane, the direction of this force corresponds to Figure 23.2, b. In both cases

$$N = m\omega^2 l, \tag{23.22}$$

where m is the load mass, ω — the angular velocity, so that in formulas (23.17), (23.18) we may set

$$\alpha l = \omega l \sqrt{\frac{ml}{EJ}}. \tag{23.23}$$

Naturally, the bending rigidity EJ must be assumed to correspond to a certain bending direction.

After this, the eigenfrequency is determined according to the simple formula

$$p = \sqrt{c : m}. \tag{23.24}$$

We may conclude our discussion here, but in the problem under consideration there is still one detail which must be clarified. When the load oscillations occur in the rotation plane of the system, a Coriolis force of inertia

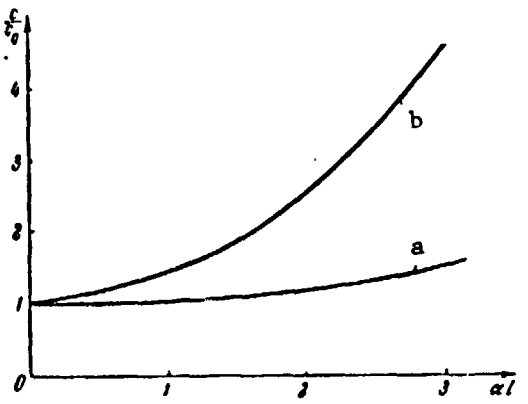

Fig. 23.3. The dependence of the bending rigidity on the dimensionless parameter αl. Curves a and b correspond to the systems in Figure 23.2.

develops, whose line of action lies in the rotation plane and is perpendicular to the vector of the relative load velocity (i.e., it is parallel to the z axis). This force changes in a cyclical manner in terms of magnitude and direction. Usually, these forces are not even mentioned when analyzing oscillations of turbine blades. However, these forces exist, although their magnitude is much less than the magnitude of the translational inertia forces. The Coriolis force of inertia reaches its largest value when the load is in its middle position. This value equals /199

$$I_c = 2m\omega v_{max}, \tag{23.25}$$

where v_{max} is the relative load velocity at the given moment. In the case of free oscillations with the frequency p and the amplitude a, we have

$$v_{max} = ap. \tag{23.26}$$

Thus,

$$I_c = 2ma\omega p. \tag{23.27}$$

Although the eigenfrequency p is always greater than the angular velocity ω (this follows from the Southwell formula), but usually has the same order of magnitude. Therefore, comparing Equations (23.27) and (23.22), we may conclude that the ratio I_c:N is on the same order of magnitude as the ratio a:l, i.e., it is very small.

According to the approximate formula of Southwell, the square of the frequency p of free oscillations of a rotating cantilever equals the sum of the squares of the angular velocity ω and the frequency p_0 of a nonrotating cantilever (see R.V. Southwell "Introduction to the Theory of Elasticity for Engineers and Physicists", Foreign Literature Press, Moscow, 1948). See the

book by A.I. Filippov "Oscillations of Mechanical Systems", published by "Naukova Dumka", Kiev, 1965, for a calculation of the Coriolis forces of inertia.

§ 24. Equal-Frequency Shock Absorber

During the operation of aircraft engines (particularly piston engines) large vibrations arise throughout the entire aircraft, which not only cause noise to the passengers, but also have a harmful influence on the equipment. The sensitive navigational devices (autopilots, altitude and velocity indicators, parts of radio and electrical equipment, etc.) wear out, lose their accuracy, and gradually become unsuitable for operation. In addition, for the same reason the normal operation of equipment is disturbed (oscillations of the pointers, noise in the radio communication, etc.). /200

A shock absorber for the equipment is one of the methods to combat these phenomena, i.e., its suspension is so soft that the high frequency vibration is barely transmitted to the objects. For this measure to be a success, the ratio of the perturbing vibration frequency to the eigenfrequency of the oscillations must be as large as possible. In addition, it is desirable that this ratio be the same for all different shock absorber objects, i.e., so that the eigenfrequencies p are the same. However, the eigenfrequency p of a system with 1 degree of freedom depends on the mass of the body m and the rigidity of the elastic connection c:

$$p=\sqrt{\frac{c}{m}}, \tag{24.1}$$

Consequently, for different values of the mass m different values of the rigidity c are necessary. It may appear that a special shock absorber is necessary for each value of the mass.

In actuality, this is not the case. Almost 20 years ago Yu.I. Iorish proposed and developed the idea of "equal-frequency" shock absorbers, i.e., elastic elements whose rigidity c changes as a function of the weight of the object being protected P = mg. An equal-frequency shock absorber fulfills

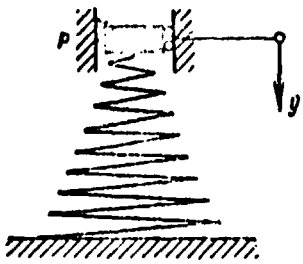

Fig. 24.1. Amortization of the load P.

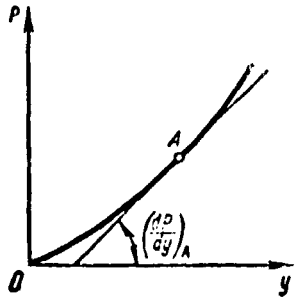

Fig. 24.2. The dependence P = P(y) is nonlinear.

its role with equal success, irrespective of the weight of the load (in very wide limits). This simplifies the standardization, and makes it possible to greatly reduce the types of shock absorbers used. The use of equal-frequency shock absorbers leads to constant values of the eigenfrequency of oscillations of a railroad car or an automobile for all possible loads in the body, as well as maintaining identical eigenfrequencies of different devices placed on elastic supports (*).

In order to clarify the idea of an equal-frequency shock absorber, we /201
shall examine Figure 24.1 and assume that the connection of a load to a spring P with the deflection y is nonlinear, as is shown in Figure 24.2.
The curve of P = P(y) shown here is a static characteristic of the elastic connection. Point A on the curve corresponds to the loading of a spring, when the weight of the load is mg. Many noncylindrical springs have such characteristics.

In the case of oscillations of the load around the static level, the force of elasticity of the spring will follow the curve P(y). However, if these oscillations are sufficiently small, the section of the curve located close to the point A may be replaced by a tangent. By this substitution,

(*) Special elastic supports constructed in the Experimental Scientific-Research Institute of Metal Cutting Equipment (Moscow) keep the eigenfrequency constant in a wide range of weights of loads (ratio of the largest weight to the least weight is 15:1).

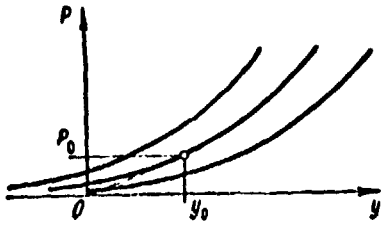

Fig. 24.3. Integral curves of Equation (24.4).

we obtain a linear oscillating system, whose rigidity is determined by the expression

$$c = \left(\frac{dP}{dy}\right)_A, \tag{24.2}$$

and the frequency is determined by formula (24.1), i.e.,

$$p = \sqrt{\frac{g\left(\frac{dP}{dy}\right)_A}{P_A}}. \tag{24.3}$$

Formula (24.3) shows that a constant frequency p (i.e., it is independent of the load P) may be achieved under the condition that the ratio $\frac{dP}{dy}$: P is constant.

Let us assume that p is the selected fixed value of the eigenfrequency. /202 Then, omitting the indices, from (24.3) we obtain the following differential equation for the characteristic P = P(y):

$$a\frac{dP}{dy} = P, \tag{24.4}$$

in which

$$a = \frac{g}{p^2} \tag{24.5}$$

is the known constant. The solution of Equation (24.4) has the form

$$a \ln P = y + C. \tag{24.6}$$

It can be immediately seen that the integral curves of Equation (24.4) have the same form and parallel each other, as is shown in Figure 24.3. Any of these characteristics satisfies the Equation(24.4), but it is necessary to determine the constant C for a valid solution, and to establish one specific integral curve — the desired static characteristic of the shock absorber. At first glance, the following initial condition can be used directly for this purpose:

$$y = 0 \quad \text{for} \quad P = 0, \tag{24.7}$$

since the static characteristic must pass through the origin. However, the difficulty arises that not one of the infinite set of integral curves (24.6) passes through the origin, and consequently cannot be used as the characteristic.

Yu.I. Iorish proposed the following way out of this difficulty. Let us assume P_0 is the least weight of the load being protected, determined by the technical requirements. In this case, for $P < P_0$ the shock absorber has a characteristic which does not satisfy the basic Equation (24.4), in particular, /203 the linear characteristic

$$P = c_0 y. \tag{24.8}$$

In addition, we shall strive to obtain a smooth transition from the linear section to the nonlinear section, as is shown by the dashed line in Figure 24.3. Thus, the selection of the desired integral curve will obey the simple geometric condition(*)

$$\frac{dP}{dy} = \frac{P}{y} \text{ for } P = P_0. \tag{24.9}$$

According to (24.6), we have

$$P = e^{\frac{y+C}{a}}; \tag{24.10}$$

Then condition (24.9) acquires the form

$$\frac{P_0}{a} = \frac{P_0}{y_0}, \tag{24.11}$$

i.e.,

$$y_0 = a, \tag{24.12}$$

where y_0 is the abscissa of the point at which the linear and nonlinear sections of the characteristic meet. In the last analysis, this quantity is determined by the given frequency p, as may be seen from formula (24.5).

Consequently, in order to find the constant C, we must not use the condition (24.7), but the condition

$$P = P_0 \text{ for } y = \frac{g}{p^2}. \tag{24.13}$$

Then, from (24.6), we obtain

$$P = P_0 e^{\frac{p^2 y}{g} - 1}, \tag{24.14}$$

and this curve begins at the point with the coordinates $y = \frac{g}{p^2}$, $P = P_0$; a straight lines passes from this point to the origin, whose Equation (24.8)

(*) Naturally, up to a certain degree this requirement is arbitrary, and may be replaced by any other.

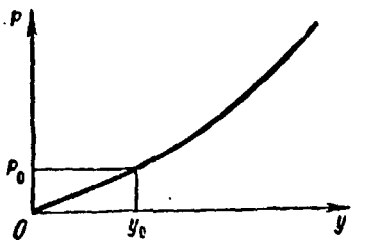

Fig. 24.4. Characteristics of equal-frequency shock absorber; the rectilinear section has a direction tangent to the curve at the point (y_0, P_0).

has the form

$$P = P_0 \frac{p^2}{g} y. \qquad (24.15)$$

Figure 24.4 shows the entire characteristic composed of two parts — (24.14) and (24.15). /204

Now the problem arises of calculating and constructing a spring, which has only the formulated characteristic. This in itself is an interesting problem which falls outside of the framework of our subject. In conclusion, we should point out that, although the characteristic of an equal-frequency shock absorber is nonlinear as a whole, since we are only studying small oscillations around the equilibrium position, the system under consideration in each specific case is linear.

For a detailed description of equal height and frequency shock absorbers, see the book by Yu.I. Iorish, "Zashchita samoletnogo oborudovaniya ot vibratsiy"(Protecting Aircraft Equipment from Vibration) (Oborongiz, 1949). This book examines large oscillations, which must include the theory of oscillations of nonlinear systems. See also his book "Vibrometriya" (Vibrometer Technology) (Mashgiz, Moscow, 1963).

§ 25. Comments on the Formulas of Rayleigh and Grammel

The formula introduced by Rayleigh(*) pertains to a number of the most popular formulas for the theory of oscillations and the stability of elastic systems. Below we shall discuss certain features of this formula, as well

(*) Strett (Lord Rayleigh), John William (1842 - 1919) — English physicist, member of the London Royal Society (since 1873), author of several studies on oscillations of elastic bodies. His well-known book "Theory of Sound" contains a fundamental description of the general theory of oscillations. A recent translation of this book into Russian was published in 1955 (Gostekhizdat, Moscow, Vol. 1 and 2).

as cases of its incorrect or unsatisfactory use. At the end of this section, we will give some information on the newer formula of Grammel.

The method of Rayleigh is generally known, and may be briefly described as follows. In the case of single-tone free oscillations of an ideally elastic system, the displacements $\xi(x, y, z, t)$, $\eta(x, y, z, t)$, $\zeta(x, y, z, t)$ /205 change in time in a cophasal manner according to the harmonic law:

$$\left.\begin{aligned}\xi &= f_1(x, y, z)\sin pt,\\ \eta &= f_2(x, y, z)\sin pt,\\ \zeta &= f_3(x, y, z)\sin pt,\end{aligned}\right\} \qquad (25.1)$$

where $f_1(x, y, z)$, $f_2(x, y, z)$ are the functions of the three-dimensional coordinates which determine the form of the oscillation under consideration. If these functions are known previously, the frequency p of the free oscillations may be found from the condition that the sum of the body kinetic energy and its potential energy are constant. This condition leads to the equation containing only one unknown p.

However, these functions were not known previously. The leading concept of the Rayleigh method consists of assigning these functions, having their selection conform with the boundary conditions and with the expected form of oscillations.

We shall investigate this idea in detail for flexural oscillations of a rod. In this case, the form of the oscillations is determined by one function of the three-dimensional coordinate z:

$$f = f(z) \qquad (25.2)$$

where z is the coordinate of the running rod cross-section, f — deflection of the axis in this cross-section. The process of free oscillations may be described by the relation

$$v(z, t) = f(z)\sin pt, \qquad (25.3)$$

according to which the potential energy of a curved rod is

$$\Pi = \frac{1}{2}\int_0^l EJ\left(\frac{\partial^2 v}{\partial z^2}\right)^2 dz, \tag{25.4}$$

and the kinetic energy is

$$T = \frac{1}{2}\int_0^l m\left(\frac{\partial v}{\partial t}\right)^2 dz. \tag{25.5}$$

Here l is the rod length, m = m(z) — intensity of the distributed rod mass. The latter expression does not take into account the inertia of rotation of the rod elements or the possible existence of concentrated masses. Taking /206 these factors into account would only complicate the computations and would not clarify the situation.

We would like to remind the reader that the quantity $\frac{\partial^2 v}{\partial z^2}$ represents the curvature of a curved axis, and $\frac{\partial v}{\partial t}$ is the velocity for transverse oscillations. According to (25.3), for these quantities we have

$$\left.\begin{aligned}\frac{\partial^2 v}{\partial z^2} &= f''\sin pt,\\ \frac{\partial v}{\partial t} &= pf\cos pt.\end{aligned}\right\} \tag{25.6}$$

Substituting (25.6) in (25.4) and (25.5), we obtain

$$\Pi = \frac{1}{2}\sin^2 pt\int_0^l EJ(f'')^2 dz, \tag{25.7}$$

$$T = \frac{p^2}{2}\cos^2 pt\int_0^l mf^2 dz. \tag{25.8}$$

With the passage of time, each of these quantities constantly changes, but — according to the law of conservation of energy — their sum remains constant, i.e.,

$$\frac{d(\Pi + T)}{dt} = 0. \tag{25.9}$$

If we substitute the Expressions (25.7) and (25.8), we obtain the Equation

$$\frac{1}{2}\int_0^l EJ(f'')^2 dz = \frac{p^2}{2}\int_0^l mf^2 dz, \tag{25.10}$$

The left side of this equation represents the greatest potential energy, and the right side represents the greatest kinetic energy. We thus obtain the Rayleigh formula, which determines the frequency of bending oscillations of a rod

$$p^2 = \frac{\int_0^l EJ(f'')^2\,dz}{\int_0^l mf^2\,dz}. \qquad (25.11)$$

If, in addition to the distributed mass, there are also concentrated loads with the masses M_i, formula (25.11) assumes the form /207

$$p^2 = \frac{\int_0^l EJ(f'')^2\,dz}{\int_0^l mf^2\,dz + \sum M_i f_i^2}. \qquad (25.12)$$

Let us discuss three problems connected with formula (25.11).

1. Can this formula be regarded as precise or approximate ?

We have traced the entire derivation, and can state that within the framework of the assumptions assumed (validity of the technical theory of rod bending, no inelastic resistances), this formula is precise, if f(z) is the true form of the oscillations. However, the function f(z) was unknown previously. In order to find its precise value, it is necessary to solve the differential equation of the problem. However, the quantity p(*) is frequently determined by means of a cumbersome solution, so that the Rayleigh formula becomes unnecessary.

The practical value of the Rayleigh formula lies in the fact that it can be used to find the eigenfrequency p, stipulating a form of the

(*) More precisely, several values of p which form the spectrum of eigenfrequencies.

oscillations f(z). The solution thus includes a more or less serious element of approximation. For this reason, the Rayleigh formula is sometimes called approximate, although the approximate character of it (unfortunately, it is always inevitable) is not connected with the formula itself, but with the methods of using it.

2. Not only the derivation of the formula (25.12) belongs to Rayleigh, but also the proof of a very important theorem: for any form of the oscillations f(z) which satisfies the kinematic boundary conditions of the problem (**), formulas (25.11) or (25.12) give a value of the fundamental frequency p, which is always higher than the true value of the fundamental frequency.

In 1939, in a book by S.A. Bernshteyn , "Principles of the Dynamics of /208
Constructions", in connection with a discussion of the Rayleigh formula, it was correctly noted that "the frequency calculated for the form of the bending, which differs from true bending, will always be greater than the true frequency". This statement was substantiated by the author by a number of purely qualitative considerations, without using the Rayleigh theorem.

Two years later, S.A. Bernshteyna found that the statement given above was not correct. In the second edition of the same book, contradicting his previous statement, he wrote "the approximate calculation of frequency according to the Rayleigh method may give both a value for the frequency which is too high or too low, depending on the form of bending selected". To support this abrupt change in position, the author used the following example.

A problem is considered of free transverse oscillations of a rod with hinged support. The form of the oscillations f(z) is assumed to have two segments of straight lines which form a triangle with the axis of the beam

(*) Thus, if the end of the rod is free, no limitations are imposed on the value of the function and its first derivative at this location. The condition $f = 0$ is imposed on the hinged, supported end, and two conditions $f = 0$, $f' = 0$ are imposed on the rigid support.

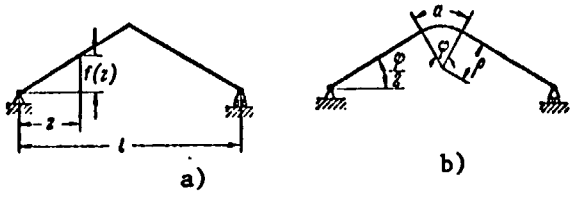

Fig. 25.1. Mode of oscillations in the form of two segments of straight lines: (a) without a smooth transition; (b) with a smooth transition (this deflection may be accomplished by two equal pairs, having the opposite direction to each other and applied at a distance a from each other).

(Figure 25.1). In addition, the author writes that — since in this case f' = 0 — the numerator in formula (25.11) vanishes, and consequently p = 0. It is thus shown that formula (25.11) gives a value which is lower than the true value. After this, we read: "Although there is an obvious flaw in this example (disturbance of the smoothness of the elastic line), a finite length of curvature could be assumed in order to restore this smoothness, without changing the calculation results". Here we are dealing with the form of bending shown in 25.1, b. It is unfortunate that S.A. Bernshteyn yielded to his first impression, and did not make the appropriate computations. /209

Let us assume that two rectilinear sections are joined to an arc of a circle with the radius ρ. If the length of this arc is a, and the central angle is φ, then $a = \rho\varphi$ (Figure 25.1, b). Then the numerator in formula (25.11) becomes

$$\int_0^l EJ(f'')^2\,dz = \int_0^a \frac{EJ}{\rho^2}\,dz = \frac{EJa}{\rho^2} = EJ\frac{\varphi}{\rho}.$$

We shall now have the length a of the rectilinear section strive to zero, assuming that the angle φ does not change. The radius of curvature will also strive to zero, and the numerator in formula (25.11) will strive to infinity. Thus, not the zero but the infinitely large value of the numerator in (25.11) corresponds to the form of oscillations shown in Figure 25.11, b.

The denominator in the Rayleigh formula can be assumed to remain unchanged with a decrease in the value of a, since the values of the function f(z) cannot change significantly with a decrease in the length of the curvilinear section. In any case, the denominator remains finite. A frequency which

equals infinity, and not zero, is obtained according to formula (25.11). This result in no way contradicts the Rayleigh theorem.

Unfortunately, up to the present time confidence is still sometimes placed in the erroneous statement of S.A. Bernshteyn. Thus, in one book published in 1963, the following commentary is made for the Rayleigh formula: "The widely held opinion that this solution must give a value of the frequency which is too high as compared with the true value was refuted by S.A. Bernshteyn in the second edition of the book 'Principles of the Dynamics of Constructions' ".

Thus, the true value of the frequency is always less than any approximate value calculated according to the Rayleigh formula, or equal to it (when the precise expression for the bending curve is substituted in formula (25.11). This property of the Rayleigh formula is not only of great importance, but also opens up great possibilities for obtaining accurate solutions. One of these possibilities was shown by V. Ritz (Ritz method).

3. Widespread use is made of the formula (25.11) which guarantees the automatic fulfillment of the boundary conditions by the function f(z). For /210 this purpose, in the solution it is assumed that a certain fictitious load q(z) is given, and not the function f(z). The bending curve caused by this load is substituted in formula (25.11). With this approach, the boundary conditions will be satisfied automatically. The advantage of this method consists of the fact that the calculation of the greatest potential energy according to the formula

$$\Pi = \frac{1}{2}\int_0^l EJ(f'')^2\,dz \qquad (25.13)$$

may be replaced by a simpler calculation of the load q(z)

$$A = \frac{1}{2}\int_0^l qf\,dz, \qquad (25.14)$$

since the quantities Π and A equal each other. Thus, the Rayleigh formula (25.12) assumes the following form:

$$p^2 = \frac{\int_0^l qf\,dz}{\int_0^l mf^2\,dz + \sum M_i f_i^2}. \tag{25.15}$$

If the given fictitious load contains only the concentrated forces P_i, then formula (25.15) assumes the form

$$p^2 = \frac{\int_0^l qf\,dz + \sum P_i f_i}{\int_0^l mf^2\,dz + \sum M_i f_i^2}. \tag{25.16}$$

It must be kept in mind that, generally speaking, the quantities M_i and P_i are not connected with each other. The former represents the masses of concentrated loads which actually exist, which the latter represent forces in the composition of the devised static load. The functions m(z) and q(z) are not related in precisely the same way.

The variations in writing (25.15) and (25.16) are in principle equivalent to writing (25.12). Nevertheless, the chances of achieving the same precision in the results are not the same in practice. Calculations according to formula (25.12) require operations of differentiation (even twice), and differentiation of a function which is approximately given always worsens the accuracy of the results. Calculations according to the formulas (25.15) and (25.16) examined here do not require differentiation, and thus differ favorably from calculations using the basic formula of Rayleigh (25.12) (the formula proposed by P. Grammel has the same advantage, which we shall discuss at the end of this section). /211

Let us now turn to formula (25.15). Frequently, the actual load from the forces of the rod length is assumed to be the load:

$$q(z) = m(z)\,g. \tag{25.17}$$

This corresponds to the assumption that the form of the oscillations coincides with the form of static bending produced by the rod weight.

If there are no concentrated masses on the beam, formula (25.15) may be written in the form

$$p^2 = g\frac{\int_0^l mf\,dz}{\int_0^l mf^2 dz}. \tag{25.18}$$

When this formula is used, the function f(z) is not selected. It represents the specific curve of static bending.

The latter edition of the Rayleigh formula is the simplest and has complete determinacy. However, it differs in principle from the formula (25.11) — the curve of bending from distributed forces of the weight does not coincide with the true bending curve in the case of oscillations. Therefore, formula (25.18) never can give an exact value of the frequency p.

If the static load contains only the concentrated loads with the masses M_i, then instead of formula (25.18) we obtain

$$p^2 = g\frac{\int_0^l mf\,dz + \sum M_i f_i}{\int_0^l mf^2 dz + \sum M_i f_i^2}. \tag{25.19}$$

This formula, just like formula (22.18), always gives an approximate result. /212

In one handbook, the Rayleigh formula is given in the form

$$p^2 = \frac{\int_0^l EJ(f'')^2\,dz + g\sum M_i f_i}{\int_0^l mf^2\,dz + \sum M_i f_i^2}, \tag{25.20}$$

This formula is generally not valid. Thus, for example, if we substitute the true function f(z) in it, we obtain an incorrect result. The presence of an extra term in the numerator is an indication of this [see for comparison formula (25.12)].

Concluding this commentary on different ways to write the Rayleigh formula, we shall now turn to the Grammel formula. This formula has great advantages, but up to the present it has not been used adequately in the technical literature (possibily due to its relative "youth" — it was proposed in 1939).

Just as above, we shall discuss the problem of free bending oscillations, which is assumed to be typical throughout this section. To save time, we shall omit the derivation and present the final result (25.25). At first glance, this formula appears strange. It may even appear that it contains an error: the numerator and the denominator are interchanged (compare the Grammel formula with the basic Rayleigh formula or any of its variations). This strange construction is completely valid, as will be seen from the following simple derivation.

Let us assume f(z) is the given form of free oscillations of a rod. Then the intensity of the maximum inertia forces is determined by the expression mp^2f, where as before $m = m(z)$ is the strength of the distributed mass, p^2 — square of the eigenfrequency of oscillations. These forces have the given value at the moment when the deflections are maximal, i.e., they are determined by the function f(z).

Let us write the expression for the greatest potential energy of bending by means of the bending moments, produced by the maximum forces of inertia:

$$\Pi_{\max} = \frac{1}{2}\int_0^l \frac{M_B^2}{EJ}\,dz. \qquad (25.21)$$

Here, EJ is the rigidity for bending, $M_B = M_B(z)$ — bending moments produced by the load mp^2f. Let us use $\bar{M}_B$ to designate the bending moment caused by an arbitrary load mf (i.e., the load is p^2 times less than the

forces of inertia). We then have

$$M_B = p^2 \bar{M}_B \tag{25.22}$$

and expression (25.21) may be written in the form

$$\Pi_{max} = \frac{p^2}{2} \int_0^l \frac{\bar{M}_B^2 \, dz}{EJ}. \tag{25.23}$$

The greatest kinetic energy which develops during the oscillations of the rod, just as above, has the form

$$T_{max} = \frac{p^2}{2} \int_0^l mf^2 dz. \tag{25.24}$$

Equating expressions (25.23) and (25.24), we arrive at the Grammel formula:

$$p^2 = \frac{\int_0^l mf^2 dz}{\int_0^l \frac{\bar{M}_B^2 dz}{EJ}}. \tag{25.25}$$

For calculations using this formula, it is first of all necessary to assign the appropriate function f(z). After this, by multiplying the function f(z) by m(z), we determine the arbitrary load mf. Using the well-known methods of resistance of materials, we then obtain the bending moments $\bar{M}_B$ produced by an arbitrary load. We must now calculate the expressions in the numerato and the denominator of the formula (25.25).

Let us illustrate this with the simplest example of free oscillations of a cantilever rod with constant cross-section. Let us assume that the left end of the rod is attached (we combine the origin with this end), and the /214
right end is free. Let us assume the following function as the form of the oscillations

$$f(z) = az^2, \tag{25.26}$$

where z is the coordinate of the cross-section, a — an unimportant constant. This expression satisfies all the kinematic conditions of the problem, and may be applied to the calculations, both for the Rayleigh formula and for the Grammel formula.

In order to use the Rayleigh formula, we must first find:

$$\int_0^l EJ(f'')^2\,dz = 4a^2lEJ, \tag{25.27}$$

$$\int_0^l mf^2\,dz = \frac{ma^2l^5}{5}. \tag{25.28}$$

Now using formula (25.12), we can determine the square of the eigenfrequency of the oscillation

$$p^2 = \frac{20EJ}{ml^4}. \tag{25.29}$$

We shoud note that this result greatly differs from the precise value

$$p^2 = \frac{12{,}36\,EJ}{ml^4}. \tag{25.30}$$

In order to calculate the eigenfrequency according to the Grammel formula, we assume the arbitrary load in the form maz^2, and we find the corresponding bending moments of this load

$$\overline{M}_B = \frac{ma}{12}(z^4 - 4zl^3 + 3l^4).$$

We now determine the denominator of the expression (25.25):

$$\int_0^l \frac{\overline{M}_B^2}{EJ}\,dz = \frac{m^2a^2l^9}{62{,}31EJ}. \tag{25.31}$$

The numerator of the same expression was already in the form of (25.28). Dividing (25.28) by (25.31), we find

$$p^2 = \frac{12{,}46EJ}{ml^4}, \tag{25.32}$$

which is much closer to the precise result than the result calculated according to the Rayleigh formula.

We should emphasize once again that the Grammel formula eliminates the /215 necessity of differentiating the approximately assumed function, i.e., the operation which always makes the error of the approximate calculations worse. It is for this reason that such high accuracy was achieved in the example just presented.

The Grammel method in its expanded form makes it possible to formulate the successive approximations and to determine the higher frequencies of oscillations. Grammel showed that the eigenfrequencies calculated according to this method are always more accurate than the eigenfrequencies calculated according to the Rayleigh method or according to Galerkin (with the same selection of the approximating functions).

The proof of the Rayleigh theorem can be found, for example, in the book of R.V. Southwell "Introduction to Elasticity Theory" (Foreign Literature Press, 1948). An example supposedly refuting it (See Figure 25.1, b above) was given by S.A. Bernshteyn in the second edition of the book "Bases of Dynamics of Constructions" (First edition, Gosstroyizdat, Moscow, 1939; second edition, Gosstroyizdat, Moscow, 1941). Critical comments on the arguments of S.A. Bernshteyn were published by M.I. Dugachev (See his article, "Solving the Problems of Stability and Oscillations of Elastic Systems by the Energy Method", Sb. Trudov Instituta stroitel'noy mekhaniki AN USSR, No. 15, 1951). The citation on page 209 is taken from the book of N.I. Bezukhov and O.V. Luzhina "Ustoychivost' i dinamika sooruzheniy (Stability and Dynamics of Constructions), Gosstroyizdat, Moscow, 1963, p. 261.

Formula (25.20) was given in the book: I.I. Gol'denblat and A.M. Sizov "Spravochnik po raschetu stroitel'nykh konstruktsiy na ustoychivost' i kolebaniya (Handbook on Designing Structures for Stability and Oscillations), Gosstroyizdat, Moscow, 1952, p. 175.

The Grammel formula was given in his article "A New Method for Solving the Eigenvalue Problem" (Ingenieur Archiv, Vol. 10, 1939) (See also the book: K. Bitseno, R. Grammel "Tekhnicheskaya dinamika" (Technical Dynamics), Gostekhizdat, 1950, Vol. 1, pp. 257 - 261.

§ 26. Lagrange Errors

The theory of oscillations of linear mechanical systems with several degrees of freedom was given by Lagrange (*) in his classic work "Analytical Mechanics". Let us recall the basic hypotheses of this theory.

Equations of free oscillations for a linear mechanical system with n degrees of freedom have, as is known, the following form (in the absence of inelastic resistances): /216

$$\sum_{k=1}^{n} (a_{ik}\ddot{q}_k + c_{ik}q_k) = 0 \qquad (i = 1, 2, \ldots, n). \tag{26.1}$$

The inertial coefficients a_{ik} and the quasi-elastic coefficients c_{ik} have the property of reciprocity

$$a_{ik} = a_{ki}, \quad c_{ik} = c_{ki}. \tag{26.2}$$

For integration of this system, the equations are assumed to be particular solutions in the form

$$q_k = A_k \sin(pt + \varphi). \tag{26.3}$$

Substituting (26.3) in (26.1) leads to a system of algebraic equations:

$$\sum_{k=1}^{n} (a_{ik}p^2 - c_{ik}) A_k = 0 \qquad (i = 1, 2, \ldots, n). \tag{26.4}$$

In this system of n equations there are n + 1 unknowns, namely — the amplitudes $A_1, A_2, \ldots, A_n$ and the frequency p.

In view of the fact that the system of equations (26.4) is homogeneous with respect to the amplitude A_k, it is satisfied by the trivial solution

$$A_1 = A_2 = \ldots = A_n = 0, \tag{26.5}$$

which corresponds to the absence of oscillations, and holds only for zero

(*) Joseph Louis Lagrange (1736 - 1813) — from the age of 19, professor of mathematics at Turin. In 1776, he replaced Euler in the Berlin Academy of Science. In 1788, he worked in Paris, where he continued his scientific research as a member of the Paris Academy of Sciences.

initial conditions

$$q_1 = q_2 = \ldots = q_n = 0, \quad \dot{q}_1 = \dot{q}_2 = \ldots = \dot{q}_n = 0. \tag{26.6}$$

Apart from this trivial solution, non-zero solutions are possible for A_k, but under the condition that the determinant of the system of equations (26.4) equals zero:

$$\Delta(p^2) = 0 \tag{26.7}$$

or, in more detail,

$$\begin{vmatrix} a_{11}p^2 - c_{11} & a_{12}p^2 - c_{12} & \ldots & a_{1n}p^2 - c_{1n} \\ a_{21}p^2 - c_{21} & a_{22}p^2 - c_{22} & \ldots & a_{2n}p^2 - c_{2n} \\ \cdots & \cdots & \cdots & \cdots \\ a_{n1}p^2 - c_{n1} & a_{n2}p^2 - c_{n2} & \ldots & a_{nn}p^2 - c_{nn} \end{vmatrix} = 0. \tag{26.8}$$

If we expand this determinant, we obtain the algebraic equation with the unknown p^2, and the power of this equation equals n, i.e., the number of degrees of freedom for the system. Solving this particular equation, we find n of the roots p_1^2, p_2^2, ..., p_n^2; it is found that all of these roots are real and positive. /217

The frequencies p are called eigenfrequencies, since they are all completely determined by the properties of the system itself, which are represented by the coefficients a_{ik} and c_{ik}.

In satisfying the condition (26.7), one of the equations in the (26.4) system is a result of the others. Therefore, definite ratios between amplitudes A_k correspond to any value of p. In other words, all the amplitudes A_k can be expressed by one of them. The relationships between the amplitudes A_k determine the eigenform of the oscillations.

Free oscillations arising after an arbitrary, beginning disturbance of the system equilibrium represent the sum of n oscillations of the (26.3) type In order to completely determine this process, it is necessary to know 2n constants (one of the amplitudes and the phase for each component). They

may be found from 2n initial conditions (in terms of two conditions for each of the generalized coordinates).

Lagrange briefly discussed the special case when there are equal roots among the roots of the particular equation (26.8). In such cases, writes Lagrange, in the solution terms arise containing the time t outside of the cosine sign ("secular" terms). For example, when two roots are equal, a solution of the following type occurs

$$q_k = (A_k + B_k t) \sin (pt + \varphi). \tag{26.9}$$

As may be seen, with an increase in the time t, the first factor increases infinitely, and the oscillations acquire a resonance character. Their amplitude will strive to infinity.

However, small free oscillations of a conservative system cannot increase infinitely — this would contradict the apparent energy considerations. With such a process, the energy of the system would increase to infinity, and the system would represent an unusual perpetual motion machine.

What can be done? Can it be that, in problems of free oscillations of conservative and autonomous mechanical systems, the case of equal roots is impossible? No, real mechanical systems may readily be found, which have /218 equal eigenfrequencies. This is the case, for example, with a spherical pendulum or an elastic system of two degrees of freedom, shown in Figure 26.1. If the rod cross section represents a rectangle with unequal sides, the eigenfrequencies will differ, naturally. However, if the rod cross section is circular or square, both eigenfrequencies will equal each other. In these examples, the fact that the two eigenfrequencies are equal does not involve any characteristics of the oscillation process, particularly an unlimited growth in the amplitude.

These two examples directly point to the case of equal roots which is physically easy to produce, while the occurrence of secular terms in the

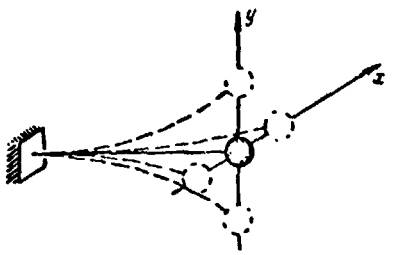

Fig. 26.1. Elastic system with 2 degrees of freedom. Both eigenfrequencies equal each other for different rigidities in the x and y directions.

solution contradicts common sense and the law of conservation of energy. However, Lagrange avoided discussing this paradox: " ... since a discussion of these cases is not of interest for the problem we are considering, we shall not dwell on it".

The statement of Lagrange about the occurrence of secular terms was published in 1788, when the first edition of his book appeared. It was abandoned by Lagrange in the second edition, which was published in 1812 — one year before the death of Lagrange. In 1853, "Analytical Mechanics" came out in the third edition, which was edited by the famous mathematician Joseph Bertrand. The statement of Lagrange was retained here.

Only in 1858 - 1859, did Weierstrass and O.I. Somov(*) state that Lagrange's conclusion was erroneous, and even in the case of equal roots of /219 a particular equation the solutions retain a purely trigonometric form, and the "secular" terms like (26.9) cannot occur.

The situation is as follows. In the case of multiple roots a system like (26.1) has an incorrect solution with the factors t, t^2, etc. But we are dealing with a special case of a system of nonlinear differential equations, which has definite symmetry properties (26.2). In this special case, with equal roots for p^2 it has a solution only like (26.3)(**).

(*) Osin Ivanovich Somov (1815 - 1876) — from 1841 Professor of the Petersburg University, and from 1857 — Associate Member of the Petersburg Academy of Science. Author of several extensive studies on mathematics and analytical mechanics.

(**) Symmetry of the matrix of the coefficients is not a necessary condition for the absence of secular solutions in the case of multiple roots. See in this respect the book by A.I.Lur'ye "Operational Calculus" (Gostekhizdat, Moscow, 1950, §§ 9, 10, pages 106 - 113).

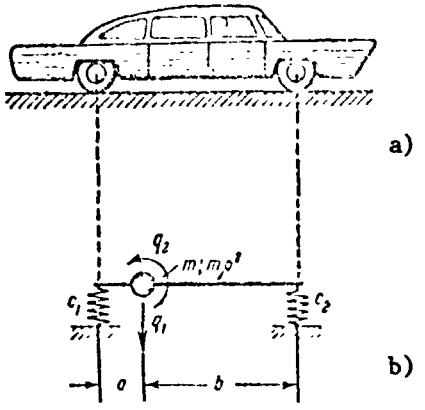

Fig. 26.2. Automobile and its dynamic system for analyzing oscillations in a vertical plane of symmetry.

Let us discuss in detail a mechanical system in which the case of equal roots is not only possible, but also desirable(*). Let us examine the problem of free vertical oscillations of an automobile which occur parallel to its plane of symmetry. Figure 26.2, a, shows an automobile, and Figure 26.2, b, shows its dynamic system. The rigidities of the forward and rear suspensions of the automobile (which take into account the rigidity of the springs and tires) are designated by c_1 and c_2. The center of gravity is located at the distances a and b, respectively, from the forward and rear supports. The mass of the body is designated by m, and the body moment of inertia with respect to the transverse axis passing thoough the center of gravity is designated by mq^2 (q — radius of inertia).

It is assumed that the deformation of the body is negligibly small as compared with the supports. Therefore, in a dynamic system a horizontal rod will be assumed to be completely rigid. In addition, we assume that the horizontal oscillations of the system are not possible. /220

This system has two degrees of freedom and the vertical displacement of the center of gravity (positive direction downwards) and the angle at which the rod turns around the center of gravity (positive direction — counterclockwise) are used as generalized coordinates q_1 and q_2. The resultants at the elastic supports equal $q_1 + aq_2$ (rear support) and $q_1 - bq_2$ (forward support).

(*) Another example is a centrifuge with a rigid rotor. In some patents of such a centrifuge, it is especially stipulated that the frequencies are equal.

Using these expressions, we may find the kinetic and potential energy of the system

$$T=\frac{m\dot{q}_1^2}{2}+\frac{mQ^2\dot{q}_2^2}{2}, \tag{26.10}$$

$$\Pi=\frac{c_1(q_1+aq_2)^2}{2}+\frac{c_2(q_1-bq_2)^2}{2}. \tag{26.11}$$

The Lagrange equations

$$\frac{d}{dt}\left(\frac{\partial T}{\partial \dot{q}_j}\right)-\frac{\partial T}{\partial q_j}=-\frac{\partial \Pi}{\partial q_j} \tag{26.12}$$

assume the form

$$\left.\begin{aligned} m\ddot{q}_1+(c_1+c_2)q_1+(c_1a-c_2b)q_2=0,\\ mQ^2\ddot{q}_2+(c_1a-c_2b)q_1+(c_1a^2+c_2b^2)q_2=0.\end{aligned}\right\} \tag{26.13}$$

After substitution of the particular solution (26.3), we obtain a homogeneous system of equations

$$\left.\begin{aligned} -mp^2A_1+(c_1+c_2)A_1+(c_1a-c_2b)A_2=0,\\ -mQ^2p^2A_2+(c_1a-c_2b)A_1+(c_1a^2+c_2b^2)A_2=0\end{aligned}\right\} \tag{26.14}$$

and we obtain the determinant of the frequencies:

$$\begin{vmatrix} c_1+c_2-mp^2 & c_1a-c_2b\\ c_1a-c_2b & c_1a^2+c_2b^2-mQ^2p^2\end{vmatrix}=0, \tag{26.15}$$

from which we obtain the particular equation

$$p^4-\left(\frac{c_1+c_2}{m}+\frac{c_1a^2+c_2b^2}{mQ^2}\right)p^2+\frac{c_1c_2(a+b)^2}{m^2Q^2}=0. \tag{26.16}$$

As a rule, this equation has <u>different</u> roots. A definite relationship between /221
the amplitudes, which determines the eigenform of the oscillations, corresponds to each of them. This relationship may be found, for example, from the first equation in the system (26.14):

$$\frac{A_2}{A_1}=\frac{mp^2-c_1-c_2}{c_1a-c_2b}. \tag{26.17}$$

This relationship follows from the second equation of the system (26.14).

Let us discuss the particular case when the following equation holds

$$\rho^2 = ab, \tag{26.18}$$

i.e., when the radius of inertia represents the geometric average between the quantities a and b. We should note that the distance a + b between the wheel axes must be much less than the overall length of the automobile (this is the case in present day automobiles).

If condition (26.18) is satisfied, then the particular equation assumes the form

$$p^4 - \frac{(c_1 a + c_2 b)}{mab}(a + b)p^2 + \frac{c_1 c_2 (a + b)^2}{m^2 ab} = 0 \tag{26.19}$$

and has the following unequal roots:

$$p_1^2 = \frac{c_1 (a + b)}{mb}, \quad p_2^2 = \frac{c_2 (a + b)}{ma}. \tag{26.20}$$

In order to determine the eigenforms, let us substitute these roots in turn in (26.17). For the first form, we obtain the following assuming $p^2 = p_1^2$:

$$\frac{A_{21}}{A_{11}} = \frac{1}{b}. \tag{26.21}$$

Here the two indices designate the number of the eigenform under consideration. After substituting $p^2 = p_2^2$ in (26.17), we obtain the second eigenform:

$$\frac{A_{22}}{A_{12}} = -\frac{1}{a}. \tag{26.22}$$

These forms are shown in Figure (26.3). Their characteristic feature is that one of the suspensions of the automobile does not move during oscillations of another suspension. In practice, this means that the suspensions of /222 an automobile oscillate independently, and the oscillations of one of them are not transmitted to the other. The dynamic system shown in Figure 26.4 graphically represents the properties of such a system. The fact that the oscillations of both suspensions of the automobile are independent is a definite operational advantage of this system. The free oscillations of each of these suspensions will be characterized by <u>different</u> frequencies.

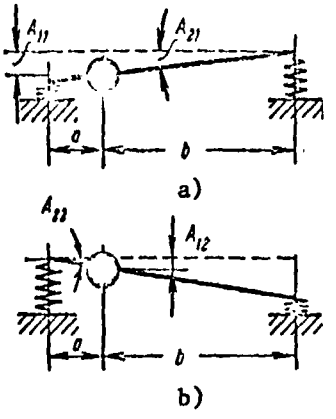

Fig. 26.3. Eigenforms of automobile oscillations for $\rho^2 = ab$.

In another particular case, when

$$c_1 a = c_2 b, \tag{26.23}$$

equations (26.14) become independent:

$$A_1(-mp^2 + c_1 + c_2) = 0, \tag{26.24}$$

$$A_2(-mQ^2p^2 + c_1a^2 + c_2b^2) = 0. \tag{26.25}$$

The independence of the equations points to the possibility of purely vertical oscillations without rotations (jumping) (Figure 26.5, a) or purely angular oscillations when the center of gravity does not move (galloping motion) (Figure 26.5, b). For the case when the automobile jumps, we have

$$A_1 \neq 0, \quad A_2 = 0 \tag{26.26}$$

and from the equation (26.24) /223

$$-mp^2 + c_1 + c_2 = 0 \tag{26.27}$$

we obtain the square of the first frequency

$$p_1^2 = \frac{c_1 + c_2}{m}. \tag{26.28}$$

For the case of galloping automobile motion, when

$$A_1 = 0, \ A_2 \neq 0, \tag{26.29}$$

from equation (26.25) we obtain the square of the second frequency

$$p_2^2 = \frac{c_1a^2 + c_2b^2}{mQ^2}. \tag{26.30}$$

Thus, the jumping and galloping frequencies p_1 and p_2 are different.

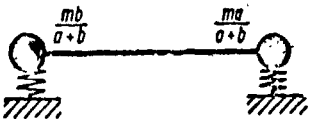

Fig. 26.4. Dynamic system of automobile with independent oscillations of both suspensions.

Can both frequencies be equal? An automobile having this property is

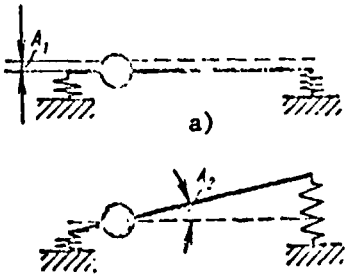

Fig. 26.5. Eigenforms of automobile oscillations for $c_1a = c_2b$.

particularly efficient, from the point of view of comfort.

It is apparent that in this case strong oscillations of the automobile only arise with a certain single frequency of jerks, whereas in the case $p_1 \neq p_2$ strong oscillations can arise for two values with this frequency.

It can be seen from equation (26.16) that its roots are equal to each other when the parameters of the automobile dynamic system satisfy the equation

$$\left[c_1 + c_2 + \frac{c_1a^2 + c_2b^2}{Q^2}\right]^2 - 4c_1c_2\frac{(a+b)^2}{Q^2} = 0. \tag{26.31}$$

It can be readily shown that it is satisfied, if both conditions (26.18) and (26.23) are satisfied <u>simultaneously</u>. In addition, it can be shown that these /224 conditions are not only sufficient, but also necessary to satisfy equation (26.31).

If a dynamic automobile system satisfies conditions (26.18) and (26.23), then a <u>single</u> eigenfrequency of the oscillations is determined by the formula

$$p = \sqrt{\frac{c_1 + c_2}{m}}. \tag{26.32}$$

Such a system is an example of equal frequencies — the case in which Lagrange felt the occurrence of secular terms was unavoidable. In actuality, such terms do not occur, and the oscillations are described in the usual way, but can have different phases:

$$\left.\begin{aligned} q_1 &= A_1 \sin(pt + \varphi_1), \\ q_2 &= A_2 \sin(pt + \varphi_2). \end{aligned}\right\} \tag{26.33}$$

The constants A_1, A_2, φ_1 and φ_2 are determined by the initial conditions. Whatever the latter may be, the oscillations with respect to each coordinate are single-frequency oscillations.

We have established that, if a mechanical system does not have dissipative properties — i.e., there is no damping — the multiple roots do not indicate the occurrence of secular terms in the solution. However, if the differential equations of motion contain the first derivatives of the desired functions, then in the case of multiple roots secular terms arise in the solution. It does not follow from this that the system must absolutely leave the equilibrium position in an infinite manner during its motion (this would be physically impossible in the case of a dissipative system).

This is the example which was given in the book by A.I.Lur'ye(see the comments on page 217). The differential equations for the motion of a system with two degrees of freedom have the form

$$\left.\begin{aligned} \ddot{q}_1 + \dot{q}_1 + q_1 + q_2 &= 0, \\ \ddot{q}_2 + 3\dot{q}_2 + q_1 + 3q_2 &= 0. \end{aligned}\right\} \tag{26.34}$$

Investigating the particular solution in the form

$$q_1 = a_1 e^{\lambda t}, \quad q_2 = a_2 e^{\lambda t}, \tag{26.35}$$

we arrive at the following characteristic equation /225

$$(\lambda^3 + 2\lambda + 2)(\lambda + 1)^2 = 0. \tag{26.36}$$

Among its roots

$$\lambda_1 = -1; \quad \lambda_2 = -1; \quad \lambda_3 = -1 + i; \quad \lambda_4 = -1 - i \tag{26.37}$$

one is a multiple root, and due to this the solution contains secular terms. With the initial conditions

$$q_1(0) = q_2(0) = \dot{q}_2(0) = 0$$

we find that the solution has the form

$$\left.\begin{aligned} q_1 &= \dot{q}_1(0)(te^{-t} + e^{-t} - e^{-t}\cos t); \\ q_2 &= \dot{q}_1(0)(te^{-t} - e^{-t}\sin t) \end{aligned}\right\} \tag{26.38}$$

and indicates damping motion (since $te^{-t} \to 0$ for $t \to \infty$), although it contains secular terms.

The translation of "Analytical Mechanics" by Lagrange into Russian was published in 1950 (Gostekhizdat, Vol. 1, 2). For the error made by Lagrange see "Lektsiyakh po kolebaniyam,(Lectures on Oscillations) "L.I. Mandel'shtam (Izdatel'stvo SSSR, Moscow, 1955, Lecture 28), and also on page 234 of the book by A.N. Krylov.

Automobile oscillations are examined in the books by R.V. Rotenberg, Teoriya podveski avtomobilya (Theory of Automobile Suspensions) (Mashgiz, 1951) and I.G. Parkhilovskiy "Avtomobil'nyye listovyye ressory (Automobile Leaf Springs) (Mashgiz, 1954).

§ 27. Formula of A.N. Krylov

In St. Petersburg in 1914 during experiments on a test stand of 12-inch marine instruments, it was found that the pressure developed in the compressor cylinders was 450 atmospheres, instead of the normal pressure of 250 atmospheres, on which the design accuracy was based. It was found that all of the compressors constructed (48 items) had to be rejected since they were incompatible with the unexpected large loads. Since each of the compressors cost 50 thousand roubles, replacing all of the compressors with new ones would entail a cost of about 2 and a half million roubles. In addition, this replacement would increase the time before the ships were ready.

This matter was submitted to the expertise of A.N. Krylov(*) who, /226 using his studies carried out in 1909, found that the recording instrument — the Vickers indicator — produced greatly distorted results, and the true maximum pressure was approximately 2 times less than that given.

(*)Aleksey Nikolayevich Krylov (1863 - 1945) — mechanist, mathematician, shipbuilder, and historian of science. Academician (from 1916), Hero of Socialist Labor (from 1943) Starting in 1890 for almost fifty years he served in Moscow as an academician in Petersburg (Leningrad). In addition to many special studies, A.N. Krylov wrote a book of memoirs entitled "Moi vospominaniya" (My Recollections).

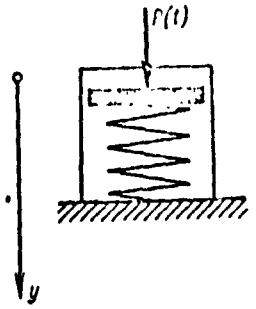

Fig. 27.1. Indicator system.

The conclusion of A.N. Krylov resulted in the fact that the replacement of the compressors was not necessary. This not only saved a great amount of money, but also made it possible to put the ships into operation in time.

The solution which A.N. Krylov obtained was not only practical, but was also of great theoretical importance. In order to understand this solution, let us investigate the action of a perturbing force P(t), given arbitrarily, on an elastic linear system with 1 degree of freedom. In particular, a spring pressure indicator may belong to such a system (Figure 27.1).

As is known, the displacement y at any moment of time t is determined by the following general expression(**)

$$y = \frac{1}{mp}\int_0^t P(\tau)\sin p(t-\tau)\,d\tau, \qquad (27.1)$$

in which m is the system mass, p — frequency of free oscillations, equal to

$$p = \sqrt{\frac{c}{m}} \qquad (27.2)$$

(c — coefficient of system rigidity). The quantity τ designates the integration variable, having the dimensionality of time.

Expression (27.1) may be given a different form, if we integrate it by parts /227

$$y = \frac{P(t)}{c} - \frac{1}{c}\int_0^t \dot{P}(\tau)\cos p(t-\tau)\,d\tau. \qquad (27.3)$$

Here

$$\dot{P} = \frac{dP}{dt} \qquad (27.4)$$

(*) The derivation is given, for example, in Section 29.

represents the rate at which the force changes. Expression (27.3) holds when P(0) = 0, and the force P(t) is continuous, as is shown in 27.2, a (this case is of interest to us in the present section).

The first term in (27.3) represents the displacement which would be caused by the force P(t) during its static action, and the second term has the meaning of a dynamic correction.

In spring indicators (of the Vickers type) it is desirable that the spring displacement be constantly proportional to the acting load. The displacement may then be used to more or less reliably determine the changes in the load (pressure). In other words, the indicator must be such that the dynamic correction is small as compared with the first term. We shall use Δy to designate the absolute value of the dynamic correction

$$\Delta y = \frac{1}{c}\left|\int_0^t \dot{P}(\tau)\cos p(t-\tau)\,d\tau\right| = \left|\frac{\cos pt}{c}\int_0^t \dot{P}(\tau)\cos p\tau\,d\tau + \frac{\sin pt}{c}\int_0^t \dot{P}(\tau)\sin p\tau\,d\tau\right| \tag{27.5}$$

and we set

$$A = \int_0^t \dot{P}(\tau)\cos p\tau\,d\tau, \quad B = \int_0^t \dot{P}(\tau)\sin p\tau\,d\tau. \tag{27.6}$$

We then have

$$\Delta y = \left|\frac{A}{c}\cos pt + \frac{B}{c}\sin pt\right|, \tag{27.7}$$

and the largest value of the correction apparently satisfies the inequality /228

$$\Delta y \leq \frac{1}{c}\sqrt{A^2 + B^2}. \tag{27.8}$$

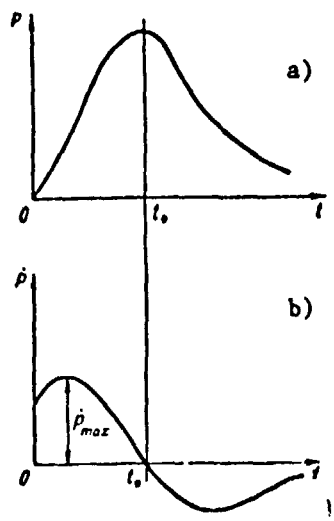

Fig. 27.2. Dependence of the force and its derivative with respect to time t. The derivative $\dot{P}$ (t) has only one maximum in the $(0,t_*)$ interval.

Following A.N. Krylov, let us investigate the case (which is basic for indicators) when the period of the eigenoscillations of the system is much less than the duration of the force increase, and we shall assume that the force changes in time according to the law shown in Figure 27.2, a. This force during a certain time t_* monotonically increases up to its greatest value, and then gradually decreases (as occurs, for example, during the action of explosions). Let us determine the greatest absolute value Δy of the dynamic correction for a certain moment $t \leq t_*$, i.e., on the ascending branch of the curve $P = P(t)$. In the integrand in (27.6), the first factor in the interval $[0, t_*]$ is positive everywhere, and the second factors periodically change sign. In order to estimate the quantities A and B, we divide the interval [0, t] by the particular intervals in which the functions cos pt and sin pt retain a positive sign. If $T_0 = \frac{2\pi}{p}$ is the period of the eigenoscillations for the system, then to calculate A we must assume the following intervals:

$$\left[0, \frac{T_0}{4}\right], \left[\frac{T_0}{4}, \frac{3T_0}{4}\right], \left[\frac{3T_0}{4}, \frac{5T_0}{4}\right], \ldots$$
$$\ldots, \left[\frac{4n-1}{4}T_0, \frac{4n+1}{4}T_0\right], \left[\frac{4n+1}{4}T_0, t\right];$$

They are given in Figure 27.3,a. In a similar manner, to calculate B such intervals are /229

$$\left[0, \frac{T_0}{2}\right], \left[\frac{T_0}{2}, T_0\right], \left[T_0, \frac{3}{2}T_0\right], \ldots$$
$$\ldots, \left[\frac{n-1}{2}T_0, \frac{n}{2}T_0\right], \left[\frac{n}{2}T_0, t\right]$$

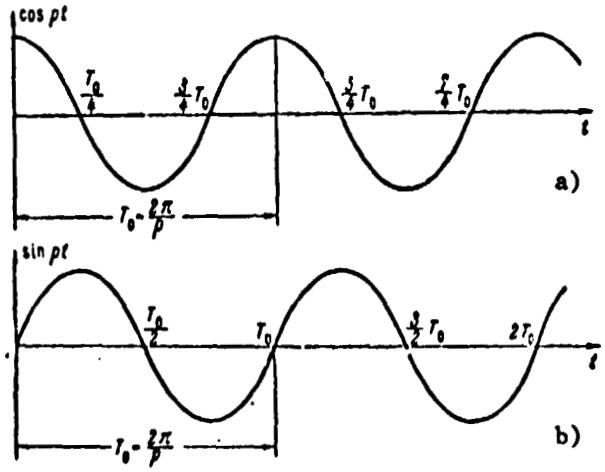

Fig. 27.3. The figure shows the time intervals, in which the functions cos pt and sin pt do not change sign.

(see Figure 27.3, b). First of all, let us estimate A. According to expression (27.6), we have

$$A=\int_0^t \dot{P}(\tau)\cos p\tau\,d\tau=\int_0^{\frac{T_0}{4}}\dot{P}(\tau)\cos p\tau\,d\tau+\int_{\frac{T_0}{4}}^{\frac{3T_0}{4}}\dot{P}(\tau)\cos p\tau\,d\tau+$$
$$+\int_{\frac{3T_0}{4}}^{\frac{5T_0}{4}}\dot{P}(\tau)\cos p\tau\,d\tau+\ldots+\int_{\frac{(4n-1)T_0}{4}}^{\frac{4n+1}{4}T_0}\dot{P}(\tau)\cos p\tau\,d\tau+ \qquad (27.9)$$
$$+\int_{\frac{4n+1}{4}T_0}^{t}\dot{P}(\tau)\cos p\tau\,d\tau.$$

In the first interval cos pτ is positive constantly; in the second interval — negative; in the third interval — positive, etc. The function $\dot{P}(\tau)$ does not change its sign and is constantly positive. Therefore, assuming the average value theorem for each of the intervals, we obtain /230

$$\int_0^{\frac{T_0}{4}} \dot{P}(\tau)\cos p\tau\, d\tau = \dot{P}(\tau_1)\int_0^{\frac{T_0}{4}} \cos p\tau\, d\tau = \frac{T_0}{2\pi}\dot{P}(\tau_1),$$
$$\int_{\frac{T_0}{4}}^{\frac{3T_0}{4}} \dot{P}(\tau)\cos p\tau\, d\tau = \dot{P}(\tau_2)\int_{\frac{T_0}{4}}^{\frac{3T_0}{4}} \cos p\tau\, d\tau = -\frac{T_0}{\pi}\dot{P}(\tau_2) \tag{27.10}$$

etc. Here $0<\tau_1<\frac{T_0}{4}$, $\frac{T_0}{4}<\tau_2<\frac{3T_0}{4}$ ..., i.e, τ_1, τ_2, ... are certain intermediate values of time within successive intervals. Thus, we have

$$A=\frac{T_0}{\pi}\left[\frac{1}{2}\dot{P}(\tau_1)-\dot{P}(\tau_2)+\dot{P}(\tau_3)-\ldots\right]. \tag{27.11}$$

In addition, A.N. Krylov assumed that the curve $\dot{P}(t)$ in the interval $[0, t_*]$ has only one maximum (see Figure 27.2, b). In this case, which is very important in practice, the absolute value of the sum, which appears between the brackets in (27.11), cannot exceed the greatest value of the components. In turn, the latter cannot exceed the maximum value of the derivative $\dot{P}$, which we designate by $\dot{P}_{max}$. Consequently,

$$|A|\leqq\frac{T_0}{\pi}\dot{P}_{max}. \tag{27.12}$$

In the same way, we find that

$$|B|\leqslant\frac{T_0}{\pi}\dot{P}_{max}. \tag{27.13}$$

Therefore,

$$\sqrt{A^2+B^2}\leqq\frac{T_0}{\pi}\sqrt{2}\dot{P}_{max} \tag{27.14}$$

and instead of (27.8), we obtain

$$\Delta y\leqq\frac{T_0}{\pi c}\sqrt{2}\dot{P}_{max}. \tag{27.15}$$

Noting that $\sqrt{2}:\pi<\frac{1}{2}$, A.N. Krylov attributed the following form to inequality (27.15) /231

$$\Delta y<\frac{T_0}{2c}\dot{P}_{max}. \tag{27.16}$$

The quantity $\frac{T_0}{2}\dot{P}_{max}$ has the dimensionality of force, and represents the largest possible increase in the force P in the time interval $\frac{T_0}{2}$, i.e., in the half-period of free oscillations. Designating this quantity by ΔP_{max}, we obtain the expressive form

$$\Delta y < \frac{\Delta P_{max}}{c}. \tag{27.17}$$

This is the A.N. Krylov formula. The right-hand side represents a displacement, which could cause a statically acting force ΔP_{max}. It is clear that the smaller is the period of free oscillations, the smaller is the value of ΔP_{max}, and consequently of Δy. A.N. Krylov wrote: "Consequently, if the period of free oscillations of a system is so small in comparison with the duration of increase in the force acting on the system that the greatest force in the time interval equal to the half-period of the free oscillations of the system can be disregarded, the deviation of the system can be calculated 'in a static manner', and the error will not exceed a value corresponding to the given change in pressure."

For correct readings of the spring indicator, it is necessary that (27.17) be very small. In turn, this means that the period of free oscillations of the indicator mass must be small as compared with the length of time the force is applied, i.e., the indicator plunger must be as light as possible, and the spring must be very rigid. These are the basic requirements which must be followed when constructing pressure indicators.

Let us determine the extent to which this was carried out in the Vickers indicators. A.N. Krylov gave the following data for the indicator: spring weight 0.817 kg, plunger weight 0.092 kg, length of spring l = 12 cm, and /232 spring rigidity coefficient

$$c = \frac{1165}{12} = 97.1 \text{ kg/cm}.$$

Using these values, we find the mass(*)

$$m = \left(0.092 + \frac{1}{3} \cdot 0{,}817\right) : 981 = 3.71 \cdot 10^{-4} \ \frac{\text{kg} \cdot \text{sec}^2}{\text{cm}}$$

and the circular frequency of the free oscillations according to formula (27.2)

$$p = \sqrt{\frac{97.1}{3.71} \cdot 10^4} = 511 \ \text{sec}^{-1}$$

Corresponding to this, the period of free oscillations of an elastic system of an indicator equals

$$T_0 = \frac{6{,}28}{511} = 0.012 \quad \text{sec}$$

(In his more precise calculation, A.N. Krylov obtained almost the same result T_0 = 0.013 sec). Such an indicator will correctly give the pressure changes only under the condition that the length of time in whhch the pressure t_* increases is much greater than 0.012 sec. In the construction studied by A.N. Krylov, the quantity t_* was not greater, but even less, than the period T . This means that the pressure is perceived by the indicator as a rapidly changing load. In this case, the Vickers indicators must give very distorted readings.

Figure 27.4 shows curves calculated by A.N. Krylov for this case. The /233
solid line shows the true value of the acting force, and the dashed line gives the corresponding change in the elastic displacement. As can be readily seen here, this form of the displacements can in no way indicate the true law governing the change in force.

The shorter is the period of time in which the force is in operation, the greater is the difference between the displacement form and the true law governing the force change. This is particularly clear when the force acts in an extremely short period of time (as compared with the period of

(*) The simplest variation of determining the reduced mass (according to Rayleigh) is used here. A.N. Krylov used more precise considerations. In his calculation, the reduction coefficient equals 0.465, and not 1/3, as was written here. This has no important influence on the final result.

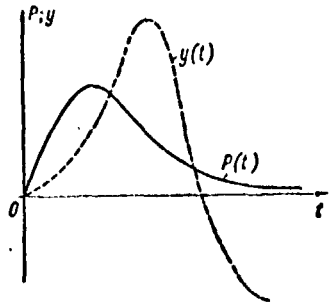

Fig. 27.4. Readings of Vickers indicator (dashed curve) are not proportional to the acting pressure (solid curve).

eigenoscillations.) In such cases, the concept of an instantaneous impulse is useful. According to this concept, the duration of the force is assumed to be zero, but the impulse S is assumed to be finite. The oscillations produced by such an impulse begin under the conditions

$$y = 0,\ v = \frac{S}{m} \quad \text{for } t = 0 \tag{27.18}$$

and follow the law

$$y = \frac{S}{mp} \sin pt, \tag{27.19}$$

i.e., they occur with the eigenfrequency p. As regards the greatest deviation

$$y_{max} = \frac{S}{mp}, \tag{27.20}$$

it may be used to determine the impulse of the force, but not the maximum value of the force.

The Krylov formula always makes it possible to make a prediction beforehand, of whether the action of a given force is static for a given system.

We shall give still one more example which we have taken from another work of A.N. Krylov. Radial oscillations of a barrel of an artillery gun loaded with an increasing internal pressure are examined. The duration of the pressure increase is (for the example given by A.N. Krylov) approximately 0.01 sec in all. However, such a pressure cannot be called a rapidly increasing pressure — the period of free oscillations of the gun barrel is much less, about 0.0003 sec. Consequently, the action of the pressure in this case /234 may be reliably assumed to be static.

The A.N. Krylov formula was derived in 1909 in his work "Sobraniye trudov" (Collected Works), Moscow, Vol. IV, 1937. Its derivation is also contained in the book "O nekotorykh differentsial'nykh uravneniyakh matematicheskoy fiziki emeyushchikh prilozheniye v tekhnicheskikh voprosakh" (Certain Differential

Equations of Mathematical Physics as Applied to Technical Problems) (Section 82-85). Section 123 in this same book examines the problem of radial oscillations of an artillery gun barrel.

§ 28. Four Methods of Solving the Problem of the Action of Periodic Instantaneous Impulses

In order to develop any branch of mechanics, attempts must be made to find improved algorithms and to improve the computational methods, even for previously solved problems. An explicit and precise solution, devoid of any superfluous factors, has been called "exceptional" (A.A. Andronov(*) wrote more expressively for these cases: "elegant solution", stressing not only the aesthetic side, but also the practical side).

In this section, we shall successively examine four variations of the solution of the same problem. All of these variations may be found in present day literature.

As we have seen, up to the present cumbersome computational methods are frequently used, although the most convenient and refined method has been well known for about half a century. For unknown reasons, it has not received its deserving study.

In certain technical problems, it is necessary to deal with brief forces, whose action is repeated over different time intervals. In these cases, an idealized concept of instantaneous impulses is used, which was discussed at the end of the preceding section, and the problem is reduced to studying the action of periodically applied instantaneous impulses S which differ from /235 each other. Let us examine and discuss the four variations of the solution of such a problem.

(*) Aleksandr Aleksandrovich Andronov (1901 - 1952) — from 1931 Professor of the Gorkiy University, from 1946 — Academician. He solved many important problems of theoretical radio engineering, the theory of nonlinear oscillations, and the theory of automatic control.

First Method. Let us assume that T is the period in which the impulses are applied. Then 0, T, 2T, ... are the moments of application of zero (initial), first, second, etc., impulses. Let us first investigate the action of only one initial impulse. The differential equation of motion

$$\frac{d^2y}{dt^2}+p^2y=0 \tag{28.1}$$

(p is the frequency of free oscillations) has a solution

$$y=\frac{S}{mp}\sin pt \quad (t>0), \tag{28.2}$$

which satisfies both equation (28.1) and the initial conditions (i.e., the conditions leading to the motion immediately after the initial impulse has disappeared):

$$y=0, \quad \frac{dy}{dt}=\frac{S}{m}. \tag{28.3}$$

The motion produced only by the subsequent first impulse may be obtained from the same expression (28.2) in the form

$$y=\frac{S}{mp}\sin p(t-T) \quad (t>T). \tag{28.4}$$

In a similar manner, we may find the result of the action of subsequent impulses. In order to obtain the general motion, it is necessary to combine these "partial" motions. For one typical interval of time [nT, (n + 1) T], i.e., in the interval between the appearance of $n^{\underline{\text{th}}}$ and $(n+1)^{\underline{\text{th}}}$ impulses, we have

$$\begin{aligned} y=\frac{S}{mp}[&\sin pt+\sin p(t-T)+\sin p(t-2T)+\ldots \\ &\ldots+\sin p(t-nT)]=\frac{S}{mp}\sum_{k=0}^{k=n}\sin p(t-kT). \end{aligned} \tag{28.5}$$

For the beginning of this time interval, i.e., for t = nT, we obtain the following from expression (28.5)

$$y=\frac{S}{mp}\sum_{k=0}^{k=n-1}\sin(n-k)pT. \tag{28.6}$$

The derivation of expressions (28.5) and (28.6) is simple and clear, and their form may even be externally compact. However, our sympathies disappear, if we only consider the necessary computations and imagine their volume. For example, let us assume we must determine the motion in the time interval /236

(99T, 100T), and find the deviations in each 10th part of this interval, i.e., in the moments $t_0 = 99T$. $t_1 = 99.1T$, $t_2 = 99.2T$, ..., $t_9 = 99.9T$, $t_{10} = 100T$. According to (28.5), we must calculate eleven sums:

$$\left.\begin{aligned} y_0 &= \frac{S}{mp}\sum_{k=0}^{k=99}\sin(99-k)pT, \\ y_1 &= \frac{S}{mp}\sum_{k=0}^{k=99}\sin(99.1-k)pT, \\ &\cdots\cdots\cdots\cdots \\ y_{10} &= \frac{S}{mp}\sum_{k=0}^{k=99}\sin(100-k)pT, \end{aligned}\right\} \qquad (28.7)$$

in each of which there are 100 (!) terms. Thus, using this method, we must:

(a) calculate a thousand values of the arguments;

(b) find as many values of the sine using the table of trigonometric functions;

(c) carry out the sumation operations indicated in expressions (28.7).

After this, we can describe (and not in very great detail) the motion only in one period [99T, 100T]. For any other period, it is necessary to do the entire process again. However, there is still one unpleasant side of these computations. Among the terms of each of the sums, there are both positive and negative terms. This makes it necessary to calculate with a large number of significant digits.

Although these drawbacks of this method are apparent, we shall not jump to conclusions. We must still examine what are the advantages and disadvantages of other methods.

Second Method. Let us begin with the general case, and investigate the /237 action of an arbitrary perturbing force P(t) on an oscillatory elastic system with one degree of freedom. As is known, the differential equation of motion

$$\frac{d^2y}{dt^2} + p^2y = \frac{P(t)}{m} \qquad (28.8)$$

(notation is the same as previously) has the following solution for zero initial conditions

$$y = \frac{1}{mp}\int_0^t P(\tau)\sin p(t-\tau)\,d\tau \tag{28.9}$$

(In the preceding section, we spoke in detail about the physical nature of the solution). It may have the following form

$$y = A\cos pt + B\sin pt, \tag{28.10}$$

where

$$\left.\begin{aligned} A &= -\frac{1}{mp}\int_0^t P(\tau)\sin p\tau\,d\tau, \\ B &= \frac{1}{mp}\int_0^t P(\tau)\cos p\tau\,d\tau. \end{aligned}\right\} \tag{28.11}$$

We may now assume that at the moments of time 0, T, 2T, ... identical impulses S are applied to the system. Then for the time interval [kT, (k + 1) T] we find the following from expressions (28.11):

$$A = -\frac{S}{mp}[\sin pT + \sin 2pT + \ldots + \sin kpT], \tag{28.12}$$

$$B = \frac{S}{mp}[1 + \cos pT + \cos 2pT + \ldots + \cos kpT]. \tag{28.13}$$

These expressions may be given a more compact form by subsequent transformations. Let us multiply the sum in expression (28.12) by $2\sin\frac{pT}{2}$, and let us write several obvious equations:

$$\begin{aligned} 2\sin\frac{pT}{2}\sin pT &= \cos\frac{pT}{2} - \cos\frac{3pT}{2}, \\ 2\sin\frac{pT}{2}\sin 2pT &= \cos\frac{3pT}{2} - \cos\frac{5pT}{2}, \\ &\ldots\ldots\ldots\ldots\ldots\ldots \\ 2\sin\frac{pT}{2}\sin kpT &= \cos\frac{2k-1}{2}pT - \cos\frac{2k+1}{2}pT. \end{aligned}$$

/238

Combining all of these equations, we obtain, instead of the expression within the brackets in formula (28.12), the following equation

$$\frac{\cos\frac{pT}{2} - \cos\frac{2k+1}{2}pT}{2\sin\frac{pT}{2}} = \frac{\sin\frac{k+1}{2}pT\cdot\sin\frac{k}{2}pT}{\sin\frac{pT}{2}}.$$

In a similar manner, the expression in the brackets in formula (28.13) may be given the following form

$$\frac{\sin\frac{2k+1}{2}pT+\sin\frac{pT}{2}}{2\sin\frac{pT}{2}},$$

Finally, the formulas (28.12) and (28.13) assume the form

$$\left.\begin{aligned} A&=-\frac{S}{mp}\frac{\sin\frac{k+1}{2}pT\cdot\sin\frac{k}{2}pT}{\sin\frac{pT}{2}},\\ B&=\frac{S}{mp}\frac{\sin\frac{2k+1}{2}pT+\sin\frac{pT}{2}}{2\sin\frac{pT}{2}}. \end{aligned}\right\} \qquad (28.14)$$

Thus, to determine the motion in any interval there is no necessity of fatiguing summation, which is necessary in the first method. We need only first find the numbers A and B according to formula (28.14), and then use the very simple expression (28.10).

Nevertheless, this method contains one great drawback.

The solution given in expressions (28.10) and (28.14) is not periodic /239 and changes from one period to another (the number k is in these expressions). Therefore, it is necessary to repeat the calculation again for each new period for a complete description of the motion. It is disappointing that apparently the main portion of the motion is undoubtedly a periodic process "imposed" on the elastic system by impulses which are repeated with the period T.

How can we explain that the solution obtained does not have this periodicity? The answer to this question is somewhat of a paradox: this solution is "too" precise — it contains not only a description of a stationary oscillating process with the period T, but also reflects the influence of the initial conditions, which in actuality is very rapidly damped due to the inelastic resistances. This "addition" to a stationary process cannot be excluded in general, since the initial equation is described for a purely elastic system devoid of inelastic resistances.

Is it possible to obtain in general a purely periodic solution, if we are dealing with this equation, i.e., terms expressing the damping are not introduced in the equation? The answer is yes, as the following two methods of solution show.

Third Method. The system we are investigating is linear, and this determines the validity of the principle of superposition, which we used above when we added the influence of the second impulse to the first impulse, and then the third impulse, etc. However, this principle may be used in a different way.

We can represent the periodic force P(t) in the right part of the differential equation of the problem (28.8) in the form of an infinite sum of harmonics with the periods T, 1/2 T, 1/3 T, ..., i.e., in the form of a Fourier series

$$P(t)=\frac{a_0}{2}+\sum_{k=1}^{\infty}a_k\cos k\frac{2\pi t}{T}+\sum_{k=1}^{\infty}b_k\sin k\frac{2\pi t}{T}. \qquad (28.15)$$

Expansion of (28.15) pertains to the first period [0, T]; the process is again repeated in all the remaining periods. In this solution, the motion produced by each of the harmonics is first found, and then — using the principle of superposition — these "partial" solutions are summed. To calculate the coefficients a_k and b_k, we must use the formulas of Fourier: /240

$$\left.\begin{aligned} a_k&=\frac{2}{T}\int_0^T P(t)\cos k\frac{2\pi t}{T}\,dt \quad (k=0,\ 1,\ 2,\ \ldots),\\ b_k&=\frac{2}{T}\int_0^T P(t)\sin k\frac{2\pi t}{T}\,dt \quad (k=1,\ 2,\ \ldots). \end{aligned}\right\} \qquad (28.16)$$

In the case of periodic instantaneous impulses, we have

$$\left.\begin{aligned} \int_0^T P(t)\cos k\frac{2\pi t}{T}\,dt&=\lim_{\Delta t\to 0}\int_0^{\Delta t} P(t)\cos k\frac{2\pi t}{T}\,dt=S,\\ \int_0^T P(t)\sin k\frac{2\pi t}{T}\,dt&=\lim_{\Delta t\to 0}\int_0^{\Delta t} P(t)\sin k\frac{2\pi t}{T}\,dt=0 \end{aligned}\right\} \qquad (28.17)$$

and we obtain the following from formula (28.16)

$$a_k = \frac{2S}{T}, \quad b_k = 0.$$

Thus, we have

$$P(t) = \frac{S}{T} + \frac{2S}{T} \sum_{k=1}^{\infty} \cos k \frac{2\pi t}{T}. \tag{28.18}$$

We must now deal not with instantaneous impulses, but with an infinite sum in expression (28.18). The general term of the sum has the form $\frac{2S}{T} \cos k \frac{2\pi t}{T}$.

Let us examine the motion which is caused by the action of only one such component. For this purpose, we must solve the differential equation of motion

$$\frac{d^2y_k}{dt^2} + p^2 y_k = \frac{2S}{mT} \cos k \frac{2\pi t}{T}. \tag{28.19}$$

The particular solution (not connected with the initial conditions) can be written in the form

$$y_k = A_k \cos k \frac{2\pi t}{T}. \tag{28.20}$$

We may find the amplitude A_k by substituting the solution (28.20) in equation (28.19): /241

$$\left(-\frac{2\pi k}{T}\right)^2 A_k + p^2 A_k = \frac{2S}{mT},$$

from which we obtain

$$A_k = \frac{2S}{mT\left[p^2 - \left(\frac{2\pi k}{T}\right)^2\right]}. \tag{28.21}$$

Thus, the solution (28.20) has the form

$$y_k = \frac{2S}{mT\left[p^2 - \left(\frac{2\pi k}{T}\right)^2\right]} \cos k \frac{2\pi t}{T}. \tag{28.22}$$

Summing the individual solutions such as (28.22), i.e., combining the motions caused by each of the harmonics in the series (28.18), we obtain the following for one period

$$y = \frac{S}{mp^2T} + \frac{2S}{mT}\sum_{k=1}^{\infty}\frac{\cos k\frac{2\pi t}{T}}{p^2 - \left(\frac{2\pi k}{T}\right)^2}. \qquad (28.23)$$

Here the first term corresponds to the first component $\frac{S}{T}$ in (28.18). The main drawback of the solution (28.23) is apparent, and consists of the necessity of summing an infinite series. However, the series converges rapidly, and this disadvantage cannot hide the important advantage of the solution (28.23) — its periodicity. This property of the solution (28.23) gives it an advantage over periodic solutions obtained by the first two methods.

It is worth investigating in greater detail the factors producing the desired periodic solution, and answering the following two questions:

(1) How can the "additions" which disturb the periodicity be removed?

(2) Is the solution obtained here more accurate than the solutions found by the two previous methods or, just the opposite, is it less accurate?

The answer to the first question is simple. The solution (28.20) of equation (28.19) represents only a stationary, i.e., a purely periodic (with the period T) part of the solution, since in our solution those terms of the complete solution which could disturb this periodicity are completely "cut off". /242

We may thus have the answer to the second question: the solution which we found (28.23) is not an accurate solution of the problem, since we have not taken into account the initial conditions. However, in actuality due to the action of the damping factors [which were not taken into account when compiling equation (28.8)], the initial conditions influence the process of motion only for a very short period, and after a certain small number of periods the process acquires a stationary character, and the subsequent action will be repeated from period to period. It may be shown that, searching for only a periodic solution, we compensate for an incomplete equation. From this point of view, the solution (28.23) more precisely reflects the true laws than do the other solutions obtained above.

Fourth Method. After the statements made above, it is difficult to imagine such a fortunate combination of advantages of periodicity and closure as in the fourth method which we are investigating now.

Let us examine one of the periods T, assuming that the moment the last impulse disappeared is the beginning moment at which the time is calculated. During the period under consideration, the oscillations are free and may be described by the following solution

$$y = A\cos pt + B\sin pt. \tag{28.24}$$

If y_0 is the initial displacement and v_0 is the initial velocity, then the constants A and B equal

$$A = y_0, \quad B = \frac{v_0}{p}, \tag{28.25}$$

Solution (28.24) may be written in the form

$$y = y_0\cos pt + \frac{v_0}{p}\sin pt. \tag{28.26}$$

Differentiating with respect to time t, we find the velocity

$$v = -y_0 p\sin pt + v_0\cos pt. \tag{28.27}$$

At the end of this period, immediately before the next impulse is applied (i.e., for t = T), we have /243

$$y_1 = y_0\cos pT + \frac{v_0}{p}\sin pT, \tag{28.28}$$

$$v_1 = -py_0\sin pT + v_0\cos pT. \tag{28.29}$$

Immediately after applying the next impulse, the displacement y retains its value (28.28):

$$y_2 = y_1 = y_0\cos pT + \frac{v_0}{p}\sin pT, \tag{28}$$

But the velocity instantaneously changes by the quantity $\frac{S}{m}$, and is the following, taking into account expression (28.29)

$$v_1 = -py_0\sin pT + v_0\cos pT + \frac{S}{m}. \tag{28.31}$$

Although these computations are simple, it is possible that the reader is not familiar with them and for this reason they are given. Everything becomes very clear after the subsequent decisive step: due to the assumed periodicity

of the process, the terms y_2 and v_2 must equal the terms y_0 and v_0, i.e.,

$$y_0 = y_0 \cos pT + \frac{v_0}{p} \sin pT, \tag{28.32}$$

$$v_0 = -py_0 \sin pT + v_0 \cos pT + \frac{S}{m}. \tag{28.33}$$

Thus, we have attained a system of two algebraic equations with two unknowns y_0 and v_0; solving it, we obtain

$$y_0 = \frac{S}{2mp} \operatorname{ctg} \frac{pT}{2}, \quad v_0 = \frac{S}{2m}, \tag{28.34}$$

and the law governing the motion (28.24) assumes the form

$$y = \frac{S}{2mp}\left(\sin pt + \cos pt \cdot \operatorname{ctg} \frac{pT}{2}\right). \tag{28.35}$$

Is this all? Yes, this is the final expression which comprehensively solves the problem. There are no finite (as in method 1) or infinite (as in method 3) sums. This method is superior to method 2 due to its periodicity. It is sufficient to formulate the law governing the motion for one period. In the subsequent periods, the motion will be completely repeated.

As we have stated above, periodicity is achieved by ignoring the given initial conditions (i.e., the conditions pertaining to the initial moment immediately before the first impulse is applied). Due to damping (which we did not take into account) in real systems, such periodic motion is achieved in the last analysis. /244

We should note that, if desired, the actually given initial conditions may be represented in the solution as follows. Let us assume that at the initial moment of time the given displacement and velocity are, respectively, y_0^* and v_0^*. Naturally, they differ from the quantities y_0 and v_0, which pertain to a purely periodic process and are given by expressions (28.34). We may write the equations:

$$\left.\begin{aligned} y_0^* &= y_0 + \left(y_0^* - \frac{S}{2mp} \operatorname{ctg} \frac{pT}{2}\right), \\ v_0^* &= v_0 + \left(v_0^* - \frac{S}{2m}\right). \end{aligned}\right\} \tag{28.36}$$

The first terms in the right-hand sides correspond to periodic (with the period T) motion (28.35), and the second terms cause free oscillations (with the period $2\pi/p$)

$$y=\left(y_0^*-\frac{S}{2mp}\operatorname{ctg}\frac{pT}{2}\right)\cos pt+\left(\frac{v_0^*}{p}-\frac{S}{2mp}\right)\sin pt. \qquad (28.37)$$

Here the time t is computed from the beginning of the process. Thus, the motion will be described by the sum of the solutions (28.35) and (28.37). We should repeat once again that the second part is of practical value in a small time interval close to the beginning of the process.

We could conclude our discussion here, but it would be useful to briefly analyze the result contained in (28.35).

First of all, let us note that if $\frac{pT}{2}=n\pi$ (where n is a whole number), then $\operatorname{ctg}\frac{pT}{2}\to\infty$; and the displacement amplitudes strive to infinity, i.e., impact resonance occurs. If $\omega=\frac{2\pi}{T}$ is the circular frequency of impulse application, then the condition of impact resonance requires the form

$$\omega=\frac{p}{n}. \qquad (28.38)$$

For all other ratios of frequencies, the deviations are finite. The amplitude of the oscillations equals the following according to (20.35) /245

$$a=\frac{S}{mp}\sqrt{1+\operatorname{ctg}^2\frac{pT}{2}}=\frac{S}{2mp\left|\sin\frac{\pi p}{\omega}\right|}. \qquad (28.39)$$

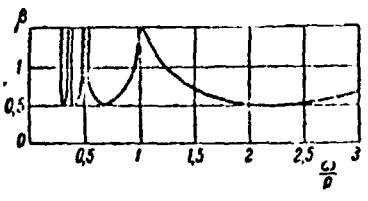

Fig. 28.1. Repetition influence coefficient in the case of periodic impulses.

Since, the fraction S : mp is the maximum deviation caused by one instantaneous impulse S, the expression

$$\beta=\frac{1}{2\left|\sin\frac{\pi p}{\omega}\right|} \qquad (28.40$$

may be called the coefficient of repetition influence. Figure 28.1 shows the dependence of β on the frequency ratio ω : p. As may be seen, a large number

of impact resonances are infinitely possible [according to formula (28.38)]. The least possible value of β equals 1/2.

By selecting the sequence of applying the four variations of the solution, we have consciously disturbed the chronological principle. The first method may be found in the book by N.K. Snitko "Metody rascheta sooruzheniy na vibratsiyu i udar" (Methods of Designing Structures for Vibration and Impact). (Gosstroyizdat, 1955, pp. 46 - 50; see also the book "Dinamika sooruzheniy" (Dynamics of Structures). (Gosstroyizdat, 1960, p. 69). The second method was proposed by A.N. Krylov (see his book "Vibratsiya sudov" (Ship Vibrations), ONTI, Sections 16, 2, 1936. For a graphic-analytical method of summation, see the book by G.S. Gorlik "Kolebaniya i volny" (Oscillations and Waves). (Fizmatgiz, Chapter II, Section 17, 1959). The third method was used by S.A. Bernshteyn in his book "Osnovy dinamiki sooruzheniy" (Bases of the Dynamics of Structures). (Gostroyizdat, Section 51, 1938). The fourth method was proposed by Duffing, and is given in all the editions of the book by A.I. Lur'ye and L.G. Loytsyanskiy "Teoreticheskaya mekhanika" (Theoretical Mechanics) as applied to the general case of a periodically disturbing force (see, for example, edition 12, Vol. II, Section 172, 1955). The relationships obtained there change into expression (28.35), if the instantaneous impulses S are used as the load. See also "Kurs stroitel'noy mekhaniki" (Course on Structural Mechanics), I.M. Rabinovich, Vol. 2 (Gosstroyizdat, Moscow, 1954), which gives the method described above for an additional calculation of the initial conditions by means of expression (28.37). The fourth method of solution may be readily extended to the case of a system with viscous resistance (see L.G. Loytsyanskiy, A.I. Lur'ye, Course on Theoretical Mechanics, Vol. II, Section 172). /246

§ 29. Superpositions: Variations of Using It in Problems of Forced Oscillations

The property of superposition (overlapping of action) is as follows. Let us assume that $P_1(t)$, $P_2(t)$, ..., $P_n(t)$ are external effects applied to a

system (for example, forces) which are given functions of time t, and $y_1(t)$, $y_2(t)$, ..., $y_n(t)$ — the phenomena caused by these effects (for example, displacement of any fixed point of a system). If, in the case of simultaneous application of all effects, i.e., for the action $P_1 + P_2 + \ldots + P_n$, the effect which is produced equals the sum of the effects $y_1 + y_2 + \ldots + y_n$, we then state that the system under consideration obeys the superposition principle.

All linear systems (not only mechanical, but also electrical, electromechanical, etc.) have this property. It is not only of great theoretical importance, but also opens up extensive and diverse possibilities for simplifying calculations in practice, particularly dynamic calculations of mechanical systems. These simplifications are as follows. An arbitrarily given perturbing force P(t) is represented by the sum of certain uniform components. In addition, a solution is formulated for the case when one of these components is in operation, and then the corresponding sum of the solutions is obtained.

In the literature on the theory of oscillations, the method of applying a perturbing force in a Fourier series is most frequently used. However, this variation far from exhausts all the possibilities inherent in the property of superposition. We may point out several different variations of applying the force P(t), and some of them have already been used in computations. Unfortunately, not enough attention has been given to the very important fact that, in spite of the external differences in the methods, they are in essence based on the general idea of superposition. We can trace the general nature of the /247 idealogical basis in five variations of a perturbing force acting on an ideally elastic system with one degree of freedom.

First Variation. Let us first of all recall that a general solution of a differential equation of free oscillations has the form

$$y = C_1 \sin pt + C_2 \cos pt. \qquad (29.1)$$

Here y = y(t) is the coordinate, t — time, p — natural frequency, C_1 and C_2 — constants subject to definition from the initial conditions of motion.

Let us now investigate the case when the motion is caused by a single instantaneous impulse S applied to the system at the moment τ. The initial conditions refer to the moment of time directly after the impulse S is applied, and have the form (m — mass of the system)

$$y=0,\quad \dot{y}=\frac{S}{m} \text{ for } t=\tau. \tag{29.2}$$

Now, determining the constants

$$C_1=\frac{S}{mp}\cos p\tau, \qquad C_2=-\frac{S}{mp}\sin p\tau, \tag{29.3}$$

we obtain the solution (29.1) in the form

$$y=\frac{S}{mp}\sin p(t-\tau). \tag{29.4}$$

This expression serves as the basis of the solution method under consideration. An arbitrary perturbing force P = P(t) may be represented in the form of a sequence of infinitely small impulses $P(\tau)d\tau$ expressed by vertical bands in Figure 29.1. Substituting the following in expression (29.4)

$$S=P(\tau)d\tau, \tag{29.5}$$

we find the oscillations caused by the action of one of the impulses. In order to determine the motion which is caused by the given force, we must apply all the influences of all the elementary impulses. Thus, we find that the displacement at the moment of time t equals /248

$$y=\frac{1}{mp}\int_0^t P(\tau)\sin p(t-\tau)\,d\tau. \tag{29.6}$$

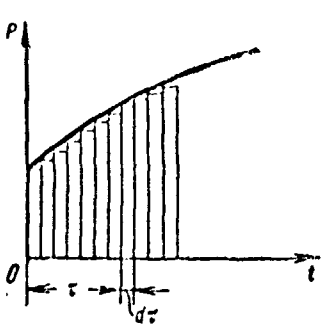

Fig. 29.1. Substitution of the force P (t) by a sequence of infinitely small impulses $P(\tau)d\tau$.

The solutions frequently have this form, when using the method of variation of constants, except that the method of derivation(*) much more graphically clarifies the "superposition" nature of (29.6).

(*) This method was given by Duhamel in 1834.

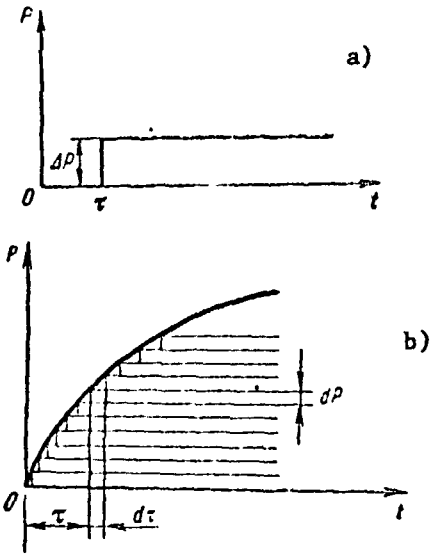

Fig. 29.2. a) Jump of the external force; b) substitution of the continuous force P(t) by a sequence of infinitely small jumps.

Second Variation. Let us again begin with a certain auxiliary problem, whose solution serves as a basis for compiling the general solution. Let us investigate the action of a jump (Figure 29.2, a), which represents the force ΔP = const applied to a system at the moment τ. In order to determine the motion of the system, it is necessary to integrate the nonnomogeneous differential equation

$$\ddot{y}+p^2y=\frac{\Delta P}{m} \quad \text{for} \quad t\geqslant\tau. \qquad (29.7)$$

The general solution of this equation has the form

$$y=C_1\sin pt+C_2\cos pt+\frac{\Delta P}{c}. \qquad (29.8)$$

Here the last term represents a particular solution (which can be easily guessed) of the differential equation (29.7) ($c = mp^2$ — coefficient of rigidity). To determine the constants, C_1 and C_2, we may use the initial conditions

$$y=0, \quad \dot{y}=0 \quad \text{for} \quad t=\tau. \qquad (29.9)$$

Using them, we obtain

$$C_1=-\frac{\Delta P}{c}\sin p\tau; \quad C_2=-\frac{\Delta P}{c}\cos p\tau \qquad (29.10)$$

and instead of (29.8) we obtain

$$y=\frac{\Delta P}{c}[1-\cos p(t-\tau)] \quad (t\geqslant\tau). \qquad (29.11)$$

We now turn to the problem of the action of an arbitrary perturbing force, and represent it in the for of a sequence of infinitely small jumps corresponding to the horizontal bands in Figure 29.2, b. In order to determine the action of one such jump, it is necessary to substitute the following in solution (29.11)

/249

$$\Delta P = \dot{P}(\tau)\, d\tau. \tag{29.12}$$

If we integrate the expression thus obtained, we obtain the result of the action of this force in the following form

$$y = \frac{1}{c}\int_0^t \dot{P}(\tau)\,[1 - \cos p\,(t-\tau)]\, d\tau = \\ = \frac{P(t)}{c} - \frac{1}{c}\int_0^t \dot{P}(\tau)\cos p\,(t-\tau)\, d\tau. \tag{29.13}$$

Finally, it is assumed here that the force P(t) has no discontinuities anywhere (i.e., finite jumps). If such discontinuities existed, they would have to be particularly isolated, and thus additional terms like (29.11) would be included in the solution (29.13) (in this case ΔP is the value of a finite jump), and the integral in (29.13) would be calculated as if the function P(t) were continuous. /250

For example, if the force P has a jump at the origin (i.e., for $\tau = 0$), as is shown in Figure 29.1, then the motion according to (29.11), caused by this jump, may be described by the law

$$y_1 = \frac{P(0)}{c}(1 - \cos pt), \tag{29.14}$$

where P(0) is the initial value of the force P. In the first term of (29.13), we must use the force P without allowance for the jump

$$y_2 = \frac{P(t) - P(0)}{c} - \frac{1}{c}\int_0^t \dot{P}(\tau)\cos p\,(t-\tau)\, d\tau. \tag{29.15}$$

Combining both motions (29.14) and (29.15), we obtain the general motion in the form

$$y = \frac{P(t) - P(0)\cos pt}{c} - \frac{1}{c}\int_0^t \dot{P}(\tau)\cos p\,(t-\tau)\, d\tau. \tag{29.16}$$

The solution (29.13) is most frequently obtained by integrating by parts expression (29.6). Thus, the physical nature of the solution remains in doubt.

Third Variation. This very popular method deals with the action of a perturbing force, whose period of change equals T:

$$P(t)=P(t+T). \tag{29.17}$$

The force (29.17) is represented in the form of a trigonometric Fourier series, i.e., it is replaced by the sum of the harmonics with the frequencies $\frac{2\pi}{T}$, $\frac{4\pi}{T}$, $\frac{6\pi}{T}$, ... The amplitude values of each of the harmonics are determined according to the formulas for the coefficients of the Fourier series. After this, /251 the typical expressions for the motions of a system are found, which correspond to each of the harmonics of the perturbing force, and then the complete solution is written in the form of the sum of these expressions. In this method, the concept of superposition is very apparent.

In many cases, a great disadvantage of the method is the necessity of allowing for a large number of components, since sometimes the amplitudes of the perturbing force harmonics decrease slightly with an increase in the number of harmonics.

Fourth Variation. This variation deals with the solution of the problem regarding forced oscillations caused by a periodic series of instantaneous impulses. This solution has been presented in Section 28 (fourth method), and we have pointed out the extreme simplicity of the final expression (28.35). Here, one useful property of this solution is important to us. Using it, we may obtain the general solution of the problem regarding the action of an arbitrary periodic perturbing force (29.17)(*). Let us assume that this force has the form shown in Figure 29.3. If we separate the periodic set of infinitely small impulses $P(\tau)d\tau$ from it, then the corresponding motion may be described by the expression (29.5), replacing S by $P(\tau)d\tau$. In addition, we should note that the letter t in expression (29.6) designates time, computed from the moment the impulse is applied. In our case, according to Figure 29.3, /252 this time equals $t-\tau$ (if $\tau < t$) and $T+t-\tau$ (if $\tau > t$).

(*) Just as in Section 28, we are discussing a steady process.

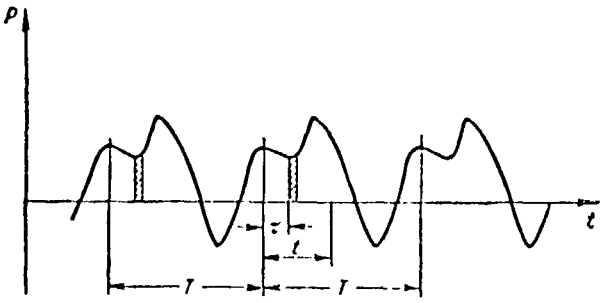

Fig. 29.3. Substitution of a periodic force by a sequence of periodic, infinitely small impulses.

The motion caused by the action of the given force $P(\tau)$ is obtained by integrating within the limits of one period (the entire set of impulses will be retained by this integration):

$$y=\frac{1}{2mp}\left\{\int_0^t P(\tau)\left[\sin p(t-\tau)+\operatorname{ctg}\frac{pT}{2}\cos p(t-\tau)\right]d\tau+\right.$$
$$\left.+\int_t^T P(\tau)\left[\sin p(T+t-\tau)+\operatorname{ctg}\frac{pT}{2}\cos p(T+t-\tau)\right]d\tau\right\}. \tag{29.18}$$

Transformations make it possible to write expression (29.18) in the form

$$y=\frac{1}{2mp}\left[A\sin pt+B\cos pt+2\int_0^t P(\tau)\sin p(t-\tau)d\tau\right], \tag{29.19}$$

where

$$\left.\begin{aligned} A&=\operatorname{ctg}\frac{pT}{2}\int_0^T P(\tau)\sin p\tau d\tau-\int_0^T P(\tau)\cos\tau d\tau,\\ B&=\int_0^T P(\tau)\sin p\tau d\tau+\operatorname{ctg}\frac{pT}{2}\int_0^T P(\tau)\cos p\tau d\tau. \end{aligned}\right\} \tag{29.20}$$

The time is computed from an arbitrarily selected moment, and the solutions (29.19) and (29.20) are valid in the case $0 \leq t \leq T$. In other periods, the motion is repeated.

Fifth Variation. This variation is particularly adapted to the case when a perturbing force has the form

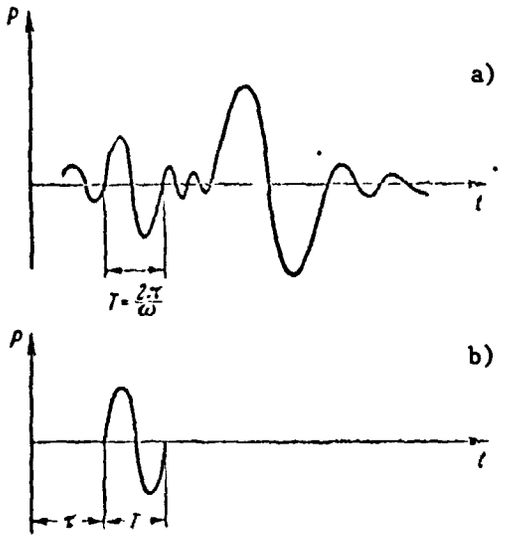

Fig. 29.4. a) Perturbing force of variable amplitude and frequency; b) elementary cycle of perturbing force.

$$P = P_0(t)\sin[\omega(t)+\sigma], \qquad (29.21)$$

i.e., it has a variable amplitude $P_0 = P_0(t)$ and a variable frequency $\omega = \omega(t)$ (see Figure 29.4, a).

First of all, let us examine the action of a force shown in Figure 29.4, b, which represents the isolated wave of a sinusoid (one cycle of change in the perturbing force, which follows a sinusoidal law of change). Let us assume the beginning of the cycle corresponds to the moment τ, and the end of the cycle corresponds to the moment $\tau + T$. Let us find the displacements of the system at the moments of time $t \geq \tau$: /253

$$y = \frac{P_0}{m(\omega^2 - p^2)}\left[\frac{\omega}{p}\sin(t-\tau) - \sin\omega(t-\tau)\right] \quad \text{for } \tau \leqslant t \leqslant \tau + T, \qquad (29.22)$$

$$y = \frac{2P_0}{m(\omega^2 - p^2)}\frac{\omega}{p}\sin\frac{\pi p}{\omega}\cos p\left(t - \tau + \frac{T}{2}\right) \quad \text{for } t > \tau + T. \qquad (29.23)$$

Now we may approximately regard the given force (Figure 29.4, a) as a series of isolated cycles (Figure 29.4, b). Naturally, this is permissible under the condition that each cycle of a given force can be replaced, with a sufficient degree of accuracy, by an isolated cycle of a strictly sinusoidal form.

In order to obtain the complete solution, it is necessary to combine the expressions (29.23), including by summation all the cycles of the load which precede the moment of time under consideration t, and also the cycle, within whose limits the moment of time t is located [according to expression (29.23)]. /254

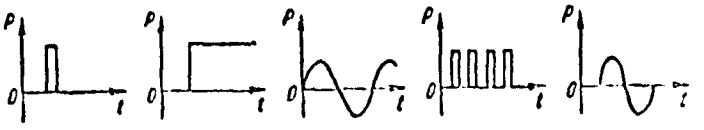

Fig. 29.5. Five variations of "supporting" effects.

We shall not describe the corresponding expressions, but we shall note that the solution may be additionally simplified, if, in the case of a large number of waves, we approximately change from summation to integration. Naturally, this change introduces a certain error into the solution.

Conclusion. Figure 29.5 shows the effects which are the basis of each of the described methods. There may be other forms of these effects. Each new variation of collecting an "elementary" effect leads to its own algorithm for solving the problem. However, any such algorithm in the last analysis will express the same universal (for linear systems) concept of superposition. Naturally, the corresponding solutions may be readily applied in these cases when the system has viscosity properties.

For details on the fifth variation, see the article by A.D. Myshkis and Ya. G. Panovko "Action of a Perturbing Force of Variable Frequency and Amplitude on a System with One Degree of Freedom" (Inzh. Sb., Izdatel'stvo AN SSSR, Vol. XXII, 1953).

§ 30. The "Inverse" Form of Differential Equations of Oscillations

The Lagrange equations represent the most general form of writing differential equations of oscillations of mechanical systems with several degrees of freedom. Let us consider a conservative system with n degrees of freedom, and q_i are the generalized coordinates, a_{ik} — inertial coefficients and c_{ik} — rigidity coefficients. The kinetic and potential energy equal /255

$$T = \frac{1}{2}\sum_{i,k} a_{ik}\dot{q}_i\dot{q}_k, \qquad \Pi = \frac{1}{2}\sum_{ik} c_{ik}q_iq_k. \tag{30.1}$$

Correspondingly, the Lagrange equations acquire the form

$$\sum_{k=1}^{n}(a_{ik}\ddot{q}_k + c_{ik}q_k) = Q_i \qquad (i = 1, 2, \ldots, n), \tag{30.2}$$

where Q_i are the generalized forces which are given functions of time (perturbing forces). In the case of free oscillations $Q_i = 0$ the differential equations (30.2) assume the form of the equation (23.1).

With the appropriate selection of the generalized coordinates, we may obtain certain simplifications of the system (30.2). Let us point out two important particular cases.

1. The generalized coordinates are selected so that $a_{ik} = 0$ for $i \neq k$. We then have

$$T = \frac{1}{2}\sum_{k=1}^{n} a_k\dot{q}_k^2 \tag{30.3}$$

and the differential equations (30.2) assume the form

$$a_i\ddot{q}_i + \sum_{k=1}^{n} c_{ik}q_k = Q_i. \tag{30.4}$$

2. The generalized coordinates are such that the expression for the potential energy does not contain the products of the coordinates

$$\Pi = \frac{1}{2}\sum_{k=1}^{n} c_kq_k^2, \tag{30.5}$$

i.e., $c_{ik} = 0$, if $i \neq k$. The differential equations (30.2) may be written in the form

$$\sum_{k=1}^{n} a_{ik}\ddot{q}_k + c_iq_i = Q_i. \tag{30.6}$$

The first form of equations (30.4) is called the normal form, and the second form (30.6) is called the inverse form. The normal form is characterized by the fact that each differential equation includes only one term which /256 contains the generalized acceleration $\ddot{q}_i$. In contrast to this, each of the equations given in inverse form contains only one term containing a generalized coordinate q_i.

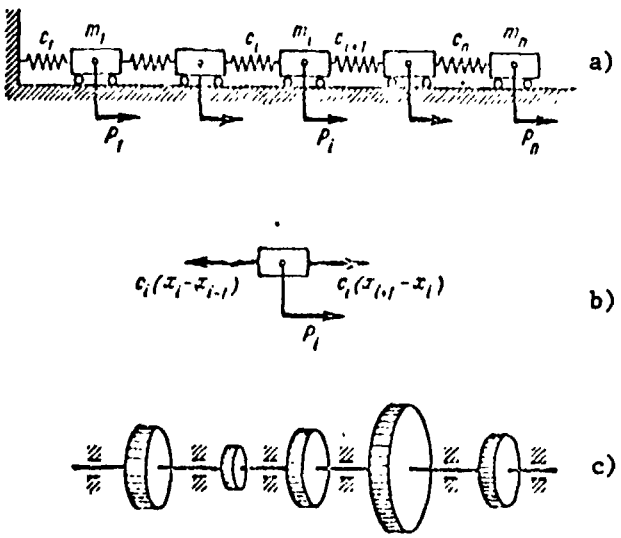

Fig. 30.1. Formulation of differential equations in normal form.

In the literature discussing oscillations of specific types of mechanical systems, both forms are encountered, but, as a rule, they are obtained by changing the procedure of compiling the Lagrange equations. We shall use examples below to explain how this is customarily done, but we would now like to point out that both forms are equivalent to each other in principle. At the same time, for each specific mechanical system preference may be given to a certain form, depending on considerations of a purely computational nature.

Let us turn to the examples. The first example is illustrated in Figure 30.1, a, and represents a chain of elastically connected loads which oscillate around a horizontal line. The notation in the figure is as follows: /257 $m_1, m_2, \ldots, m_n$ — mass of the loads, $c_1, c_2, \ldots, c_n$ — spring rigidity coefficients, $P_1(t), P_2(t), \ldots, P_n(t)$ — given perturbing forces. Let us assume $x_1, x_2, \ldots, x_n$ are the deviations of the loads from the position of equilibrium. Then the force of elasticity which develops in the $i^{\underline{th}}$ spring and acts on the $i^{\underline{th}}$ load is written in the form $c_i(x_i - x_{i-1})$. Separating out the $i^{\underline{th}}$ load, we can write the following differential equation of motion

for it (Figure 30.1, b):

$$P_i = c_{i+1}(q_{i+1} - q_i) - c_i(q_i - q_{i-1}) - m_i\ddot{q}_i \qquad (30.7)$$

(Naturally, we must assume $c_{n+1} = 0$ in the last equation, i.e., for $i = n$). Thus, we arrive at the differential equations in normal form. This will always be obtained when we write differential equations of motion for solid bodies included in the system, assuming that the generalized coordinates are their displacements of the centers of gravity and the angles of rotation around the center of gravity. In actuality, the kinetic energy will be written in the form (30.3) with such a selection of generalized coordinates.

The normal form is suitable when the elastic forces may be simply expressed by the generalized coordinates. In particular, this pertains to systems of the chain type. For example, for systems with several disks which have torsional oscillations (Figure 30.1, c), the same form (30.7) may be used, if the angles of rotations for the disks are used as the coordinates, and if we write the differential equations of rotating motion for each of them. Naturally, in this case, instead of P_i, we may substitute the perturbing moments M_i; instead of the linear displacements x_i — the angles of rotation of the disks φ_i; instead of m_i — the moments of inertia of the disks, and finally, instead of c_i — the rigidity coefficients of the shaft sections.

However, let us turn to the system shown in Figure 30.1, a. To obtain the inverse form of the differential equations, just as before we must separate the loads. We must then consider not the loads, but the elastic skeleton of the system which remains after separating out the loads and which has no mass (Figure 30.2, a). This system is loaded both with the given perturbing forces P_i, and the forces of inertia of the separated masses — $m_i\ddot{x}_i$.

Let us use δ_{ik} to designate the static influence coefficient ("single displacement"), i.e., the displacement of the point i under the action of a single force applied at the point k. In this case, we have /258

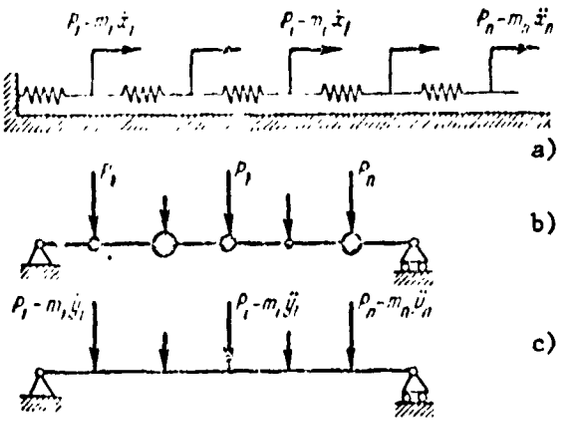

Fig. 30.2. Formulation of differential equations in inverse form.

$$\left.\begin{aligned} \delta_{ik} &= \sum_{j=1}^{i} \frac{1}{c_j}, \quad \text{if} \quad k > i; \\ \delta_{ik} &= \sum_{j=1}^{k} \frac{1}{c_j}, \quad \text{if} \quad k < i. \end{aligned}\right\} \tag{30.8}$$

The complete displacement of the i^{th} point is determined by superposing the displacements caused by each of the forces applied to the elastic skeleton, and consequently we have

$$x_i = \sum_{k=1}^{n} (P_k - m_k \ddot{x}_k)\,\delta_{ik}. \tag{30.9}$$

As may be seen, this procedure leads to the inverse form of the differential equations of motion.

This form is used quite frequently when studying the bending oscillations of rods supporting several concentrated masses. Figure 30.2, b shows a system of this type, and Figure 30.2, c — its elastic skeleton, to which (similarly /259 to the scheme shown in Figure 30.2, a) perturbing forces and forces of inertia of discarded loads are applied at the same time. In this case, the differential equations of motion have the same inverse form (30.8). The advantage of this form lies in the fact that, to calculate the coefficients of influence, there are well-developed methods (the formula of Moore, Vereshchagin formula, etc.).

Thus, there are two opposite concepts for writing the differential equations of oscillations. In both cases, a mental separation of the systems is assumed by separating the loads having a mass from the elastic skeleton of the system. However, in the first case the laws governing the motion of loads are described, while in the second case — the relationships determine the motion of an elastic skeleton without a mass. The first method leads to the normal form of differential equations of motion, and the second method — to the inverse form of these equations.

Let us discuss the second method in more detail, dealing with the action of real forces $P_k - m_k\ddot{x}_k$ on an elastic skeleton of a structure, i.e., on a system of connections with no mass. Although the concept of a skeleton without any mass contains a certain element of artificiality, in essence it closely coincides with the basic concepts of the mechanics of restricted systems. Let us repeat again: this discussion fully corresponds to the basic concept of the D'Alembert's principle, and does not contain those fictions which correspond to the usual discussion of this principle.

We usually speak about the arbitrary application of fictitious forces of inertia to the masses of the system. For the beam considered above, this is illustrated in Figure 30.3. This system differs from the system in Figure 30.2, c: in one case, we are discussing the action of real forces on a system of real connections (Figure 30.2, c), and in the other case — the action of fictitious forces on a given system (Figure 30.3). Naturally, the latter approach does not lead to any errors in the equations. However, it must be noted that it is not dictated by the essence of the problem, and only confuses a physically clear picture. We can only hope that in the literature devoted to applied problems of the theory of mechanical oscillations the inverse form of the equations is most frequently obtained by this method.

Thirteen years ago, Ye.L. Nikolay wrote: "We can hardly conceive of another theorem of mechanics which could have caused as much misunderstanding as the D'Alembert's principle. Were those forces of inertia which were discussed in this principle real or fictitious; if they are fictitious, then /260

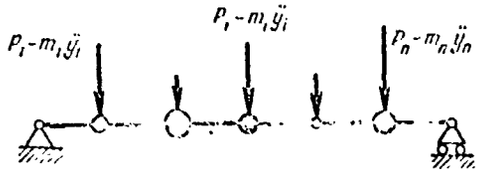

Fig. 30.3. Normal kinetostatic system.

how can these forces of inertia cause such completely real phenomena as the interruption of a fly wheel or a train leaving the tracks and breaking down, etc.? These are questions which can cause endless debates, and not only among those beginning to study mechanics".

The situation as a whole has now improved: in several contemporary mechanics handbooks, these problems are comprehensibly explained. However, in the technical literature devoted to applied problems, the requisite discussion is rarely encountered. The authors of this book feel that the concept of an elastic skeleton without mass(*) (or body) of a structure can greatly clarify this situation. Without this, the concepts are frequently somewhat ambiguous.

Naturally, this pertains not only to problems of oscillations, but also in general to any problems of dynamics of mechanical systems. When it is assumed that forces of inertia act on an airplane when calculating the strength of aircraft, this is an unfortunate choice of terms, since forces of inertia cannot act on an aircraft which represents a set of internal connections ("skeleton") and masses distributed over its volume. It is true, most authors use such terms in reference to the D'Alembert principle. In this way, formal invulnerability of the text is achieved, but at the expense of a certain clarity.

At the same time, the expression "when an aircraft performs any maneuvers, /261 forces of inertia act on its frame with no mass" accurately corresponds to the nature of the problem (the strength of the frame is calculated for these forces, just as for the external load), does not contain any ambiguity, and

(*) This term is arbitrary. In essence, we are discussing a system of internal connections.

corresponds to the D'Alembert principle(*). In other words, a distinction must be made between the concept of a mechanical system and its frame with no mass.

See the book by I.M. Babakov "Teoriya kolebaniy" (Theory of Oscillations). (2nd Edition, "Nauka" Press, Moscow, 1965). See the article by Ye.L. Nikolai "The D'Alembert Principle and Forces of Inertia", in his book "Trudy po mekhanike" (Works on Mechanics). (Gostekhizdat, Moscow, 1955, pp. 407 - 418).

§ 31. Terminology References: Impedance, Receptance, Admittance, Response, Anti-Resonance

Scientific and technical progress leads to the continuous creation of new concepts, and along with that — to the occurrence of new terms. In our days, this progress has been so intense that the dictionary writers — explanatory and translation dictionaries — cannot keep up with it.

Thus, in the contemporary literature in the English language devoted to problems of mechanical oscillations, more and more frequently the following terms are encountered: "impedance," "receptance," "admittance," "response." It is very difficult to translate them.

Let us give two examples of the titles of three articles:

1. "Mechanical Impedances for Thin Plates." (Thomas Dan A., J. Acoust. Soc. America, No. 10, 1960.)

2. "The Receptances of Uniform and Nonuniform Rotating Shafts." (Gladwell G.M.L., Bishop R.E.D., J. Mech. Engng. Sci., No. 1, 1959.)

(*) The true meaning of this principle may be seen in the fact that the equations of equilibrium are always valid for a frame with no mass investigated in this way.

3. "Response of Rigid Frame to a Distributed Transient Load." (De Hart R.C., J. Struct. Div. Proc. Amer. Soc. Civil Engrs., No. ST5, 1956.)

Following are our translations of these titles: /262

1a. "Mechanical Impedances for Thin Plates."

2a. "Receptances of Rotating Shafts of Constant and Variable Cross Section."

3a. "Reaction of a Rigid Frame to a Distributed Impact Load."

In the first two cases the translators took the path of least resistance and, in essence, retained the terms without translation, since in the Russian literature on mechanics the term "impedance" is still not legalized, and the term "receptance" is generally not used. These terms exist in the literature on electrical engineering. However, this is of no great help, since, for example, the term "impedance" which is used in electrical engineering must be changed from the "electrical engineering" language to the "mechanical" language.

The translation of the third term "response" is formally correct, since in any dictionary one of the variations for translating this word is the word "reaction"(*). However, the term "reaction" has a definite meaning in Russian terminology used in mechanics. This meaning does not coincide with the meaning of the word "response" in the title of this article.

Thus, in the first two cases, the translation is in general not a translation, and in the third case — the translation may cause a false association in the reader. Encountering these terms in the original (1, 2, 3) or in the translation (1a, 2a, 3a), we find ourselves in a difficult position.

(*) We shall not discuss the incorrect translation of the word "transient." Naturally, we are not talking about an impact, but about a brief load.

In the present section, we shall clarify what concepts must be attributed to these terms, as well as the English term "admittance" and the term "anti-resonance", which is frequently used in our literature.

To explain retaining the term "impedance", we shall turn to the problem of forced oscillations of an elastic system with one degree of freedom, when the perturbing force changes according to the law

$$P = P_0 \sin \omega t. \tag{31.1}$$

As is known, this displacement equals /263

$$y = \frac{P_0 \sin \omega t}{c - m\omega^2}, \tag{31.2}$$

where m is the reduced mass, c — rigidity coefficient of the system. We use c to designate the relationship of the statically applied force P_{st} to the displacement caused by it y_{st}

$$c = P_{st} : y_{st} \tag{31.3}$$

which determines the angle of inclination of the static characteristic and which characterizes the ability of the system to resist static deformation.

By analogy, we may introduce the concept "dynamic rigidity" as the ratio of the harmonic force (31.1) to the dynamic displacement caused by it (31.2):

$$\frac{P}{y} = c - m\omega^2. \tag{31.4}$$

This quantity depends not only on the parameters of the system c and m, but also on the frequency ω of the perturbing force. Thus, with a very slow change in the external force ($\omega \to 0$), the dynamic rigidity becomes static rigidity. For a specific value of the frequency

$$\omega = \sqrt{\frac{c}{m}} \tag{31.5}$$

the dynamic rigidity vanishes, i.e., the system is completely devoid of rigidity, and the perturbing force of an arbitrarily small amplitude P_0 causes an infinitely large displacement (resonance). The concept of dynamic rigidity

is a completely clear physical concept, and is widely used in the theory of oscillations for this reason. The same meaning is sometimes attributed to the expression "mechanical impedance" (see, for example, the translation of the book by J. Den-Gartog "Mechanical Oscillations", Fizmatgiz, 1960). In the book by T. Karman and M. Biot "Mathematical Methods in Engineering" (Gostekhizdat, 1948)the second variation of this term is also given: the ratio of the amplitude of the force to the amplitude of the velocity. It is frequently encountered in this sense in our literature, and acquires a complex form for systems with viscous resistance (see Yu.I. Iorish "Vibrometriya" (Vibrometry), Mashgiz, 1963).

Let us now turn to the terms "receptance" and "admittance", and we should /264 particularly like to point out that they are completely different. In order to clarify their meaning, we must recall that, along with the concept of rigidity (static or dynamic), there is a "mutual" concept of compliance (also static or dynamic).

A quantity which is the opposite of static rigidity y_{st}: $P_{st} = 1 : c$ is called <u>static compliance</u> (or simply, compliance). In structural mechanics of rod systems, compliance is the same as "unit displacement", i.e., displacement caused by a force which equals unity (the influence function for displacements serves as the analog in the theory of elasticity).

The concept of <u>dynamic compliance</u> is formulated in the following way. Let us divide (31.2) by (31.1):

$$\frac{y}{P} = \frac{1}{c - m\omega^2}. \qquad (31.6)$$

This quantity determines the displacement amplitude, if the amplitude of the disturbing force equals unity. With a slow change in the perturbing force, when $\omega \to 0$, the dynamic compliance does not differ from static compliance. If the frequency ω coincides with the value of (31.5), then dynamic compliance strives to infinity (resonance), etc. In present day literature in the English language, dynamic compliance is called "receptance" (or "admittance").

a) b)

Fig. 31.1. Action of force P on system with one and two degrees of freedom.

The verb "to respond", which is designated in Russian by "to answer", "to respond to", "to react to", corresponds to the English word "response". Correspondingly, the word "response" may be translated as "answer", "response", and even "reaction". However, in the latter case we must keep the fact in mind that we are not dealing with a reactive force, but with the "reaction" of a certain mechanical system to given external influences (usually dynamic loads of a certain type). Recently, the term "response" has been most widely used, and is preferable.

Finally, let us clarify the meaning of the term "anti-resonance", which is frequently used in our literature, which is devoted to torsional oscillations of shafts.

Let us first of all present certain elementary considerations pertaining to the staticsof elastic systems. Let us assume that a concentrated force /265 is applied statically to an elastic system. The displacement of the point of application for the force in the direction of the force cannot equal zero. This follows, for example, from the fact that the potential deformation energy, which equals the work of the external force, cannot equal zero. Thus, it cannot be concluded that, under the action of a force applied to an elastically fixed mass (Figure 31.1, a), the latter would remain in place. This is also impossible in the case of a more complex system, for example, that shown in Figure 31.1, b.

The situation is completely different in dynamic problems. Thus, for example, if a force changes harmonically in time

$$P = P_0 \sin \omega t, \tag{31.7}$$

under certain conditions the point at which the force is applied remains immobile always. It is true that this can only be the case if the system has at least two degrees of freedom (Figure 31.1, b). This phenomenon is not only of theoretical interest, but is also of great practical interest.

Let us examine forced oscillations of a two-mass system, shown in Figure 31.1, b. If we use m_1 and m_2 to designate the masses of both bodies, and c_1 and c_2 to designate the rigidity of both springs, then the equations of motion may be written in the following form

$$\left.\begin{aligned} -c_1 y_1 + c_2 (y_2 - y_1) + P_0 \sin \omega t = m_1 \ddot{y}_1, \\ -c_2 (y_2 - y_1) = m_2 \ddot{y}_2. \end{aligned}\right\} \tag{31.8}$$

where $y_1 = y_1(t)$ and $y_2 = y_2(t)$ are the displacements of both masses, which are the desired functions of time. The system of equations (31.8) may be satisfied by the solution /266

$$\left.\begin{aligned} y_1 = a_1 \sin \omega t, \\ y_2 = a_2 \sin \omega t, \end{aligned}\right\} \tag{31.9}$$

which indicates that the operations occur with the frequency ω of the perturbing force. This is a particular solution, but it describes the most important, stationary part of the process. Another part of the solution, describing oscillations with eigenfrequencies, rapidly disappears due to the action of unavoidable damping forces.

Substituting (31.9) in (31.8), we obtain two equations with two unknown amplitudes of the oscillations a_1 and a_2:

$$\left.\begin{aligned} -a_1 m_1 \omega^2 + c_1 a_1 - c_2 (a_2 - a_1) = P_0, \\ -a_2 m_2 \omega^2 + c_2 (a_2 - a_1) = 0. \end{aligned}\right\} \tag{31.10}$$

Solving this system of equations, we find

$$\left.\begin{aligned} a_1 = \frac{P_0 (c_2 - m_2 \omega^2)}{(c_1 + c_2 - m_1 \omega^2)(c_2 - m_2 \omega^2) - c_2^2}, \\ a_2 = \frac{P_0 c_2}{(c_1 + c_2 - m_1 \omega^2)(c_2 - m_2 \omega^2) - c_2^2}. \end{aligned}\right\} \tag{31.11}$$

These formulas may be used to determine the amplitudes of oscillations of both masses, which essentially depend on the frequency ω of the perturbing force. In particular, for definite values of ω, the denominators in (31.11) vanish, and the quantities a_1 and a_2 strive to infinity. This indicates that resonance has entered the system. There are two such values for the frequency, and they may be found from the equation

$$(c_1 + c_2 - m_1\omega^2)(c_2 - m_2\omega^2) - c_2^2 = 0. \tag{31.12}$$

We should recall that the resonance frequencies are precisely equal to the eigenfrequencies of the system under consideration, and their number always equals the number of their degrees of freedom.

The resonance properties of elastic systems are well known, and we shall not discuss them. We shall discuss another property of the system connected with the possibility of the numerator vanishing in the first of the formulas (31.11). In order that this numerator may equal zero, it is necessary that the frequency ω be

$$\omega_* = \sqrt{\frac{c_2}{m_2}}. \tag{31.13}$$

Using this value of the frequency and formulas (31.11), we obtain /267

$$\left.\begin{aligned} a_1 &= 0, \\ a_2 &= -\frac{P_0}{c_2}. \end{aligned}\right\} \tag{31.14}$$

The first result is of particular interest. The first mass remains immobile, although a perturbing force is applied to it. This is a remarkable phenomenon which is impossible in static problems. Sometimes the state of the system in the case $\omega = \omega_*$ is called "anti-resonance".

Figure 31.2 shows the change in the amplitude a_1 as a function of the perturbation frequency ω. Anti-resonance is clearly apparent here (for $\omega = \omega_*$), and also two resonances (in the case $\omega = p_1$ and $\omega = p_2$). We assumed that $P_0 = 1$, $c_1 = c_2 = 1$, $m_1 = m_2 = 1$ for the calculations.

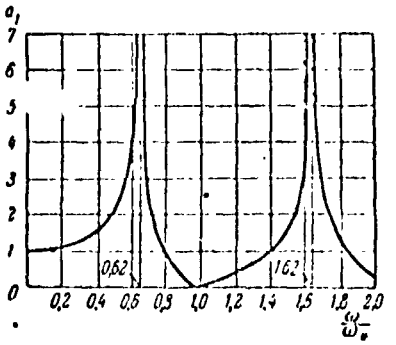

Fig. 31.2. Dependence of amplitude a_1 on frequency of perturbing force ω. For $\omega = 0.62\omega_*$ and for $\omega = 1.62\omega_*$ resonance occurs and for $\omega = \omega_*$ anti-resonance occurs.

The possibility of anti-resonance is used in practice for a dynamic oscillation damper. For example, let us assume a one-mass system (Figure 31.1, a), to which a harmonic perturbing force (31.7) is applied. Anti-resonance is impossible in this one-mass system, and oscillations of the mass are unavoidable for any parameters of the system.

One of the methods of extinguishing the oscillations consists of introducing into the system an additional mass with an elastic connection, and a two-mass system is obtained, as shown in Figure 31.1, b. As we have just seen, oscillations of the basic (first) mass completely disappear if the parameters c_2 and m_2 of an additional part of the system are selected according to condition (31.12). In this case, the second mass plays the role of a dynamic damper of oscillations of the first mass.

With the appropriate adjustment of the vibration damper, when oscillations /268 of the basic structure disappear, the additional mass, as a rule, vibrates very strongly. The amplitudes a_2 of the oscillations of the damper equal the ratio of the perturbing force P_0 amplitude to the rigidity of the additional spring [for a light damper, when the value of m_2 is small, this rigidity must also be small — as required by the adjustment of the damper (31.13)].

The idea of a dynamic vibration damper is unusual, and it may even be a panacea from all undesirable vibrations. Unfortunately, there is one serious drawback in a dynamic vibration damper: it can only damp oscillations of a strictly fixed frequency ω. Any change in the perturbation frequency disturbs the condition (31.13), and the supplementary mass loses the properties of a damper. It is even possible that the operational conditions of the basic system are not improved, but worsened.

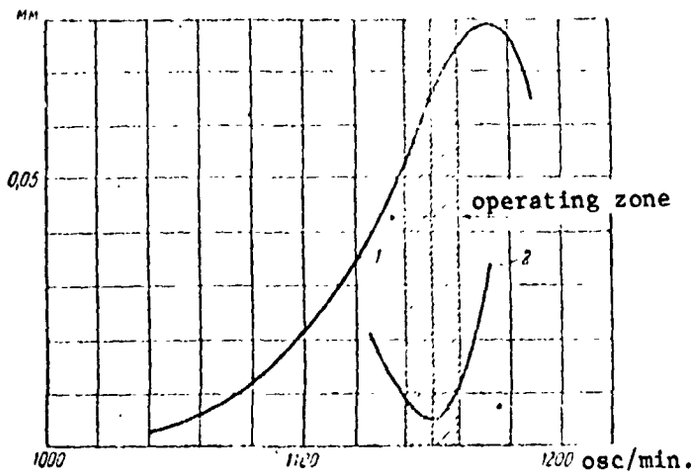

Fig. 31.3. Oscillation amplitude of stern of ship; 1 — without damper; 2 — with damper.

It may be seen from Figure 31.2 that the second mass damps oscillations only in a small vicinity of the frequency $\omega = \omega_*$. If, for example, the perturbation frequency is $\omega = p_2$, then resonance arises, which could not exist in the absence of such a "damper" (the quotation marks are not used here at random).

By introducing viscous resistance into the damper system, we may somewhat expand the range of frequencies within which intense damping of oscillations occurs. Therefore, in the majority of cases, dampers with resistance are used. In particular, these dampers were used to eliminate vibrations in the stern of river boats of the "Volgo-Don" type. The experimental curves in Figure 31.3 show the effectiveness of this measure.

At the present time, there are several types of so-called controlled vibration dampers. The main idea underlying these devices is an automatic change in the eigenfrequency of the damper when the frequency of the perturbing force changes. Special systems of automatic control are used for this purpose. The controlled vibration dampers are complex, but in return they assist in the successful struggle against vibrations in a wide range of perturbing force frequencies.

One of the recently published works analyzed the influence of a vibrometer, located on a comparatively light oscillating system to measure its vibrations, upon the oscillations of this system. It was found that for certain parameters /269 of the system the vibrometer plays the role of the vibration damper. The objectivity of its readings may naturally be greatly disturbed. This is an unusual example of the influence of a measuring device on the process being studied !

The terms used above were not chosen at random. They have appeared recently in the literature on mechanics, and have been widely used. It is sufficient to note that the three English terms given above were borrowed from one of the abstract journals "Mechanics", No. 8, 1961, which also gives translations of the terms which are necessary for an explanation.

See the following works regarding the dynamic rigidities and compliances: F.M. Dimentberg "Application of the 'Dynamic Rigidity Method' in Calculating Connected Oscillations" (see "Dinamika i prochnost' kolenchatykh valov" [Dynamics and Strength of Crankshafts], Izdatel'stvo AN SSSR, 1949); M.L. Kempner "Methods of Dynamic Compliance and Rigidity for Calculating Bending Oscillations of Elastic Systems with Several Degrees of Freedom" (Sb: "Poperechnyye kolebaniya i kriticheskiye skorosti" [Collection: Transverse Oscillations and Critical Velocities], No. 1, Izdatel'stvo AN SSSR, 1951).

A practical example of using vibration dampers was borrowed from the book of: A.M. Alekseyev, A.K. Sborovskiy "Sudovyye vibrogasiteli" (Ship Vibration Dampers) (Sudpromgiz, Leningrad, 1962).

The influence of a vibrometer on oscillations in a structure being /270 studied is discussed in the article by I.I. Klyukin "Influence of a Vibrometer on the Motion of an Oscillating Surface" (Akusticheskiy Zhurnal, No. 1, 1959).

§ 32. Parametric Excitation of Oscillations

Let us investigate the elastic system shown in Figure 32.1 — it is simplest to begin the discussion by considering the so-called parametric excitation of oscillations. As is shown in the figure, the concentrated mass 1 is fixed at the end of a weightless rod 2, and the freedom of the rod displacements is additionally limited by the bushing 3. Let us write the formula for free oscillations of the system, assuming that they take place in the drawing plane. If at the moment of time t the mass displacement is y, the restoring elasticity force of the rod equals cy, the equation of motion for the mass has the form

$$-cy = m\ddot{y}, \tag{32.1}$$

where c is the system rigidity coefficient. The bushing 3, if it is sufficiently short, produces conditions which are similar to the conditions of hinged support of the rod. The rigidity coefficient c may be determined according to the formula

$$c = \frac{3EJ}{l(l-s)^3}. \tag{32.2}$$

It is assumed that the rod has a constant transverse cross section with the moment of inertia J. We used E to designate the elasticity modulus of the rod material. Thus, the differential equation (32.1) assumes the form

$$\ddot{y} + \frac{3EJ}{ml(l-s)^3}y = 0. \tag{32.3}$$

If the distance s is constant, the differential equation (32.3) describes the free oscillations of the mass around its middle position, and the fraction /271
tion $3EJ:ml(l-s)^2$ represents the square of the free oscillation frequencies.

Let us now assume that the bushing 3 slides along the rod 2, according to the law

$$s = s_0 - A\cos\omega t, \tag{32.4}$$

i.e., it completes harmonic oscillations with the amplitude A and the circular frequency ω. Here s_0 is the average distance from the bushing to the upper hinge. In this case, the rigidity coefficient is a function of time:

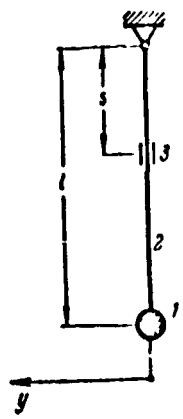

Fig. 32.1. In the case of oscillations of a bushing 3 along a rod, the bending rigidity of the system changes periodically.

$$c = \frac{3EJ}{l(l - s_0 + A\cos\omega t)^3}, \qquad (32.5)$$

and the differential equation (32.3) becomes an equation with variable coefficients

$$\ddot{y} + \frac{3EJ}{ml(l - s_0 + A\cos\omega t)^3}y = 0. \qquad (32.6)$$

Oscillations of the mass 1 cannot be called free now, since they take place under an external influence, which is fixed in time, in the form of a periodic change in the system rigidity. On the other hand, they cannot be called forced, since the external influence is not a perturbing force, and is included in the left side of the equation of motion. The oscillations of such systems, which occur with a given change in the system parameters (in this case, rigidity), are called parametrically forced oscillations, or more simply — parametric oscillations.

As we shall see below, in certain regions of excitation frequencies, the amplitudes of the parametric oscillations gradually increase. This phenomenon is parametric resonance, or "ordinary" resonance which occurs only for precisely given values of the external perturbation frequency.

There are many mechanical systems which are subjected to parametric excitation. We shall give several such examples below, and would like to stress that in many cases which are important in practice the differential equation of parametric oscillations may be reduced to the standard form

$$\frac{d^2y}{d\tau^2} + (a - 2q\cos 2\tau)y = 0, \qquad (32.7)$$

where a and q are constants.

Thus for example, if the amplitude of the bushing oscillations is very small as compared with the average dimension $l - s_0$ in the mechanical system /272

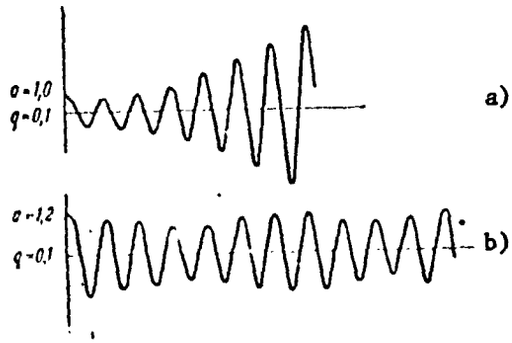

Fig. 32.2. Two solutions of the Mathieu equation: a) unstable; b) stable.

examined above (Figure 32.1), then, instead of (32.5), we approximately obtain

$$c \approx \frac{3EJ}{l(l-s_0)^3}\left(1-\frac{2A}{l-s_0}\cos\omega t\right), \qquad (32.8)$$

and the differential equation (32.6) assumes the form

$$\ddot{y}+\frac{3EJ}{ml(l-s_0)^3}\left(1-\frac{2A}{l-s_0}\cos\omega t\right)y=0. \qquad (32.9)$$

Now changing to the dimensionless time τ:

$$2\tau=\omega t, \qquad (32.10)$$

we have

$$\frac{d^2y}{dt^2}=\frac{\omega^2}{4}\frac{d^2y}{d\tau^2}, \qquad (32.11)$$

and the differential equation (32.9) assumes the standard form (32.7), and

$$a=\frac{12EJ}{m\omega^2l(l-s_0)^3}, \quad q=\frac{24AEJ}{m\omega^2l(l-s_0)^3}. \qquad (32.12)$$

Transformations of this type are typical for cases of small pulsation intensity of the variable parameter for the system.

Let us now turn to the basic equation of the problems (25.7) considered above, which is called the Mathieu equation. The solutions of the Mathieu equation are oscillatory in nature. Their main properties depend on specific values of the parameters a and q. In some cases, oscillations limited in amplitude correspond to a given combination of a and q, and in other cases — oscillations with an increasing amplitude. In essence, additional details of the oscillations are not important, since the tendency of an oscillatory process is of primary importance — if the amplitudes remain limited, then the system is stable. Otherwise, parametric resonance occurs, and the system is unstable.

The results of solving the Mathieu equation for two different combinations of a and q are shown in Figure 32.2 (these solutions were obtained on an analog computer). Although in both cases the parameter q of the system is the same

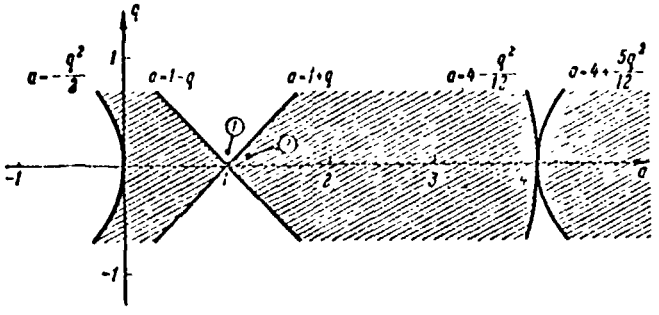

Fig. 32.3. Part of the Haynes-Strett diagram for small values of the parameter q. Points 1 and 2 correspond to solutions a) and b) in Figure 32.2.

(q = 0.1), the oscillations differ greatly due to differences between values /273
of the parameter a (a = 1; a = 1.2). In the first case, they increase, i.e., the system is unstable, and in the second case they remain limited, i.e., the system is stable.

For practical purposes, the boundaries between the regions of stable and unstable solutions are of the greatest importance. This problem has been greatly studied, and the final results are given below in the form of a diagram drawn in the plane of the parameters a and q. It is called the Haynes-Strett diagram. Figure 32.3 shows part of the Haynes-Strett diagram pertaining to small values of the parameter q. A point with the coordinates a, q on the Haynes-Strett diagram ("the image point") corresponds to each given system characterized by the parameters a and q. If the image point is located within the crosshatched fields of the diagram, the system is stable. Image points located in the white fields correspond to unstable systems.

By way of an example, the diagram shows points 1 and 2 corresponding to the parameters $a_1 = 1$, $q_1 = 0.1$; $a_2 = 1.2$, $q_2 = 0.1$ (the solution of the Mathieu equation for these cases is given in Figure 32.2). Point 1 is located in the white zone (instability), and oscillations occur with increasing amplitudes (Figure 32.2, a). Point 2 is located within the crosshatched zone. It /274
corresponds to motion with a limited amplitude (Figure 32.2, b).

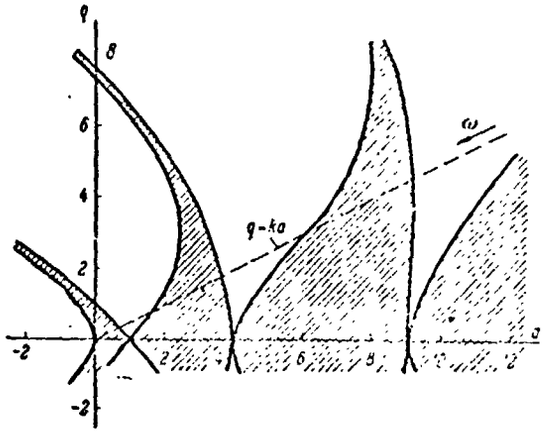

Fig. 32.4. Haynes-Strett diagram. The dashed line is the geometric location of the image points of a given mechanical system. When the frequency ω increases, the image point approaches the origin.

The complete Haynes-Strett diagram is shown in Figure 32.4. As may be seen, in the plane of the parameters a, q the stability regions alternate with regions of instability. The widest, and therefore the most important, region of instability contains the point a = 1, q = 0.

The Haynes-Strett diagram completely eliminates the necessity of any operations to solve the Mathieu equation. It is sufficient to write this equation, i.e., to find the parameters of the system a and q. After this, the diagram immediately gives the answer to the question of whether the system has stability or not.

Let us trace the change in the properties of parametric oscillations with a gradual change in the excitation frequency. Turning to the expressions (32.12) for an example, we see that both parameters a and q decrease in proportion to an increase in frequency. Since the ratio of both parameters remains constant, the successive stages of the system are determined by the image points on the dashed line q = ½a passing through the origin. Figure 32.4 clearly shows the alternation of stable and unstable states with increasing values of the excitation frequency.

We may give several possible reasons for parametric excitation of mechanical systems:

a) Periodic change of rigidity (as in the system studied above); /275

b) periodic change in so-called parametric loads(*); c) periodic change in inertia of the system. We shall give examples of all three types of parametric excitation, and we shall then indicate cases of a mixed character, when periodic changes in rigidity and inertia are simultaneously the cause of parametric excitation.

a) Periodic change in rigidity. The elastic part of the system shown in Figure 32.5 is a slotted shaft 1; the disk 2 is located at the lower end of the shaft. A slotted, massive bushing 3 is connected with the shaft. This bushing may slide along the shaft's axis, and perform harmonic oscillations in the vertical direction. Parametric excitation not only of bending oscillations, but also of torsional oscillations, is possible in this system. Let us assume that the free length of the shaft at the moment of time t is /276

$$l = l_0 + A\cos\omega t; \tag{32.13}$$

Thus, the torsional rigidity coefficient for the shaft is

$$c = \frac{GJ_p}{l} = \frac{GJ_p}{l_0 + A\cos\omega t}. \tag{32.14}$$

If the amplitude of the oscillations A is much less than the average value of the length l_0, expression (32.14) may be represented in the form

$$c = \frac{GJ_p}{l_0}\left(1 - \frac{A}{l_0}\cos\omega t\right), \tag{32.15}$$

which fully coincides in its structure with (32.8). Therefore, torsional oscillations of the system under consideration may also be described by the Mathieu equation (32.7), and

$$a = \frac{4GJ_p}{l_0\omega^2}, \quad q = \frac{2GJ_pA}{l_0^2\omega^2}. \tag{32.16}$$

Another example of a system with a periodic change in rigidity is shown in Figure 32.6. The system contains a disk 1 which is fastened in the middle of a vertical shaft 2. In a portion of the length, the shaft has a transverse cross section with different main moments of inertia (for example, a

(*) Loads under whose static influence stability loss is possible in the Euler sense are called parametric loads.

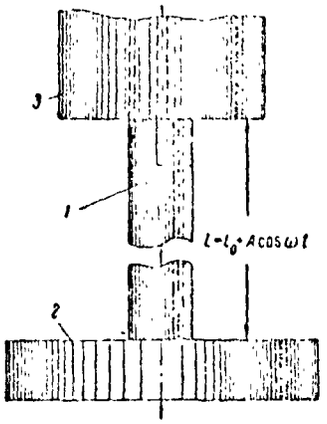

Fig. 32.5. For oscillations of a slotted bushing 3 along the axis 1, the twisting rigidity of the shaft changes periodically.

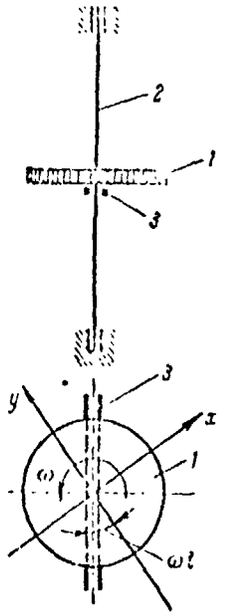

Fig. 32.6. The shaft may bend in the vertical plane fixed by the guides 3. If the bending rigidities in the main directions x and y are identical, the bending rigidity along the directrices depends on the angle ωt of the rotation for the system xy.

rectangular cross section). For this reason, the shaft rigidity is not the same in the two main directions x and y. The guides 3 fix the plane in which the shaft bends. Therefore, when the shaft rotates, the bending rigidity in the given direction changes periodically, and parametric excitation of the oscillations is possible(*).

For an instructive example of parametric excitation of oscillations, let us deal with the operation of a single mine shaft (Figure 32.7). The guides 1, along which the cage 2 moves, are solid beams with multiple supports. Their lateral rigidity depends on the level at which the cage is located: when the cage is located against the support 2, the rigidity is the greatest, and when the case is located in the middle of the span, the rigidity is the least. /277

(*) We should note that, if there are no guides, the shaft may oscillate in two planes. It may be found by an elementary method that the shaft is unstable in all regions of angular velocities $[\omega_1, \omega_2]$ (here $\omega_1=\sqrt{c_1:m}$, $\omega_2=\sqrt{c_2:m}$; c_1, c_2 are coefficients of main shaft rigidities).

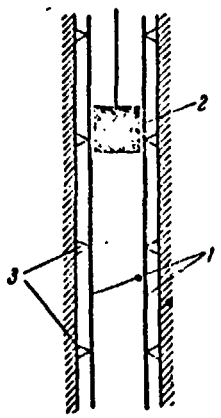

Fig. 32.7. Diagram of a mine shaft.

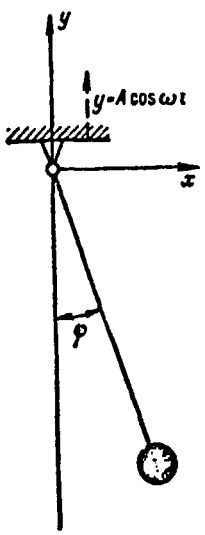

Fig. 32.8. Pendulum with a point suspension oscillating along the vertical.

When the cage moves along the vertical, the lateral rigidity periodically changes, which creates the danger of parametric resonance. In the case which we are discussing, in actuality significant oscillations arise in a certain range of cage velocities. In order to eliminate the oscillations, we must greatly change the structure of the shaft. Only after this, is the system free from parametric resonance.

A pendulum with an oscillating point suspension belongs to this group (Figure 32.8).

$$-mgl\varphi + mA\omega^2 l\varphi\cos\omega t = ml^2\ddot{\varphi}.$$

If the point of the suspension is fixed, then the unit moment with respect to this point is the moment of force of the weight — mgl_φ (m — pendulum mass, l — its length, φ — angle of deflection), and the differential equation of small oscillations of the pendulum takes the form

$$-mgl\varphi = ml^2\ddot{\varphi}. \qquad (32.17)$$

Let us assume that the suspension point oscillates along the y axis according to the law

$$y = A\cos\omega t. \qquad (32.18)$$

When writing the equation of the moments, we must take into account the transferable force of inertia — $m\ddot{y} = mA\omega^2\cos\omega t$. Its moment is $mA\omega^2 l_\varphi\cos\omega t$, and the differential equation for the pendulum oscillations may be written in the form /278

(32.19)

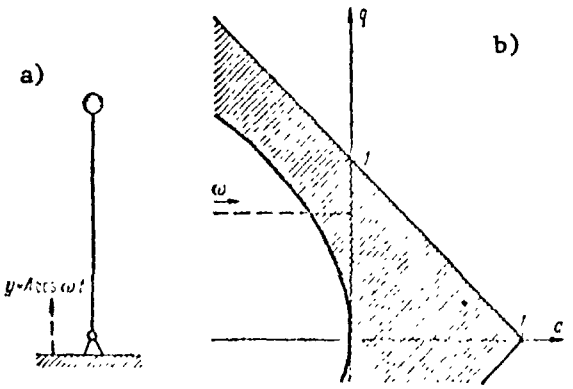

Fig. 32.9. a) "Tilted" pendulum with a point suspension oscillating along the vertical; b) "tilted" pendulum may be stable with sufficiently large frequency values.

i.e.,

$$\ddot{\varphi} + \left(\frac{g}{l} - \frac{A\omega^2}{l}\cos\omega t\right)\varphi = 0. \quad (32.20)$$

This equation may be reduced to the standard form (32.7), if we set

$$2\tau = \omega t; \quad a = \frac{4g}{\omega^2 l}; \quad q = \frac{2A}{l}. \quad (32.21)$$

It may be immediately seen from the Haynes-Strett diagram that the parameter a does not depend on the oscillation amplitude of the suspension point and the amplitude A may be small. The instability of the lower position of the pendulum arises close to the values a = 1, 4, 9, ..., i.e., in the case

$$\omega = 2\sqrt{\frac{g}{l}};\ \sqrt{\frac{g}{l}};\ \frac{2}{3}\sqrt{\frac{g}{l}};\ \ldots \quad (32.22)$$

Let us now turn to the possibility of stability of the upper position of the pendulum (Figure 32.9, a). With an immovable support, this position is naturally unstable. However, vibrations of the base may cause this position to be stable. In order to obtain the equation of motion for this case, it is sufficient to change the sign before the term containing the acceleration g in equation (32.20). We correspondingly obtain in (32.21)

$$a = -\frac{4g}{\omega^2 l} \quad (32.23)$$

(the remaining terms remain as before).

It may be seen from Figure 32.9, b that the upper position of the pendulum may be stable. For small amplitudes A of the suspension point oscillations (when $0 < |q| < 1$) the stability of the upper position is achieved, if the inequality $|a| < \frac{q^2}{2}$ is satisfied. According to expressions (32.21), this stability condition assumes the form

$$\omega > \frac{\sqrt{2gl}}{A}. \quad (32.24)$$

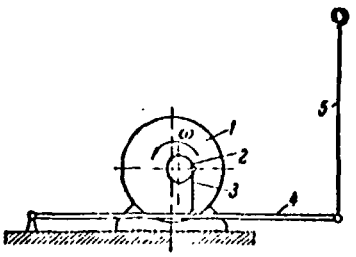

Fig. 32.10. Device of P.L. Kapitsa.

It may be seen that the upper /280
suspension position may become stable by high-frequency vertical vibrations of the base. Incidentally, we should note that inequality (32.24) in essence determines the lower level of maximum oscillation velocity ωA, at which this effect is achieved: the maximum oscillation velocity must exceed the velocity of the free fall of the body from a height equal to the pendulum length (i.e., the value $\sqrt{2gl}$).

P.L. Kapitsa has written about this interesting phenomenon:

"The demonstration of stability of a pendulum with an oscillating suspension is no less than the phenomenon of gyroscopic stability of a gyroscope. Experiments with a pendulum having an oscillating suspension, although they are simple, still involve greater difficulties than experiments with a gyroscope, since a special mechanism is required to impart rapid oscillations to the pendulum suspension.

"We have done this by using a simple device, which is schematically shown in Figure 32.10. On the axis of a small electric motor 1 with a large rpm (we have used an electric motor from a small Swiss machine)is mounted in an eccentric manner a ball bearing 2. A bar 3 is attached to the ring of the bearing; this bar causes the arm 4 to oscillate. One end of the arm 4 rotates in a fixed support, and a rod of the pendulum 5 is suspended at the other end, so that it may swing freely.

"When the device is set in action, the pendulum rod behaves as though there were a special force, directed along the axis of the suspension oscillations. Since the suspension oscillation frequency is very large, the picture of the pendulum rod appears somewhat blurred to the eye, and the oscillatory motion cannot be noticed. Therefore, the phenomenon of stability produces an unexpected impression. If the pendulum is pushed to one side, it begins to

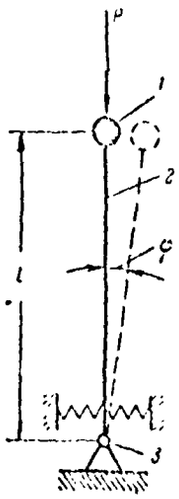

Fig. 32.11. Rod under the influence of a parametric force P.

swing like an ordinary pendulum. These oscillations are damped, and the pendulem changes to a vertical position". /281

b) Periodic change of parametric loads.

Let us examine the system shown in Figure 32.11. The mass 1 is attached at the upper end of a vertical, absolutely rigid rod 2. There is a support 3 below the rod, which resists rotation elastically ("elastic hinge"). A vertical force P is in operation at the upper end of the rod.

This force is a parametric load. If it changes in time, its critical value P_{cr} exists, which may be found by means of the Euler method. Let us assume φ is the angle of rod deflection from the vertical, and c is the hinge rigidity coefficient. Then the restoring moment (moment of the elastic hinge) is $c\varphi$, and the equation for the rod equilibrium in a deflected state takes on the form

$$Pl\varphi - c\varphi = 0. \tag{32.25}$$

We find from $\varphi \neq 0$ that the deflected state of equilibrium is possible if the force P equals

$$P_{cr} = \frac{c}{l} \tag{32.26}$$

This formula may be used to determine the critical value of the static acting force P (for example, the weight of the load 1).

This value may be found by examining the free oscillations of the mass 1. In contrast to the equation of statics (32.25), the equation of moments with respect to the hinge 3 contains the inertia term, and has the form

$$Pl\varphi - c\varphi = ml^2\ddot{\varphi}, \tag{32.27}$$

i.e.,

$$\ddot{\varphi} + \frac{c - Pl}{ml^2}\varphi = 0. \tag{32.28}$$

In the case

$$c = Pl \tag{32.29}$$

the frequency of the free oscillations of the system vanishes, i.e., the system becomes unstable. For a critical force, the previous result (32.26) follows from (32.29). /282

If the force P changes according to a harmonic law

$$P = P_0 + P_1 \cos \omega t, \tag{32.30}$$

the equation for the rod oscillations (25.19) may be written in the form

$$(P_0 + P_1 \cos \omega t) l\varphi - c\varphi = ml^2\ddot{\varphi}, \tag{32.31}$$

i.e.,

$$\ddot{\varphi} + \frac{1}{ml^2}(c - P_0 l - P_1 l \cos \omega t)\varphi = 0. \tag{32.32}$$

This equation may be reduced to the standard form of the Mathieu equation (32.7), if we set

$$2\tau = \omega t; \quad a = \frac{4}{m\omega^2 l}\left(\frac{c}{l} - P_0\right); \quad q = \frac{2P_1}{m\omega^2 l}. \tag{32.33}$$

With an increase in the frequency ω, the parameters a and q decrease in proportion. The crosshatched area in Figure 32.4 indicates that the system passes through several alternating stable and unstable states. The inclination of this area is determined by the relationship

$$k = \frac{q}{a} = \frac{P_1}{2(P_{cr} - P_0)} \tag{32.34}$$

where P_{cr} is the static critical force, given by the expression (32.26).

For a given value of P_1, the quantity k depends on the difference $P_{cr} - P_0$. The more the static component P_0 approximates the critical value P_{cr}, the shorter is the area and the wider are the intersected sections of the instability regions. This is naturally the case, since approximation of the force P_0 to the Euler force must make it easier for instability to occur. On the other hand, stability loss is possible with arbitrarily small compressive forces P_0, and even for tensile stresses. However, for $P_0 < 0$ the area $q = ka$ is mildly sloping, but also intersects several instability regions.

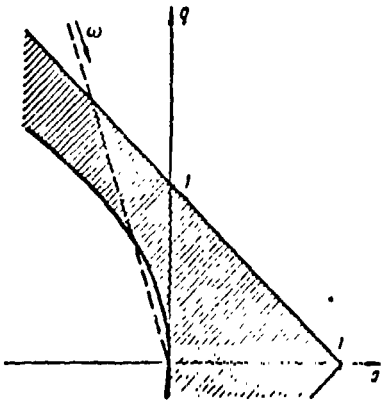

Fig. 32.12. The stand shown in Figure 32.11 may be stable in the case $P_0 = P_{cr}$; a rather large frequency ω is necessary for this.

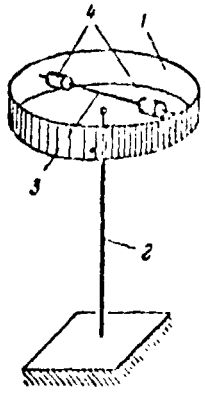

Fig. 32.13. System with variable inertia (distance between the loads 4 changes periodically.)

On the other hand, the Haynes-Strett diagram indicates that the system may be stable in the case $P_0 = P_{cr}$, even in the case $P_0 > P_{cr}$.

If $P_0 = P_{cr}$, then $a = 0$, the region $q = ka$ coincides with the ordinate axis of the Haynes-Strett diagram, and the system remains stable if $0<|q|<1$. According to (32.33), it is necessary that the inequality pertaining to the oscillation frequency of the force be satisfied: /283

$$\omega > \sqrt{\frac{2P_1}{ml}}. \qquad (32.35)$$

Thus, under certain conditions oscillations of the force can stabilize the system, which is unstable in the absence of oscillations.

In the case $P_0 > P_{cr}$, the region $q = ka$ is located in the second quadrant of the Haynes-Strett diagram. It may be seen in Figure 32.12 that in this case the system may be stable (in an appropriately selected range of changes in the frequency ω).

c) Periodic change in inertia. Figure 32.13 shows a disk 1 which is located horizontally and has the form of a dish attached to an elastic, vertical rod 2. The ends of a rigid bar 3 are attached to the disk.

Two loads 4 which are located symmetrically may slide along the bar. We shall /284 assume that the loads are given a harmonic motion with respect to the disk, which is described by the law

$$r = r_0 + A\cos\omega t, \tag{32.36}$$

and it is necessary to study the torsional oscillations of the disk around the rod axis. If I_0 is the eigenmoment of inertia for the disk relative to the axis, the complete moment of inertia for the disk-load system is

$$I = I_0 + 2mr^2. \tag{32.37}$$

Substituting expression (32.36), we obtain

$$I = I_0 + 2m(r_0 + A\cos\omega t)^2. \tag{32.38}$$

It may thus be seen that the moment of inertia of the system under consideration is a periodic function of time.

It must not be assumed that, to allow for this factor, it is sufficient to substitute into the differential equation

$$I\ddot{\varphi} + c\varphi = 0 \tag{32.39}$$

the function of time (32.38), instead of I. The situation is somewhat more complex. The differential equation (32.39) is valid only for a solid body which has a constant moment of inertia, and for the system under consideration it does not hold in general. The correct differential equation is obtained by the theorem of a change in the momentum of the system in the form

$$\frac{d}{dt}(I\dot{\varphi}) + c\varphi = 0, \tag{32.40}$$

i.e.,

$$\ddot{\varphi} + \frac{\dot{I}}{I}\dot{\varphi} + \frac{c}{I}\varphi = 0. \tag{32.41}$$

In contrast to equation (32.39), this equation contains the first derivative of the desired function $\dot{\varphi}$, and the Mathieu equation in the form (32.7) does not immediately follow from it. Nevertheless, a buildup of oscillations is possible in this system, since the coefficient periodically changes in time for the function φ.

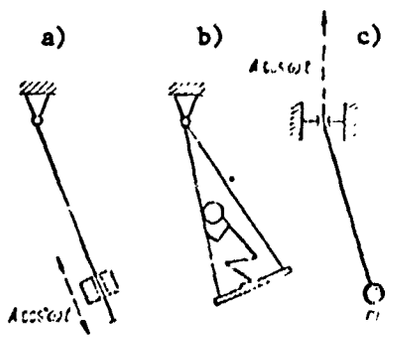

Fig. 32.14. Mixed cases: a) a mass slides along a rod according to a periodic law; b) distance from the swinging axis to the center of gravity fluctuates due to periodic pushes on the swing ; c) length of pendulum changes periodically due to the oscillatory motion of the end of the wire passing through the upper rings.

d) Mixed cases. Cases are possible when both the rigidity and the inertia change periodically in a mechanical system. For example, let us investigate system shown in Figure 32.14, a. /285 Here a point load slides along a rod, obeying a harmonic law of motion, while the rod itself may freely rotate around a hinge.

Let us write the load momentum with respect to the center of the hinge:

$$K = m\dot{\varphi}l = m\dot{\varphi}(l_0 + A\cos\omega t). \quad (32.42)$$

The time derivative of this moment

$$\frac{dK}{dt} = m[\ddot{\varphi}(l_0 + A\cos\omega t) - \dot{\varphi}A\omega\sin\omega t] \quad (32.43)$$

equals the moment of the external forces with respect to the same center

$$M = -mgl = -mg(l_0 + A\cos\omega t). \quad (32.44)$$

Consequently,

$$\ddot{\varphi}(l_0 + A\cos\omega t) - \dot{\varphi}\omega A\sin\omega t + g(l_0 + A\cos\omega t) = 0. \quad (32.45)$$

As may be seen, the inertia (see the coefficient for $\ddot{\varphi}$) and the rigidity (see the coefficient for φ) are the variables in this system. The term containing the first derivative $\dot{\varphi}$ corresponds to a similar term in the differential equation (32.41), although due to this component the final equation differs somewhat from the Mathieu equation, but parametric excitation of oscillations is possible here.

For example, the problem of oscillations of swings (Figure 32.14, b) belongs to this system. Buildup of oscillations occurs due to periodic pushes by a man standing on the swings, and the system center of mass is displaced as shown in Figure 32.14, a.

The arrangement for a pendulum of a variable length may be demonstrated /286
by the scheme shown in Figure 32.14, c. The pendulum length is changed by imparting a periodic motion to the end of the wire passing through the upper end.

We would like to make two comments to conclude this section.

In addition to the cases described by the differential equation of Mathieu, there are several cases when parametric oscillations obey a periodic, and non-harmonic law (for example, the "square sine" law).

The influence of inelastic resistances (for example, viscous friction) has also been studied. It has been found that such resistances somewhat constrict the boundaries of the instability regions.

The stability of elastic systems under the action of periodic parameter forces was first studied by N.M. Belyayev. He studied the stability of a flexible rod with hinged-supported ends, loaded by a longitudinal force (25.23). The rod mass was assumed to be uniformly distributed along its length (see his article "Stability of Prismatic Rods under the Action of Longitudinal Periodic Forces", in the collection "Inzhenernyye sooruzheniya i stroitel'naya mekhanika" (Engineering Structures and Structural Mechanics) (Leningrad, 1924). Several problems of this type were solved later. The present day status of the problem is discussed in the book by V.V. Bolotin "Dinamicheskaya ustoychivost' uprugikh sistem" (Dynamic Stability of Elastic Systems) (Gostekhizdat, Moscow, 1956).

B.N. Chelomey (see his article "The Possibility of Increasing Stability of Elastic Systems by Means of Vibrations", Doklady AN SSSR, Vol. 110, No. 3, 1956) has pointed out the possibility of stabilizing elastic systems by means of vibrations.

An experiment with an inverted pendulum was described in an article by P.L. Kapitsa "Dynamic Stability of a Pendulum with an Oscillating Point of

Suspension" (Zhurnal Eksperimental'noy i teoreticheskoy fiziki, Vol. 21, No. 5, 1951).

Parametric resonance in mine shafts was studied by Yu.G. Ispolov (see his article in Trudy Leningradskogo politekhnicheskogo instituta im. M.I. Kalinina, No. 265, 1965).

Figure 32.2 was borrowed from the book by V. Cunningham "Vvedeniye v teoriyu nelineynykh sistem" (Introduction to the Theory of Nonlinear Systems) (Gosenergoizdat, Moscow-Leningrad, 1962). The equations for the boundary lines of the Haynes-Strett diagram may be found in the book by G. Cauderer "Nonlinear Mechanics", (Foreign Literature Press, Moscow, 1961).

§ 33. Destabilizing Action of the Forces of Viscous Friction

The origin of forces of friction — unavoidable companions of any oscillatory processes in real mechanical systems — is very diverse and complex. However, to simplify the analysis viscous properties are most frequently assigned to these forces, and it is assumed that they are proportional to the /287 displacement velocities (or deformation velocities). In many cases, the forces of viscous resistance play a damping role: due to these forces, the free oscillations are damped, the amplitudes of the forced oscillations decrease, and the regions of stability are expanded in the case of parametric excitation of oscillations. Therefore, it is not unusual that it has been the custom for a long time to observe only a damping factor in the forces of viscous friction.

The error assumed by A. Lees in his work published in 1923 becomes understandable against this background. This author studied the free bending oscillations of a rotating flexible shaft, assuming that the shaft material had elastic-viscous properties. In writing the correct differential equations for the problem, Lees did not carefully analyze their solution, but apparently confined himself to the single comment that viscous friction in the material must contribute to damping the free oscillations.

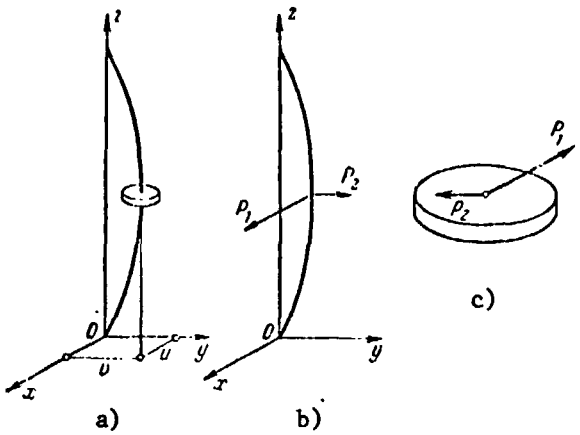

Fig. 33.1. The problem of the stability of rotation of a flexible shaft: a) curved axis; b) forces acting on the shaft; c) forces acting on the disk.

It very quickly appeared that this statement by Lees was erroneous. In 1924 Kimball examined in detail the possible solutions for the differential equations of this problem. It was found that internal viscous friction damped the oscillations only at angular velocities which are less than the critical value, and in the supercritical region they play the opposite role, and contribute to the buildup of oscillations. The Kimball theory explained the unexpected results obtained before by B. Newkirk. In these experiments, the shaft instability was found not only at the critical angular velocity, but also in the supercritical region. The theory was developed further by B.L. Nikolay, I.B. Barger, F.M. Dementberg, et al.

If we disregard the secondary phenomenon, a simplified theory of the problem may be formulated by means of the following model.

A disk of mass m is located in the middle of a rotating, vertical, doubly-supported shaft with a circular cross section and completely balanced on the shaft. At a certain moment, from which the time is computed, the center of the disk is deflected from the axis of rotation Oz in some manner, and the center of the disk begins to move (Figure 33.1, a). Let us examine the subsequent process of motion, assuming that the shaft is only bent, and does

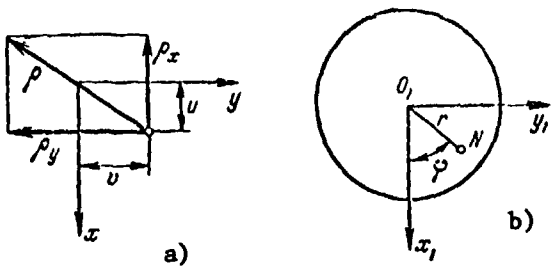

Fig. 33.2. Problem of stability of rotation of a flexible shaft: a) displacement scheme; b) transverse shaft cross section; the x_1, y_1 axes are parallel to the fixed axes x, y.

not undergo torsional deformation. In addition, let us /288 assume that the angular rotation rate of the shaft ω remains constant (this assumes the presence of an engine which provides constant ω) for any deflections of the disk center.

We shall use a fixed system of coordinate axes xyz, and we shall connect the axis z with a line passing through the center of the bearings. We shall use u = u(t) and v = v(t) to designate the components of bending in the middle of the shaft in the direction of the x and y axes. We shall separate the disk from the shaft mentally, and we shall replace the action of the disk on the shaft by the forces P_1 and P_2 (Figure 33.1, b). The diagram of the forces acting on the disk is shown in Figure 33.1, c. These forces are equal in magnitude and opposite in direction to the forces P_1 and P_2. The differential equations for the disk motion have the form

$$m\ddot{u} = -P_1, \quad m\ddot{v} = -P_2. \tag{33.1}$$

These two differential equations contain four unknown functions of time: u(t), v(t), $P_1(t)$ and $P_2(t)$. To formulate the two missing equations, we must examine the shaft bending.

Let us use ρ to designate the radius of curvature of the shaft axis in /289 the middle of its cross section. The projection of ρ on the x and y axes is designated by ρ_x and ρ_y (Figure 33.2, a). The corresponding curvatures are proportional to the bending. We may use the methods of strength of materials to establish the following relationships

$$\frac{1}{\rho_x} = \frac{12}{l^2}u, \quad \frac{1}{\rho_y} = \frac{12}{l^2}v. \tag{33.2}$$

Let us now examine the average cross section of a shaft (Figure 33.2, b), and connect the fixed system of axes x_1, y_1 — which constantly remains parallel to the fixed axes x, y — with the center of gravity O_1 of this cross section. A certain point N, which is located at a distance r from the cross section center of gravity, has the coordinates

$$x_1 = r\cos\varphi, \quad y_1 = r\sin\varphi, \tag{33.3}$$

and we have $\varphi = \omega t$ according to the statements given above.

The strain at the point N is the following, due to the shaft bending

$$\varepsilon_z = -\frac{x_1}{\rho_x} - \frac{y_1}{\rho_y}. \tag{33.4}$$

Substituting (33.2) and (33.3), we obtain

$$\varepsilon_z = -\frac{12r}{l^3}(u\cos\omega t + v\sin\omega t). \tag{33.5}$$

Let us assume that E is the elasticity modulus and k — viscosity coefficient of the shaft material. Then the normal stress at the point N is /290

$$\begin{aligned}\sigma_z = E\varepsilon_z + k\dot{\varepsilon}_z = -\frac{12Er}{l^3}(u\cos\omega t + v\sin\omega t) - \\ -\frac{12kr}{l^3}(\dot{u}\cos\omega t - u\omega\sin\omega t + \dot{v}\sin\omega t + v\omega\cos\omega t).\end{aligned} \tag{33.6}$$

Returning again to the coordinates x_1, y_1, we have

$$\sigma_z = -\frac{12x_1}{l^3}(Eu + k\dot{u} + kwv) - \frac{12y_1}{l^3}(Ev + k\dot{v} - k\omega u). \tag{33.7}$$

The system of elementary forces σdF forms the bending moments with respect to the axes x_1, y_1:

$$\left.\begin{aligned}M_1 = -\int_{(F)}\sigma_z y_1\,dF = \frac{12J}{l^3}(Ev + k\dot{v} - k\omega u), \\ M_2 = -\int_{(F)}\sigma_z x_1\,dF = \frac{12J}{l^3}(Eu + k\dot{u} + k\omega v),\end{aligned}\right\} \tag{33.8}$$

where J is the moment of inertia of the shaft cross section with respect to any of the axes x_1 or y_1. Now turning to Figure 33.1, b, we may note that the bending moment M_1 caused by the action of the force P_2, and the bending moment M_2 caused by the action of the force P_1 are

$$M_1 = \frac{P_2 l}{4}, \quad M_2 = \frac{P_1 l}{4}. \tag{33.9}$$

Equating the right hand sides of equations (33.8) and (33.9), we obtain

$$\left.\begin{aligned} Ev + k\dot{v} - k\omega u &= \frac{P_1 l^3}{48J}, \\ Eu + k\dot{u} + k\omega v &= \frac{P_2 l^3}{48J} \end{aligned}\right\} \qquad (33.10)$$

or

$$\left.\begin{aligned} P_1 &= \frac{48J}{l^3}(Eu + k\dot{u} + k\omega v), \\ P_2 &= \frac{48J}{l^3}(Ev + k\dot{v} - k\omega u). \end{aligned}\right\} \qquad (33.11)$$

It must be noted that the forces P_1 and P_2 depend not only on the displacements u and v, bu_ also on the velocities $\dot{u}$ and $\dot{v}$. The relationships (33.11) represent two supplementary differential equations, which form a complete /291 system with the differential equations (33.1). Substituting (33.11) in (33.1), we obtain the differential equations of motion for the disk center of gravity

$$\left.\begin{aligned} \ddot{u} + p^2\left(u + \frac{k}{E}\dot{u} + \frac{k}{E}\omega v\right) &= 0, \\ \ddot{v} + p^2\left(v + \frac{k}{E}\dot{v} - \frac{k}{E}\omega u\right) &= 0, \end{aligned}\right\} \qquad (33.12)$$

where $p^2 = \frac{48EJ}{ml^3}$ is the square of the eigenfrequency of the disk oscillations on a nonrotating, ideally elastic shaft (or,which is the same thing, the square of the critical angular velocity). To solve the homogeneous system of differential equations (33.12), we set

$$u = ae^{\lambda t}, \quad v = be^{\lambda t}, \qquad (33.13)$$

where a, b, λ are constants.

Substituting (33.13) in (33.12), we obtain a system of algebraic equations which is homogeneous with respect to a and b:

$$\left.\begin{aligned} \left(\lambda^2 + p^2 + p^2\frac{k}{E}\lambda\right)a + p^2\frac{k}{E}\omega b &= 0, \\ -p^2\frac{k}{E}\omega a + \left(\lambda^2 + p^2 + p^2\frac{k}{E}\lambda\right)b &= 0. \end{aligned}\right\} \qquad (33.14)$$

Naturally, this system is satisfied by the trivial solution a = 0, b = 0, but this solution indicates the possible existence of the non-bent form of shaft equilibrium. To study the motion arising after a certain initial perturbation, we must examine the condition of non-zero solutions for a and b, which has the form

$$\begin{vmatrix} \lambda^2+p^2+p^2\frac{k}{E}\lambda & p^2\frac{k\omega}{E} \\ -p^2\frac{k\omega}{E} & \lambda^2+p^2+p^2\frac{k}{E}\lambda \end{vmatrix}=0. \tag{33.15}$$

The characteristic equation of the fourth power for λ follows from (33.15):

$$\left(\lambda^2+p^2\frac{k}{E}\lambda+p^2\right)^2+\left(p^2\frac{k\omega}{E}\right)^2=0. \tag{33.16}$$

If one of the roots of equations (33.16) has a positive real part, then expressions (33.13) include terms which increase infinitely with time. /292
Therefore, in order that solutions (33.13) represent a damped process, i.e., in order that the system may be stable, all real parts of the roots of equation (33.16) must be negative. This occurs if the Hurwitz conditions are satisfied

$$A_0>0;\quad A_1>0;\quad A_2>0;\quad A_3>0; \tag{33.17}$$

$$A_1A_2A_3>A_1^2+A_0A_3^2, \tag{33.18}$$

where A_s is the coefficient in the case of λ^s. Conditions (33.17) are satisfied for any values of the system parameters. Therefore, the condition of stable motion has the form of inequality (33.18). In our case, it reduces to the simple form

$$\omega < p. \tag{33.19}$$

It thus follows that, while the angular rotation rate of the shaft is less than the critical rate, the rectilinear form of equilibrium is stable. For $\omega > p$, this form becomes unstable. Thus, in the supercritical region the internal friction has a damping action, leading to the formation of instability.

We can establish that the external viscous friction produces the opposite influence. We assume that the force of external friction has the components $\alpha\dot{u}$ and $\alpha\dot{v}$ (Figure 33.3). Then the differential equations of motion (33.1) assume the form

$$m\ddot{u}=-P_1-\alpha\dot{u};\quad m\ddot{v}=-P_2-\alpha\dot{v}. \tag{33.20}$$

Substituting the expressions (33.11) found previously for the forces P_1 and P_2, instead of (33.20) we obtain

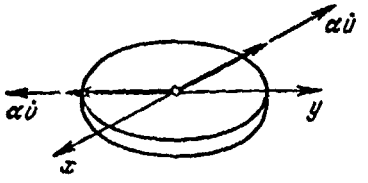

Fig. 33.3. Forces acting on a disk.

$$\left.\begin{aligned}\ddot{u}+p^2\left(u+\frac{k}{E}\dot{u}+\frac{k}{E}\omega v\right)+\frac{\alpha}{m}\dot{u}=0,\\ \ddot{v}+p^2\left(v+\frac{k}{E}\dot{v}-\frac{k}{E}\omega u\right)+\frac{\alpha}{m}\dot{v}=0.\end{aligned}\right\} \qquad (33.21)$$

Substituting the solution in the form of (33.13), we obtain /293

$$\left.\begin{aligned}\left[\lambda^2+\lambda\left(p^2\frac{k}{E}+\frac{\alpha}{m}\right)+p^2\right]a+p^2\frac{k}{E}\omega b=0,\\ -p^2\frac{k}{E}\omega a+\left[\lambda^2+\lambda\left(p^2\frac{k}{E}+\frac{\alpha}{m}\right)+p^2\right]b=0.\end{aligned}\right\} \qquad (33.22)$$

Instead of (33.16), the characteristic equation assumes the form

$$\left[\lambda^2+\lambda\left(p^2\frac{k}{E}+\frac{\alpha}{m}\right)+p^2\right]^2+\left(p^2\frac{k\omega}{E}\right)^2=0. \qquad (33.23)$$

Utilizing inequalities (33.17) and (33.18), we arrive at the condition of stability in the form

$$\omega<p+\frac{E\alpha}{kpm}. \qquad (33.24)$$

It can be immediately seen that external friction (expressed by the coefficient α) expands the stability region of the shaft. For this reason, in the supercritical region instability is not always observed.

The work of Lees was published in the journal "Phil. Mag.", Vol. 45, No. 6, 1929. The articles by Kimball and Newkirk are given in the journal "General Electric Review", Vol. 27, 1924. The article by B.L. Nikolay "Theory of a Flexible Shaft" was published in "Trudy Leningradskogo industrial'nogo instituta", Vol. 6, 1937. For the work by I.B. Barger, see "Trudy LPI im. M.I. Kalinina", No. 3, 1947. The work by F.M. Dimentberg was published in "Inzh. Sbornike", Vol. 16, 1953; see also his book "Izgibnyye kolebaniya vrashchayushchikhsya valov" (Bending Oscillations of Rotating Shafts) (Izdatel'stvo AN SSSR, Moscow, 1959).

§ 34. Linear Realizations of Dry Friction Forces

The real properties of dry friction forces may be most simply described by means of the Coulomb law(*)

$$T = -fN. \tag{34.1}$$

Here T is the projection of the friction force in the direction of the velocity, /294 f — friction coefficient which depends only on the properties of the adjacent surfaces, N — normal pressure. When the direction of motion changes, i.e., when the sign of the velocity changes, the friction force also changes, and as a whole the friction characteristic is essentially nonlinear, as is shown graphically in Figure 34.1, a.

It would appear that in the present chapter, which is devoted to linear problems, it would not be valid to consider the action of nonlinear forces. However, we are discussing particular cases, in which — due to the properties of the mechanical systems — there is an interesting transformation of the Coulomb friction into a force having a linear character — into viscous resistance and even into a linear restoring force.

Coulomb friction as a restoring force. Let us examine the system shown in Figure 34.1, b. A uniform rod is freely placed on two cylindrical pulleys

(*) Charles Augustin Coulomb (1736-1806) was a French physicist. From 1782 he was a member of the Paris Academy of Sciences. The studies of Coulomb in the field of mechanics have been devoted to friction and torsion of elastic rods. The basic laws governing electrostatic and magnetic effects have been established by the torsion balances invented by Coulomb.

Although Coulomb made a significant contribution to science concerning friction, the traditional expressions "Coulomb friction", "Coulomb law" are not valid with respect to (34.1). In actuality, this law was clearly formulated by Guillaume Amonton (1663-1705) almost forty years before Coulomb was born. In 1699 Amonton clearly wrote "It would be erroneous to assume, as is usually done, that the friction of two adjacent bodies increases with an increase in the area of contact. Based on experiments, friction increases only with an increase in the load".

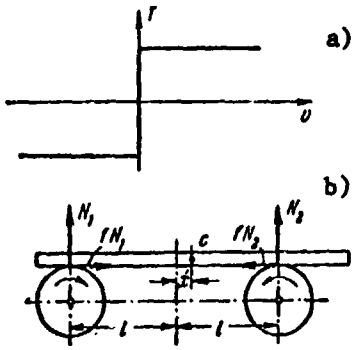

Fig. 34.1. When the rod center of gravity is displaced, the magnitude of the friction forces changes.

which have the same radius and which rotate in opposite directions. The centers of the pulleys are located on a horizontal line. The friction forces developing at the points where the rods touch the pulleys obey the Coulomb law, i.e., they are proportional to the corresponding pressure. Let us study the motion of the rod after it is no longer in equilibrium, for whatever reason.

Let us assume that at the moment of time t the center of gravity C of the rod is located at the distance x from the axis of symmetry. Then the reactions of the pulleys are /295

$$N_1=\frac{l-x}{2l}mg; \quad N_2=\frac{l+x}{2l}mg. \tag{34.2}$$

Here m is the mass of the rod, $2l$ — distance between the centers of the pulleys. The projections of the friction forces will be

$$T_1=\frac{l-x}{2l}fmg; \quad T_2=-\frac{l+x}{2l}fmg, \tag{34.3}$$

where f is the friction coefficient. Thus, the total friction force has the form

$$T=T_1+T_2=-\frac{fmg}{l}x, \tag{34.4}$$

i.e., it is proportional to the displacement x and has the opposite direction. It is very clear here that in this system the friction force plays a role which is not characteristic of it, and is transformed in a remarkable manner into a restoring force.

Let us solve the problem, and write the differential equation of rod motion in the projection on the horizontal axis

$$-\frac{fmg}{l}x=m\ddot{x}. \tag{34.5}$$

This equation takes on the customary form of a differential equation of free nondamped oscillations

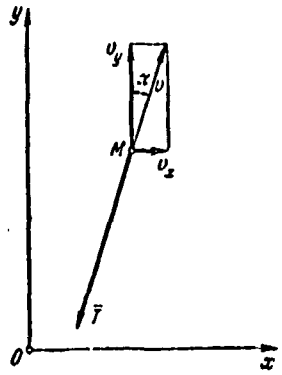

Fig. 34.2. Coulomb friction force is directed opposite to the relative slipping velocity.

$$\ddot{x} + p^2 x = 0, \tag{34.6}$$

if we set

$$p = \sqrt{\frac{fR}{l}}. \tag{34.7}$$

The general solution of the differential equation (34.7) has the specific form

$$x = \frac{v_0}{p} \sin pt + x_0 \cos pt, \tag{34.8}$$

where x_0 and v_0 are the initial displacement and the initial velocity.

Thus, the rod motion will represent harmonic oscillations. This may be predicted from the form of (34.4), which is used to establish the "elastic" character of the friction force. The circular frequency of the oscillations is determined according to (34.7). This formula may be used to determine the friction coefficient f from the values of the circular frequency p observed in the experiments.

The motion of a system in which the Coulomb friction force plays the role of a restoring force is the subject of problem No. 837 of the book of problems by I.V. Meshcherskiy. /296

Coulomb friction as a viscous force. Let us examine the motion of a material point M along a rough plane xOy. Let us assume the motion is such that, in addition to the constant velocity component v_y, there is a much smaller variable component v_x (Figure 34.2). Let us find the expressions for the projection of the Coulomb friction force T. For this purpose, we should note that the vector of the total velocity makes a small angle α with the axis y

$$\alpha \approx \operatorname{tg} \alpha = \frac{v_x}{v_y}. \tag{34.9}$$

The direction of the total friction force $\bar{T}$ may be determined from this angle. Consequently, the projections of the friction force on the coordinate axes are (within an accuracy of small terms of second order)

$$\left.\begin{aligned} T_x &= -Ta = -T\frac{v_x}{v_y}; \\ T_y &= -T. \end{aligned}\right\} \tag{34.10}$$

If we set the constant

$$T : v_y = k, \tag{34.11}$$

then the projection T_y assumes the form

$$T_x = -kv_x, \tag{34.12}$$

i.e., it is proportional to the velocity v_x.

Therefore, it would not be erroneous to say that T_x appears in the form of the force of linear viscous friction. When writing the differential equation of motion in the projection on the x axis, this force must be included in the form $-k\dot{x}$, which is typical for viscous friction forces. This property can only occur under the condition that $|v_x| \ll |v_y|$, i.e., when there is very rapid motion in the direction of the y axis.

For example, let us assume that the pivot of a rapidly rotating shaft is located in a sliding bearing, and the friction properties of this kinematic pair are described by the Coulomb law. With a relatively slow movement of the pivot along the shaft axis, the component of the friction force must be assumed to be viscous. /297

This property is beginning to be of practical importance in machine construction. It is known that the customary dry friction dampers have one drawback: in a certain operational frequency zone, they are unstable. Therefore, the transformation of dry friction into viscous friction described above is very advantageous. The damper of V.A. Kudinov shown in Figure 34.3, a, is based on this principle. Figure 34.3, b, shows a scheme of combining the damper with the object to be damped. The damper consists of two parts, which are connected separately with those units whose relative oscillations must be damped. One part represents a housing 1 of an arbitrary configuration, in which there are two parallel openings. The second part consists of the crankcase 2, in which two rollers 3 are mounted on the bearings. These rollers have parallel axes and are connected with each other by the gear 4. One of the /298

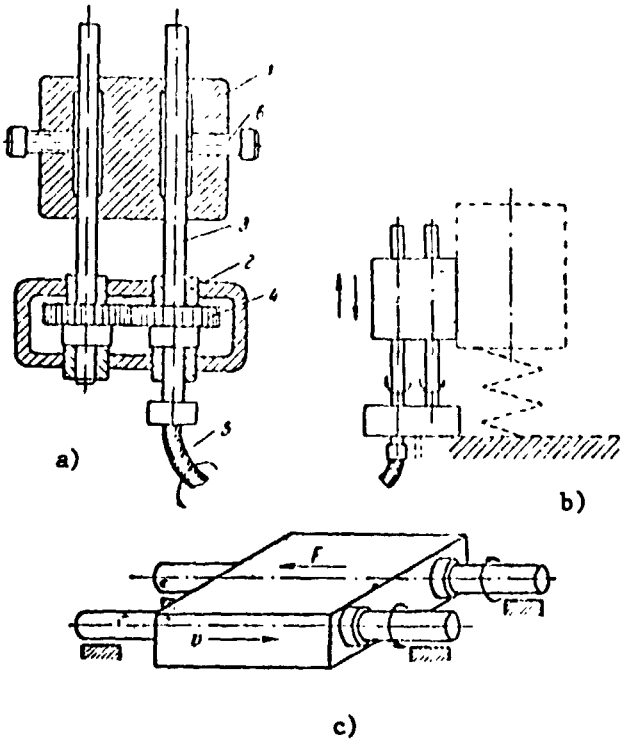

Fig. 34.3. a) Damper scheme; b) scheme for attaching the dampers; c) scheme for cancelling dry friction in the feed mechanism.

rollers is rotated, for example, by means of the flexible roller 5. The rollers enter the opening of the housing 1 with friction, whose magnitude is regulated by the screws 6. In the case of oscillations of the object to be damped, a resistance force develops in the damper, which is practically proportional to the velocity of the relative motion.

The same principle is used in the feed mechanism system shown in Figure 34.3, c. The guides are in the form of two rotating rods (rollers), along which an object moves on bushings. With relatively small, longitudinal motion of the object, a longitudinal force arises, which depends linearly on the velocity of the longitudinal displacement (naturally the rotation may be applied to the bushings, and not the rollers; it is clear that this does not

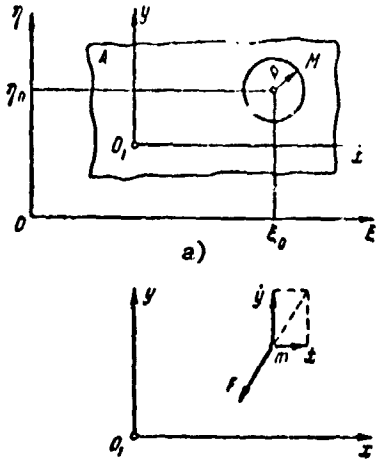

Fig. 34.4. The ξOη coordinate system is fixed. An arbitrary point M of the movable platform A performs a circular motion.

change anything). This construction also provides stable damping of longitudinal oscillations, if they arise for any reason. In addition, this construction is good in that there is no "dead zone" in it at the beginning of motion in the opposite direction. This zone always arises in systems with dry friction.

In all systems of this type, rapid motion in one direction makes it easier to overcome the friction in the perpendicular direction. This property may be used, in particular, to explain the phenomenon of <u>vibration separation</u> in engineering. To analyze this phenomenon, it is necessary to discuss the following problem of N.Ye. Zhukovskiy(*) ("problem of planar separation").

Let us assume that ξOη is a fixed system of axes lying in a horizontal plane, xO_1y is a system of axes lying in the same plane and rigidly connected with the horizontal platform A which has a rough surface. The x, y axes are parallel to the ξ,η axes (Figure 34.4, a). We shall assume that the platform A gradually moves, remaining in the same plane ξOη, while each point completes uniform motion along a circle of radius R. Thus, the motion of any point /299

(*)Nikolay Yegorovich Zhukovskiy (1847 - 1921) — Professor of Mechanics at Moscow Technical Institute (from 1879) and Moscow University (from 1886); Associate Member of the Petersburg Academy of Sciences (from 1894). Author of several basic works in the field of hydro- and aerodynamics. N.Ye. Zhukovskiy played an important role in establishing and developing domestic aviation. He formed the Central Aerodynamic Institute (TsAGI)

on the platform may be described by the equations

$$\left.\begin{aligned}\xi &= \xi_0 + R\cos\omega t;\\ \eta &= \eta_0 + R\sin\omega t,\end{aligned}\right\} \qquad (34.13)$$

so that the projections of acceleration of a point on the fixed axes ξ, η have the form

$$\left.\begin{aligned}\ddot{\xi} &= -R\omega^2\cos\omega t;\\ \ddot{\eta} &= -R\omega^2\sin\omega t.\end{aligned}\right\} \qquad (34.14)$$

Naturally, they are the same for all points, i.e., they are not related with the coordinates ξ_0, η_0. We shall also assume that there is a material point on the platform (plane particle) with the mass m. The particle coordinates in the moveable system of axes are designated by x and y. If a particle moves with respect to the platform A (slides along it), then x = x(t), y = y(t), and the projections of the particle acceleration will contain two components:

$$w_\xi = \ddot{x} + \ddot{\xi} = \ddot{x} - R\omega^2\cos\omega t; \quad w_\eta = \ddot{y} + \ddot{\eta} = \ddot{y} - R\omega^2\sin\omega t. \qquad (34.15)$$

The former components determine the relative particle acceleration, and the latter components — the acceleration of following.

A friction force of constant magnitude F = fmg acts upon the particle; this force is directed opposite to the relative velocity, having the projections $\dot{x}$ and $\dot{y}$. Consequently, the projections of the friction force on the ξ, η axes (or on the x, y axes) have the form (Figure 34.4, b). /300

$$\left.\begin{aligned}F_\xi &= -fmg\frac{\dot{x}}{\sqrt{\dot{x}^2+\dot{y}^2}},\\ F_\eta &= -fmg\frac{\dot{y}}{\sqrt{\dot{x}^2+\dot{y}^2}}.\end{aligned}\right\} \qquad (34.16)$$

We may now write the differential equations of motion for the particle

$$mw_\xi = F_\xi; \quad mw_\eta = F_\eta. \qquad (34.17)$$

Substituting the expressions (34.15) and (34.16), we obtain

$$\left.\begin{aligned}\ddot{x} + fg\frac{\dot{x}}{\sqrt{\dot{x}^2+\dot{y}^2}} &= R\omega^2\cos\omega t,\\ \ddot{y} + fg\frac{\dot{y}}{\sqrt{\dot{x}^2+\dot{y}^2}} &= R\omega^2\sin\omega t.\end{aligned}\right\} \qquad (34.18)$$

These equations hold under the condition that the particle slides along the platform, i.e., if $\sqrt{\dot{x}^2+\dot{y}^2} \neq 0$.

In the case of relative rest $\dot{x} \equiv \dot{y} \equiv 0$ the equations (34.17) assume the form

$$\left.\begin{aligned} -mR\omega^2\cos\omega t &= F_\xi, \\ -mR\omega^2\sin\omega t &= F_\eta \end{aligned}\right\} \tag{34.19}$$

and determine the friction force at rest. The modulus of this force

$$F^0 = mR\omega^2 \tag{34.20}$$

must be less than the limiting value of the friction force

$$F^0_{max} = fmg. \tag{34.21}$$

Thus, the condition of the relative particle rest has the form $F^0 < F^0_{max}$, i.e.,

$$\frac{fg}{R\omega^2} \geqslant 1.$$

The condition of relative motion has the form

$$\frac{fg}{R\omega^2} < 1. \tag{34.22}$$

We shall assume that the latter condition is satisfied. It may be shown /301 that the differential equations (34.18) have a particular periodic solution

$$\left.\begin{aligned} x &= R\sqrt{1-\left(\frac{fg}{R\omega^2}\right)^2}\sin(\omega t - \alpha) + x_*, \\ y &= -R\sqrt{1-\left(\frac{fg}{R\omega^2}\right)^2}\cos(\omega t - \alpha) + y_*, \end{aligned}\right\} \tag{34.23}$$

where

$$\alpha = \arccos\frac{fg}{R\omega^2}. \tag{34.24}$$

The constants x_* and y_* in the solution (34.23) are coordinates of the center of the particle circular trajectory on the moving axes xO_1y. The slipping velocity is constant:

$$v_r = \sqrt{\dot{x}^2 + \dot{y}^2} = R\omega\sqrt{1-\left(\frac{fg}{R\omega^2}\right)^2} = \text{const}. \tag{34.25}$$

In order to determine the trajectory of the relative motion, we eliminate the time t from the equations of motion (34.23). We thus find that this solution describes the relative motion of a particle along a particular trajectory with the radius

$$r = R\sqrt{1-\left(\frac{fg}{R\omega^2}\right)^2} \tag{34.26}$$

which is somewhat less than the radius R of absolute trajectories of points on the platform A.

With an increase in the friction coefficient, the trajectory radius decreases, and in the case

$$fg = R\omega^2 \tag{34.27}$$

vanishes. The "adhesion" of a particle to the platform corresponds to this. On the other hand, with a decrease in the friction coefficient the particle trajectory radius increases, and in the limiting case, when f = 0, equals the radius R. The particle thus freely slides along the platform, and its relative motion precisely reproduces the migratory motion of the platform, but in the opposite direction. The particle is fixed in the $\xi O\eta$ coordinate system.

In order to establish the physical validity of the motion found, it is /302 necessary to verify the stability of the periodic solution (34.23). This important contribution to the solution of N.Ye. Zhukovskiy was made by Tszya Shu-khuay. As was found, the solution (34.23) is stable.

Using this solution of the N.Ye. Zhukovskiy problem, we may now explain the vibration separation process.

Let us assume that a vessel filled with a certain free-flowing medium is located on the horizontal platform A, and the particle m is located within the medium, above the platform level. We shall assume that the specific weight of the particle is greater than the specific weight of the medium. If the platform and the free-flowing liquid are at rest, the particle may fall ("sink") into the free-flowing medium under the action of its own weight. However, this will only occur under the condition that the limiting value of the vertical friction force for the particle in the free-flowing medium is sufficiently small(*). The opposite case is of practical interest — namely, the case when this limiting value is large. Then the particle will be at rest in the free-flowing medium.

(*) The friction force is arbitrarily assumed to mean the equivalent force of the resistance of the medium to the motion of the particle under consideration.

Let us now assume that the horizontal platform has the same motion as in the N.Ye. Zhukovskiy problems solved above, and the free-flowing medium connected with it completes plane-parallel motion together with the platform. As we now know, when condition (34.22) is satisfied the particle penetrates through the medium, trying to move in the horizontal plane along a circular trajectory.

However, due to the circular motion in the horizontal plane, the particle m does not encounter the same resistance along the vertical as in the case when the free-flowing medium is at rest. In other words, the circular motion produces the conditions for the particle to fall into the free-flowing medium, just as the rotation of a pivot facilitates its motion along a bearing.

Thus, motion along the vertical is superimposed on the circular motion of a particle in a horizontal plane. A spiral serves as the particle trajectory. These phenomena comprise the main basis of the vibration separation process /303 of free-flowing mixtures: the heavier particles can gradually penetrate below, and the motion along the vertical is very similar to a body entering a viscous medium.

This line of reasoning simplifies the sometimes incomprehensible statements about "dilution" of a free-flowing body when it vibrates.

The damper of V.A. Kudinov is described in the "Byulleten izobreteniy", of the Committee on Inventions and Discoveries under the Soviet of Ministers, No. 8, 1961. The scheme shown in Figure 34.3 was borrowed from the article by V.A. Kudinov in the journal "Stanki i instrument", No. 1, 1961. See also the book by S.P. Timoshchenko "Kolebaniya v inzhenerom dele" (Oscillations in Engineering), (Fizmatgiz, Moscow, 1959, p. 70).

For the problem of N.Ye. Zhukovskiy, see his article "Notes on Planar Separation" (Sobr. Soch. [Collected Works], Vol. 3, Gostekhizdat, 1949) and also the book by I.I. Blekhman and G.Yu. Dzhanelidze "Vibratsionnoye peremeshcheniye (Vibration displacement) (Fizmatgiz, Moscow, 1964, pp 225 - 230). The explanation

given above for the vibration separation process was given by I.I. Blekhman, V.V. Gortinskiy, and G.Ye. Putshkina in the article "Particle Motion in an Oscillating Medium in the Case of Resistance of the Dry Friction Type", (Izvestiya AN SSSR, OTN, Mekhanika i mashinostroyeniye, No. 4, 1963). See also the book by I.I. Blekhman and G.Yu. Dzhanelidze (Chapter XII).

§ 35. Paradox Connected with Damping Coverings

One of the ways to combat oscillations of elastic structures is to use special coverings which intensely absorb (scatter) the oscillation energy. In particular, such coverings are effective in sound-insulating partitions.

It has been found experimentally that coverings, whose material is characterized by a large absorption coefficient, frequently cannot damp oscillations as well as coverings with a small absorbing coefficient. This paradoxical phenomenon was established by Yu.K. Favstov, who developed the explanation of this paradox which is given below.

Let us first recall the basic methods of determining the damping properties of oscillating systems. For this purpose, the concepts of logarithmic decrement and absorption coefficient are frequently used.

The following quantity is called the logarithmic decrement of oscillations(*) /304

$$\delta = \ln \frac{a_m}{a_{m+1}}, \tag{35.1}$$

where a_m and a_{m+1} are two adjacent amplitudes of free damping oscillations. If, as is usually the case, the damping is not too large, the difference Δa_m between two consecutive amplitudes is small as compared with the amplitudes themselves, and we may approximately set

(*) Sometimes it is incorrect to speak of, or to write, "logarithmic decrement of damping". This term contains a tautology, since the word "decrement" itself (from the Latin "decrementum") designates "to decrease", i.e., "to damp".

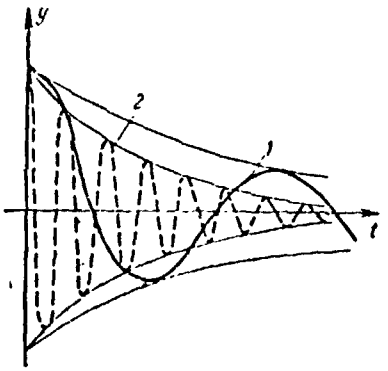

Fig. 35.1. Which oscillations (see curves 1 and 2) damp more rapidly?

$$\delta = \ln \frac{a_m}{a_{m+1}} \approx \approx \ln\left(1 + \frac{\Delta a_m}{a_m}\right) \approx \frac{\Delta a_m}{a_m}. \qquad (35.2)$$

It is of interest to turn our attention to the arbitrary nature of determining the damping rate from the logarithmic decrement. Figure 35.1 shows vibrograms of two different processes of damped oscillations. Based on the behavior of the envelopes, we may say that the damping of process 1 occurs more slowly than the damping of process 2, although the logarithmic decrement of oscillations in the first case is greater than in the second case. The fact is that the logarithmic decrement of oscillations characterizes damping not in an objective unit of time (for example, in one second), but in one period of oscillations.

Ordinarily the logarithmic decrement of oscillations depends on the level of maximum deformations of the material, and consequently on the displacement amplitude. Therefore, calculations using formulas (35.1) and (35.2) yield different results, depending on what region of the vibrogram is used to determine the amplitude a_m. Usually, close to the origin of the vibrogram (at large amplitudes), the system logarithmic decrement of oscillations is large, and then gradually decreases. /305

An exception (but not the rule !) is the damping of oscillations according to an exponential law, when the equation of the envelopes has the form

$$a(t) = \pm a_0 e^{-kt}, \qquad (35.3)$$

where a_0 is the deviation of the system for t = 0, k — a quantity characterizing the damping rate. In actuality, in this case

$$\left.\begin{aligned} a_m &= a_0 e^{-km\tau}, \\ a_{m+1} &= a_0 e^{-k(m+1)\tau}, \end{aligned}\right\} \qquad (35.4)$$

and using formula (35.1) it is found that the logarithmic decrement of oscillations is

$$\delta = kT, \tag{35.5}$$

i.e., it is constant for the entire process of damped oscillations. In particular, the case of viscous resistance represents such an exception, i.e., resistance which is proportional to the displacement rate. On the other hand, as is now known, the elastic-viscous model of a solid body, proposed by Kelvin(*) and Focht, reflects very poorly the actual properties of the majority of real structural materials (for example, steel).

Another method of determining absorbing properties is based on formulating the energy $\Delta\Pi_m$ scattered in one cycle of oscillations, with the greatest potential energy of the cycle

$$\psi = \frac{\Delta\Pi_m}{\Pi_m}, \tag{35.6}$$

The quantity ψ is called the absorption coefficient. This quantity may be /306 determined both in the process of forced oscillations (measuring the energy losses in a reliable manner), and in the process of free oscillations (using a vibrogram). In the latter case, we must use the expression for the potential energy

$$\Pi_m = \frac{ca_m^2}{2}, \tag{35.7}$$

in which c is the system rigidity. We then have

$$\Delta\Pi_m = \frac{ca_m^2}{2} - \frac{ca_{m+1}^2}{2} = \frac{c}{2}(a_m + a_{m+1})(a_m - a_{m+1}) \approx \approx ca_m\Delta a_m. \tag{35.8}$$

According to formula (35.6), the absorption coefficient equals

$$\psi = 2\frac{\Delta a_m}{a_m}. \tag{35.9}$$

(*) Kelvin (V. Tomson, 1824 - 1907) — English physicist. Founder of the theory of electric oscillations and the theory of vortex motion of liquids. He developed problems of the potential theory and the heat conductivity theory. The author of many inventions. From 1851 — Member of the London Royal Society. From 1877 — Associate Member, and from 1896 — Full Member of the Petersburg Academy of Sciences.

Consequently, the absorption coefficient of the system under consideration is two times larger than the logarithmic decrement of the oscillations.

The absorption coefficient thus determined is, in essence, characteristic of the damping properties of the sample, and does not only depend on the material, but also on the form of the sample, as well as the nature of the load. Along with this, there is a more objective characteristic of the damping properties of the material — the absorption coefficient of the material:

$$\psi_* = \frac{\Delta\Pi_*}{\Pi_*}. \tag{35.10}$$

Here we use Π_* to designate the greatest potential energy per unit volume, and $\Delta\Pi_*$ — the energy scattered in one cycle also per unit volume. For a direct determination of ψ_*, it is necessary that the sample be in a homogeneous, stress state, when all its elements scatter the energy in a similar way, i.e., when the energy scattering is also homogeneous. In this case, for the entire sample we have:

$$\Pi = \Pi_* V, \quad \Delta\Pi = \Delta\Pi_* V$$

(V is the sample volume) and the sample absorption coefficient is

$$\psi = \frac{\Delta\Pi}{\Pi} = \frac{\Delta\Pi_*}{\Pi_*} = \psi_* \tag{35.11}$$

and coincides with the absorption coefficient of the material. /307

This occurs, for example, in the case of expansion-compression of a cylindrical sample, if the inertia of the rod itself is negligibly small as compared with the inertia of the oscillating mass connected with the free end of the rod (the latter condition is important because the inherent inertia of the rod elements makes the longitudinal stresses vary over the length, i.e., it disturbs the homogeneity of the stress state).

It must be noted that such experimental conditions are very difficult to realize, primarily due to the extremely small magnitude of the displacements which correspond to the elastic state of the material. Therefore, usually experiments are performed on deformed (or twisted) samples, when the displacements are sufficiently large even in the case of moderate stresses.

In these cases, due to the nonhomogeneity of the stress state the absorption coefficients ψ and ψ_* are different. The formulas for the change from the observed values ψ to the desired values ψ_* essentially depend on the design of the specimen and the nature of its load.

For an example, let us discuss the case when the absorption coefficient of the material ψ_* is connected with the deformation amplitude ε by the power relationship

$$\psi_* = \alpha\varepsilon^{n-1}, \tag{35.12}$$

α and n are the material constants(*). The energy scattered in one cycle is

$$\Delta\Pi_* = \psi_*\Pi_* = 2\frac{E\varepsilon^{n+1}}{2}. \tag{35.13}$$

We shall assume that the rod undergoes pure bending, and the curvature changes in a symmetrical cycle. If the rod has a rectangular transverse cross section with the height h, the amplitude of the longitudinal deformation at a distance of y from the neutral axis is

$$\varepsilon = \frac{2|y|}{h}\varepsilon_0, \tag{35.14}$$

where ε_0 is the amplitude of the longitudinal deformation for $y = \frac{h}{2}$, i.e., /308 at the edge of the cross section. Any separately examined, elementary layer with a volume of $bl\,dy$ (b — cross section width, l — rod length, dy — layer height) is under conditions of a homogeneous stress state. Therefore, according to formula (35.13) the following energy is scattered in one cycle in this layer

$$\frac{\alpha E\varepsilon^{n+1}}{2}bl\,dy = 2^n\alpha E\varepsilon_0^{n+1}\left|\frac{y}{h}\right|^{n+1}bl\,dy. \tag{35.15}$$

Integrating over the coordinate y, we find the energy scattered in one cycle throughout the entire volume of the rod

$$\Delta\Pi = 2^{n+1}\alpha E\varepsilon_0^{n+1}bl\int_0^{\frac{h}{2}}\left(\frac{y}{h}\right)^{n+1}dy = \frac{\alpha E\varepsilon_0^{n+1}}{2(n+2)}V. \tag{35.16}$$

(*) The relationship $\psi_* = \psi_*(\varepsilon)$ for the majority of materials has this character.

We now find the greatest potential energy of the entire rod:

$$\Pi = \int_V \frac{E\varepsilon^2}{2} dV = \frac{4Eble_0^2}{h^n} \int_0^{\frac{h}{2}} y^n dy = \frac{E\varepsilon_0^2}{6} V. \tag{35.17}$$

Dividing expression (35.16) by (35.17), we find the absorption coefficient for the rod

$$\psi = \frac{3\alpha\varepsilon_0^{n-1}}{n+2}. \tag{35.18}$$

Comparing this with (35.12), we obtain

$$\psi = \frac{3}{n+2}\psi_*. \tag{35.19}$$

As may be seen, the absorption coefficients of the material and the rod are different. Thus, for example, if n = 2 (steel), then

$$\psi = 0{,}75\psi_*, \quad \psi_* = 1{,}33\psi. \tag{35.20}$$

Let us now turn to the basic theme of the present section, i.e., the case when the same rod is covered with thin damping layers both above and below. The layers are made of material whose absorption coefficient equals ψ_a. We shall find the absorption coefficient ψ_c of a rod covered with these layers.

Just as before, we shall use ψ to designate the absorption coefficient of the rod without damping coverings. We shall designate the greatest potential energy and the energy scattered in one cycle by Π_a, Π_c, Π and $\Delta\Pi_a$, $\Delta\Pi_c$ and $\Delta\Pi$ (for a covering, for a sample with a damping covering, for the same sample without a covering). We thus have /309

$$\Pi_c = \Pi + \Pi_a \tag{35.21}$$

$$\Delta\Pi_c = \Delta\Pi + \Delta\Pi_a \tag{35.22}$$

In addition, by definition we have

$$\Delta\Pi_c = \psi_c\Pi_c, \quad \Delta\Pi_a = \psi_a\Pi_a \quad \Delta\Pi = \psi\Pi, \tag{35.23}$$

so that equation (35.22) assumes the form

$$\psi_c(\Pi + \Pi_a) = \psi\Pi + \psi_a\Pi_a \tag{35.24}$$

We thus find the absorption coefficient for a rod with a damping covering

$$\psi_c = \psi \frac{\Pi}{\Pi + \Pi_a} + \psi_a \frac{\Pi_a}{\Pi + \Pi_a}. \tag{35.25}$$

We now note that for both thin-layer coverings with the thickness h, we have

$$\Pi_a = 2bl h \frac{E_a \varepsilon_0^2}{2} = E_a V_a \varepsilon_0^2 \tag{35.26}$$

(V_a is the volume of one covering layer), and for the rod itself, according to formula (35.17),

$$\Pi = \frac{E\varepsilon_0^2}{6} V.$$

Therefore, the rod absorption coefficient equals

$$\psi_c = \psi \frac{1}{1 + 6\frac{E_a V_a}{EV}} + \psi_a \frac{1}{1 + \frac{EV}{6E_a V_a}}. \tag{35.27}$$

Since the volume of the covering is much less than the volume of the rod itself, and the elasticity moduli E and E_a are of at least the same order of magnitude, we have

$$\frac{6E_a V_a}{EV} < 1, \quad \frac{EV}{6E_a V_a} > 1;$$

For purposes of simplification, we may approximately assume

$$\psi_c = \psi + \psi_a \frac{6E_a V_a}{EV}. \tag{35.28}$$

Thus, the absorption coefficient ψ_c for a rod with a covering is $\psi_a \frac{6E_a V_a}{EV}$ times greater than the absorption coefficient of the same rod without a covering.

Let us pay particular attention to this correction, which determines the advantage in absorbing properties. As must be the case, this correction is proportional to the absorption coefficient of the covering material ψ_a. However, it does not follow that the material for the covering must be selected only with this property. The correction also depends on the elasticity modulus E_a of the covering material, and in the last analysis it is necessary

to determine the damping properties of the covering, not by the quantity ψ_a, but by the product $\psi_a E_a$. Unfortunately, frequently materials with a high value of ψ_a have an elasticity modulus E_a which is too low. Therefore, the use of such materials as coverings is comparatively less effective.

For the article by Yu.K. Favstov, see "Izvestiya AN SSSR, OTN, Mekhanika i mashinostr.", No. 3, 1963.

For a discussion of energy scattering in the case of oscillations, see the book by E.S. Sorokin "K teorii vnutrennego treniya pri kolebaniyakh uprugikh sistem" (Theory of Internal Friction in the Case of Oscillations of Elastic Systems), (Gosstroyizdat, Moscow, 1960); Ya.G. Panovko "Vnutrenneye treniye pri kolebaniyakh uprugikh sistem" (Internal Friction in the Case of Oscillations of Elastic Systems), (Fizmatgiz, Moscow, 1960); G.S. Pisarenko "Rasseyaniye energii pri mekhanicheskikh kolebaniyakh" (Energy Scattering in the Case of Mechanical Oscillations), (Izdatel'stvo AN USSR, Kiev, 1962).

§ 36. Damping of Pipeline Oscillations by Coriolis Forces

Recently, the problems of pipeline oscillations have acquired much greater significance. It is known that the liquid flow rate greatly influences the oscillatory properties of pipelines. For a pipeline with fixed ends, it has been established that the frequency of eigenoscillations decreases with an increase in the flow rate, and a critical state may occur which is characterized by a zero value of the frequency. This must be regarded as one of phenomena which destabilizes the flow with a constant velocity. On the other /311 hand, pulsation of pressure and velocity may also lead to harmful oscillations which threaten the strength of the pipeline and the strength of the connections.

Nevertheless, there may be equipment in which the liquid flow unexpectedly produces a damping action. It should be noted that such cases are unusual. However, an analysis of these particular systems may help to clarify the mechanism of the flow and the pipeline interaction. Let us turn to the

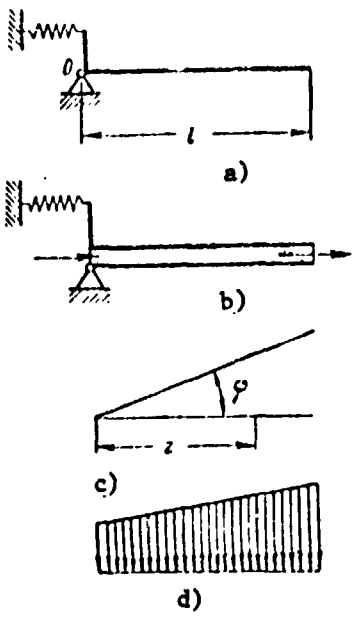

Fig. 36.1. a) An elastically fixed rigid cantilever; b) elastically fixed cantilever tube; c) scheme for tube displacement; d) diagram of load on tube.

simplest problem of this type, and examine a completely rigid cantilever, whose left end is fixed elastically (Fig. 36.1, a), and c is the fastening elasticity coefficient (the moment which stops when the cantilever turns at an angle equal to unity). Let m be the mass of a unit length of the cantilever, and l — its total length. Then the eigenfrequency of the centilever oscillations is determined by the formula

$$p = \sqrt{\frac{c}{I}} = \sqrt{\frac{3c}{ml^3}} \qquad (36.1)$$

(I is the cantilever moment of inertia with respect to the axis passing through the point O perpendicularly to the plane of the drawing). Let us now complicate the problem, and assume that the cantilever represents a tube, i.e., it has a longitudinal channel along which the liquid flows from left to right continuously. There is a free outflow of liquid at the right end (Figure 36.1, b). We shall designate the mass of a unit length of the flow by m_*, and the flow rate by v.

How is the influence of the flow upon the oscillatory properties of the system manifested? We would like to immediately point out the following: it would be erroneous to assume that the system retains its conservative properties and that the eigenfrequency must only be determined by formula (36.1), replacing m by the sum $m + m_*$. For a correct answer to the problem just proposed, we must carefully examine the forces arising during oscillations, write the differential equation of oscillations, and then study its solution. /312

Let us use z to designate the coordinate of the pipeline cross section, and $\varphi = \varphi(t)$ to designate the angle of turn of the tube at the current moment

of time (Figure 36.1, c). In the case of small oscillations, φz, $\dot{\varphi} z$, $\ddot{\varphi} z$ are, respectively, the displacement, velocity, and acceleration of the tube cross section. For oscillations between the particles of the liquid and the tube, forces of interaction arise which are perpendicular to the tube axis and depend both on the coordinate z and on the time t. Let us refer these forces to a unit of length and designate their strength by

$$F = F(z, t), \tag{36.2}$$

so that the force F dz on the side of the pipeline influences a particle of the liquid occupying a portion of the length dz along the system axis. Since the particle mass equals $m_* dz$, the differential equation of its motion assumes the form

$$F = m_* w, \tag{36.3}$$

where w is the total acceleration of a particle which is also perpendicular to the z axis. We may regard the particle motion as complex, connecting the moving coordinate system with the tube. The relative particle acceleration equals zero, and consequently

$$w = w_e + w_c, \tag{36.4}$$

where $w_e = \ddot{\varphi} z$ is the acceleration of following, i.e., the acceleration of the corresponding tube cross section, $w_c = 2\dot{\varphi} v$ — Coriolis acceleration. Combining (36.3) and (36.4), we obtain the strength of the forces acting from the side of the tube on the liquid flow

$$F = m_* (\ddot{\varphi} z + 2\dot{\varphi} v). \tag{36.5}$$

Turning now to the tube, we must assume that the same forces (36.5) act upon it from the liquid, but these forces have a different direction (Figure 36.1, d). These forces produce a negative moment with respect to the center of the elastic fastening /313

$$M = -\int_0^l m_* (\ddot{\varphi} z + 2\dot{\varphi} v) z \, dz = -m_* \left(\ddot{\varphi} \frac{l^3}{3} + \dot{\varphi} v l^2 \right). \tag{36.6}$$

In addition, the moment of the elastic fastening acts upon the tube. This moment equals $-c\varphi$, and therefore the differential equation of motion for the tube assumes the form

$$-c\varphi + M = I\ddot{\varphi}, \tag{36.7}$$

where as before $I = \frac{m l^3}{3}$. Substituting expression (36.6), we obtain

$$\frac{(m+m_*)l^2}{3}\ddot{\varphi} + m_* v l^2 \dot{\varphi} + c\varphi = 0 \qquad (36.8)$$

or finally

$$\ddot{\varphi} + \frac{3m_* v}{(m+m_*)l}\dot{\varphi} + \frac{3c}{(m+m_*)l^2}\varphi = 0. \qquad (36.9)$$

The first derivative is retained in this equation, and the coefficient in this case is positive. It is thus apparent that the oscillations of the system under consideration have a damping character, and it is also possible that, instead of oscillations, the tube will perform an aperiodic motion toward the equilibrium position. The damping will thus be more intense, the greater the velocity of the liquid.

How can we physically explain the origin of the damping in the system under consideration?

In the differential equation (36.9), the "quasi-viscous" component containing the first derivative of the tube angle of rotation arises due to the Coriolis effect. It must be emphasized that the Coriolis force $-2m_* v\dot{\varphi}$ is a real force acting on the tube from the flow. This force is proportional to the angular velocity $\dot{\varphi}$ and produces the moment of the opposite sign.

A more graphic explanation is possible, based on a simple comparison of the energy of the flow particles at the tube input, and not at its output. The kinetic energy of a particle $m_* dz$ at the tube input equals $m_* dz \frac{v^2}{2}$, and /314 at the tube output the same particle has a greater energy: $m_* dz \frac{v^2 + (\dot{\varphi}z)^2}{2}$. Consequently, each particle has the energy $m_* dz \frac{(\dot{\varphi}z)^2}{2}$, which is the reason for the damping of the oscillations. In particular, it is clear that, if both ends of the tube are fixed, irrespective of the possible bending of the tube, the energy of the incoming liquid particles precisely equals the energy of the outgoing particles, and damping naturally does not arise.

It must once again be stressed that we are dealing with systems of a special form. It is sufficient to take into account the transverse compliance

of a support to explain the reverse, i.e., the destabilizing, influence of the flow on the tube (in order to represent this phenomenon, it is sufficient to stay within the framework of a rigid nozzle of a watering hose).

This phenomenon was indicated by A.P. Kovrevskiy. His experiments on an elastic cantilever tube (the root section was rigidly fixed) revealed an increase in the damping with an increase in the liquid flow rate (see the article by A.P. Kovrevskiy in "Izvestiya vysshikh uchebynkh zavedeniy BSSR", Minsk, No. 4, 1964).

CHAPTER VII

DYNAMIC ACTION OF A MOVING LOAD

The present chapter is devoted to the problem of the action of moving loads on elastic structures. In § 37 a brief historical sketch is given of the origin and development of the theory. In the subsequent section § 38, the erroneous solution of one of the simple problems is described. Although it was advanced more than a hundred years ago, an analysis of this error is still instructive today. The last two sections 39 and 40 contain the solutions of two, in a certain sense mutually exclusive, problems regarding the action of a moving load.

§ 37. Brief Historical Sketch

The theory of the dynamic action of a moving load arose long before the theory of the static calculation of rod systems, and has a somewhat more secular history. The collapse of the Chester bridge (England) in 1847 was the immediate cause for the formulation of the first theoretical and experimental studies of the dynamic action of moving loads. This catastrophe was accompanied by human deaths, and caused serious misgivings among English civil engineers. Researchers were confronted with the problem of the extent to which the phenomena produced in an elastic structure by a moving load (deflection and internal stresses) differ from the corresponding phenomena which arise under conditions of a static load. One of the first attempts to solve this problem theoretically led to the conclusion that the dynamic phenomena are two times greater than the static phenomena. The author of this conclusion H.L. Cox reasoned as follows. Let us assume P is the weight of the load moving along a hinge-supported beam, EJ — the rigidity of the /316
transverse cross section of the beam in the case of bending, l — span of the beam, f — deflection of the beam at the moment the load passes through the middle of it (Figure 37.1). The force P performs the work Pf at this moment.

The potential bending energy of the beam at the same moment is $\frac{48EJ}{l^3} \cdot \frac{f^2}{2}$. Equating both expressions, Cox found $f = \frac{Pl^3}{24EJ}$, i.e., the dynamic deflection was twice as great as the static deflection $f_{st} = \frac{Pl^3}{48EJ}$. As may be seen, in this line of reasoning the mass of the beam is assumed to equal zero (otherwise, it would be necessary to take into account the kinetic energy of the beam).

This result was obtained in 1848, but even in 1849 it was refuted by Stokes(*). Stokes turned his attention to the error in the balance of energy: Cox omitted the work of a horizontal force necessary to maintain the load velocity constant along the beam. If it is assumed that this force does not exist, then the velocity of the load, which moves along a curvilinear path, cannot remain constant, and the change in the kinetic energy of the load must be taken into account.

A large number of theoretical and experimental studies were published after this time. They were primarily related to the action of a moving load on a bridge. Later, an important region in which to apply the theory appeared — the action of a liquid on flexible pipelines.

There are four different variations for formulating the problem of the action of a moving load, depending on the method of schematizing the inertia forces of the system. The different features of these variations are given in the following table.

(*) George Gabriel Stokes (1819 - 1903) — English physicist and mathematician, Member (from 1851) and President (1885 - 1890) of the London Royal Society. The works of Stokes are devoted to optics, hydrodynamics, and mathematical physics.

Variant of Problem Formulation	Allowance for the Mass	
	of the beam	of the load
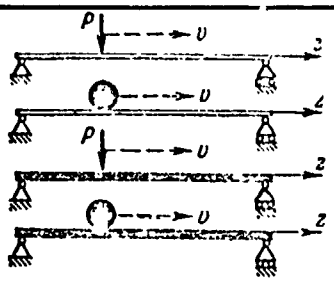	no	no
	no	yes
	yes	no
	yes	yes

/317

We shall briefly characterize each of these variants.

Variant 1. All of the inertia phenomena are assumed to be negligibly small, and the pressure of the load on the beam is assumed to equal the weight of the load mg (m — mass of the load). With this formulation, not the "dynamic nature" but the "kinematic nature" of the load is taken into account, i.e., the variability of the distance x which depends on the time t (x = vt, where v is the constant velocity of the load).

In 1868, independently from each other, E. Winkler and O. Mohr, when solving such problems, constructed special graphs called lines of influence (in old Russian technical literature, they are called influence lines). The graphs show the change in the internal forces or the displacements, as a function of the load coordinate. The graphs were based on the assumption that the load equals unity. For purposes of illustration, Figure 37.2 shows examples of such lines of influence: The lines of influence of the left-hand reactive force (Figure 37.2, a), the line of influence of the bending moment /318
in the middle of the span (Figure 37.2, b), and the line of influence of deflection in the middle of the beam (Figure 37.2, c).

Using the lines of influence, we may readily determine the effect of applying any system of loads, and may also find their worst location. The lines of influence are widely used in the static calculation of bridges.

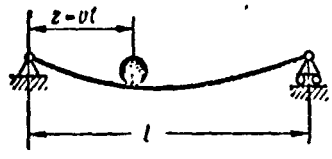

Fig. 37.1. Transverse bending of a doubly-supported beam under the action of a moving point load.

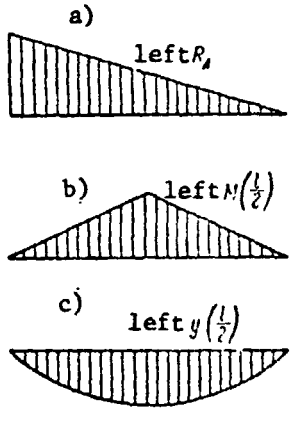

Fig. 37.2. Lines of influence of a left-hand reactive force, bending moment in the middle of the span, and deflection of the middle of the beam.

It is known that such a "non-inertia" formulation of the problem is suitable only for sufficiently small velocities v of the load.

Variant 2. It is assumed that the mass of an elastic structure is small, but the force N of the load differs from the static load. Assuming that the positive deflections are directed downward, we may write the force N of the load on the beam in the form

$$N = mg - m\frac{d^2y}{dt^2} = mg - m\frac{d^2y}{dz^2}v^2. \quad (37.1)$$

In expression (37.1), y designates the load displacement along the vertical (i.e., deflection of the beam under the load). The second term of this expression represents the vertical force of inertia of the load.

This form of the problem was first formulated in 1849 by a professor of the Cambridge University, F. Willis. Assuming that the beam buckles under the influence of a single active force N, Willis found that the beam deflection under a load is

$$y = \frac{Nz^2(l-z)^2}{3lEJ}. \quad (37.2)$$

This expression is obtained from a purely static solution. However, the value of N which was not known previously, according to (37.1), depends on the deflection y. Excluding the force N from equations (37.1) and (37.2), Willis obtained the following differential equation for the basic variable problem — the deflection y:

$$\frac{d^2y}{dz^2} + \frac{3lEJ}{mv^2(lz-z^2)^2}y = \frac{g}{v^2}. \quad (37.3)$$

However, Willis could not solve this complex equation, and turned for help to Stokes, who in the same year obtained a solution to the equations (37.3) in the form of an algebraic series. In the first approximation, the ratio of the maximum dynamic deflection to the corresponding static deflection /319 (dynamic coefficient) was found to equal

$$\mu = 1 + \frac{ml}{3EJ} v^2. \tag{37.4}$$

In this formula, the influence of a new factor is very apparent — the load velocity. Stokes obtained the solution to equation (37.3) in closed form.

Replacing the variables sometimes makes it possible to transform the differential equation with variable coefficients into an equation with constant coefficients. There are no universal methods for performing substitutions — it is all a matter of skill in mathematics. In 1883 J.V. Boussinesq(*) pointed out the following clever transformation of variables for the differential equation (37.3):

$$\xi = \frac{1}{2} \ln \frac{z}{l - z}, \qquad \eta = y \frac{8v^2}{gl^2} \operatorname{ch} \xi, \tag{37.5}$$

after which the equation assumes the simple form:

$$\frac{d^2\eta}{d\xi^2} + k^2\eta = \frac{2}{\operatorname{ch}^2 \xi}, \tag{37.6}$$

where

$$k^2 = \left| \frac{12EJ}{mlv^2} - 1 \right|. \tag{37.7}$$

Naturally, we cannot dwell on the solution of (37.6).

The formulation of the problem described here was used in several other studies. However, its practical value is very small, since the mass of the structure cannot be neglected as compared with the mass of the load (which is usually much less).

(*) Joseph Valentyn Boussinesq (1842 - 1929) — Specialist in the field of elasticity theory. Member of the Paris Academy of Sciences from 1886.

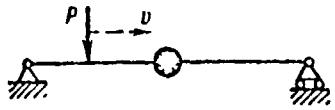

Fig. 37.3. Action of a moving force on a beam with a concentrated mass.

Variant 3. This problem is solved under the assumption that the dynamic effect is only connected with the inertia of the beam itself. The force of the load on the beam is assumed to equal its weight. This formulation of the problem is diametrically opposed to the preceding one (see Part 2), where the forces of inertia of the beam itself are ignored, but the inertia of the load is taken into account.

A.N. Krylov in 1905 provided the most complete solution of this problem /320 regarding a moving force. A.N. Krylov also solved the problem of the action of a moving pulsating force on a beam; this problem illustrates the action of unbalanced wheels of a locomotive on a bridge. This formulation of the problem is of great practical value, and its solution assumes many useful generalizations due to the linear nature of the problem.

In the solution of A.N. Krylov, the beam mass is assumed to be continuously distributed over the length. Along with this most precise solution, there are approximate solutions based on the concentration of the beam mass at one or several cross sections. For example, we have the beam shown in Figure 37.3 with one concentrated mass, when a force P moves along a beam at a constant velocity.

Let us discuss the solution of this problem. The deflection in the middle of the beam is determined by the expression

$$y = P\delta_{1P} - m\ddot{y}\delta_{11}. \tag{37.8}$$

Here δ_{1p} is the static deflection in the middle, caused by the force P, and δ_{11} is the static deflection at the same point, if a unit force is applied to it. Thus, the first component expresses the deflection caused by the force P, and the second component represents the deflection caused by the force of inertia $m\ddot{y}$. The unit displacement δ_{11} is

$$\delta_{11} = \frac{l^3}{48EJ}, \tag{37.9}$$

and the unit displacement δ_{1p} is determined as a function of the abscissa z of the point where the force P is applied by the formulas

$$\left.\begin{aligned} \delta_{1P} &= \frac{z(3l^2-4z^2)}{48EJ} \quad \text{for } z \leqslant \frac{l}{2}, \\ \delta_{1P} &= \frac{(l-z)(8lz-4z^2-l^2)}{48EJ} \quad \text{for } z \geqslant \frac{l}{2}. \end{aligned}\right\} \tag{37.10}$$

In the case of uniform motion of the force along the beam at the velocity v, we must set z = vt in these formulas. Then, for the motion of the load along the left half of the beam, when $t \leq \frac{1}{2v}$, equation (37.8) assumes the form /321

$$\ddot{y} + \frac{48EJ}{ml^3} y = \frac{Pvt(3l^2-4v^2t^2)}{ml^3}, \tag{37.11}$$

and for this stage of motion along the right half of the beam, when $t \geq \frac{1}{2v}$, it assumes the form

$$\ddot{y} + \frac{48EJ}{ml^3} y = \frac{P(l-vt)(8lvt-4v^2t^2-l^2)}{ml^3}. \tag{37.12}$$

Equation (37.11) must be integrated for the initial conditions.

$$y = 0, \quad \dot{y} = 0 \quad \text{for} \quad t = 0 \tag{37.13}$$

This solution, which is valid for the entire interval of time $0 < t \leq \frac{1}{2v}$, may be used to find the values of y and $\dot{y}$ at the moment of time $t = \frac{1}{2v}$. These values must be used as the initial conditions to solve the equation (37.12).

Thus, the problem reduces to the consecutive solution of two differential equations (37.11) and (37.12) for the given initial conditions. It is not difficult to obtain the solutions, but we shall not discuss this here. It is more advantageous to regard the initial scheme shown in Figure 37.3.

Usually, systems of this type with concentrated masses are used to simplify real systems with a continuous distribution of the mass. However, such systems are only useful if the form of the bending curve does not change in time, but only its scale changes (for example, for free oscillations with respect to one of the eigenforms). If the bending curve does not remain

the same in time, the concept of the reduced concentrated mass loses any apparent meaning. In particular, this pertains to problems regarding the action of a moving load, since the moving load causes a continuous change not only in the scale, but also in the form of the bending. Therefore, the scheme shown in Figure 37.3 in this case must be regarded as problematical, although, as we have seen, a solution may be rapidly reached by using it.

Variant 4. Both the mass of the load and the mass of the beam are considered. This formulation of the problem, which is most complex, was encountered in certain studies carried out in the last century. However, the first attempt to solve this problem was extremely approximate, and was not based on valid assumptions. The first important results in this field were only obtained in the first thirteen years of this century, and were obtained by representing the solution in the form of a series. /322

Comparative calculations lead to the interesting conclusion: if the velocity of the load is so great that the static consideration (variant 2) cannot be assumed, then, as a rule, the influence of inertia of the construction and inertia of the load is of the same order of magnitude (if the load does not have a spring; otherwise, the inertia of the load plays an unimportant role).

The latter conclusion was reached by Yu.M. Mayzel' in his study, "Magnitude of the Dynamic Coefficient for Beams Under the Influence of a Moving Load" (see Nauchnyye trudy Dnepropetrovksogo metallurgicheskogo instituta, No. 34, 1958).

For greater details about the history of this problem, see the article by Ya.G. Panovko "Historical Sketch of the Development of the Theory of the Dynamic Action of a Moving Load" (Trudy Leningradskoy Krasnoznamennoy voyenno-vozdushnoy inzhenernoy akademii, No. 17, 1948).

The classical work of A.N. Krylov "On the Forced Oscillations of Smooth Bars" was published in 1905 (Mathematische Annalen, Vol. 61, 1905).

The results of A.N. Krylov have been reproduced in the majority of courses on the theory of oscillations and the dynamics of structures.

An effective method for simultaneously calculating the mass of a moving load and the mass of a structure was published in the work: Schallenkamp, A. "Oscillations of Supporting Beams in the Case of Live Loads" (Ingenieur-Archiv, Vol. 8, 1937).

§ 38. Bresse Error

In the problem concerning the action of a moving load, the trajectory of motion of the load and the curve for the bent axis of the beam are of course completely different curves. Confusing these different curves nas often been the source of errors. We shall discuss them below.

In 1859 Bresse published the solution given below for the problem for the motion of a point load along a doubly-supported weightless beam (see § 37 in the present book; second variant). The reasoning of Bresse can be reduced to the following (see Figure 37.1). For the moment of time $t = \frac{1}{2v}$ /323 (v — load velocity, l — span), when the load is located in the middle of the beam, Bresse writes the expression for the bending moment in the middle of the span in the form

$$M = \frac{Pl}{4} + \frac{Pl}{4g} \cdot \frac{v^2}{Q} \tag{38.1}$$

(P — weight of the load, g — acceleration of gravity). The first term on the right-hand side indicates the influence of the load weight, and the second — the influence of its force of inertia. In addition, Bresse writes

$$M = \frac{EJ}{Q} \tag{38.2}$$

and, solving the system of two equations with the unknowns M and q, we obtain

$$M = \frac{Pl}{4 - \frac{Plv^2}{EJg}}.$$

This solution indicates the unusual influence of velocity on the bending moments, and in particular makss it possible to find the critical velocity

$$v_{cr} = \sqrt{\frac{4EJ}{Pl}}, \tag{38.3}$$

at which the bending moments and the deflection strive to infinity.

This is an amazingly simple solution; however, it is incorrect due to the error which Bresse made. Possibly, the reader may have already noted it.

We have in mind the similar meaning of the symbols ρ in equations (38.1) and (38.2). One and the same letter in these equations designates completely different quantities. In the first equation, according to the notation, ρ is the radius of curvature of the trajectory of the load when it is in the middle of the beam. In the second equation, ρ is the radius of curvature of the beam axis at the same moment of time.

To explain the great difference between these terms, let us examine Figure 38.1, which shows the bent axis of the beam at different moments of time. The corresponding positions of the moving load (points 1, 2, 3, 4) are /324 shown here. The dashed line shows the trajectory of the load (for purposes of clarity, the states of the beam pertaining to the motion of the load only along its left half are given). We assume that the bent axis 4 corresponds to the moment that the load passes through the middle. The quantity ρ in formula (38.2) represents the radius of curvature of the bent axis (for $z = l/2$), since the quantity ρ in formula (38.1) represents the radius of curvature of the trajectory (also for $z = l/2$).

Thus, Bresse made two different quantities the same. It may be seen in Figure 38.1 that two curves — the trajectory and the bent axis — are completely different. These curves are different for the static formulation of the problem. Let us determine this difference, assuming that the process has no inertia. Utilizing the elementary methods of resistance of materials, we find the expression for the curvature of the bent axis of the beam

Fig. 38.1. Form of a bent beam with different positions of the load (solid lines) and load trajectory of motion (dashed curve).

($0 \leq z \leq l/2$), when the load is in the middle of the beam (i.e., $z = l/2$):

$$\frac{1}{\rho_1} = \frac{Pl}{4EJ}. \qquad (38.4)$$

It is a little more complex to find the curvature of the load trajectory. For the case when the load P is located at the distance a from the left support, the equation of the bent beam axis at the section from 0 to a has the form

$$y = -\frac{Pz(l-a)(2al-a^2-z^2)}{6EJl}.$$

If we set $a = z$, we obtain the equation describing the beam deflected by the load P:

$$y = -\frac{Pz^3(l-z)^3}{3EJl}, \qquad (38.5)$$

i.e., the equation for the load trajectory.

Differentiating (38.5) twice with respect to z and assuming $l/\rho \approx y''$, /325 we obtain the following expression for the curvature of the load trajectory:

$$\text{For} \qquad \frac{1}{\rho} = -\frac{P}{3EJl}(2l^3 - 12lz + 12z^2). \qquad (38.6)$$

At the moment when $z = 1/2$, we have

$$\frac{1}{\rho} = \frac{Pl}{3EJ}. \qquad (38.7)$$

Thus, the curvatures of two different curves, which are incorrectly made the same, differ by 1.33 times in the case $x = 1/2$. This estimate pertains to the purely static problem, and only gives a general representation of the possible magnitude of the error.

It is interesting that this long established error has had a setback. In one of the handbooks on theoretical mechanics, the following problem is presented:

"A steam locomotive with the weight P = 180 tons passes along a bridge at the velocity v = 72 km/hr. At the moment when the locomotive is located in

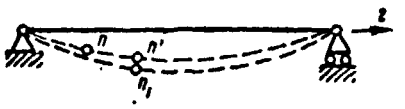

Fig. 38.2. Sketch of Renaudot article.

the middle of the bridge, the deflection of the bridge equals $h = 0.1$ m. Let us determine the extra pressure on the bridge at this moment, assuming that the bridge may be regarded as a single-span beam with excess mass, constant cross section, and a length of $l = 100$ m, with hinge supported edges. We shall disregard the dimensions of the locomotive".

Further on, the answer is given:

$$\frac{12Phv^2}{gl^2} = 0{,}88 \text{ ton}.$$

Based on the conditions, this is the problem of Willis (see § 37), reduced to a complex differential equation (37.3). It is astonishing that this problem is included in a handbook for students.

However, the writer evidently assumed that the simple, but erroneous solution of Bresse was correct, which was discussed above. This is how this solution appeared in this case. If the concentrated force N is applied at the middle of the span of a doubly-supported beam, the curvature of the bent /326 axis of the latter is determined by the expression

$$\frac{1}{\varrho} = \frac{Nl}{4EJ}, \tag{38.8}$$

and the deflection in the middle of the span is given by the expression

$$h = \frac{Nl^3}{48EJ}. \tag{38.9}$$

With respect to the problem being discussed, N designates the total force of the load, i.e., the sum of the weight P and the centrifugal force

$$N = P + \frac{mv^2}{\varrho}. \tag{38.10}$$

We may find the curvature from equations (38.8) and (38.9)

$$\frac{1}{\varrho} = \frac{12h}{l^2}. \tag{38.11}$$

It thus follows that the desired additional force equal to the centrifugal force is

$$\frac{mv^2}{\rho} = \frac{P}{g} \cdot v^2 \cdot \frac{12h}{l^2} = 0{,}88 \text{ ton}. \tag{38.12}$$

The error in this solution lies in the fact that expression (38.11) does not determine the curvature of the load trajectory, which is needed for substitution in (38.10), but rather the curvature of the bent beam axis.

In the new edition of this same handbook, the following statement was made after the text: "In determining the trajectory curvature, we assume a static form of the elastic line of the beam". Careful researchers even at the time of Bresse apparently discovered the difference between the two curves. Figure 38.2 reproduces a drawing from an article published in 1861 by the French engineer Renaudot. He accompanied this drawing with the following explanations.

Let us assume that at the time t a load is located at the point n. In the time interval dt, this load moves to the point n', if the curved axis of the beam does not change. In the segment of time dt the curved axis of the /327
beam changes its position, and the load is at the point n_1. The difference is clearly apparent here between the element nn' of the bent beam axis and the element nn_1 of the load trajectory.

The solution of Bresse is given in the book: "Cours de Mecanique Appliquée", 1859, Paris, Vol. 1, Chapt. VI. The problem of a steam locomotive is given in the handbook by I.V. Meshcherskiy (problem No. 666). Its solution which repeats the error of Bresse is given by Neiber in the book: "Lösungen zur Aufgabensammlung Mestscherski" (Solution to the Meshcherskiy Problem) (VEB Deutscher Verlag der Wissenschaften, Berlin, 1961). The article by Renaudot was published two years after the book by Bresse was published (see the "Annales des Ponts et Chaussées", 1861, No. 1, pp. 145 - 204.

§ 39. A Travelling Bending Wave

In the general formulation of the problem regarding the action of a moving load on elastic systems, it is necessary to take into account the mass both of the load and of the structure itself. If we disregard any of these quantities, then the solution is more or less approximate. The first three variants in section § 37 are an example of this. However, we may point out two particular problems, which are in a certain sense an exception. In one of them the mass of the moving load plays no role, and in the second one — the mass of the structure itself. This section is devoted to the first problem. The second problem is examined in § 40.

Let us assume a load with the weight P moves uniformly at the velocity v along an infinite beam lying on a solid, uniform elastic base (Figure 39.1, a).

One unusual feature of this problem is the possibility of a stationary regime of motion, in which deflection under a load remains constant, and the load moves along the horizontal. The picture of the beam axis bending will not change, but will move uniformly with the velocity of the load and will seem to accompany the load (Figure 39.1, b). Therefore, for the observer /328 the beam bending will always appear to be the same. This makes it possible to call this phenomenon a traveling bending wave(*).

Since the vertical coordinate of the load is unchanged, the vertical acceleration of the load equals zero, and the load pressure on the beam equals the weight P. This is the unusual feature of the problem under consideration.

We shall assume that the base of the beam is linearly deformable and follows the Winkler hypothesis:

$$r = -ky, \tag{39.1}$$

(*) We could expand the problem and also study beam oscillations around this stationary regime. We shall not do this.

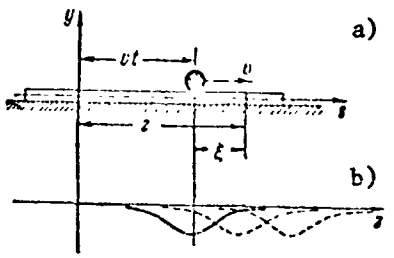

Fig. 39.1. Action of a moving load P on an infinite beam lying on a solid elastic base.

where r is the reaction rate of the base, y — deflection, k — coefficient of proportionality characterizing the rigidity of the base and called the carrier coefficient. It is well known that this model has faults, and has been greatly criticized in problems of statics of beams on an elastic base. Nevertheless, we shall use this model as well as the schematization route, assuming that the elastic base has no properties of inertia or damping. Thus, elasticity remains a single physical property, which our model of an elastic base will have.

Let us assume z is the abscissa of the beam cross section, determined from a certain fixed origin, t — time. Then the differential equation of the beam bending may be written in the form

$$EJ\frac{\partial^4 y}{\partial z^4} = -m\frac{\partial^2 y}{\partial t^2} - ky. \tag{39.2}$$

The right-hand side represents the load strength at the point z at the moment of time t, and consists of two terms: the inertia load (m — mass per unit length of the beam) and the reaction of the elastic base. We should note that the differential equation of bending has the same form for all problems of dynamics of beams on an elastic base (schematicized as shown above), if there are no distributive perturbing forces [if such a load is given, for example, in the form q(z,t), it must be introduced into the right-hand side of the equation]. /329

Let us rewrite equation (39.2) in the form

$$\frac{\partial^4 y}{\partial z^4} + 2a\frac{\partial^2 y}{\partial t^2} + b^2 y = 0, \tag{39.3}$$

where

$$2a = \frac{m}{EJ}, \quad b^2 = \frac{k}{EJ}. \tag{39.4}$$

We shall expand the solution of this equation in the form

$$y = f(z - vt). \tag{39.5}$$

Here the argument z — vt represents the abscissa of the beam cross section calculated from the moving origin connected with the load.

Our problem is to determine the form of the newly introduced function f(z — vt).

If we use primes to designate differentiation of this function with respect to its argument z — vt, then the derivatives of the function y which we need may be written in the form

$$\frac{\partial^4 y}{\partial z^4} = f^{IV}(z - vt); \quad \frac{\partial^2 y}{\partial t^2} = v^2 f''(z - vt). \tag{39.6}$$

The partial differential equation (39.3) changes into the following ordinary differential equation

$$f^{IV} + 2av^2 f'' + b^2 f = 0. \tag{39.7}$$

The possibility of changing to a simpler equation follows from the nature of our problem. For an observer connected with the load, as we saw above, the bending curve does not change in time. It may be stated that equation (39.7) represents the differential equation of a traveling wave (for a moving observer z — vt is the abscissa of the cross section). The linear differential equation (39.7) has constant coefficients(*), and we — not wishing to dwell on the details of its simple solution — will give the final result:

$$f = e^{-\alpha\xi}(C_1 \sin \beta\xi + C_2 \cos \beta\xi) + e^{\alpha\xi}(C_3 \sin \beta\xi + C_4 \cos \beta\xi), \tag{39.8}$$ /330

where

$$\xi = z - vt. \tag{39.9}$$

Here the quantities α and β are determined by the coefficients of the equation (39.7) using the formulas:

$$\alpha = \sqrt{\frac{b - av^2}{2}}, \quad \beta = \sqrt{\frac{b + av^2}{2}}. \tag{39.10}$$

(*)With a variable velocity v, it is in general impossible to use this equation, since the stationary regime assumed when it was formulated is impossible.

We shall assume that the solution (39.8) pertains to that part of the traveling wave which is located ahead of the moving load (i.e., for $\xi > 0$). For another part of the wave (for $\xi < 0$), the equation of the bent axis has the same form:

$$f_1 = e^{-\alpha\xi}(D_1 \sin \beta\xi + D_2 \cos \beta\xi) + \\ + e^{\alpha\xi}(D_3 \sin \beta\xi + D_4 \cos \beta\xi), \tag{39.11}$$

but with different values of the constants.

For a complete solution of the problem, it is necessary to find the eight constants C_i and D_i in expressions (39.8) and (39.11). For this purpose, we must use the following conditions:

At infinity:

$$\left.\begin{aligned} f &= 0 \quad \text{for} \quad \xi = \infty, \\ f_1 &= 0 \quad \text{for} \quad \xi = -\infty; \end{aligned}\right\} \tag{39.12}$$

Under a load:

$$\left.\begin{aligned} f(0) &= f_1(0), \\ f'(0) &= f_1'(0), \\ f''(0) &= f_1''(0), \\ f_1'''(0) - f'''(0) &= \frac{P}{EJ}. \end{aligned}\right\} \tag{39.13}$$

We find four constants from condition (39.12)

$$D_1 = D_3 = C_3 = C_4 = 0.$$

To determine the remaining constants, we use the condition (39.13). In this way we obtain

$$C_1 = -D_2 = -\frac{P}{2EJ\beta(\alpha^2 + \beta^2)}, \quad C_2 = D_4 = -\frac{P}{2EJ\alpha(\alpha^2 + \beta^2)}.$$

Thus, the traveling wave has an absolutely symmetrical form, and to analyze the results obtained it is sufficient to study, for example, part of the wave in the case $\xi \geq 0$: /331

$$f = -\frac{Pe^{-\alpha\xi}}{2EJ(\alpha^2+\beta^2)\alpha\beta}(\alpha\sin\beta\xi + \beta\cos\beta\xi). \tag{39.14}$$

The deflection under load is of the greatest interest, i.e., when $\xi = 0$:

$$f(0) = -\frac{P}{2EJ_2(\alpha^2+\beta^2)}. \tag{39.15}$$

To clarify the effect of the velocity v on the quantity f() f(0), we substitute the expression for the parameters α and β given in formulas (39.10). We then find

$$f(0) = -\frac{P}{EJb\sqrt{2(b-av^2)}}. \tag{39.16}$$

In particular, when v = 0, i.e., in the case of a fixed load, we obtain a specific result for the deflection f_{st} under a force applied to an infinitely long beam on an elastic base. At the velocity v > 0, the deflection under the load will exceed the quantity f_{st}. The ratio $\mu = f:f_{st}$ may be called the dynamic coefficient. With allowance for formulas (39.4), it equals

$$\mu = \sqrt{\frac{1}{1-\frac{mv^2}{2\sqrt{kEJ}}}}. \tag{39.17}$$

The influence of all the parameters in the system may be seen directly from this formula. With an increase in the velocity v, the dynamic coefficient increases and at the velocity

$$v = \sqrt{\frac{2\sqrt{kEJ}}{m}} \tag{39.18}$$

strives to infinity. The value of the velocity which is found is critical. Figure 39.2 shows a graph of the change in the dynamic coefficient.

For values of v less than the critical value, the traveling wave has the form of a sinusoid, but with decreasing amplitudes. Damping of the amplitudes is determined by the factor $e^{-\alpha\xi}$ in equation (39.14). When the velocity

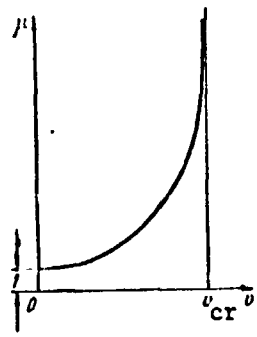

Fig. 39.2. Dependence of the dynamic coefficient on the load velocity v.

approaches its critical value, according to the first formula (39.10) the parameter α vanishes, and equals zero at the critical velocity. Corresponding to this, the curve of (39.14) indicates constantly decreasing damping, and at the critical velocity becomes a pure sinusoid. /332

We must refer to our results with a certain caution, because we have ignored the inertial and damping properties of the base. At the same time, these properties will be more noticeable, the faster is the motion of the load and the more dynamic is the process as a whole. For this reason, it would be incorrect to investigate the region of velocities close to the critical region using these assumptions. Nevertheless, the solution obtained qualitatively reflects correctly the tendency of the deflection to increase with an increase in the load velocity.

The author of this solution is V.L. Biderman (see the book: S.D. Ponomarev, V.L. Biderman, K.K. Likharev, V.M. Makushin, V.N. Feodos'yev "Osnovy sovremennykh metodov rascheta na prochnost' v mashinostroyenii (Bases of Contemporary Methods of Designing for Strength in Machine Construction), Mashgiz, Moscow, 1952, pp. 198 - 202.

§ 40. Action of an Infinite Strip of a Moving Load

In the preceding section we discussed the particular case of the action of a moving load, in which the load mass is of no importance. Here we shall discuss another particular case, in which, however, the mass of the elastic structure, along which the load moves, does not play a role.

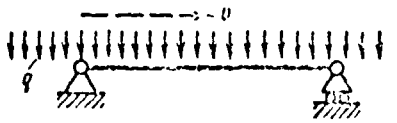

Fig. 40.1. Analysis of the action of an infinite strip of a uniformly distributed moving load.

In contrast to the problems examined above, here we are discussing the motion of a single load, analyzing the action of an infinite strip of a uniformly distributed moving load (Figure 40.1). From the very beginning, it is important to note that there is a quasi-static regime /333 in this system, to which the beam bending curve, which does not change in time, corresponds. At the same time, this curve is also the trajectory of motion of elements of the moving load. Due to the curvature of the trajectory, the pressure of any element of the moving load does not equal its weight, but is determined by the sum of the weight qdz and the force of inertia $\frac{q}{g}\frac{d^2y}{dt^2}dz$ (q — the weight of the moving load, y — beam deflection, i.e., the ordinate of the trajectory of motion for a load element, $\frac{d^2y}{dt^2}$ — vertical acceleration of a load element). Thus, the load strength on the beam is

$$q+p-\frac{q}{g}\frac{d^2y}{dt^2}=q+p-\frac{q}{g}\cdot\frac{d^2y}{dz^2}v^2. \tag{40.1}$$

Here p is the weight of the beam, v — velocity of motion. According to this, the differential equation for a bent beam axis has the form

$$EJ\frac{d^4y}{dz^4}=q+p-\frac{q}{g}\cdot\frac{d^2y}{dz^2}v^2. \tag{40.2}$$

If we assume the origin is at the left end of the beam, the solution of the differential equation (40.2) may be written in the form

$$y=\frac{(p+q)l^2}{4EJu^2}\left\{\frac{1}{2}(z^2-lz)+\frac{l^2}{u^2}\left[\frac{\cos\left(\frac{2z}{l}-1\right)u}{\cos u}-1\right]\right\}, \tag{40.3}$$

where we set

$$u=\frac{vl}{2}\sqrt{\frac{q}{gEJ}}. \tag{40.4}$$

In particular, the greatest beam deflection (in the middle of the span) equals

$$y\left(\frac{l}{2}\right)=\frac{(p+q)l^4}{32EJu^2}\left[\frac{8}{u^2}\left(\frac{1}{\cos u}-1\right)-1\right]. \tag{40.5}$$

As we can see, it increases with an increase in the velocity v, and becomes infinite for $u = \frac{\pi}{2}$. Thus, the velocity /334

$$v = \frac{\pi}{l}\sqrt{\frac{EJ}{q}} \tag{40.6}$$

is critical. It is useful to note that this formula coincides with (4.49) found in § 4 in the study of pipeline stability. In this case, the rigidity is the moving load.

In their general outlines, these are the basic properties of a quasi-static regime, which is characterized by the curve (which is unchanged in time) of the beam bent axis. It is of definite interest to study the properties of the process of free oscillations, which the system will perform near the quasi-static regime, if it is disturbed by any disturbance.

With these oscillations, the bent axis will not remain unchanged in time, and its equation represents the function of two variables

$$y = y(z, t). \tag{40.7}$$

The forces of inertia of the beam elements appear, and the forces of inertia of a moving load will be described in a more complex manner than in the case of a quasi-static regime.

The strength of the beam force of inertia is determined by the partial derivative

$$r_p = -\frac{p}{g}\frac{\partial^2 y}{\partial t^2}. \tag{40.8}$$

In order to determine the forces of inertia of a moving load, it is necessary to assume that the three-dimensional coordinate z of a load element depends on the time

$$z = vt. \tag{40.9}$$

Therefore, the projection of the velocity of a moving load element on the axis y equals the total derivative

$$\frac{dy}{dt} = \frac{\partial y}{\partial t} + \frac{\partial y}{\partial z}\cdot\frac{dz}{dt} = \frac{\partial y}{\partial t} + \frac{\partial y}{\partial z}v. \tag{40.10}$$

In a similar manner, the vertical acceleration of the moving load element must be written in the form /335

$$\frac{d^2y}{dt^2}=\frac{d}{dt}\left(\frac{\partial y}{\partial t}\right)+\frac{d}{dt}\left(\frac{\partial y}{\partial z}v\right). \tag{40.11}$$

The first component yields

$$\frac{d}{dt}\left(\frac{\partial y}{\partial t}\right)=\frac{\partial^2 y}{\partial t^2}+\frac{\partial^2 y}{\partial t\,\partial z}\frac{dz}{dt}=\frac{\partial^2 y}{\partial t^2}+\frac{\partial^2 y}{\partial t\,\partial z}v, \tag{40.12}$$

and the second component yields

$$\frac{d}{dt}\left(\frac{\partial y}{\partial z}v\right)=\frac{\partial^2 y}{\partial z\,\partial t}v+\frac{\partial^2 y}{\partial z^2}\frac{dz}{dt}v=\frac{\partial^2 y}{\partial z\,\partial t}v+\frac{\partial^2 y}{\partial z^2}v^2. \tag{40.13}$$

Thus, the desired acceleration equals

$$\frac{d^2y}{dt^2}=\frac{\partial^2 y}{\partial t^2}+2v\frac{\partial^2 y}{\partial z\,\partial t}+\frac{\partial^2 y}{\partial z^2}v^2, \tag{40.14}$$

and consequently,

$$r_q=-\frac{q}{g}\left(\frac{\partial^2 y}{\partial t^2}+2v\frac{\partial^2 y}{\partial z\,\partial t}+\frac{\partial^2 y}{\partial z^2}v^2\right). \tag{40.15}$$

Equation (40.2) now assumes the form

$$\frac{\partial^4 y}{\partial z^4}+a\frac{\partial^2 y}{\partial t^2}+b\frac{\partial^2 y}{\partial z\,\partial t}+c\frac{\partial^2 y}{\partial z^2}=0, \tag{40.16}$$

where

$$a=\frac{p+q}{gEJ},\quad b=\frac{2qv}{gEJ},\quad c=\frac{qv^2}{gEJ}. \tag{40.17}$$

Frequently, the third component in (40.16) plays a secondary role, and in one case even precisely equals zero(*). We shall not perform a complete investigation, and shall confine ourselves to the solution of the simplified equation

$$\frac{\partial^4 y}{\partial z^4}+a\frac{\partial^2 y}{\partial t^2}+c\frac{\partial^2 y}{\partial z^2}=0. \tag{40.18}$$

(*) This case pertains to the problem (which is similar to this subject) of the counter motion of two bands of a load with the velocities v and — v along a doubly-supported beam (the motion of two trains along a bridge in the opposite directions).

The function

$$y = A \sin \frac{n\pi z}{l} \sin pt, \tag{40.19}$$

satisfies this equation and the boundary conditions of a hinged-support. In this equation p is the circular oscillation velocity. Substituting (40.19) in (40.18), we obtain /336

$$\left(\frac{n\pi}{l}\right)^4 - ap^2 - c\left(\frac{n\pi}{l}\right)^2 = 0. \tag{40.20}$$

We thus find the eigenfrequency of the system

$$p = \sqrt{\frac{\left(\frac{n\pi}{l}\right)^4 - c\left(\frac{n\pi}{l}\right)^2}{a}}. \tag{40.21}$$

It is important to note that the eigenfrequency depends on the load velocity.

The critical state is assumed to be that state when the eigenfrequency vanishes (and the period — strives to infinity). This state is determined by the condition

$$\left(\frac{n\pi}{l}\right)^4 - c\left(\frac{n\pi}{l}\right)^2 = 0. \tag{40.22}$$

We thus have

$$c = \frac{qv^2}{gEJ} = \left(\frac{n\pi}{l}\right)^2, \tag{40.23}$$

i.e., the critical velocity of the liquid flow is

$$v_{cr} = \frac{n\pi}{l}\sqrt{\frac{gEJ}{q}} \tag{40.24}$$

and its smallest value (in the case n = 1) corresponds with the result (40.6).

The solution of the problem for the quasi-stationary regime was given by Bresse in his book on page 327.

The book by H. Ashley and G. Havilland "Bending Oscillations of a Tube Containing a Flowing Liquid" (Journal of Applied Mechanics, 1950, No. 3) contained errors when the basic differential equation of the problem was formulated. Concerning this matter, see the article by V.I. Feodoz'yev

"Oscillations and Stability of a Tube When a Liquid Flows Through It" (Inzh. Sb., Vol. X, Izdatel'stvo AN SSSR, 1951). A more complete analysis of the problem is given in the articles by O.N. Mukhin "Dynamic Stability Criteria of a Pipeline Containing a Flowing Liquid" (Izvestiya AN SSSR, Mekhanika, No. 3, 1965) and A.A. Movchan, "One Problem of Tube Stability with a Liquid Flowing Through It" (PMM, Vol. 29, No. 4, 1965, pp. 760 - 762).

See the book by I.I. Gol'denblat "Sovremennyye problemy kolebaniy i ustoychivosti inzhenernykh sooruzheniy" (Contemporary Problems of Oscillations and Stability of Technical Structures) (Gosstroyizdat, Moscow, 1947).

CHAPTER VIII
AEROELASTIC OSCILLATIONS

We should like to remind the reader that we have already discussed the problems of aeroelasticity in § 3 in Chapter 1, where we examined the static stability loss under the action of aerodynamic forces. Here we shall discuss the specific features of the dynamic problems of aeroelasticity theory. /337

§ 41. Dynamic Problems of Aeroelasticity Theory

In a dynamic formulation of the problems of aeroelasticity theory, forces of inertia must be included as well as the aeroelastic and elastic forces. The development of the deformation process in time must also be studied. This study reveals the important features of aeroelastic phenomena, which cannot be determined with a purely static formulation. In particular, we wish to establish new possibilities of stability losses of elastic structures located in a gas flow. Most frequently, the dynamic stability loss occurs at velocities which are less than the critical velocities, calculated on the basis of static concepts. Therefore, the danger of the dynamic stability loss is particularly pressing.

The scheme shown in Figure 41.1 gives a graphic characterization of the different types of aeroelasticity problems.

At the apexes of the symbolic triangle, the letters A, Y and I designate all three categories of forces participating in the aeroelasticity phenomena. Four circles corresponding to definite types of problems are connected by dashed lines with the apexes of the triangle.

If we consider only the forces of elasticity (Y) and forces of inertia (I) we arrive at the problem of free oscillations of a mechanical system (point M in Figure 41.1).

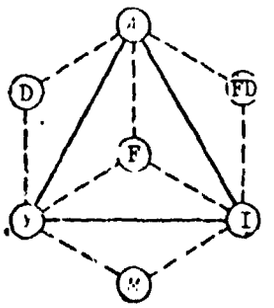

Fig. 41.1. Collar force triangle. The upper triangle shows 3 forms of forces considered in problems of aeroelasticity (A — aerodynamic forces, Y — elastic forces, I — inertia forces).

In solving the problem of divergence, /338 we only considered the aerodynamic (A) and elastic forces (Y). This formulation corresponds to the circle with the letter D in Figure 41.1.

The problem of the flight dynamics of a rigid aircraft is designated in Figure 41.1 by the letters F, D (these problems are not considered in our book, which is devoted to deformable systems).

In each of these three cases, only two categories of forces are considered. The most complete formulation of the aeroelasticity problems simultaneously considers all three categories of forces (the letter F in Figure 41.1).(*) The letter F was not selected at random. Flutter must be regarded as one of the most important and dangerous aeroelastic phenomena. Following are the words which one of the most important specialists in the field of aircraft flight tests wrote about the development of aviation in the last thirty years of our century:

"With the appearance of new high speed aircraft in aviation, there is hardly any country in the world which has not encountered a wave of unexplained catastrophes.

(*) This formulation of a set of mechanical problems by means of a single scheme was proposed by Collar in 1930. We have only reproduced here part of the Collar scheme, and have not considered certain other phenomena which also are well illustrated by means of the Collar triangle. It must be noted that there are no perturbing forces in the Collar scheme, i.e., the forces which change in time in a given manner. For this reason, the Collar scheme does not include problems of forced oscillations of mechanical systems. Allowance for perturbing forces would require a change from a triangle to a rectangle.

"Accidental eye witnesses who observed these catastrophes from the earth in almost every case saw the same picture: the aircraft flew absolutely normally, with no indications of the least danger, and then suddenly some unknown force, like an explosion, rocked the aircraft — and mutilated fragments fell to the /339 earth: the wing, the fuselage, the tail . . .

"All of the eyewitnesses, who did not talk with each other, used the same expression — explosion, since there were no other possible reasons for such a lightning-like and complete destruction. However, an examination of the fragments did not substantiate this interpretation: there were no traces of an explosion — soot or burns.

"As a rule, it was not possible to use the most reliable source of information — the report of the crew on the fatal aircraft. Those few fliers, whose number may be counted on the fingers of one hand, who were able to escape from the fuselage and use a parachute, had nothing of great importance to add to the stories of the eyewitnesses on earth. The event was very unexpected and happened rapidly: a few seconds before the catastrophe there was nothing to indicate it, and then all at once — a shock, crackling, a roar, and the aircraft disintegrated into pieces!

"This new phenomenon has been given the name of "flutter" (from the English flutter — trembling), but, if I am not mistaken, as Moller wrote, it does not make it any easier for the patient to know what his sickness is called in Latin.

"One after another, alarming reports were circulated about the mysterious loss of French, English and American high speed aircraft.

"Nor have we escaped this bitter cup."

Thus, at first engineers and fliers did not recognize in this phenomenon a special form of oscillatory instability. Only after several extensive theoretical investigations, and also after real and model tests, was it established that flutter represents oscillations with rapidly increasing amplitudes.

If problems of the static, aeroelastic instability pertain to phenomena described by the theory of Euler (see Chapter 1), then flutter must pertain to the phenomena of stability loss by changing from rest to motion, i.e., to the phenomena which were discussed above in Chapters III and IV. However, the specific nature of the problems of dynamic aeroelasticity compel us to discuss the problems of flutter in a separate chapter.

The nature of the so-called "classical" flutter — dangerous oscillations /340 of an aircraft, which we discussed briefly above — is discussed in § 42. The subsequent section § 43 discusses the famous Tacoma catastrophe. Its analysis shows that engineering structures, particularly suspension bridges, also are subjected to flutter (in this case, the so-called "stall flutter" occurs, whose theory is far from complete).

There is one type of flutter to which the skins of aircraft are subjected — "panel flutter". We shall not discuss this phenomenon here.

The literature devoted to different types of flutter will be given at the end of each of the following sections. The citation given above was borrowed from the writings of the Soviet flier-inventor, Hero of the Soviet Union, M.L. Gallaya ("Novyy mir", No. 7, 1960, p. 113).

§ 42. "Classical" Flutter

To explain the nature of flutter, let us investigate the oscillations of an elastically fixed plate shown in Figure 42.1. In contrast to the scheme used in studying divergence (Figure 4.9), the plate has two degrees of freedom, and its position is characterized by the two coordinates — the angle of rotation φ and the vertical displacement y of the middle of the plate. It is assumed that the horizontal displacements are impossible. Both coordinates φ and y are functions of time

$$\varphi = \varphi(t), \quad y = y(t). \tag{42.1}$$

Our problem is to determine the form of these functions, and then to estimate the possibility of flutter. The rigidities of both springs c_1 and c_2 are

assumed to be different. We shall assume that the mass of the plate is uniformily distributed over its surface, and we shall use m to designate the mass corresponding to a unit area of the middle plate plane. /341

When the plate moves, a lifting force acts upon it

$$Y=\frac{dc_y}{d\alpha}\varphi\frac{\rho v^2}{2}bl, \tag{42.2}$$

which passes at the distance a from the right edge of the plate, and also — reactions of the elastic supports which are proportional to the displacements of the plate edges

$$\left.\begin{aligned} R_1&=-\left(y+\frac{b}{2}\varphi\right)c_1l,\\ R_2&=-\left(y-\frac{b}{2}\varphi\right)c_2l. \end{aligned}\right\} \tag{42.3}$$

Reducing this reaction to the plate center of gravity, we obtain the force

$$R=R_1+R_2=-(c_1+c_2)ly-\frac{b}{2}(c_1-c_2)l\varphi \tag{42.4}$$

and the moment

$$M=-\left(y+\frac{b}{2}\varphi\right)c_1l\frac{b}{2}+\left(y-\frac{b}{2}\varphi\right)c_2l\frac{b}{2}. \tag{42.5}$$

Let us write the differential equations of motion. One of them describes the displacement of the plate center of mass

$$Y+R=mbl\frac{d^2y}{dt^2} \tag{42.6}$$

(mbl — mass of the entire plate), and the other describes the rotation of the plate around the horizontal axis z passing through the center of gravity:

$$Y\left(a-\frac{b}{2}\right)+M=\frac{mb^2l}{12}\frac{d^2\varphi}{dt^2}. \tag{42.7}$$

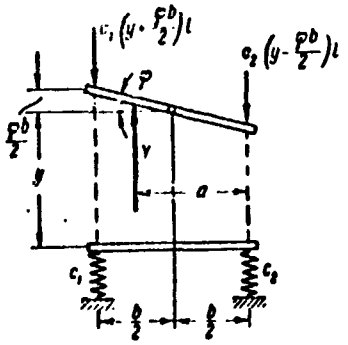

Fig. 42.1. Diagram of forces acting on an inclined plate.

Substituting the expressions (42.2), (42.4) and (42.5) for Y, R and M, we obtain the following system of

differential equations

$$\left.\begin{aligned}\frac{d^2y}{dt^2}+a_{11}y+a_{12}\varphi=0,\\ \frac{d^2\varphi}{dt^2}+a_{21}y+a_{22}\varphi=0,\end{aligned}\right\} \tag{42.8}$$

where /342

$$\left.\begin{aligned}a_{11}=\frac{c_1+c_2}{mb},\quad a_{21}=\frac{3(c_1+c_2)}{mb}+6\frac{dc_y}{da}\frac{\varrho v^2}{2}\cdot\frac{b-2a}{mb^2},\\ a_{12}=\frac{c_1-c_2}{2m}-\frac{dc_y}{da}\cdot\frac{\varrho v^2}{2}\cdot\frac{1}{m},\quad a_{22}=\frac{6(c_1-c_2)}{mb^2}.\end{aligned}\right\} \tag{42.9}$$

We shall first determine under what conditions <u>divergence</u> of the plate is possible. For this, we must assume that y and φ are constants. Then their second derivatives become equal to zero, and equations (42.8) assume the form

$$\left.\begin{aligned}a_{11}y+a_{12}\varphi=0,\\ a_{21}y+a_{22}\varphi=0.\end{aligned}\right\} \tag{42.10}$$

The condition of non-zero solutions of the system of equations (42.10) has the form

$$\begin{vmatrix}a_{11} & a_{12}\\ a_{21} & a_{22}\end{vmatrix}=a_{11}a_{22}-a_{12}a_{21}=0. \tag{42.11}$$

Substituting the expressions (42.9) for the coefficients, we arrive at the following formula which determines the critical divergence velocity

$$v_{cr}=\sqrt{\frac{2c_1c_2b}{\varrho\frac{dc_y}{da}[c_1(a-b)+c_2a]}}. \tag{42.12}$$

With infinite rigidity of the right support, this formula changes into the formula (4.23) obtained in Chapter 1. For $c_2 \leq c_1\left(\frac{b}{a}-1\right)$ the divergence becomes impossible. For large values of c_2, the critical velocity is larger than is the case with formula (4.23). Consequently, [illegible]crease in the right support rigidity leads to a decrease in the danger c[illegible]vergence.

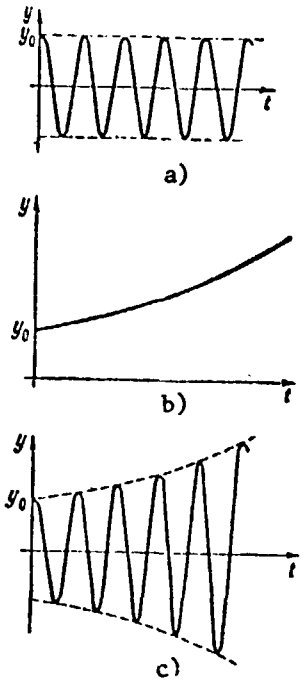

Fig. 42.2. Types of motion of a plate after initial deflection: a) harmonic oscillations (stability); b) aperiodic increase in deflection y (aperiodic instability — divergence); c) oscillations with increasing amplitudes (oscillatory instability — flutter).

Let us now study the possible motions of a plate, and we shall expand the solution of the homogeneous system of differential equations (42.8) in the form

$$y = Ae^{i\omega t}, \quad \varphi = Be^{i\omega t}, \tag{42.13}$$

i.e., we shall assume that both coordinates change cccording to one and the same law, and are constantly proportional to each other.

Below we obtain the expression for /343 ω^2, from which it can be seen that both the quantity ω and $-\omega$ satisfy the problem. Therefore, for the coordinate y the solution will have the form

$$y = A_1 e^{i\omega t} + A_2 e^{-i\omega t} \tag{42.14}$$

(in a similar manner — for the coordinate φ). If we substitute

$$A_1 = \frac{A_1' - A_2' i}{2}, \quad A_2 = \frac{A_1' + A_2' i}{2}, \tag{42.15}$$

i.e., we change to the new constants

$$A_1' = A_1 + A_2, \; A_2' = -(A_1 - A_2) i, \tag{42.16}$$

then expression (42.14) may be written as

$$y = A_1' \frac{e^{i\omega t} + e^{-i\omega t}}{2} + A_2' \frac{e^{i\omega t} - e^{-i\omega t}}{2i} = A_1' \cos \omega t + A_2' \sin \omega t. \tag{42.17}$$

Let us examine three possible cases.

1. If ω is a real umber, then expression (42.13) will represent the harmonic motion (Figure 42.2, a). In this case, the system state of equilibrium is apparently stable.

2. If ω is an imaginary number, for example, $\omega = i\beta$, then instead of (42.14) we obtain

$$y = A_1 e^{-\beta t} + A_2 e^{\beta t}. \tag{42.18}$$

This solution (see the second term) will indicate an infinite and monotonic increase in the deflections (Figure 42.2, b). In this case, the system state of equilibrium must be designated as unstable.

3. If ω is obtained as a complex number, for example, $\omega = \alpha + i\beta$ then /344
the solution will also be $\omega = -\alpha - i\beta$. Correspondingly, instead of (42.13) we obtain

$$y = A_1 e^{i\alpha t} \cdot e^{-\beta t} + A_2 e^{-i\alpha t} \cdot e^{\beta t}. \tag{42.19}$$

Let us turn our attention to the factor $e^{-\beta t}$ and $e^{\beta t}$. Whatever the term β may be (positive or negative), one of the components will increase infinitely. Due to the factors $e^{i\alpha t}$ and $e^{-i\alpha t}$, the motion will be oscillatory in nature, but with an infinitely increasing amplitude (Figure 42.2, c). This state is <u>flutter</u>.

It follows from the above that it is necessary that ω be a real number for stability of a system. In turn, this means that ω^2 must be a number which is first <u>real</u>, and secondly <u>positive</u>.

We shall now turn to the system of equations (42.8), substituting (42.13) in it. We obtain

$$\begin{aligned} A(-\omega^2 + a_{11}) + Ba_{12} &= 0, \\ Aa_{21} + B(-\omega^2 + a_{22}) &= 0. \end{aligned} \tag{42.20}$$

The determinant of this system must equal zero.

$$\begin{vmatrix} -\omega^2 + a_{11} & a_{12} \\ a_{21} & -\omega^2 + a_{22} \end{vmatrix} = 0, \tag{42.21}$$

i.e.,

$$\omega^4 - \omega^2(a_{11} + a_{22}) + (a_{11}a_{22} - a_{12}a_{21}) = 0. \tag{42.22}$$

We thus obtain

$$\omega^2 = \frac{a_{11} + a_{22}}{2} \pm \sqrt{\left(\frac{a_{11} + a_{22}}{2}\right)^2 - (a_{11}a_{22} - a_{12}a_{21})}. \tag{42.23}$$

The condition of ω^2 being real assumes the form

$$a_{11}a_{22} - a_{12}a_{21} \leqslant \left(\frac{a_{11} + a_{22}}{2}\right)^2, \tag{42.24}$$

and the condition for ω^2 being positive is

$$a_{11}a_{22} - a_{12}a_{21} \geqslant 0. \tag{42.25}$$

Thus, it is necessary that the difference $a_{11}a_{22} - a_{12}a_{21}$ occur in the interval $0, \left(\frac{a_{11} + a_{22}}{2}\right)^2$ in order that the mechanical system under consideration be stable. It is apparent that the boundaries of this interval correspond to the critical states, i.e., the equation /345

$$a_{11}a_{22} - a_{12}a_{21} = \left(\frac{a_{11} + a_{22}}{2}\right)^2; \quad a_{11}a_{22} - a_{12}a_{21} = 0.$$

We discovered this equation when studying the possible divergence of a system, and obtained formula (42.12). If the equation $a_{11}a_{22} - a_{12}a_{21} = 0$ is satisfied, then according to (42.23) we have

$$\omega_1^2 = a_{11} + a_{22}; \quad \omega_2^2 = 0.$$

The instability is determined by the second root, to which the constant deflection of the system corresponds. If the velocity v is greater than the critical divergence velocity, then the difference $a_{11}a_{22} - a_{12}a_{21}$ becomes negative. Correspondingly, one of the values of ω^2 is obtained with a minus sign. Aperiodic motion, which is shown in Figure 42.2, b corresponds to this. For purposes of simplification, we shall assume in addition that $a = 0.5b$. As follows from formula (42.12), divergence is then only possible under the condition $c_1 < c_2$.

Let us now turn to the inequality (42.24), and write it in the form

$$(a_{11} - a_{22})^2 + 4a_{12}a_{21} > 0. \tag{42.26}$$

If $c_1 < c_2$, then this inequality is always satisfied (since the product $a_{12}a_{21}$ is positive). Consequently, if the rigidity of the left support

is less than the rigidity of the right support, the structure can be threatened only with aperiodic departure from the state of equilibrium (divergence). An oscillatory form of instability is impossible.

Let us now investigate the opposite case, when $c_1 > c_2$, and the rigidity of the left support exceeds the rigidity of the right support. Thus, the condition (42.25) is always satisfied (even for $v = 0$ and expecially for $v > 0$), and we must now examine only condition (42.24). Substituting in it the expression for the coefficients we obtain the critical velocity, i.e., the value of the velocity v at which the inequality (42.24) turns into the equation

$$v_{cr} = 2\sqrt{\frac{1}{3\rho\frac{dc_y}{d\alpha}}\cdot\frac{c_1^2 - c_1c_2 + c_2^2}{c_1 - c_2}}. \qquad (42.27)$$

When the velocity v equals this value, the sum, under the root in (42.23), /346
vanishes. For a small increase in the velocity above the value v_{cr}, this sum becomes negative, and ω^2 is a complex number. The motion acquires the character shown in Figure 42.2, c.

Thus, formula (42.27) determines the velocity at which flutter occurs.

Let us give some results. For any ratio of rigidities, one of the inequalities (42.24) and (42.25) is always satisfied, and the other may be violated, but only for a sufficiently large value of the flow velocity v.

Thus, if $c_1 < c_2$, for any values of v condition (42.24) is satisfied, and the critical velocity, indicating that divergence has set in, is determined from condition (42.25) (used in the form of the equation).

If $c_1 > c_2$, then — irrespective of the value of the velocity v — condition (42.25) is satisfied, and the critical state is established from an analysis of inequality (42.24). Thus, the flutter velocity is determined.

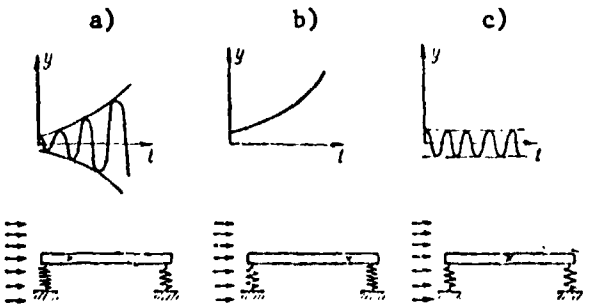

Fig. 42.3. Influence of the rigidity axis position on plate stability. The rigidity axis is designated by the x. It is assumed that the center of gravity is located in the middle of the span.

It thus follows that a structure of this type for a = 0.5b can lose stability only in the form of divergence, or in the form of flutter. The development of a certain danger depends on the location of the rigidity axis (we should recall that the geometric location of points having the same property as the vertical load applied at these points is the plate rigidity axis, and does not produce rotations of the plate).

The case when both rigidities are equal $c_1 = c_2$ is a particular case. Thus, according to (42.9), the coefficient a_{21}, expression (42.23) depends on the velocity v and gives two real positive roots

$$\omega_1^2 = a_{11}, \quad \omega_2^2 = a_{22}, \tag{42.28}$$

i.e., the system in general does not lose stability.

Figure 42.3 shows the conditions for the occurrence of different types of motion as a function of the position of the rigidity center.

It is advantageous to turn our attention to the conclusion indicated above that counter-flutter stability is absolutely established with a "rear" location of the rigidity axis, i.e., when the center of rigidity is farther /347 from the forward edge than is the center of gravity for the plate.

This conclusion is valid for real aircraft wings and ailerons, which are now always constructed so that the cross section centers of gravity are located ahead of the rigidity axis.

Several types of "classical" flutter of the lifting surface of aircraft are known, and one of the necessary conditions for the development of flutter is the existence of several degrees of freedom of the oscillatory system. A typical form of aircraft wing flutter is bending-torsional flutter. When studying the possibility of its development, it is necessary to consider both bending and torsion of the wing.

Figure 42.4 shows the displacements y and φ of an aircraft wing cross section, which are important when studying the bending-torsional flutter. If /348 we disregard all the degrees of freedom except one (for example, if we take into account only the wing twisting), it is not possible in general to detect oscillatory instability.

We must keep the fact in mind that the results obtained above cannot be regarded as quantitatively correct, even for such a simple system as an elastically supported plate. Aerodynamic loads in actuality depend not only on the angle of attack, as we have assumed, but also on the displacement velocity. In order to understand how this occurs, let us investigate, for example, the scheme shown in Figure 42.5, a. We shall assume that the plate moves in a translational manner perpendicularly to the flow at the velocity v_y. In this case, the aerodynamic forces will be the same as if the plate were fixed, and the air particles had a vertical velocity v_y in the upward direction (except for the basic horizontal velocity v_x) — see Figure 42.5, b.

The simultaneous existence of two velocities v_x and v_y is equivalent to the total velocity v which has the direction shown in Figure 42.5, c. Therefore, the effective angle of attack is the angle between the direction of the vector v and the plane of the plate which equals

$$\alpha = \alpha_0 + \frac{v_y}{v_x},$$

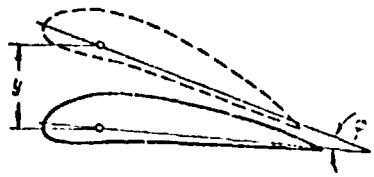

Fig. 42.4. Displacement of the wing cross section in the case of bending-torsional flutter.

where α_0 is the "apparent" angle of attack, i.e., the angle between the direction of the velocity v_x and the plane of the plate (if the velocity v_y is much less than the velocity v_x, then it is assumed that the small angle is replaced by its tangent). This must be assumed in problems of dynamic aeroelasticity. Along with the functions y and φ themselves and their second derivatives, their first derivatives are also included in the equations of motion.

On the other hand, in a precise solution we would also have to take into account the influence of the so-called apparent masses of air.

One of the first Soviet researchers on flutter was Ye.P. Grossman [see his work "Flatter" (Flutter), Trudy TsAGI, No. 284, 1937, as well as the book "Kurs vibratsiy chastey samoleta" (Course on Vibration of Aircraft Parts), Oborongiz, Moscow, 1940]. /349

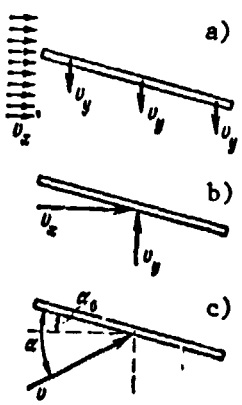

Fig. 42.5. Influence of velocity v_y on effective angle of attack.

In a simple formulation, the problem of flutter is discussed in the following book: T. Karmon and M. Biot "Mathematical Methods in Engineering" (Gostekhizdat, 1946, pp. 196 - 202); J. Rocard "Instability in Mechanics" (Foreign Literature Press, 1959, pp. 79 - 86). In the last book there is a more complete description of the theory of flutter, but it is better in the following books: Y.G. Fung "Introduction to the Theory of Aeroelasticity" (Fizmatgiz, 1959); R.L. Bisplinghoff. H. Ashley, R.L. Halfman "Aeroelasticity" (Foreign Literature Press, 1958).

§ 43. Tacoma Catastrophe; Separation Flutter

Not only aviation structures, but also engineering structures are subjected to flutter. This section describes the catastrophe of a bridge, which is famous in history — the collapse of the bridge at the narrows at Tacoma (USA) in 1940. It gives brief characteristics of the aeroelastic phenomena which occurred in the catastrophe. At the same time, we point out other important cases of aeroelastic oscillations of the same type.

Suspension bridges have several indisputable technical, economic, and aesthetic advantages as compared with other types of bridge construction. Many of them represent outstanding engineering structures, and the greatest spans have been covered by suspension bridges. However, it was recently noted that suspension bridges are very unreliable in the case of strong winds, and the history of bridge technology contains cases of the destruction of suspension bridges in strong winds. Although the theory of static design of bridges has been improved with the years and more and more daring designs are being made, the destruction of suspension bridges has inexorably been repeated.

In 1852 the bridge of Laroche-Bernare collapsed, which had a span of 196 m. The bridge was quickly restored, and again collapsed in 1871. Two years later, a bridge with a span of 336 m across the river Ogayo collapsed near the city of Wheeling. Following are the words of one eyewitness to this event: "For several minutes we watched the oscillations with alarm; they were similar to the tossing of a ship in a storm. Once the bridge rose almost to the height of the pylons, and then dropped. There was twisting along the entire span, and one half of the thoroughfare almost completely turned over. Then the enormous construction fell from the giddy height down to the river with a roar and crash". Subsequent great catastrophes occurred in 1864 and 1889 with suspension bridges over the Niagra River. The bridge spans were 320 m and 386 m, respectively. /350

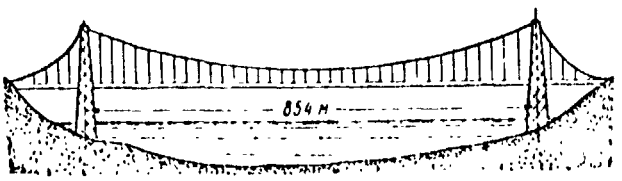

Fig. 43.1. Tacoma Bridge.

The facts concerning the catastrophes are not reliably known, with the exception of the fact that they occurred in a strong wind and were preceded by very strong oscillations. These accidents alarmed engineers, but it did not keep them from building new suspension bridges. They continued to build them, particularly in cases when it was necessary to go across very large spans.

In 1938 the famous bridge "Golden Gate" was opened in San Francisco — from that time until 1964 it held the record for length of span, 1280 m. In the summer of 1940, the construction was finished of the Tacoma Bridge, which was third in terms of the span (854 m). Since no great traffic was expected in this location, for purposes of economy the bridge was built very narrow (11.9 m), and the thoroughfare was designed only for two lanes of automobiles. The bed of the bridge was laid on two steel cables, with a diameter of 44 cm each, and a sag of 70.7 m (Figure 43.1).

Immediately after the bridge was constructed, its great sensitivity to the action of wind was discovered, which produced strong oscillations with amplitudes amounting to one and a half meters. Different structural measures were taken to remove this disadvantage, which caused great alarm (by introducing additional connections and mounting hydraulic dampers on the pylons).

However, this did not avoid the catastrophe, which occurred November 7, 1940. Beginning at 8 o'clock in the morning there were very strong vertical bending oscillations of the bridge with a frequency of 0.6 oscillations per /351 second. It is interesting that the wind had not too large a velocity — about 17 m/sec, whereas before this there were cases when the bridge stood

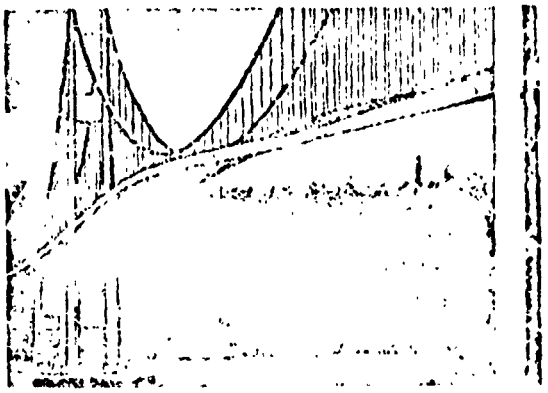

Fig. 43.2. Oscillations of the thoroughfare of the Tacoma Bridge before the catastrophe.

up against a stronger wind without any damage(*).

At about 10 o'clock in the morning, the wind velocity increased somewhat (up to 18.7 m/sec), and bending-torsional oscillations were established with an extremely small frequency (0.2 oscillations per second) and an extremely large amplitude. When the twisting reached a maximum, the thoroughfare was inclined to the ground at an angle of 45°. Apparently, there was a sharp change in the oscillation frequency due to the breaking off of some important connections in the structure. The bridge withstood these oscillations for about an hour, after which part of the thoroughfare broke in half and fell to the water.

It is interesting that the Tacoma Bridge disaster was record n a film. This film has provided extremely valuable material for studying the causes of the catastrophe. Figure 43.2 reproduces one of the frames of this film, /352 showing the condition of the bridge a half hour before the damage. The bending height and torsional nature of the oscillations is clearly apparent here.

The destruction of the Tacoma Bridge naturally attracted enormous interest on the part of researchers. Almost immediately after the catastrophe, T. Karman published an analysis of the critical velocity of the Tacoma Bridge divergence. According to the calculations of Karman, this velocity was 22.2 m/sec. However, the destruction of the Tacoma Bridge was definitely

(*) The bridge was designed for a static wind load from a wind with a velocity of approximately 50 m/sec.

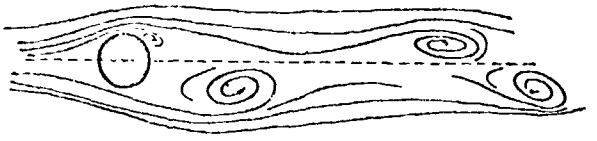

Fig. 43.3. Vortex trail ("Karman Trail").

caused by oscillations, and therefore an analysis of the aerodynamic instability requires not a static but a dynamic formulation of the problem.

Several attempts were made later to connect the Tacoma Bridge disaster with the phenomenon of the classic flutter of a structure. However, recently another explanation has been generally accepted, which is connected with the particular aerodynamic phenomena, which we must discuss in greater detail.

If there is a barrier in a flow of air (liquid) around which it is difficult to pass, a vortex trail is formed behind it, and the vortices move with a certain periodicity which depends on the form and dimensions of the structure, as well as on the flow velocity. Thus, for example, in the case of flow around a cylinder a vortex trail is formed, which is shown in Figure 43.3. The direction of the vortices coming from the cylinder changes alternately, and the number of vortices moving per second is determined by the expression

$$f = \frac{0.22v}{D} \ \text{sec}^{-1} \qquad (43.1)$$

where v is the flow velocity (m/sec), D — diameter of the cylinder (m). The coefficient 0.22 represents the Strouhal number (for a given type of structure located in a flow). As a result of the vortex detachment alternately from both sides of the cylinder, a harmonically changing force acts upon the latter, which is perpendicular to the direction of flow. The law governing the change /353 in time of this force has the form

$$F = c_k \frac{\rho v^2}{2} S \sin 2\pi ft. \qquad (43.2)$$

Here S is the area of the barrier projection on a plane perpendicular to the flow direction, c_k — coefficient depending on the form of the barrier (for a circular cylinder $c_k = 1$). The more difficult it is for flow to pass around the structure, the larger is the coefficient c_k and the amplitude of the force F, respectively. Thus, for example, flow around an aircraft wing at small angles of attack is very smooth. The vortex trail is very weakly

expressed, and the coefficient c_k is very small. The situation is different for the structure of a suspension bridge, around which it is difficult for a flow to pass. It is natural to assume here the development of a force F of a large amplitude.

Thus, a structure located in an air flow undergoes the action of the perturbing force (43.2) and, consequently, changes into a state of forced oscillations. The extent of the danger of this motion regime depends on whether the eigenfrequency (or, to phrase it better, any of the eigenfrequencies of the structure) is close to the frequency of the perturbing force $2\pi f$. When the frequencies coincide, resonance occurs, and the oscillations can be destructive, if the system does not have adequate damping.

Large oscillations of this type have been observed repeatedly in engineering practice. Thus, for example, resonance caused by a vortex separation was observed in steel factory pipes. In 1953 a steel pipe with a diameter of 4.8 m and a height of 90 m was in a state of resonance with a wind velocity of about 80 km/hr. Great damage to the pipes made it necessary to replace their upper parts, and to introduce hydraulic dampers into the exhaust system.

Even larger amplitudes of the force F develop in those cases when a flow with a great density ρ (for example, a flow of water) passes around a structure. Resonance phenomena have been repeatedly observed in periscopes of submarines at velocities of about 8 km/hr. The oscillation ranges were very great, since a periscope is a very flexible structure: with a diameter of about 20 cm, the length of a periscope may be 6 m (when extended). Strong oscillations of the periscope produce not only a blurred image, but also threaten its strength. /354

The phenomenon described above of great oscillations caused by a vortex trail is called <u>separated flutter</u>. In an aircraft wing, this phenomenon may only occur at large angles of attack, i.e., when the smoothness of the flow

is disturbed. Ship propellers are subjected to separated flutter to a much greater degree, as well as blades of turbines and compressors, which sometimes operate at large angles of attack.

It has presently been established that oscillations of this nature were the cause of the Tacoma Bridge disaster.

A new bridge has been built at Tacoma, but having a completely different form. Its width has been increased more than one and a half times, and is 18 m, while the thoroughfare has a box-like cross section with a height of 10 m, instead of the previous H-form 2.4m in height. In addition, the solid beams have now been replaced with open girders, which greatly reduces the amplitude of aerodynamic perturbations.

In the form described above, separated flutter cannot be regarded as a phenomenon pertaining to aeroelasticity. For aeroelastic phenomena, the influence of elastic displacements on aerodynamic forces is typical. However, in this section, we did not point out this influence above, as if aerodynamic forces were given perturbing forces which swing an elastic structure, but are not changed themselves with these oscillations.

In actuality, the process of separated flutter is more complex. As soon as large oscillations arise, vortex formation begins to depend on the regime of motion of the structure, and its oscillations begin to <u>influence</u> considerably the aerodynamic forces — the process acquires the characteristic feature of an aeroelastic phenomenon.

Only direct experiments are a reliable basis for studying the danger of separated flutter.

The problems which we have discussed in this section, were treated in the following books: R.L. Bisplinghoff, H. Ashley and R.L. Halfman "Aeroelasticity" (Foreign Literature Press, 1958, pp. 541 - 546);

F.G. Fung "Introduction to the Theory of Elasticity" (Fizmatgiz, 1959, pp. 76 - 96, 351 - 361); J. Rocard "Instability in Mechanics" (Foreign Literature Press, 1959, Chapter VI); F.D. Dmitriyev "Krusheniya inzhenernykh sooruzheniy" (Torsion in Engineering Structures) (Gosstroyizdat, 1953, pp. 81 - 94). /355

The theory of a vortex trail was first advanced by T. Karman in 1911. The first article by Karman on the Tacoma catastrophe was given in the journal "Engineering News Records", Vol. 125, 21 November 1940. The results of extensive experimental studies on the aerodynamic instability of suspension bridges are contained in five issues of a work by F.B. Farquarson et al. "Aerodynamic Stability of Suspension Bridges with Special Reference to the Tacoma Narrows Bridge", University of Washington Experiment Station Bulletin No. 116, 1954.

See also the following regarding the Tacoma catastrophe: I.I. Gol'denblat "Sovremennyye problemy kolebaniy i ustoychivosti inzhenernykh sooruzheniy" (Contemporary Problems of Oscillations and Stability of Engineering Structures) (Gosstroyizdat, 1947), J. Rocard "Instability in Mechanics" (Foreign Literature Press, 1959). We borrowed Figure 43.2 from the last book.

CHAPTER IX

PROBLEMS OF NONLINEAR SYSTEM OSCILLATIONS

This chapter begins with the simplest problem of the theory of self-synchronization (§ 44), and we shall discuss a system with one degree of freedom. In § 45 and 46 we shall investigate the stability of stationary regimes of oscillations of mechanical systems with two degrees of freedom. We must assume the solutions which were proposed by Rocard, and in particular we shall note an error in one of them. In § 47 we present variants of the method of slowly changing amplitudes, which is an adequately general approximate method for solving the problem of oscillations of systems with slight nonlinearity (curvilinear systems). Section § 48 gives an example of applying this method to the specific problem of self-oscillations of a system with dry friction. In the next section (§ 49) we examine friction self-oscillations, but when they have an explosive character. We shall not use the method of slowly changing amplitudes here, but rather the method of appropriation. The last section in this chapter (§ 50) is devoted to a graphic-analytical method of studying oscillatory processes by means of a phase picture.

§ 44. Vibration Maintenance of Rotation

In present day technology, in order to produce vibrations which are necessary for certain production processes (compressing concrete mixtures, screening, vibration transport, vibration hammering, etc.), mechanical vibrators are widely used. The main part of a mechanical vibrator is an unbalanced /357 rotor which is rotated by an electric engine.

In heavy vibrating machines (sifters, crushers, conveyors, disintegrators, etc.) there is usually not one, but several mechanical vibrators on a common base. Due to this, the bearings of the vibrators are unloaded. These bearings are the most vulnerable units, and the perturbing load is uniformly

distributed over the entire working part of the machine. In order that the operation of several vibrators be coordinated, it is necessary to have synchronous rotation and to maintain specific relationships between their phases of rotation. As a rule, for this purpose kinematic connections are used between the vibrator rotors, for example, toothed or chain drive. In this way, forced synchronization of the operation of several vibrators is achieved.

However, about 15 years ago the self-synchronization of rotors was first observed — the phenomenon of automatically maintaining equal angular velocities and phases in different vibrators when there were no connections of this kind.

Huyghens in the second half of the XVII century established that two clocks, running differently,were sychronized when they were placed on a sufficiently pliable common base (on a light beam). Following are the observations of Huyghens:

"The pendulum on these clocks was 9 inches long and weighed half a pound. The mechanism was set in motion by gears which were located in the box together with the mechanism. The box was 4 feet long. It was weighted below with at least 100 pounds of lead. The following interesting observation was made with these clocks.

"Two such clocks were placed on the same beam, located on two supports. The two pendulums always moved in opposite directions, and their oscillations coincided so closely that no divergences could be observed. The ticking of both clocks was very audible, and took place at the same instant. If this agreement was artificially disturbed, it was restored in a very short time. At first I was astonished by this strange phenomenon, but finally — after careful investigation, I found that the reason was the slight motion of the beam itself. The oscillations of the pendulum imparted a certain motion to the clocks, no matter how heavy they were. This motion was transmitted to /358 the beam, and if the pendulums themselves did not move in opposite directions, then this of necessity occurred".

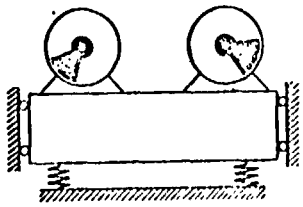

Fig. 44.1. Only the left vibrator is turned on in the system.

It is probable that this is the first recorded case of self-synchronization of technical objects. Similar phenomena were observed at the end of the last century by Rayleigh for organ pipes and tuning forks. Later — approximately at the beginning of this century — the self-synchronization phenomena were discovered in electric furnaces and in certain electromechanical systems.

At the present time, self-synchronization is being used more and more extensively in new vibration machines, since sometimes, due to self-synchronization, it is possible to completely avoid forced (kinematic or electric) synchronization of a vibrator system. Self-synchronization has the general property of individual objects of a "technical collective" adapting to the operational rhythm of the collective at whole. The opinion has been expressed in the literature that such properties are not inherent only to technical devices, but they are also manifested in many physical phenomena, and even in the life of biological collectives.

We shall examine the phenomenon of self-synchronization with the simplest example of a two-vibrator system, when the engine of only one of the vibrators is turned on in the network, and the unbalanced rotor of the second vibrator is the usual freely suspended physical pendulum. It is found — and we are convinced of this — that under these conditions the rotor of the second vibrator also rotates at the same angular velocity. In this case, self-synchronization can be explained by the vibrations of the common base. The latter serves as an unusual connection between the vibrators, which can make their motions agree. Such "weak" connections are characteristic for all self-synchronizing systems.

Figure 44.1 shows a scheme of this system. It is assumed that only the left vibrator is turned on. The rotor of this vibrator rotates with a given angular velocity ω. Thus, the circular velocity of the base oscillations /359

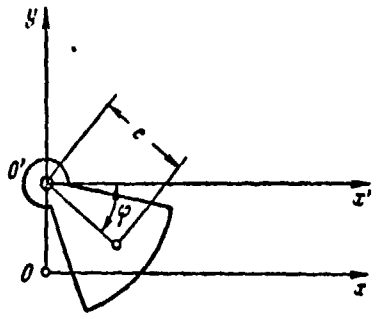

Fig. 44.2. Scheme for compiling the equation of motion of a free rotor.

will also equal ω. For purposes of simplicity, we shall assume that all points on the base oscillate over the same vertical. In this case, the vertical oscillations of a point on the suspension of the right rotor (which belongs to the vibrator which is not turned on in the network) may be described by the law

$$y = A \sin \omega t, \tag{44.1}$$

where A is the amplitude of the oscillations.

We shall assume that the state of relative rest of the free rotor is disturbed. We shall write the equation of the relative motion, setting: ρ — radius of inertia of the free rotor, e — eccentricity, m — rotor mass, φ — angle of rotor rotation, calculated from the x axis in the clockwise direction (Figure 42.2). The moment of the weight must be included in the equation of moments with respect to the oscillating axis O'

$$M_1 = mge \cos \varphi \tag{44.2}$$

and the friction moment, which we shall assume is proportional to the angular velocity $\dot{\varphi}$

$$M_2 = -k\dot{\varphi}. \tag{44.3}$$

In addition, we must take the fact into account that the coordinate system x'O'y' moves with respect to the fixed coordinate system xOy. Therefore, the moment of the translational force of inertia must be introduced into the equation of moments. This force is directed along the vertical and equals

$$-m\ddot{y} = mA\omega^2 \sin \omega t, \tag{44.4}$$

so that the corresponding moment is

$$M_3 = -(mA\omega^2 \sin \omega t)\, e \cos \varphi. \tag{44.5}$$

Thus, the differential equation of relative motion of a free rotor may be written in the form

/360

$$mgc\cos\varphi - k\dot{\varphi} - mcA\omega^2\cos\varphi\sin\omega t = m\rho^2\ddot{\varphi}, \qquad (44.6)$$

where $m\rho^2$ is the rotor moment of inertia.

As a result, we arrive at the very complex nonlinear differential equation with variable coefficients, which assumes a solution of several different types. Let us confine ourselves to answering the main question of self-synchronization: under any conditions, is rotation of a rotor at the angular velocity ω possible? For this, we must determine whether the function

$$\varphi = \omega t + \alpha \qquad (44.7)$$

is the solution of the differential equation (44.6) (α — constant). Using the law governing the rotor motion in the form (44.7), we assume that the rotor is synchronized, but moves with a certain phase shift α with respect to the oscillations of the base(*). Substituting (44.7) in the differential equation (44.6), we obtain

$$mc\cos(\omega t + \alpha)(g - A\omega^2\sin\omega t) = k\omega. \qquad (44.8)$$

Since the left side is variable, and the right side is constant, this equation is apparently not satisfied identically. This means that function (44.7) is not the precise solution of equation (44.6).

However, we must not reach the conclusion about the unsuitability of (44.7) for describing the rotor motion, and must establish whether it is possible to regard the function (44.7) as the approximate solution of the differential equation (44.6). For this purpose, we shall discard the unsatisfied requirement regarding the identical fulfillment of relationship (44.8), and shall replace it with the less rigid requirement of satisfying the equations (44.8) on the average.

The left-hand side of (44.8) represents a certain periodic functi of time with the period $2\pi:\omega$. Therefore, to determine the average value of this function we must integrate it over the time interval $\left[0, \frac{2\pi}{\omega}\right]$ and divide the

(*) Due to inelastic resistances, a certain phase shift is also possible for the rotation of the left vibrator and oscillations of the base.

results by the value of the period $\frac{2\pi}{\omega}$. Integration yields /361

$$me\int_0^{\frac{2\pi}{\omega}}\cos(\omega t+\alpha)(g-A\omega^2\sin\omega t)\,dt=\pi meA\omega\sin\alpha. \tag{44.9}$$

Dividing expression (44.9) by the period, we obtain the average value of the left side of equation (44.8). Equating the result obtained with the right-hand side of (44.8), we obtain

$$\frac{meA\omega^2}{2}\sin\alpha=\kappa\omega. \tag{44.10}$$

Thus, the function (44.7) is an approximate solution of the differential equation (44.8), under the condition that the system parameters are satisfied by (44.10). The following expression thus follows

$$\sin\alpha=\frac{2k}{meA\omega}. \tag{44.11}$$

On the one hand, this expression makes it possible to determine the phase shift, and on the other hand — which is very important for our purposes — makes it possible to formulate the condition of self-synchronization in the form

$$\frac{2k}{meA\omega}<1. \tag{44.12}$$

Thus, the greater the disbalance me and the greater the vibration of the rotor axis Aω, the easier it is to achieve the self-synchronization. There is one factor which may prevent self-synchronization — this is friction in the system, represented by the coefficient k. The smaller is the friction, the better are the conditions for self-synchronization to develop.

The solution given above may be interpreted by means of several physical representations. The right-hand side of (44.8) expresses the retarding moment of friction, and the left-hand side — the moment of the forces contributing to the rotor rotation. Therefore, the operation of averaging the left-hand side, which was used above, is equivalent to replacing the latter moment by its constant component.

We may use (44.10) also, when investigating the energy relationships. Let us multiply both parts of the differential equation (44.6) by $d\varphi = \dot{\varphi}dt$, /362 and let us integrate the equation over the time interval $\left[0, \frac{2\pi}{\omega}\right]$.

We then obtain

$$mge\int_0^{\frac{2\pi}{\omega}}\dot{\varphi}\cos\varphi\,dt-k\int_0^{\frac{2\pi}{\omega}}\dot{\varphi}^3dt-mc\lambda\omega^3\int_0^{\frac{2\pi}{\omega}}\dot{\varphi}\cos\varphi\sin\omega t\,dt=$$
$$=mQ^3\int_0^{\frac{2\pi}{\omega}}\ddot{\varphi}\dot{\varphi}dt. \qquad (44.13)$$

The right-hand side may be written in the form

$$mQ^3\int_0^{\frac{2\pi}{\omega}}\ddot{\varphi}\dot{\varphi}\,dt=mQ^3\int_0^{\frac{2\pi}{\omega}}\dot{\varphi}\cdot\frac{d\dot{\varphi}}{dt}\cdot dt=mQ^3\int_{\dot{\varphi}_0}^{\dot{\varphi}_T}\dot{\varphi}\,d\dot{\varphi}=$$
$$=mQ^3(\dot{\varphi}_T^2-\dot{\varphi}_0^2). \qquad (44.14)$$

Here $\dot{\varphi}_0$ and $\dot{\varphi}_T$ are the values of the angular velocity at the beginning and end of the period. Expression (44.14) represents the increase in the kinetic energy in one period. If the rotation is uniform on the average, this increase must equal zero. Consequently, the left side of equation (44.13) must equal zero. If we approximately substitute (44.7) in this side, then we again obtain (44.10). Thus, the operation of averaging and the energy method are equivalent to each other, in essence.

Both variations of the solution are approximate. What will the rotor motion be like in actuality? A more precise theory provides the answer to this question. The real law governing the rotor motion has the form

$$\varphi=\omega t+\alpha(t), \qquad (44.15)$$

where $\alpha(t)$ is a periodic function of time with the period $2\pi:\omega$. Thus, the angular velocity of the rotor is

$$\dot{\varphi}=\omega+\dot{\alpha}, \qquad (44.16)$$

i.e., it oscillates around the value of ω. Thus, synchronization is achieved only on the average, since periodic oscillations obeying the law $\alpha(t)$ are applied to the uniform rotation of the rotor with the angular velocity ω. However, these oscillations are small, and in expression (44.16) their velocity $\dot{\alpha}$ can be disregarded in practice, as compared with the angular velocity ω. The approximate analysis given above is based on this. /363

In conclusion, we should note that the vibration maintenance of rotation is used in so-called planetary vibrators. Figure 44.3 shows the scheme of such a vibrator with a cylindrical cavity. The main portion of the vibrator

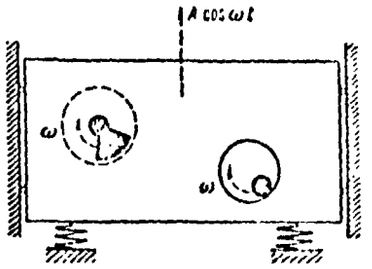

Fig. 44.3. Planetary vibrator (on the right) rotates due to oscillations of the base.

is a massive cylinder, which is freely inserted into the cylindrical cavity with a large diameter. In the case of vibrations (for example, vertical ones) of the housing, the cylinder rolls along the inner surface of the cavity and has an action similar to the action of a unbalanced vibrator. Such mechanisms can be used not only as oscillation exciters, but also as the working units of a machine. Thus, vibrational pressures work on this principle. Rolling along the cavity, the cylinder crushes material which enters it.

This theory was used in 1960 by T. Caughey to explain the nature of the ring rotation in the well known game "hula-hoop" (see his work: "Hula-Hoop: An Example of Heteroparametric Excitation", American Journal of Physics, Vol. 28, No. 2, 1960).

Concerning the observations of H. Huyghens, see his "Three Memoirs on Mechanics" (Izdatel'stvo AN SSSR, 1951, pp. 30 - 31). The theory of self-synchronization was developed completely in the works by I.I. Blekhman. See his article "Rotation of an Unbalanced Rotor Caused by Harmonic Oscillations of Its Axis" (Izvestiya AN SSSR, OTN, No. 8, 1954), in connection with the simple problem discussed above. He examined a more general case in this work.

§ 45. Dynamics of the Boisse-Sarda Regulator

The mechanism studied here was advanced by the French engineers Boisse and Sarda to ensure the uniform dropping of a load on a cable. After solving the differential equations of motion, the possibility is explained of two /364 essentially different operational regimes. Which of them is used in actuality?

Let us investigate the scheme shown in Figure 45.1. A drum with the radius R containing a cable is fastened on the axis AA. A load is fastened

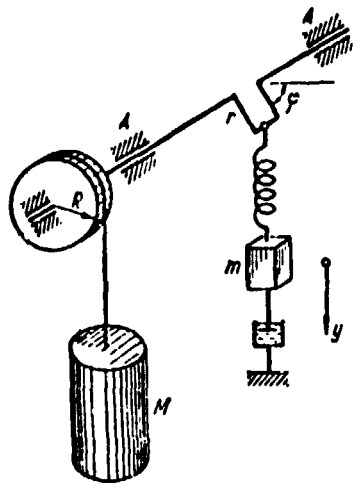

Fig. 45.1. Boisse-Sarda regulator scheme.

to the lower end of the cable, which drops down due to its own weight. In the absence of additional devices, the load would drop with a uniform acceleration. In order that it drops uniformly, a crank is attached to the axis AA, and the mass m of the regulator is elastically suspended at the radius r. The rigidity coefficient of the spring is c. In addition, viscous resistance is introduced into the system. The viscocity coefficient equals k. It is assumed that the regulator mass only completes vertical oscillations.

This system has two degrees of freedom. The vertical displacement y of the mass m and the angle φ of the crank rotation are used as the generalized coordinates. When writing the equations of motion, we naturally did not use the assumption of a uniform drum rotation (although the regulator is designed to provide such rotation).

When the system moves, three forces act on the mass m: the weight of the load mg, the viscosity force — $k\dot{y}$, and the spring force of elasticity — $c(y - r \sin \varphi)$; the latter is proportional to the difference in the displacements y (of the mass m) and r sin φ (and of the crank). Thus, the differential equation of motion for the regulator mass has the form

$$m\ddot{y} = mg - k\dot{y} - c(y - r\sin\varphi), \tag{45.1}$$

i.e.,

$$\ddot{y} + 2\varepsilon p\dot{y} + p^2 y = \frac{cr}{m}\sin\varphi + g, \tag{45.2}$$

where we set

/365

$$\varepsilon = \frac{k}{2mp}, \quad p^2 = \frac{c}{m}.$$

The second differential equation pertains to the drum rotation. We should first note that the vertical acceleration of the load M equals $\ddot{\varphi}R$, and the tension of the cable T is $T = M(g - \ddot{\varphi}R)$[*]. Consequently, the moment of the force T with respect to the axis ... equals $MR(g - \ddot{\varphi}R)$.

The moment of the spring tensile strength may be found by multiplying this force by $r\cos\varphi$. With allowance for the signs, we find that this moment equals $c(y - r\sin\varphi)\, r\cos\varphi$. Thus, the second equation of motion has the form:

$$MR(g - \ddot{\varphi}R) + c(y - r\sin\varphi)\, r\cos\varphi = I\ddot{\varphi},$$

where I is the shaft moment of inertia. Consequently,

$$(I + MR^2)\ddot{\varphi} - c(y - r\sin\varphi)\, r\cos\varphi = MgR. \tag{45.3}$$

We must now solve concurrently the system of nonlinear equations (45.2) and (45.3). We should first of all determine whether uniform rotation of the drum is possible, i.e., whether the equations of the problem are satisfied by the solution

$$\varphi = \omega t, \tag{45.4}$$

where ω is the angular velocity of the drum rotation. Naturally, the quantity ω was unknown previously. If the solution of (45.4) satisfies the system of equations, we shall then try to determine the quantity ω, which determines the rate at which the load falls.

If the drum rotation is uniform and expression (45.4) is the solution, then equation (45.2) assumes the form

$$\ddot{y} + 2\varepsilon p\dot{y} + p^2 y = \frac{cr}{m}\sin\omega t + g \tag{45.5}$$

and has the well-known solution

$$y = \frac{r}{\sqrt{\left(1 - \frac{\omega^2}{p^2}\right)^2 + \frac{4\varepsilon^2\omega^2}{p^2}}}\sin(\omega t + \alpha) + \frac{g}{p^2}, \tag{45.6}$$

(*) This follows from the equation of motion for the mass M:

$$Mg - T = M\ddot{y}R.$$

where the displacement of the phase α is determined by the equation /366

$$\operatorname{tg}\alpha = -\frac{2\varepsilon\omega p}{p^2 - \omega^2}. \tag{45.7}$$

Let us now examine the second equation of our problem — equation (45.3). Under the condition that φ is determined by (45.4), we have $\ddot{\varphi} = 0$, i.e., the right-hand term on the left side of (45.3) vanishes, and the second term equals:

$$-c(y - r\sin\varphi)r\cos\varphi = \\ = -c\left[\frac{r\sin(\omega t + \alpha)}{\sqrt{\left(1 - \frac{\omega^2}{p^2}\right)^2 + \frac{4\varepsilon^2\omega^2}{p^2}}} + \frac{g}{p^2} - r\sin\omega t\right]r\cos\omega t. \tag{45.8}$$

It may be readily seen that this quantity is variable. It does not satisfy equation (45.3), the right-hand side of which is constant. It does follow that (45.4) does not satisfy the system of equations for the problem, i.e., it is impossible for the load to fall uniformly

Nevertheless, we may write an approximate solution, assuming that the average value of the function (45.8) coincides with the right side of equation (45.3). This method of averaging is widely used in the theory of nonlinear oscillations. In particular, it is used in § 47.

Removing the brackets in the right side of (45.8), we obtain the sum of the components, whose variable parts are the trigonometric functions $\sin\omega t \cdot \cos\omega t$, $\cos\omega t$ and $\cos^2\omega t$. We should note that the average value in one period of the first two functions equals zero, and the average value of the latter is

$$\frac{\omega}{2\pi}\int_0^{\frac{2\pi}{\omega}} \cos^2\omega t\, dt = \frac{1}{2}. \tag{45.9}$$

Therefore, the average value of the function on the right side of (45.8) may be expressed by one term and is

$$-\frac{cr^2}{2\sqrt{\left(1 - \frac{\omega^2}{p^2}\right)^2 + \frac{4\varepsilon^2\omega^2}{p^2}}}\sin\alpha = -\frac{c\varepsilon r^2\omega}{p\left[\left(1 - \frac{\omega^2}{p^2}\right)^2 + \frac{4\varepsilon^2\omega^2}{p^2}\right]}. \tag{45.10}$$

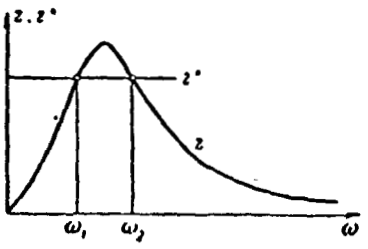

Fig. 45.2. Graphic solution of equation (45.11).

We have substituted the expression following from relationship (45.7) here, instead of sin α. Thus, instead of (45.3), we obtain /367

$$\frac{\varepsilon\omega}{p\left[\left(1-\frac{\omega^2}{p^2}\right)^2+\frac{4\varepsilon^2\omega^2}{p^2}\right]}=\frac{MgR}{cr^2}. \qquad (45.11)$$

This equation almost completes the solution. This equation may be regarded as the equation for determining the angular velocity ω of the drum rotation. In view of the nonlinearity of equation (45.11) with respect to ω, it has more than one root. This indeterminacy of the solution requires further analysis of stability of the solutions.

To solve the equations (45.11), we use a graphic method, and first of all compile a graph of the function

$$z=\frac{\varepsilon\omega}{p\left[\left(1-\frac{\omega^2}{p^2}\right)^2+\frac{4\varepsilon^2\omega^2}{p^2}\right]}. \qquad (45.12)$$

This graph has the form shown in Figure 45.2. We now draw a horizontal line

$$z^*=\frac{MgR}{cr^2}; \qquad (45.13)$$

Then the points where the lines (45.12) and (45.13) intersect determine the real roots of the equation (45.11). Figure 45.2 shows the cases when the curve z intersects the line z^* twice. The greater the moment MgR of the weight of the load being dropped, the higher is the corresponding line z^*. With sufficiently large moments, the graphs of z and z^* do not intersect in general. In these cases, the assumption ω = const was not even approximately valid, i.e., it is impossible for a load to drop uniformily (or, more correctly, "almost uniformly") in general.

In order that the regulator can handle this problem, it is necessary that the location of the line of (45.13) be low enough. This may be done, for example, by increasing the radius of the crank r.

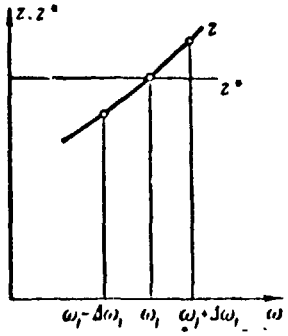

Fig. 45.3. Investigation of stability of rotation at the angular velocity ω.

We shall assume that the regulator parameters are selected reliably, and the line (45.13) intersects the curve (45.12) twice. But then the problem arises which was presented at the beginning of this section: which of the two motions is performed — with the lower frequency ω_1 or the higher frequency ω_2? /368

The answer to this question is connected with the stability of each of the two operational regimes found.

To determine the stability, let us turn to the equation (45.3). Replacing the second term in it by its average value (45.10), and setting $\ddot{\varphi} = \dot{\omega}$, after dividing by cr^2 we obtain

$$\frac{I+MR^2}{cr^2}\dot{\omega} = \frac{MgR}{cr^2} - \frac{\varepsilon\omega}{p\left[\left(1-\frac{\omega^2}{p^2}\right)^2+\frac{4\varepsilon^2\omega^2}{p^2}\right]},$$

or, more simply

$$\frac{I+MR^2}{cr^2}\dot{\omega} = z^* - z. \qquad (45.14)$$

Under conditions of a stationary regime, when $\omega = \omega_1$ or $\omega = \omega_2$, both parts vanish. What occurs, for example, if the angular velocity ω_1 decreases somewhat and becomes equal to $\omega_1 - \Delta\omega_1$? It may be seen from Figure 45.3 that in this case $z^* > z$. Therefore, it follows from equation (45.14) that $\dot{\omega} > 0$, i.e., the angular velocity increases, trying to restore its unperturbed value ω_1. If the angular velocity increases somewhat and assumes the value $\omega_1 + \Delta\omega_1$, then $z > z^*$, and we find that $\omega < 0$ from (45.14). This means that the angular velocity decreases, i.e., it strives to the value ω_1. From this it is clear that the rotational regime of the system with an angular velocity ω_1 is stable.

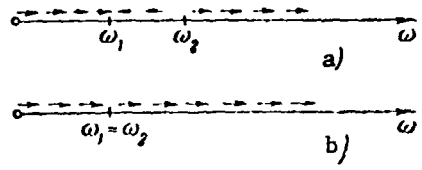

Fig. 45.4. Behavior of the system motion after perturbation of the angular velocity ω_1 or ω_2: a) case $\omega_1 \neq \omega_2$; b) case $\omega_1 = \omega_2$.

Using equation (45.14), we can in the same way establish that rotation at the angular velocity ω_2 is unstable.

Thus, the Boisse-Sarda regulator /369 may provide that the mass M drops "almost uniformly"(i.e., uniform throughout the period, on the average). The smaller of the roots in equation (45.11) corresponds to a stable regime.

Does the second root $\omega = \omega_2$ have any practical value? Based on the above statements, it would appear that the answer is negative. However, in actuality, the value of ω_2 is of some interest — this value determines the upper boundary of the permissible perturbances of the angular velocity ω. A stationary regime $\omega = \omega_1$ will only be retained if the possible perturbations of the angular velocity are small enough. If the perturbation is so great that the threshold $\omega = \omega_2$ is changed, then the system, as it is usually expressed, "moves and accelerates", and the angular velocity ω will increase indefinitely. The behavior of the system motion may be characterized by arrows as is done in Figure 45.4, a.

Consequently, for stable operation of the regulator in a sufficiently wide region it is necessary that the solutions ω_1 and ω_2 differ considerably. The difference between these values may be assumed to be the stability reserve. The smaller the stability reserve, the less reliable is the regulator operation. When $\omega_1 = \omega_2$, the system becomes "half-stable" (Figure 45.4, b). Therefore, it would be particularly desirable that the line z^* could pass lower.

This solution of the problem regarding the Boisse-Sarda regulator belongs to J. Rocard (see the third edition of the book "Dinamique Générale des Vibrations", Paris, 1960, pp. 312 - 315). This problem was studied in greater

detail by I.I. Blekhman and G.Yu. Dzhanelidze (see their article "Dynamics of the Boisse-Sarda Regulator", Izvestiya AN SSSR, OTN, No. 10, 1955. In particular, they established that in the case of viscous resistance to rotation there are not two, but three stationary regimes, and in the case of large perturbations in the system there is a jump-like transition from the first regime into the third (the second regime is unstable). /370

§ 46. Sommerfeld Effect

It is usually assumed that an eccentric vibrator generates the perturbing force

$$P = P_0 \cos \omega t \tag{46.1}$$

($P_0 = m\omega^2 e$, ω — angular rotation velocity of the vibrator axis, m — unbalanced mass, e — its eccentricity). It is most frequently tacitly assumed that the value of ω is given ahead of time, and does not depend on the oscillations of the elastic system on which the vibrator is located.

In actuality, this is not the case, if an engine is used which has a small power. In this case the oscillations of the elastic system have a great influence on the value of ω, and the latter also oscillates around a certain average value.

Due to the opposite influence of the structure oscillations on the angular velocity of rotation, the vibrator operation in a certain range of angular velocities $[\omega_1, \omega_2]$ becomes unstable. This effect has been called the Sommerfeld effect — from the well-known physicist who first published it in 1904, and demonstrated the instability on an experimental device. A simplified theory of the Sommerfeld effect is given below.

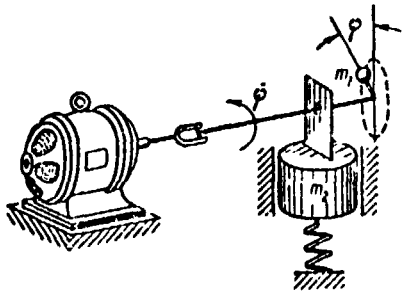

Fig. 46.1. Scheme of an oscillatory electromechanical system.

Let us examine the oscillations of an electromechanical system shown in Figure 46.1. An electric engine rotates a cam with the mass m_1, whose axis is connected with an elastically suspended mass m_2. It assumed that the mass m_2 can only complete vertical oscillations, and small sags in the cam axis are compensated by a Cardan connection, and are not transmitted to the engine axis. /371

Let us assume φ is the angle of the rotor rotation, which equals the angle of rotation of the cam axis. The starting point of further computations consists of the fact that oscillations of the mass m_2 influence the angular velocity of rotor rotation, and that the moment M transmitted by the stator to the rotor is a quantity which depends on the angular velocity $\dot{\varphi}$ of rotation.

The relationship

$$M = M(\dot{\varphi})$$

is called the characteristic of the engine, and is determined by its construction and parameters.

In many cases, the characteristic of electric engines may be assumed to have the form of the linear function

$$M = M_0 - a\dot{\varphi}, \qquad (46.2)$$

and the quantity M_0 depends on the working voltage. A rheostat may be used to change the engine characteristic — on the graph, this is shown by its displacement parallel to itself (Figure 46.2).

The motion of the system as a whole is determined by two coordinates — the angle φ, which was already discussed, and the vertical displacement y of the mass m_2. The displacement of y is calculated from the position of equilibrium (Figure 46.3).

The equations of the system motion may be written in the Lagrange form. For this purpose, we must first of all write the expression for the kinetic energy T. Three components corresponding to three elements of the system which have mass, are included in it (rotor, mass m_1 and mass$_2$). The kinetic

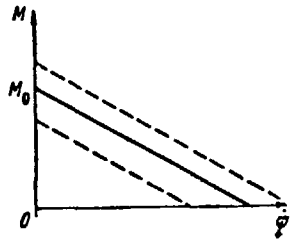

Fig. 46.2. Characteristics of an engine. With a change in the working voltage, the line shifts parallel to itself.

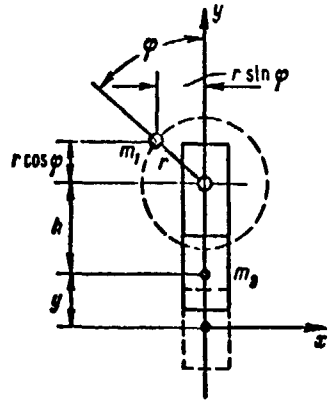

Fig. 46.3. Coordinate axes.

energy of the rotor is

$$T_0 = \frac{I_1 \dot{\varphi}^2}{2}, \qquad (46.3)$$

where I_1 is the rotor moment of inertia with respect to its axis. The expression /372 for the kinetic energy of the mass m_1 is written in a somewhat more complex manner. Its vertical coordinate is

$$y_1 = y + h + r \cos \varphi, \qquad (46.4)$$

and the horizontal coordinate is determined by the expression

$$x_1 = -r \sin \varphi \qquad (46.5)$$

(see Figure 46.3). Differentiating expressions (46.4) and (46.5) with respect to time, we find the vertical and horizontal projections of the velocity of the mass m_1:

$$\dot{y}_1 = \dot{y} - r\dot{\varphi} \sin \varphi, \qquad (46.6)$$

$$\dot{x}_1 = -r\dot{\varphi} \cos \varphi. \qquad (46.7)$$

Therefore, the kinetic energy of the mass m_1 is

$$T_1 = \frac{m_1}{2}[(\dot{y} - r\dot{\varphi} \sin \varphi)^2 + (-r\dot{\varphi} \cos \varphi)^2]. \qquad (46.8)$$

Finally, the kinetic energy of the mass m_2 may be written in the form

$$T_2 = \frac{m_2 \dot{y}^2}{2}. \qquad (46.9)$$

Combining expressions (46.3), (46.8) and (46.9), we obtain the kinetic energy of the system, which is described by the generalized coordinates and velocities:

$$T = \frac{(I_1 + m_1 r^2)\dot{\varphi}^2}{2} + \frac{(m_1 + m_2)\dot{y}^2}{2} - m_1 r \dot{y} \dot{\varphi} \sin \varphi. \qquad (46.10)$$

If we introduce an abbreviated notation

$$\left.\begin{aligned} I &= I_1 + m_1 r^2, \\ m &= m_1 + m_2, \end{aligned}\right\} \qquad (46.11)$$

then the kinetic energy is written in the form

$$T = \frac{I\dot{\varphi}^2}{2} + \frac{m\dot{y}^2}{2} - m_1 r \dot{y}\dot{\varphi} \sin \varphi. \tag{46.12}$$

We now write the left-hand sides of the Lagrange equations /373

$$\left.\begin{aligned} \frac{d}{dt}\left(\frac{\partial T}{\partial \dot{y}}\right) - \frac{\partial T}{\partial y} &= m\ddot{y} - m_1 r (\ddot{\varphi} \sin \varphi + \dot{\varphi}^2 \cos \varphi), \\ \frac{d}{dt}\left(\frac{\partial T}{\partial \dot{\varphi}}\right) - \frac{\partial T}{\partial \varphi} &= I\ddot{\varphi} - m_1 r \ddot{y} \sin \varphi. \end{aligned}\right\} \tag{46.13}$$

The generalized forces are the right-hand sides of the Lagrange equations. For the coordinate y, the spring elasticity force is the generalized force

$$Q_y = -cy,$$

where c is the spring rigidity coefficient. For the coordinate φ the sum of the rotating moment (46.2) and the moment of the friction forces, which we assume is proportional to the angular velocity $\dot{\varphi}$, is the generalized force Q_φ:

$$Q_\varphi = M_0 - a\dot{\varphi} - k\dot{\varphi}, \tag{46.14}$$

where k is the resistance coefficient.

Thus, the Lagrange equations have the form

$$m\ddot{y} - m_1 r (\ddot{\varphi} \sin \varphi + \dot{\varphi}^2 \cos \varphi) = -cy, \tag{46.15}$$

$$I\ddot{\varphi} - m_1 r \ddot{y} \sin \varphi = M_0 - (a + k)\dot{\varphi} \tag{46.16}$$

It is important to note that these equations do not include time in an explicit form. They describe the motion of an autonomous system.

It may be readily shown that this system of equations is not satisfied by the solution

$$\dot{\varphi} = \omega, \quad \varphi = \omega t, \tag{46.17}$$

which expresses the process of uniform rotor rotation. In actuality, in this case (46.15) would assume the form

$$m\ddot{y} + cy = m_1 r \omega^2 \cos \omega t \tag{46.18}$$

and we would have a solution with the following form

$$y = A \cos \omega t. \tag{46.19}$$

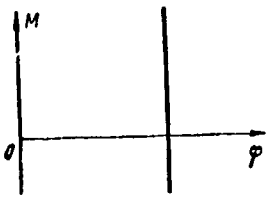

Fig. 46.4. Characteristic of engine with infinite power.

Substituting the latter expression in equation (46.16), we would obtain the variable $m_1 r\omega^2 A \cos \omega t \sin \omega t$ (its average value equals zero) in the left-hand side, whereas the right - hand side is constant. It thus /374 follows that the angular velocity of rotor rotation cannot be assumed to be constant. This is one of the important features of the problem under consideration.

However, we can indicate the limiting form of the engine characteristics, when the solution (46.17) is correct. It is shown in Figure 46.4(*). In this case, the rotating moment is an indefinite quantity, i.e., the left-hand side of equation (46.16) may be whatever is desired, and the solution (46.17) does not contradict the system of equations (46.15), (46.16).

It is known that the more powerful is the engine, the steeper is its characteristic (a small change in the velocity $\dot{\varphi}$ corresponds to large changes in the load M). Therefore, it may be stated that the characteristic shown in Figure 46.4 pertains to an engine with an infinitely large power. Consequently, solution (46.17) will correspond (and only approximately) only to engines with very great power. For engines with limited power, we cannot use the solution (46.17)

Unfortunately, it is impossible to obtain a precise solution of the system of equations (46.15) and (46.16) in a closed form. Therefore, we shall substitute a more modest, but still achievable goal — to formulate the first approximation, which can reflect the main properties of oscillations in the system under consideration.

(*) Just as in Figure 46.2, this characteristic may move to the right or to the left, depending on the working voltage.

The general scheme of the computations is as follows. Using equation (46.15), we express y by the variable φ. Here, for the sake of simplification, we must introduce a certain inaccuracy into the solution. We substitute the expression y in equation (46.16), and then analyze the possible solutions. We thus find the effect which we discussed at the beginning.

First of all, instead of equation (46.15) we write

$$\ddot{y} + p^2 y = \frac{m_1 r}{m}(\ddot{\varphi}\sin\varphi + \dot{\varphi}^2\cos\varphi). \tag{46.20}$$

The right-side may be represented in a more compact form /375

$$\ddot{\varphi}\sin\varphi + \dot{\varphi}^2\cos\varphi = -\frac{d^2}{dt^2}(\cos\varphi), \tag{46.21}$$

after which equation (46.20) assumes the form

$$\ddot{y} + p^2 y = -\frac{m_1 r}{m}\frac{d^2}{dt^2}(\cos\varphi). \tag{46.22}$$

The structure of the right-hand side suggests the advantage of changing to a new variable u = u(t) connected with the function y(t) as follows:

$$y = u. \tag{46.23}$$

Then equation (46.22) becomes

$$\ddot{u} + p^2 u = -\frac{m_1 r}{m}\frac{d^2}{dt^2}(\cos\varphi). \tag{46.24}$$

Now, after integrating twice, we obtain the following equation:

$$u + p^2 u = -\frac{m_1 r}{m}\cos\varphi + p^2(a_1 + b_1 t). \tag{46.25}$$

The linear function $p^2(a_1 + b_1 t)$, which arises during integration of equation (46.24), is not important for the subsequent calculations. We shall attempt to satisfy the equation (46.25) by the solution

$$u = A\cos\varphi + a_1 + b_1 t, \tag{46.26}$$

where in contrast to (46.19) A = A(t) — a function of time t, and the quantity φ does not coincide with the product ωt.

Substituting (46.26) in (46.25), we obtain the equation

$$\left(\ddot{A} - A\dot{\varphi}^2 + Ap^2 + \frac{m_1 r}{m}\right)\cos\varphi - (2\dot{A}\dot{\varphi} + A\ddot{\varphi})\sin\varphi = 0, \tag{46.27}$$

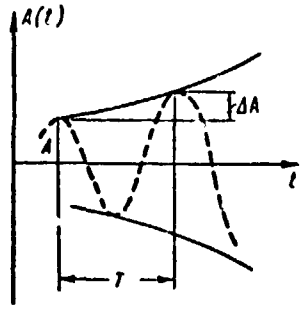

Fig. 46.5. Increase in ΔA in a period which is much less than A.

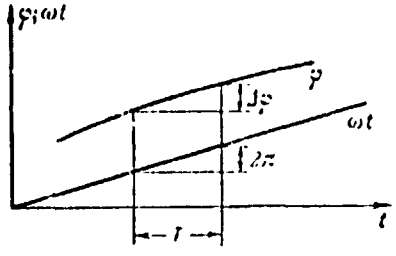

Fig. 46.6. Increase in Δ_φ in a period which is very close to the value of 2π.

which does not contain the cited function. To identically satisfy equation (46.27), it is necessary that both expressions in the parentheses equal zero separately:

$$\ddot{A} - A\dot{\varphi}^2 + Ap^2 + \frac{m_1 r}{m} = 0, \tag{46.28}$$

$$2\dot{A}\dot{\varphi} + A\ddot{\varphi} = 0. \tag{46.29}$$

Up until now, our calculations have been strictly rigorous, but now in order to make the solution possible, we shall assume certain inaccuracies. We shall /376 start from the assumption that the displacement y(t) changes according to a law which is close to the law governing simple harmonic oscillations. However, according to relationships (46.23) and (46.26)

$$y = \frac{d^2}{dt^2}(A\cos\varphi), \tag{46.30}$$

Therefore, it is natural to assume that the function A cos φ also changes according to a law which is close to the law governing harmonic oscillations. Being close to harmonic oscillations means that the function A(t) changes slowly in the expression (46.26) and the quantity φ(t) almost changes according to a linear law as a function of time.

Slowness of changes in the function A(t) means that in one period of oscillations the function A(t) cannot change significantly, i.e., increment ΔA is small as compared with A (Figure 46.5):

$$\Delta A = \dot{A}T + \ddot{A}\frac{T^2}{2} + \ldots < A, \tag{46.31}$$

i.e.,

$$\left.\begin{aligned}\dot{A}T &\ll A \quad \text{or} \quad \dot{A} \ll \omega A,\\ \ddot{A}T &\ll \dot{A} \quad \text{or} \quad \ddot{A} \ll \omega^2 A.\end{aligned}\right\} \tag{46.32}$$

The assumption about the change in (t) may be formulated as follows: an increasein the function φ in one period is close to the increase (also in one period) of the linear function ωt. However, the increase in the function φ in one period is (Figure 46.6)

$$\Delta\varphi = \dot{\varphi}T + \ddot{\varphi}\frac{T^2}{2} + \ldots, \tag{46.33}$$

and the increase in the function ωt is 2π. Therefore, we may write

$$\dot{\varphi}T + \ddot{\varphi}\frac{T^2}{2} + \ldots \approx 2\pi, \tag{46.34}$$

i.e., in the first approximation

$$\dot{\varphi}T \approx 2\pi, \quad \dot{\varphi} \approx \omega. \tag{46.35}$$

In addition,

$$\ddot{\varphi}\frac{T^2}{2} \ll \dot{\varphi}T \quad \text{or} \quad \ddot{\varphi} \ll \omega^2. \tag{46.36}$$

We now turn to equation (46.28). Taking into account (46.32) and (46.34), we may write

$$-A\omega^2 + Ap^2 + \frac{m_1 r}{m} = 0; \tag{46.37}$$

and we thus find the approximate expression

$$A = \frac{m_1 r}{m(\omega^2 - p^2)}, \tag{46.38}$$

which coincides with the solution according to the customary simplified theory.

We must also find the derivative $\dot{A}$. Naturally, it is impossible to do this using the approximate expression (46.38), and we shall use equation (46.29), from which we have the following without any simplications:

$$\dot{A} = -A\frac{\varepsilon}{2\dot{\varphi}}. \tag{46.39}$$

Now, using expression (46.26), we form the derivative $\ddot{y} = \ddot{u}$ which is necessary to us. Consequently, differentiating (46.29) we shall systematically find all terms having an order of smallness which is higher than the first. We thus obtain the expression $\ddot{u}$ which is accurate up to a second order of smallness. According to conditions (46.32) and (46.36), those terms which /378

have the factors $\ddot{A}$, $\dot{A}^2$, $\dddot{\varphi}$, $\ddot{\varphi}^2$ and $\dot{A}\ddot{\varphi}$ are terms of the second order of smallness. Proceeding in this manner, we finally obtain the following expression

$$\ddot{u} = A\dot{\varphi}^4 \cos\varphi + (6A\dot{\varphi}^2\ddot{\varphi} + 4\dot{A}\dot{\varphi}^3)\sin\varphi. \tag{46.40}$$

Taking into account (46.39) for the derivative $\dot{A}$, we obtain

$$\ddot{y} = A(\dot{\varphi}^4 \cos\varphi + 4\dot{\varphi}^2\ddot{\varphi}\sin\varphi). \tag{46.41}$$

Let us now substitute the approximate expression (46.38) for the function $\dot{A}$:

$$\ddot{y} = \frac{m_1 r}{m(\omega^2 - p^2)}(\dot{\varphi}^4 \cos\varphi + 4\dot{\varphi}^2\ddot{\varphi}\sin\varphi). \tag{46.42}$$

Thus, the second component in the left-hand side of equation (46.16) is determined in the form

$$-m_1 r\ddot{y}\sin\varphi = \frac{m_1^2 r^2}{m(p^2 - \omega^2)}(\dot{\varphi}^4 \sin\varphi\cos\varphi + 4\dot{\varphi}^2\ddot{\varphi}\sin^2\varphi). \tag{46.43}$$

The next operation, which we carry out with the last expression, is also approximate in nature, and is related to the fact that the variables in the parentheses have <u>different rates of change</u>. According to the statements made above, the quantities $\dot{\varphi}^4$ and $\dot{\varphi}^2\ddot{\varphi}$ are slowly changing functions, i.e., their increases in one period are small, whereas the trigonometric functions $\sin\varphi$ $\cos\varphi$ and $\sin^2\varphi$ complete a cycle of change in one period. Since we are interested in the <u>general nature</u> of the process, i.e., its behavior in a very large number of periods, we shall ignore the details pertaining to the motion within the limits of one period.

Mathematically, this means replacing the rapidly changing variables $\sin\varphi$, $\cos\varphi$ and $\sin^2\varphi$ with their averaged values in the period 2π:

$$\frac{1}{2\pi}\int_0^{2\pi} \sin\varphi\cos\varphi\, d\varphi = 0, \quad \frac{1}{2\pi}\int_0^{2\pi} \sin^2\varphi\, d\varphi = \frac{1}{2}. \tag{46.44}$$

Therefore, we may assume the following, instead of (46.43) /379

$$-m_1 r\ddot{y}\sin\varphi \approx \frac{2m_1^2 r^2}{m(p^2 - \omega^2)}\dot{\varphi}^2\ddot{\varphi} \approx \frac{2m_1 r^2\omega^2}{m(p^2 - \omega^2)}\ddot{\varphi}. \tag{46.45}$$

Here we assume $\dot{\varphi} = \omega$ in the final computation.

Equation (46.16) now acquires the form of a linear differential equation with constant coefficients:

$$\left[I+\frac{2m_i^2r^2\omega^2}{m(p^2-\omega^2)}\right]\ddot{\varphi}+(a+k)\dot{\varphi}=M_0. \tag{46.46}$$

To solve this equation, to its partial solution

$$\varphi=\frac{M_0}{a+k}t \tag{46.47}$$

(expressing the uniform rotation of an engine rotor at the angular velocity $\omega = \frac{M_0}{a+k}$), we add the solution of the corresponding homogeneous differential equation

$$\varphi=C_1e^{\lambda_1 t}+C_2e^{\lambda_2 t}, \tag{46.48}$$

where λ_1 and λ_2 are the roots of the characteristic equation

$$\lambda\left\{\left[I+\frac{2m_i^2r^2\omega^2}{m(p^2-\omega^2)}\right]\lambda+(a+k)\right\}=0. \tag{46.49}$$

One of the roots equals zero. No important effects are connected with this root.

The value of the second root is determined by the sign of the sum in the brackets in expression (46.49). If this sum is positive, then the root is negative, and the corresponding motion is aperiodic damping motion. The positive root, to which the aperiodic egress of the system from the stationary regime (46.47) corresponds, appears in the case of a negative sum

$$I+\frac{2m_i^2r^2\omega^2}{m(p^2-\omega^2)}<0. \tag{46.50}$$

Thus, the condition for the motion instability has the form

$$\omega>\frac{p}{\sqrt{1-\frac{2m_i^2r^2}{Im}}}. \tag{46.51}$$

For values of ω which satisfy inequality (46.51), the motion will not be periodic, and the angular velocity $\dot{\varphi}$ will increase infinitely /380

Figure 46.7 shows the resonance curve for the system under consideration, compiled with the equation (46.38). Parts of the right-hand side, designated by the crosses, correspond to unstable regimes.

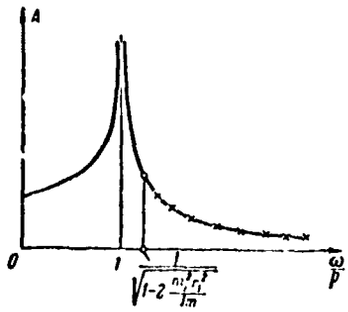

Fig. 46.7. Unstable regimes are designated by the crosses.

It is interesting that the location of the instability region does not depend on the parameters of the engine a, k and M_0. However, the valuesof the unstable roots, naturally, depend on a and k. They influence the rate at which the system aperiodically leaves a stationary regime.

These conclusions are basically valid if there is viscous resistance to motion of the mass m_2 (we assumed above that there is no such resistance). However, such viscous resistance appears at the boundary of the instability region.

The solution described above was given by J. Rocard in the book "Dynamique Générale des Vibrations" (First Edition, 1943; Second Edition, 1949; Third Edition 1960). One and the same error appears in all editions of this book: the minus sign is omitted in the right side of (46.21). Due to this, the second term in the brackets of equation (46.45) has a positive sign, and as a result the instability region was found on the left branch of the resonance curve, which does not agree with the experimental observations of Sommerfeld (see his article in VDI, No. 18, 1904).

I.I. Blekhman in his work "Self Synchronization of Vibrators on Certain Vibration Machines" (Inzhenernyy Sbornik, Vol. XVI, 1953) discovered unstable regimes on the right side of the resonance curve. See also the article by I.I. Blekhmen and G.Yu. Dzhanelidze "Dynamics of the Boisse-Sarda Regulator" (Izvestiya AN SSSR, OTN, No. 10, 1955). In later studies of B.O. Konenko and other authors, the action of an engine with limited power upon the nonlinear and parametric elastic systems was investigated. The present state of the problem is discussed very concisely in the book by B.O. Konenko "Kolebatel'nyye sistemy s ogranichennym vozbuzhdeniyem" (Oscillatory Systems with Limited Excitation), ("Nauka" Press, 1964).

§ 47. Self Oscillations; Method of Slowly Changing Amplitudes /381

Nondamped oscillations in mechanical systems are usually produced by perturbing forces of a periodic nature. However, in several cases nondamped oscillations may be sustained due to energy sources, which do not have oscillatory properties. We have already encountered such cases above when we examined the phenomenon of flutter in an air flow (§ 42) and oscillations of the Boisse-Sarda regulator (§ 45). Although the aerodynamic forces developing during flutter are periodic in nature, this periodicity is not specified beforehand, and results from oscillations of the elastic structure itself. The energy source of oscillations — the flow — has a constant velocity. The constant force of the weight of a load suspended from a cable is precisely the same source of oscillations in the mass of the Boisse-Sarda regulator.

Systems of this type are called self-oscillating (or self-exciting), and are widely used in present day technology. In particular, many systems with dry friction are self-oscillating(*).

If the equilibrium state of a self-oscillating system is unstable, then after any initial perturbation at first there is an increase in the oscillation amplitude. Then they gradually stabilize, and a certain stationary regime is established, which is characterized by unchanged values of amplitude and frequency, which do not depend on the initial conditions (Figure 47.1). These /382 parameters of steady self-oscillations are usually of the greatest interest,

(*) Processes such as the beating of the heart or a periodic change in the quantity of animals under certain conditions are also self-oscillating processes, which are far removed from technology. For example, the "fur cycle" in certain regions of Canada is well known, when the number of rabbits regularly increases, and then decreases. This phenomenon may be explained as follows. Let us imagine a region in which there are rabbits and lynx. The basic foods for lynx are rabbits, and if the number of lynx is very great, then the number of rabbits begins to decrease. However, with a decrease in the number of rabbits, the lynx begin to be very hungry, and their number decreases. This creates conditions for an increase in the number of rabbits, and consequently leads to the disappearance of hunger in the lynx. The number of the latter increases, the destruction of the rabbits increases, etc.

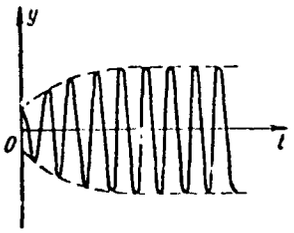

Fig. 47.1. Process of establishing self-oscillations.

but sometimes it is necessary to have a complete description of the entire motion and, in particular, its first stage — "the establishment process".

Due to unavoidable scattering of energy, in linear systems the nondamped oscillations can be subjected only to periodic external influences. It thus follows that all self-oscillating systems are primarily nonlinear.

In § 42 we were able to solve the problem of flutter as a linear problem, only because the only aim of the study was to determine self-excitation conditions. Linearizing the system, we were able to establish the initial behavior of the oscillations, but were not able to predict the further course of the process (at large amplitudes). On the other hand, in the problem of classical flutter, such a prediction is not required of the theory. Experience has shown that, if the critical velocity is reached, (i.e., self-excitation becomes possible), then disturbance of the real structure is practically unavoidable, and occurs very rapidly after the beginning of oscillations.

Linearization cannot be used here, since we shall be interested not only in the conditions of self-excitation, but also in the subsequent process of oscillations.

Frequently the nonlinearity of a self-oscillating system is represented in the equations of motion by small (but important) nonlinear terms, and the self-excitations have a harmonic nature. Such systems are called quasi-linear (slightly nonlinear, Thomson systems). This section as well as the following one are devoted to these systems.

A differential equation of motion of a quasi-linear system with one degree of freedom is usually written in the form

$$\ddot{y} + p^2 y = \mu f_1(y, \dot{y}),$$

where p is the eigenfrequency of the corresponding degenerate linear system, $f_1(y,\dot{y})$ — nonlinear function of the coordinate y and the velocity $\dot{y}$, μ — small parameter characterizing the similarity between the system under consideration and a linear conservative system. Separating out the small parameter is not obligatory, if the method given below is used, which provides only the first approximation. The right-hand side of the equation may be designated by $f(y,\dot{y})$, and we must simply recall that we are discussing a "small" nonlinear function. Therefore, we shall use the following /383

$$\ddot{y} + p^2 y = f(y, \dot{y}). \tag{47.1}$$

For an approximate solution of this equation, the following procedure is most advantageous (variants of the basis of this procedure will be investigated below). Instead of y and $\dot{y}$, we substitute the following in $f(y,\dot{y})$

$$y = A\cos\varphi, \quad \dot{y} = -Ap\sin\varphi, \tag{47.2}$$

i.e., the function is formed

$$f(y, \dot{y}) = f(A\cos\varphi, -Ap\sin\varphi) \tag{47.3}$$

and the integrals are calculated

$$\left.\begin{aligned} \Phi(A) &= \int_0^{2\pi} f(A\cos\varphi, -Ap\sin\varphi)\sin\varphi\, d\varphi, \\ \Psi(A) &= \int_0^{2\pi} f(A\cos\varphi, -Ap\sin\varphi)\cos\varphi\, d\varphi, \end{aligned}\right\} \tag{47.4}$$

under the assumption that A is a constant. After this, we may write the two differential equations

$$\left.\begin{aligned} \frac{dA}{dt} &= -\frac{\Phi(A)}{2\pi p} \\ \frac{d\xi}{dt} &= \frac{\Psi(A)}{2\pi p A} \end{aligned}\right\} \tag{47.5}$$

for the functions A(t) and $\xi(t)$. Naturally, it is assumed that A is a variable. It may be found by integrating the first equation. Then, after integrating the second equation, we obtain the function $\xi = \xi(t)$. The initial conditions for determining the integration constants may be given in the form

$$A(0) = A_0, \quad \xi(0) = 0. \tag{47.6}$$

Finally, the final solution of the equation (47.1) is obtained: /384

$$y = A(t)\cos[pt - \xi(t)]. \tag{47.7}$$

Thus, the function A = A(t) represents the envelope of the graph for the steady self-oscillations. For self-oscillating systems, it is typical for the amplitude to strive to a certain limit with an infinite increase in the time t. The amplitude of stationary self-oscillations serves as this limit. It may be found from the condition that it is constant, i.e., the relationship

$$\frac{dA}{dt}=0. \tag{47.8}$$

According to (47.4), this condition leads to the final equation

$$\Phi(A)=\int_0^{2\pi} f(A\cos\varphi,\ -Ap\sin\varphi)\sin\varphi\,d\varphi=0, \tag{47.9}$$

from which we must find A = const.

We have dealt purely with the effect, and must still find the cause. Now, having become familiar with the calculation procedure, let us examine two variants of the basis for the sequence of operations given above.

a) Van der Pol method. The Dutch scientist B. Van der Pol advanced the following approximate method for solving the nonlinear differential equation (47.1). According to this method, the solution may be expanded in the form

$$y=a(t)\cos pt+b(t)\sin pt. \tag{47.10}$$

Depending on the nature of the functions a and b again introduced, the form of the solution may be more or less similar to purely harmonic oscillations with the frequency p. For the constants a and b, it precisely describes the harmonic oscillations. In the case of slight nonlinearity ("quasi-linearity"), the systems of a and b are apparently "almost constant", i.e., they are slowly changing functions of time. On the other hand, up to a certain point in the calculations, we did not assume a slow change in a and b.

Replacing one unknown function y(t) by two unknown functions a(t) and b(t) does not adequately determine the latter, and some additional condition is still necessary to provide a specific transition to new functions. The correct selection of this condition can simplify the solution. Van der Pol

/385

assumed the following as such a condition:

$$\dot{a}\cos pt + \dot{b}\sin pt = 0. \tag{47.11}$$

A considerable simplification of the expression for the velocity $\dot{y}$ is thus achieved. In actuality, differentiating (47.10), we obtain, taking into account (47.11),

$$\dot{y} = -ap\sin pt + bp\cos pt, \tag{47.12}$$

i.e., the same expression as if the quantities a and b were constant. Therefore, the expression for the acceleration $\ddot{y}$ is relatively simple, and will not change the two derivatives $\ddot{a}$ and $\ddot{b}$. Differentiating (47.12), we have

$$\ddot{y} = -\dot{a}p\sin pt - ap^2\cos pt + \dot{b}p\cos pt - bp^2\sin pt. \tag{47.13}$$

Now substituting expressions (47.10), (47.12) and (47.13) in the given equation (47.1), we obtain the first order equation:

$$\begin{aligned} -\dot{a}p\sin pt + \dot{b}p\cos pt = \\ = f(a\cos pt + b\sin pt,\ -ap\sin pt + bp\cos pt). \end{aligned} \tag{47.14}$$

We may find the following expression for the derivatives a and b from the equations (47.11) and (47.14):

$$\left.\begin{aligned} \dot{a} = -\frac{1}{p} f(a\cos pt + \\ + b\sin pt,\ -ap\sin pt + bp\cos pt)\sin pt, \\ \dot{b} = \frac{1}{p} f(a\cos pt + \\ + b\sin pt,\ -ap\sin pt + bp\cos pt)\cos pt. \end{aligned}\right\} \tag{47.15}$$

Up until now, all of the computations have been very rigorous, and only now do we make a simplification which introduces a certain approximation into the solution. Assuming that the system is quasi-linear, we may assume that the variables a and b do not significantly increase in one period $2\pi:p$, and /386 the derivatives $\dot{a}$ and $\dot{b}$ are constant throughout any one period. Therefore, although these derivatives may be expressed by complex nonlinear functions of time (47.15), there will not be any great error, if we replace the functions by their average (in one period) values. To find these average values, we must alternately integrate [illegible] of the functions over the interval $\left[0, \frac{2\pi}{p}\right]$,

and then divide by the period. Thus, instead of the exact equations (47.15), we obtain

$$\left.\begin{aligned}\dot{a} &= -\frac{1}{2\pi}\int_0^{2\pi/p} f(a\cos pt + \\ &+ b\sin pt, -ap\sin pt + bp\cos pt)\sin pt\,dt, \\ \dot{b} &= \frac{1}{2\pi}\int_0^{2\pi/p} f(a\cos pt + \\ &+ b\sin pt, -ap\sin pt + bp\cos pt)\cos pt\,dt.\end{aligned}\right\} \tag{47.16}$$

Naturally, in performing integration, we assume that the quantities a and b in the right-hand sides are constant.

These equations are called the abbreviated equations, or the establishment equations of Van der Pol.

After squaring we obtain two equations of first order, but unfortunately, with nonseparated variables. To separate the variables, we turn to the new variables A and ξ, introducing them by means of the equations

$$\left.\begin{aligned}a &= A\cos\xi, \\ b &= A\sin\xi.\end{aligned}\right\} \tag{47.17}$$

Then the derivatives $\dot{a}$ and $\dot{b}$ acquire the form

$$\left.\begin{aligned}\dot{a} &= \dot{A}\cos\xi - A\dot{\xi}\sin\xi, \\ \dot{b} &= \dot{A}\sin\xi + A\dot{\xi}\cos\xi.\end{aligned}\right\} \tag{47.18}$$

In addition, by means of (47.17) we obtain the following expressions for the coordinate y and the velocity $\dot{y}$:

$$\left.\begin{aligned}y &= a\cos pt + b\sin pt = A\cos(pt-\xi), \\ \dot{y} &= -ap\sin pt + bp\cos pt = -Ap\sin(pt-\xi).\end{aligned}\right\} \tag{47.19}$$

Substituting (47.18) in the left-hand side of equations (47.16), and /387 expressions (47.19) in the right-hand side, we obtain

$$\left.\begin{aligned}
&\dot{A}\cos\xi - A\dot{\xi}\sin\xi = \\
&= -\frac{1}{2\pi}\int_0^{2\pi/p} f[A\cos(pt-\xi), -Ap\sin(pt-\xi)]\sin pt\,dt, \\
&\dot{A}\sin\xi + A\dot{\xi}\cos\xi = \\
&= \frac{1}{2\pi}\int_0^{2\pi/p} f[A\cos(pt-\xi), -Ap\sin(pt-\xi)]\cos pt\,dt.
\end{aligned}\right\} \qquad (47.20)$$

Multiplying the first equation by cos ξ, and the second by sin ξ, and then combining the equations, we obtain

$$\dot{A} = -\frac{1}{2\pi}\int_0^{2\pi/p} f[A\cos(pt-\xi), -Ap\sin(pt-\xi)]\sin(pt-\xi)\,dt. \qquad (47.21)$$

Multiplying the first equation (47.20) by sin ξ, and the second equation by cos ξ, and subtracting the first equation from the second, we obtain

$$\dot{\xi} = \frac{1}{2\pi A}\int_0^{2\pi/p} f[A\cos(pt-\xi), -Ap\sin(pt-\xi)]\cos(pt-\xi)\,dt. \qquad (47.22)$$

We now introduce the variable

$$\varphi = pt - \xi, \qquad (47.23)$$

then we obtain (47.21) and (47.22) in the final form:

$$\left.\begin{aligned}
\dot{A} &= -\frac{1}{2\pi p}\int_0^{2\pi} f(A\cos\varphi, -Ap\sin\varphi)\sin\varphi\,d\varphi, \\
\dot{\xi} &= \frac{1}{2\pi pA}\int_0^{2\pi} f(A\cos\varphi, -Ap\sin\varphi)\cos\varphi\,d\varphi.
\end{aligned}\right\} \qquad (47.24)$$

These equations with separated variables coincide with the equations (47.5), which were given above.

For a certain amount of time, the accuracy of the Van der Pol solution remained unclear, since it can be estimated only by means of a more rigorous theory. /388

L.I. Mandel'stam and N.D. Papaleksi, using the method of the small parameter, found that the Van der Pol solution is valid in the first approximation. We should note that this method may be used to formulate higher approximations for equations of this type.

b) Method of energy balance. Let us begin by studying stationary self-oscillations, and let us try to find the solution of equation (47.1) in the form

$$y = A \cos pt. \tag{47.25}$$

The solution (47.25) does not satisfy the equation (47.1) — the term $f(y, \dot{y})$ which represents a certain nonlinear force prevents this. If, instead of y and $\dot{y}$, we substitute A cos pt and Ap sin pt, the expression f(A cos pt, — Ap sin pt) does not identically equal zero. Nevertheless, we shall use the solution in the form (47.25), assuming that it is approximate. With respect to the "excess" of the force $f(y, \dot{y})$ introduced in the equation, its influence may be "smoothed out" as follows.

Let us study the possibility of stationary self-oscillations. If the work of the force $f(y, \dot{y})$ in a period is negative (for example, as occurs in the linear case of viscous friction), then the energy of the system in a period must decrease, but then the oscillations will be damped, which does not agree with the assumption of constant amplitudes. When the work of the force $f(y, \dot{y})$ is positive, the energy of the system increases, i.e., there is a jump in the oscillations. This also contradicts the condition of stationary self-oscillations.

Thus, only the requirement that the work of the force $f(y, \dot{y})$ equal zero in a period may provide results which are satisfactory in terms of energy. This condition lies at the basis of the method under consideration. In the last analysis, the method of the energy balance consists of the fact that, although the governing principles are violated within a separate period, we nevertheless see that they are satisfied as a whole in each period, I i.e., "on the average".

The work of the force f(y, ẏ) in the interval dy equals f(y, ẏ)dy or f(y, ẏ)ẏ dt. Therefore, the requirement formulated above takes on the form

$$\int_0^{2\pi/p} f(A\cos pt, -Ap\sin pt)\sin pt\,dt = 0. \tag{47.26}$$

Substituting pt = φ, we again obtain the equation (47.9) to determine the amplitude of the steady self-oscillations.

For the establishment process it is also possible to use the energy balance method, assuming that the amplitude $\dot{A}$ (just as in the Van der Pol method) is variable, but slowly changes.

In the establishment process, the energy continuously increases [the force f(y, ẏ) introduces it], and therefore the condition for the energy balance may not be written in the form (47.26), but rather

$$-Ap\int_0^{2\pi/p} f(A\cos pt, -Ap\sin pt)\sin pt\,dt = \Delta W, \tag{47.27}$$

where ΔW is the increase in the system energy in one period, calculated per unit of mass.

At any moment of time, the energy is approximately

$$W = \frac{cy^2}{2} + \frac{m\dot{y}^2}{2} = \frac{cA^2}{2}\cos^2 pt + \frac{mp^2A^2}{2}\sin^2 pt. \tag{47.28}$$

If we use ΔA to designate the increase in the amplitude A in one period T = 2π:p, then the energy at the beginning and end of the period under consideration is

$$W(0) = \frac{cA^2}{2},\quad W(T) = \frac{c(A+\Delta A)^2}{2}. \tag{47.29}$$

Thus, the desired energy increase ΔW, pertaining to a unit of mass, equals

$$\Delta W = tA\,\Delta A : m = p^2 A\,\Delta A \tag{47.30}$$

(the component of second order of smallnesses containing ΔA^2 is naturally omitted in the calculations). Substituting (47.30) in the energy balance equation (47.27), we obtain

$$-Ap\int_0^{2\pi/p} f(A\cos pt,\ -Ap\sin pt)\sin pt\,dt = p^2A\Delta A, \qquad (47.31)$$

or, dividing both parts of the equation by $2\pi pA = p^2AT$ and returning to the previous notation $\Phi(A)$, we find /390

$$\frac{\Delta A}{T} = -\frac{\Phi(A)}{2\pi p}. \qquad (47.32)$$

Let us now change from the finite differences of amplitude (ΔA) and time (T) to the differentials dA and dt. This leads to

$$\frac{dA}{dt} = -\frac{\Phi(A)}{2\pi p}, \qquad (47.33)$$

which completely coincides with the establishment equation (47.5).

The method given by Van der Pol was first published in the article: Van der Pol B. "A Theory of the Amplitude of Free and Forced Triode Vibration", Radio Review, Vol. I, 1920, p. 701.

An effective and general method of solving nonlinear problems, which makes it possible in particular to formulate the higher approximations, was advanced by N.M. Krylov and N.N. Bogolyubov. The basic results of their studies are given in the books: N.M. Krylov and N.N. Bogolyubov "Novyye metody nelineynoy mekhaniki v ikh primenenii k izucheniyu raboty elektronnykh generatorov" (New Methods of Nonlinear Mechanics in Their Application to the Operation of Electronic Oscillators) (ONTI, 1934); "Introduction to Nonlinear Mechanics" (Izdatel'stvo AN USSR, 1937). See also the book by N.N. Bogolyubov and Yu.A. Mitropol'skiy "Asimptoticheskiye metody v teorii nelineynykh kolebaniy" (Asymptotic Methods in the Theory of Nonlinear Oscillations) (Fizmatgiz, 1963).

The energy balance method was subsequently used in the book by K.F. Teodorchik "Avtokolebatel'nyye sistemy" (Self-Oscillatory Systems) (Gostekhizdat, Third Edition, 1955).

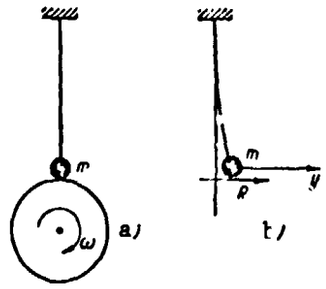

Fig. 48.1. Simplest scheme of an elastic-friction self-oscillatory system.

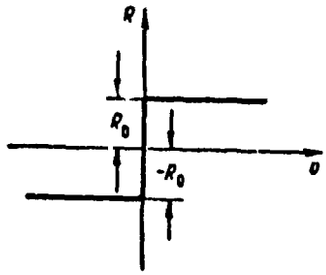

Fig. 48.2. Simplest characteristic of dry friction force. Using this characteristic, it is impossible to explain the nature of self-oscillations.

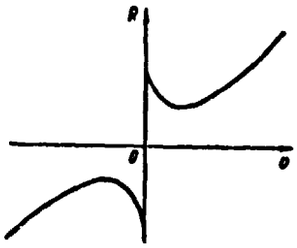

Fig. 48.3. Real characteristic of dry friction force.

§ 48. Self-Oscillations of a Quasi-System with Dry Friction

Figure 48.1, a shows a simple mechanical system, in which frictional self-oscillations are possible. This scheme may be used when studying the structure of friction brakes or when examining the interaction of tool and workpiece on a lathe. When the disk rotates, a friction force R arises in the zone of contact between the disk and the elastically fixed mass m, which is clamped to the disk. Under the action of the friction force, the mass will turn to the right, and a specific equilibrium position will occur, in which the mass is not fixed, and the slipping velocity is constant (Figure 48.1, b). However, under certain conditions this state of equilibrium may be unstable, and self-oscillations arise.

The possibility of frictional self-oscillations is closely connected with the properties of the friction characteristics, i.e., the dependence of the friction force R on the slipping velocity v. When solving the elementary problems of mechanics, a primitive description of the dry friction force is used, assuming /391

$$R = \pm R_0. \qquad (48.1)$$

The corresponding characteristic is shown in Figure 48.2. However, using the law (48.1), we could not explain the development of frictional self-oscillations. This more complex problem requires a more precise description of the dry friction forces in order to solve it. It has been experimentally established that the real characteristic of dry friction forces in its general outlines is as shown in Figure 48.3.

We must stress that the reason for frictional self-oscillations must be connected with the existence of the decreasing section of the characteristic. In the state of rest, two forces act on the mass m: the friction force R, corresponding to the nominal slipping velocity $v_0 = \omega r$ (ω — angular velocity of disk rotation, r — its radius), and the restoring force of an elastic cantilever — cy_0 (c — cantilever rigidity coefficient, y_0 — static displacement of the mass m). /392

We first assume that v_0 and R_0 correspond to the ascending section of the characteristic. It follows from the condition of equilibrium of the mass m that the static displacement is

$$y_0 = \frac{R_0}{c}. \tag{48.2}$$

Let us assume that the state of rest for the mass m is disturbed in some way. Then the subsequent motion will be described by the differential equation

$$R - cy = m\ddot{y}. \tag{48.3}$$

Naturally, when the mass m moves, its slipping velocity differs from the velocity v_0 and is

$$v = v_0 - \dot{y}. \tag{48.4}$$

Due to this, the friction force R, following the characteristic (Figure 48.3), changes. If $\dot{y}$ is small, we may set

$$R = R_0 + \left(\frac{dR}{dv}\right)_0 (v - v_0) = R_0 - \left(\frac{dR}{dv}\right)_0 \dot{y}, \tag{48.5}$$

where $\left(\frac{dR}{dv}\right)_0$ is the value of the derivative $\frac{dR}{dv}$ for $v = v_0$.

Substituting (48.5) in (48.3), we obtain

$$m\ddot{y} + \left(\frac{dR}{dv}\right)_0 \dot{y} + cy = R_0. \tag{48.6}$$

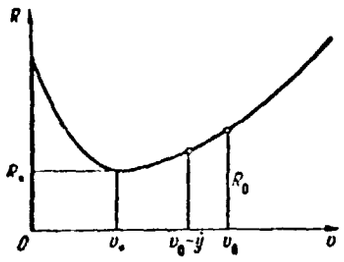

Fig. 48.4. For $\dot{y} > 0$ the slipping rate decreases and the friction force decreases (on the ascending curve of the characteristic).

This is an ordinary equation of free damped oscillations of a linear system and it may be immediately seen from it that the mass m will complete damped oscillations under the condition that $\left(\frac{dR}{dv}\right)_0 > 0$.

The opposite case is particularly important, when the nominal regime corresponds to the decreasing section of the characteristic (which may occur for a small angular velocity ω). Here the derivative $\frac{dR}{dv}$ is negative, i.e., negative damping would seem to appear in the system, and the oscillations will take place with an increase in amplitude.

Thus, for $v_0 > v_*$ (ascending section of the characteristic) the oscillations are damped, and for $v_0 < v_*$ (descending section of the characteristic),/393 they are increasing. Here v_* is the abscissa of a point on the characteristic minimum. This value of the velocity may be called the critical velocity of frictional self-oscillations. In contrast to the problem concerning flutter it is necessary that the slipping velocity v_0 be greater than the critical velocity for stability of the system.

Naturally, this analysis is very incomplete. Due to the linearization of the equation, just as in the problem concerning flutter, we have established only the conditions for which self-exciting oscillations may arise. However, such a procedure cannot provide an answer to the problem of the parameters of a steady self-oscillating process.

We shall not limit outselves here to a simple statement of the fact that at the slipping velocity $v_0 < v_*$ build-up of the oscillations begins. Our problem has become much broader, and we shall try to trace the subsequent behavior of these oscillations. This formulation of the problem does not

lead us outside the framework of a stability investigation "in the small", when linearization of the friction characteristic is permissible. In order to explain the process by which self-oscillations are established and the properties of a stationary self-oscillating regime, it is necessary to take into account the real nonlinearity of the friction characteristic. We shall assume that the friction characteristic corresponds to Figure 48.4, and is described by the relationship

$$R=3R_*\left(1-\frac{v}{v_*}+\frac{v^3}{3v_*^3}\right), \tag{48.7}$$

where v_*, R_* are the coordinates of a point on the characteristic minimum. We shall assume that the nominal velocity v_0 is less than the critical velocity v_*, and therefore self-oscillations are unavoidable. We shall also assume that the variable slipping velocity v

$$v=v_0-\dot{y} \tag{48.8}$$

remains positive always, i.e., the quantity $\dot{y}$ never exceeds the velocity /394 $v_0 = \omega r$. This enables us to use only that branch of the friction characteristic which is included in the first quadrant.

Substituting the velocity v with respect to (48.8) in the expression for the friction force (48.7), we obtain

$$R=R_0+R_1\dot{y}+R_2\dot{y}^2-R_3\dot{y}^3, \tag{48.9}$$

where, for purposes of brevity, we have introduced the positive coefficients

$$\left.\begin{aligned} R_0&=3R_*\left(1-\frac{v_0}{v_*}+\frac{v_0^3}{3v_*^3}\right),\\ R_1&=\frac{3R_*}{v_*}\left(1-\frac{v_0^2}{v_*^2}\right),\\ R_2&=\frac{3R_*v_0}{v_*^2},\\ R_3&=\frac{R_*}{v_*^3}. \end{aligned}\right\} \tag{48.10}$$

Expression (48.9) must be substituted in the equation of motion (48.3):

$$R-cy=m\ddot{y}; \tag{48.11}$$

and we then obtain

$$m\ddot{y}-R_1\dot{y}-R_2\dot{y}^2+R_3\dot{y}^3+cy=R_0. \tag{48.12}$$

It is more advantageous to locate the beginning of the displacement calculations to the right on the segment with the length R_0:c, i.e., to calculate the coordinate y from the position of the equilibrium of the mass m, when the force R_0 acts upon it. Then, instead of equation (48.12), we shall have

$$m\ddot{y} - R_1\dot{y} - R_2\dot{y}^2 + R_3\dot{y}^3 + cy = 0, \tag{48.13}$$

or, dividing by the mass m, we obtain

$$\ddot{y} - r_1\dot{y} - r_2\dot{y}^2 + r_3\dot{y}^3 + p^2y = 0, \tag{48.14}$$

where

$$r_1 = \frac{R_1}{m}, \quad r_2 = \frac{R_2}{m}, \quad r_3 = \frac{R_3}{m}, \quad p^2 = \frac{c}{m}. \tag{48.15}$$

If we discard the nonlinear terms in equation (48.14), we then obtain an equation for oscillations of the system with negative damping, which is described by the term $r_1\dot{y}$. As we have shown above, using such a linearized equation, we may only find the conditions for the beginning of self-excitation.

We shall investigate the complete equation (48.14). It contains three terms which depend on the velocity $\dot{y}$ and which determine either the damping or the self-excitation of the oscillations. Only one of them (term $r_3\dot{y}^3$) is included in the equation with a plus sign, and produces positive damping. The role of this term increases with an increase in the velocity $\dot{y}$, i.e., with the development of an oscillatory process. For sufficiently large oscillations, this influence becomes sufficient to compensate for the negative damping and to maintain the further increase in the oscillation amplitude. This contains the explanation for the possibility of stationary self-oscillations. /395

Let us use the method of the solution, which was proposed in § 47. The sequence of calculations indicated there as applied to our problem is as follows. According to equation (48.14), we write

$$f(y, \dot{y}) = r_1\dot{y} + r_2\dot{y}^2 - r_3\dot{y}^3 \tag{48.16}$$

and, following the second of the expressions (47.2), we obtain

$$f(A\cos\varphi - Ap\sin\varphi) = -r_1Ap\sin\varphi + r_2A^2p^2\sin^2\varphi + \\ + r_3A^3p^3\sin^3\varphi \tag{48.17}$$

Now we shall calculate the integrals (47.4):

$$\left.\begin{aligned}\Phi(A)&=\int_0^{2\pi}[-r_1Ap\sin\varphi+r_2A^2p^2\sin^2\varphi+\\&\quad+r_3A^3p^3\sin^3\varphi]\sin\varphi\,d\varphi=-\pi r_1pA+\frac{3}{4}\pi r_3p^3A^3,\\\Psi(A)&=\int_0^{2\pi}(-r_1A\sin\varphi+r_2A^2\sin^2\varphi+\\&\quad+r_3A^3\sin^3\varphi)\cos\varphi\,d\varphi=0.\end{aligned}\right\}\qquad(48.18)$$

Thus, the equations of establishment (47.5) assume the form

$$\left.\begin{aligned}\frac{dA}{dt}&=\frac{r_1A}{2}-\frac{3}{8}p^2r_3A^3,\\\frac{d\xi}{dt}&=0.\end{aligned}\right\}\qquad(48.19)$$

Integrating these equations for the initial conditions (47.6), we find /396

$$A=\frac{A_0}{\sqrt{\left(1-\frac{3r_3p^2}{4r_1}A_0^2\right)e^{-r_1t}+\frac{3r_3p^2}{4r_1}A_0^2}};\quad\xi=0.\qquad(48.20)$$

Consequently, the approximate solution of equation (48.14), according to (47.7), has the form

$$y=\frac{A_0\cos pt}{\sqrt{\left(1-\frac{3r_3p^2}{4r_1}A_0^2\right)e^{-r_1t}+\frac{3r_3p^2}{4r_1}A_0^2}}.\qquad(48.21)$$

This solution describes the entire process for the development of self-oscillations. Figure 48.5 shows the envelopes of graphs of the oscillations for different values of the initial deflections A_0. As may be seen, with the passage of time all the envelopes strive to one and the same horizontal lines, corresponding to a stationary regime of self-oscillations with a constant amplitude. The value of the latter may be found from expression (48.20), setting $t\to\infty$:

$$A=\frac{2}{p}\sqrt{\frac{r_1}{r_3}}.\qquad(48.22)$$

Substituting the expressions (48.15) divided by m, we obtain /396

$$A=\frac{2v_*}{p}\sqrt{1-\frac{v_*^2}{v_0^2}}.\qquad(48.23)$$

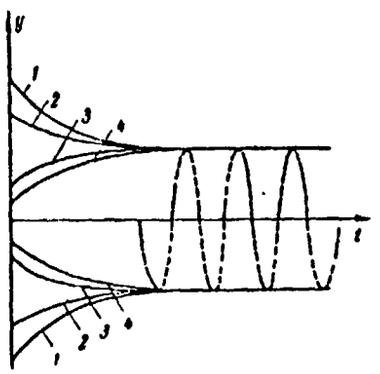

Fig. 48.5. Envelopes of graphs showing the establishment of self-oscillations. One and the same stationary regime is established, irrespective of the magnitude of the initial deflection with time.

Finally, the last result may be obtained directly from equation (47.9), which in our case assumes the form

$$\Phi(A) = -\pi r_1 p A + \frac{3}{4}\pi r_3 p^3 A^3 = 0. \quad (48.24)$$

We thus have the formula (48.23).

It may now be seen that, with an increase in the velocity v_0 and its approximation to the value v_*, the amplitude of the self-oscillations increases. For $v_0 \geq v_*$, self-oscillations are impossible. With a decrease in the velocity v_0, the amplitude of the self-oscillations increases, and for a sufficiently small velocity v_0 the slipping velocity (48.4) may vanish. This means that "adhesion" of the load occurs during self-oscillations in certain time intervals. Such a system is not quasi-linear.

The problem of self-oscillations was discussed for example in detail in following books: K.F. Teodorchik "Avtokolebatel'nyye sistemy" (Self-Oscillatory Systems) (Gostekhizdat, 1948); A.A. Andronov, A.A. Vitt, S.E. Khaykin "Teoriya kolebaniy" (Theory of Oscillations) (Fitmatgiz, 1959); N.V. Butenin "Elementy teorii nelineynykh kolebaniy" (Elements of the Theory of Non-Linear Oscillations) (Sudpromgiz, 1962); H. Kauderer "Non-Linear Mechanics" (Foreign Literature Press, 1960), and also the extensive literature on the theory of automatic control. For a popular discussion, see the book by A.A. Kharkevich "Avtokolebaniya" (Self-Oscillations) (Gostekhizdat, 1953).

The problem of frictional self-oscillations is particularly discussed in the book by Yu.I. Kosterina "Mekhanicheskiye kolebaniya pri sukhom trenii" (Mechanical Oscillations in the Case of Dry Friction) (Izdatel'stvo AN SSSR, 1960).

§ 49. Discontinuous Self-Oscillations in the Case of Dry Friction

The widely used expression "the torments of Tantalus" is connected with the well-known ancient myth regarding Tantalus, who invoked the anger of the gods with his crimes. Thundering Zeus overthrew Tantalus in the gloomy reign of the brother of Aida; there he met a horrible punishment. Tormented with thirst, he stood in clear water reaching up to his chin, but when Tantalus bent to slake his thirst, the water disappeared.

A simple hydraulic system ("Tantalus vessels") has been named after /398 the mythical Tantalus. Its action is as follows (see Figure 49.1). A stream of water constantly passes through a vessel. A thick curvedtube passes through the bottom of it. When the water reaches the level H, the vessel rapidly empties to the level h, and no more water passes through until it again reaches the level H. Then the process is repeated.

The period of oscillations for the liquid level in the Tantalus vessel is determined only by the parameters of the system itself, and equals the sum of the time intervals for filling the vessel and emptying it. With a sufficiently large diameter of the output tube, the time for emptying the vessel is very low, so that the period of oscillations may be approximately determined by the formula

$$T=\frac{\pi D^2(H-h)}{Q},$$

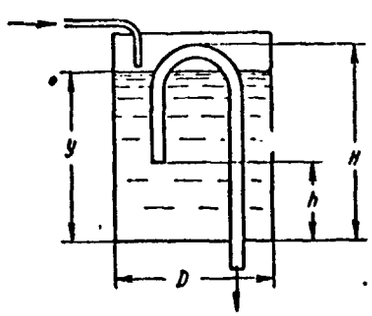

Fig. 49.1. Tantalus vessel.

in which D is the vessel diameter, Q — flow rate of the water passing through the filled tube.

It is assumed that the Tantalus vessel is the first self-oscillating system in the history of technology. In this device, the basic property of self-oscillating systems may be

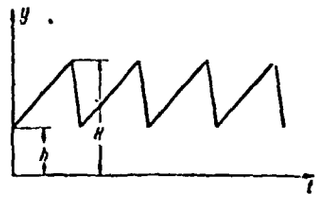

Fig. 49.2. Discontinuous self-oscillations of the liquid level in a Tantalus vessel

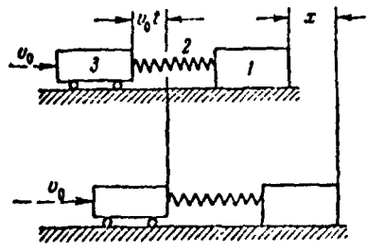

Fig. 49.3. For the uniform motion of the drive link 3, the load 1 performs self-oscillations around the state of uniform motion.

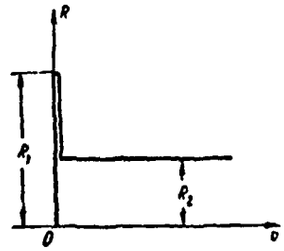

Fig. 49.4. Characteristic of Coulomb friction.

clearly seen — the existence of the oscillation regime, when the external influence is not oscillatory in nature. Here the oscillations are maintained due to uniform entry of the water into the vessel. It must be noted that self-oscillations of the water level in a Tantalus vessel obey a law, which sharply differs from a harmonic law. A graph showing the processes (Figure 49.2) has a sawtoothed nature, and the sections of the graph pertaining to the intervals in which the vessel is emptied are almost vertical. Such self-oscillations are called discontinuous or relaxation.

Self-oscillations of this type sometimes occur in mechanical systems due to dry friction, which acts between the moving elements of the system. The simplest case of discontinuous self-oscillations in a system with dry friction is described below (with a direct relationship to the motion of the support of a metal-cutting stand). /399

Let us examine the motion of a massive load 1, connected by a spring with a drive link 3 (Figure 49.3). The velocity of the latter is assumed to be constant and to equal v_0. For the characteristic of the friction, we use the Coulomb law (Figure 49.4), which takes into account the difference between the friction force at rest R_1 and the friction force in motion R_2. This simplified characteristic differs

greatly from the real law, but is adequate for the analysis of at least the main features of the self-oscillatory process being studied.

It is apparent that an unperturbed regime is possible, when the velocity of the load 1 also equals v_0, and the friction force is R_2. The spring compression force also equals R_2. However, if the velocity v_0 is very small, then a small random obstacle may be sufficient for stopping the load. If this occurs, then a self-oscillating process begins. /400

Let us assume that the load is stopped. Since the limiting friction force increases to the value R_1, then a certain period of time is necessary so that the spring compression force P reaches the same value which is necessary for the load to separate from its location. For the present let us omit this stage of rest for the load, and assume that it occurs immediately after the separation. The friction force decreases monotonically to the value R_2. Since the spring compression force does not change instantaneously, at the first moment of the initial motion it will equal R_1, as previously. We shall assume that this moment of the load separation is the beginning of calculating the time (t = 0). Thus, both the initial displacement x and the initial velocity $\dot{x}$ equal zero, i.e.,

$$x(0)=0, \qquad \dot{x}(0)=0. \tag{49.1}$$

The second condition follows from the fact that an instantaneous jump in the load velocity is impossible (an infinitely large acceleration would correspond to such a jump, and consequently an infinitely large force). The end force $R_1 - R_2$ acts on the load in the first moment of motion(*).

Since in the subsequent motion the velocity of the load $\dot{x}$ differs from the velocity v_0, the spring length will change. At the moment of time t, the additional extension of the spring is $x - v_0 t$. The spring elasticity force decreases by the quantity $c(x - v_0 t)$, and will equal

(*) The acceleration increases instantaneously from zero to $(R_1 - R_2)$: m; interruption of acceleration in mechanics is sometimes called soft impact (in contrast to hard impact - in the case of velocity interruption) or impact.

$$P(t) = R_1 - c(x - v_0 t) \tag{49.2}$$

(c — spring rigidity coefficient). Therefore, the differential equation of motion for the load has the form

$$R_1 - c(x - v_0 t) - R_2 = m\ddot{x},$$

where m is the load mass, or

$$\ddot{x} + p^2 x = p^2 v_0 t + \frac{R_1 - R_2}{m}, \tag{49.3}$$

where /401

$$p^2 = \frac{c}{m}. \tag{49.4}$$

The solution of this equation, which corresponds to the initial conditions (49.1), has the form

$$x = v_0 t - \frac{v_0}{p} \sin pt + \frac{R_1 - R_2}{c}(1 - \cos pt). \tag{49.5}$$

The first component in the right-hand side expresses the uniform motion at the velocity of the drive link, and the remaining components — additional load oscillations. The velocity of the load changes according to the law

$$\dot{x} = v_0 - v_0 \cos pt + \frac{p(R_1 - R_2)}{c} \sin pt. \tag{49.6}$$

The load subsequently stops at the moment when $\dot{x}$ again vanishes. The condition for the stopping $\dot{x} = 0$ leads, according to expression (49.6), to the transcendental equation

$$v_0 - v_0 \cos pt_1 + \frac{p(R_1 - R_2)}{c} \sin pt_1 = 0, \tag{49.7}$$

in which t_1 designates the time from the separation to the new stopping.

Let us introduce the dimensionless parameter

$$\alpha = \frac{p(R_1 - R_2)}{cv_0} = \frac{g}{pv_0}\Delta f, \tag{49.8}$$

where Δf is the difference between the coefficients of friction at rest and in motion. Then the stopping condition (49.7) assumes the form

$$\alpha \sin pt_1 = \cos pt_1 - 1, \tag{49.9}$$

from which we have

$$\sin pt_1 = -\frac{2\alpha}{1+\alpha^2}, \quad \cos pt_1 = \frac{1-\alpha^2}{1+\alpha^2}. \tag{49.10}$$

Finding the value t_1, using formula (49.5) we may determine the abscissa x_1 at the moment of stopping, i.e., the path traversed by the load in the time t_1:

$$x_1 = v_0 t_1 - \frac{v_0}{p} \sin pt_1 + \frac{R_1 - R_2}{c}(1 - \cos pt_1) = \\ = v_0 t_1 + \frac{2av_0}{p}. \tag{49.11}$$

With allowance for the expressions obtained, using formula (49.2) we find the spring compression force at the moment of stopping: /402

$$P(t_1) = 2R_2 - R_1. \tag{49.12}$$

Since, $R_2 < R_1$, then $P(t_1) < R_1$. Consequently, after the load stops, it remains for a certain period of time in place, while the spring elasticity force P again reaches the limiting force of friction at rest R_1.

During the time in which the load is at rest, the compression force of the spring increases by the value

$$\Delta P = R_1 - P(t_1) = 2(R_1 - R_2), \tag{49.13}$$

and the corresponding contraction of the spring is

$$\Delta l = \frac{\Delta P}{c} = \frac{2(R_1 - R_2)}{c}. \tag{49.14}$$

The path traversed by the leading unit during the period of time the load remains in place equals this value. Consequently, the length of time the load is at rest is

$$t_2 = \frac{\Delta l}{v_0} = \frac{2(R_1 - R_2)}{cv_0} = \frac{2a}{p}. \tag{49.15}$$

The same result may be obtained from the condition

$$v_0(t_1 + t_2) = x_1, \tag{49.16}$$

which expresses the equality of the displacements of the load and the leading unit in a period.

Thus, the period of load self-oscillations is determined by the formula

$$T = t_1 + t_2. \tag{49.17}$$

To use this formula, it is first necessary to find t_1 by means of any of the expressions (49.10), and then t_2 from the formula (49.15). At the moment $t = T$, the subsequent separation of the load occurs, and a new cycle of self-oscillations begin.

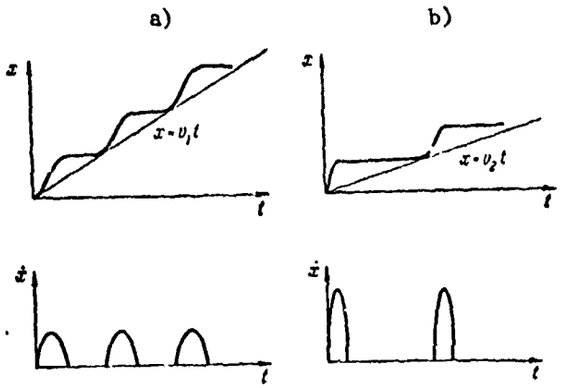

Fig. 49.5. Self-oscillations expressed more vividly in the case of reduced velocity of the drive link ($v_2 < v_1$).

The slower the velocity of the leading unit, the more sharply expressed is the self-oscillation process. In actuality, for small values of v_0 the dimensionless parameter α becomes very large. In this case, we may approximately obtain the following from expression (49.10)

$$t_1 \approx \frac{\pi}{\rho}, \tag{49.18}$$

And, with allowance for the expression (49.15) found above the period of self- /403
oscillations approximately equals

$$T \approx \frac{\pi + 2\pi}{\rho}. \tag{49.19}$$

The value of the second term increases with a decrease in the velocity v_0. The nature of the motion for two different small velocities $v_0 = v_1$ and $v_0 = v_2$ is shown in Figure 49.5. As is seen, with a decrease in the velocity v_0 the period T increases, and simultaneously the quantity y_1 increases.

With an increase in the velocity v_0, the stopping time decreases, and the motion acquires a more uniform nature.

The problem described here is discussed in the book by Ya.G. Panovko "Osnovy prikladnoy teorii uprugikh kolebaniy" (Fundamentals of the Applied Theory of Elastic Oscillations) (Mashgiz, Moscow, 1957). A less schematic characteristic of the friction force in this problem is given in the work by M. Ye. El'yasberg

"Designing the Feed Mechanisms of Machine Tools" ("Stanki i instrumenty", No. 11-12, 1951). See also the works: Singh B.R., Mohanti H.B. "Experimental Investigations on Stick-Slip Slidings", Engineer, No. 207, 1959; Häussler F.W., Wonka A. "Zur Berechnung des Stickslip-Vorganges" (Calculating the Stick-Slip Process), Maschinenbautechnik, Vol. 8, No. 1, 1959; D.R. Merkin "Relaxation Self-Oscillations of a Body When It Rises Along an Inclined Plane by Means of a Cable" (Tr. Leningradskogo in-ta inzh. vodnogo transporta, No. 83, 1965); Kemper J.D. "Torsional Instability from Frictional Oscillations", J. Franklin Inst., 1965, 279, No. 4.

§ 50. Delta Method /404

One of the effective methods for solving nonlinear problems, particularly problems of self-oscillations, is the delta method described here. It is connected with the mapping of real motion on the phase plane, and therefore we must first of all recall the basic properties of this mapping.

Phase plane refers to a plane of variables y and $\dot{y}$. When mapping motion on a phase plane, although we do not obtain a graphic dependence of the displacement y on the time t, this disadvantage is overcome by other advantages of the method.

Figure 50.1 by way of an example represents simply harmonic oscillations on a phase plane in the y, $\dot{y}$ coordinates. One point in Figure 50.1 (for example, point C_1) corresponds to each state of the system characterized by the quantities y and $\dot{y}$. This point is called the image point. In a small interval of time, the state of the system will be different, and another image point will represent it (for example, point C_2).

Thus, with the passage of time the image point will move along a certain curve called the phase trajectory. If the motion is periodic, then the state of the system is repeated with each period, and the image point returns to the previous position on the y, $\dot{y}$ plane. Correspondingly, the phase trajectory is a closed curve.

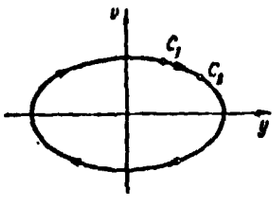

Fig. 50.1. Image point moves along a phase trajectory in the clockwise direction.

We should note that the direction of motion of the image point may only be in the clockwise direction. A system in the state C_1 has a positive velocity and, consequently the coordinate must increase. Therefore, in the upper half-plane (i.e., for $\dot{y} > 0$) the motion of the image point must go from left to right. Similar reasoning leads to the conclusion that the image point moves from right to left on the lower half-plane. /405

In this case, the phase trajectory differs greatly from the initial conditions. Thus, for other initial conditions the phase trajectories will differ from that shown in Figure 50.1, and form a set of ellipses which are inserted in each other and have a common center at the origin (Figure 50.2). The origin corresponds to the state of equilibrium for the system. A set of phase trajectories describes the possible motions of the system and is the phase picture (phase diagram) of the system.

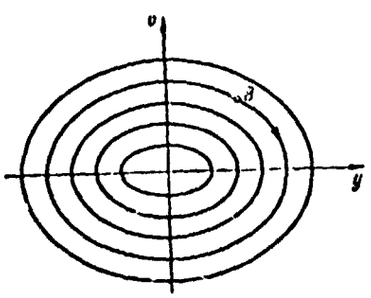

Fig. 50.2. Phase picture of a linear, conservative oscillatory system. The existence of a certain phase trajectory depends on the initial conditions (see, for example, point B).

Figure 50.3 shows the phase picture of a certain self-oscillating system. Here we may see only one closed curve A. It describes the stationary self-oscillations whose existence was established above. In addition, there are two phase trajectories in the picture: phase trajectory I, located within curve A, and phase trajectory II, located on the outside.

Let us assume that the state of equilibrium (the origin corresponds to

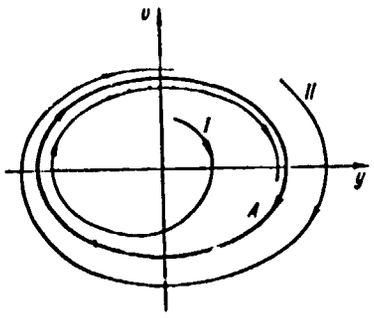

Fig. 50.3. Closed curve A describes stationary self-oscillations. Curves I and II describe establishment processes. Both curves infinitely approximate the limiting cycle A (outside or inside, depending on the initial conditions).

it) is disturbed so that the initial values of y_0, v_0 determine the image point located within the curve A. Then build-up of oscillations begins, and the phase trajectory, having the form of a spiral, will unfold, infinitely approaching the trajectory A. After a large initial push, when the system is thrown beyond the contour A, the phase trajectory is also a spiral, which is wound around the curve A on the outside.

Isolated closed curves, which the contiguous phase trajectories infinitely approach, are called stable limiting cycles. In our case, the limiting cycle describes a stationary regime of /406
self-oscillations. All the remaining phase trajectories describe the establishment process.

Figure 50.4 shows the phase picture of a system containing two limiting cycles A and B. In addition, it shows three typical phase trajectories — curve I, which begins close to the origin, curve II, which begins in the circular region between the limiting cycles A and B, and finally III, which begins in the region outside of the limiting cycle A. The nature of these phase trajectories indicates that for small initial perturbations (curve I) the system strives to a state of equilibrium (the origin), but for sufficiently large initial perturbations (curves II and III) the system strives to the motion of the limiting cycle A. The motion along the

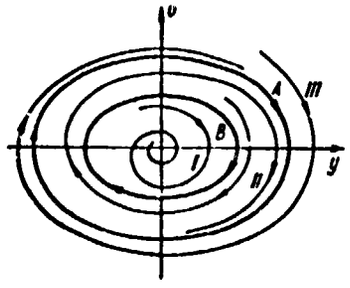

Fig. 50.4. A — stable limiting cycle; B — unstable limiting cycle (rigid self-excitation).

limiting cycle B is apparently unstable, since for any small perturbation of this motion the system either begins to move toward the position of equilibrium (curve I) or toward the limiting cycle A (curve II). The latter is a stable limiting cycle.

Thus, the system under consideration belongs to self-oscillatory systems, but for stable self-oscillations a sufficiently large initial perturbation of /407 the state of equilibrium is necessary. In these cases we are talking about rigid self-excitation. In the case to which Figure 50.3 refers, we have soft self-excitation. It is apparent that rigid self-excitation assumes stability (limited stability) of the state of equilibrium, whereas only systems with an unstable state of equilibrium may have soft self-excitation.

It is clear that it is impossible to establish the properties of the system by one phase trajectory. Thus, for example, it is impossible to determine the properties of the system, by regarding the phase trajectory shown in Figure 50.1. This trajectory may describe the behavior of a linear oscillatory system (for the corresponding initial conditions), but may also be a limiting cycle (both stable and unstable) for a nonlinear oscillatory system. We may say that the individual phase trajectory is only a part of the picture, making it impossible to determine the properties of the system as a whole. However, we may use the phase picture as a whole to obtain a complete picture of the possible states of motion for the system, and, in addition, to estimate their instability or stability.

Recalling the rule of "reading" the phase pictures, let us turn to the methods of compiling them.

It is not difficult to compile a phase picture after the general solution is found, i.e., the function y = y(t). For a known law governing the motion

$$y = y(t) \tag{50.1}$$

we must form the derivative

$$\dot{y} = \dot{y}(t) \tag{50.2}$$

and then exclude time t from the two equations (50.1) and (50.2). This gives the necessary connection between the variables y and $\dot{y}$. We may say that the expressions (50.1) and (50.2) serve as equations of phase trajectories in the parametric form (parameter — time t).

For example, in the case of harmonic oscillations, when

$$y = A\cos(pt-\xi) \tag{50.3}$$

(A and ξ — constants which depend on initial conditions), we have

$$\dot{y} = -Ap\sin(pt-\xi). \tag{50.4}$$

Squaring these equations and combining them, we obtain the equation for the /408 phase trajectory

$$y^2 + \frac{\dot{y}^2}{p^2} = A^2, \tag{50.5}$$

i.e., the equation for the set of ellipses shown in Figure 50.2.

If the phase picture is formulated from the well-known solution of the problem, them it plays a role only of illustration, which is still very graphic and always useful. However, there are methods for directly compiling the phase picture using the differential equation of the problem without solving the latter. These methods eliminate the necessity of formulating the analytic solution (wiich is frequently very cumbersome) and make it possible to study the motion by completely independent methods on the phase plane.

To formulate the phase trajectories, we usually start with the general form of the differential equation, describing the motion of an autonomous nonlinear system:

$$\ddot{y} + p^2 y = f(y,\dot{y}). \tag{50.6}$$

We set:

$$\frac{dy}{dt} = v; \tag{50.7}$$

and then we may write the following, instead of equation (50.6)

$$\frac{dv}{dt} = f(y,v) - p^2 y. \tag{50.8}$$

Dividing (50.8) by (50.7), we obtain the basic differential equation for the phase trajectories

$$\frac{dv}{dy} = \frac{\overset{\bullet}{f}(y, v) - p^2 y}{v}. \qquad (50.9)$$

The set of integral curves for this differential equation is formed by the phase picture of the system.

First of all, we should note that the derivative $\frac{dv}{dy}$ has a definite value everywhere, except for those points on the phase plane at which both the numerator and the denominator of the fraction in the right part of the equation (50.9) simultaneously equal zero. These unusual points on the phase plane are called <u>particular points</u>. The numerator on the right-hand side of equation (50.9) represents the force (per unit of mass), and the denominator represents /409 the velocity. Therefore, the fact that these quantities equal zero means that the <u>state of equilibrium</u> corresponds to the particular point. The stability or instability of equilibrium may be determined from the character of the phase trajectories in the vicinity of this point.

If the origin is surrounded by closed trajectories (Figure 50.2), then the state of equilibrium is stable. This particular point is called the <u>center</u>. The state of equilibrium in Figure 50.4 is also stable. A particular point of this type (i.e., surrounded by converging spirals) is called the <u>stable focus</u>.

The unstable state of equilibrium corresponds to the origin in Figure 50.3. The particular point, surrounded by diverging spirals, is called the <u>unstable focus</u>. There are particular points, in whose vicinity the phase trajectories have a different appearance. We shall not discuss these cases (particular points of the "saddle" and "nodal" type).

The <u>delta method</u> makes it possible to obtain the phase trajectories by simple and uniform geometric formulations. Let us explain this method, using

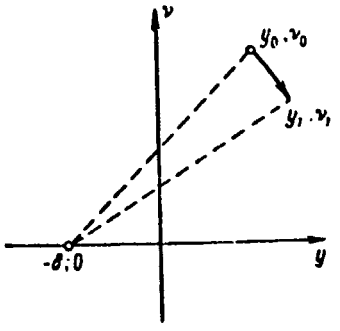

Fig. 50.5. Formulating an element of the phase trajectory by means of the delta method.

(50.6) as the initial equation(*). The latter may be advantageously changed somewhat, by using the dimensionless time τ as the independent variable:

$$\tau = pt, \tag{50.10}$$

and using the derivative $\frac{dy}{d\tau}$, which we designate by ν:

$$\nu = \frac{dy}{d\tau} = \frac{v}{p}. \tag{50.11}$$

The dimensionality of the variable ν coincides with the dimensionality of the variable y, and therefore the phase plane (y, ν) acquires a certain **isotropism**.

Substituting (50.11) in the differential equation (50.9), we have

$$p\frac{d\nu}{dy} = \frac{f(y, p\nu) - p^2 y}{p\nu}; \tag{50.12}$$

Let us set /410

$$\delta(y, \nu) = -\frac{f(y, p\nu)}{p^2}, \tag{50.13}$$

and we obtain the transformed equation

$$\frac{d\nu}{dy} = -\frac{\delta(y, \nu) + y}{\nu}. \tag{50.14}$$

The function δ(y, ν) depends on the two variables y and ν, but for small intervals of time (and small increases in the variables y and ν) it may be assumed to be constant . If we assume that δ is constant, then the variables y and ν are separated in the differential equation (50.14), and after integration we obtain the equation

$$\nu^2 + (y + \delta)^2 = \text{const}. \tag{50.15}$$

(*) The delta method may be applied to non-autonomous systems, when the nonlinear part of equation (50.6) depends on the time t and has the form f(y, ẏ, t). It also applies to non-oscillatory, nonlinear systems, when $p^2 y$ does not appear in the left-hand side of (50.6).

This equation describes a circle whose center is located at the axis of the abscissa at the point $y = -\delta$, $\nu = 0$. Thus, for a small interval of time a section of the phase trajectory describes the arc of a circle with the center at the given point.

The compilation of the phase trajectory begins at the point having the coordinates $y_0 = y(0)$, $\nu_0 = \nu(0)$, which are determined by the initial conditions for $\tau = 0$. These values of y and ν are substituted in expression (50.13), and $\delta_0 = \delta(y_0, \nu_0)$ is determined. The value of δ which is found determines the abscissa of the center of the circle (Figure 50.5).

We may now draw a small arc of a circle from the beginning point of the phase trajectory (y_0, ν_0) in a clockwise direction. Thus, we determine the first element of the phase trajectory. We may use the drawing to find new values of the phase coordinates y_1, ν_1, again substituting them in (50.13), and to find $\delta_1 = \delta(y_1, \nu_1)$, i.e., to determine the position of the new center of the circle on the abscissa axis. We may use this center to compile the second element of the phase trajectory, etc.

Naturally, when doing this we must follow the general rule of graphic solutions, and in particular, must not select lengths of consecutive segments of the arc which are too large. /411

Depending on the physical meaning of the problem, the delta function may depend only on one of the variables y or ν. These cases hold when the differential equation (50.6) has the form

$$\ddot{y} + p^2 y = f(y) \tag{50.16}$$

or

$$\ddot{y} + p^2 y = f(\dot{y}). \tag{50.17}$$

Equation (50.16) describes the free oscillations of a conservative nonlinear system, and equation (50.17) — the oscillations of a dissipative or self-oscillatory system [depending on the form of the function $f(\dot{y})$]. In each of these cases, it is advantageous to first compile the graphs of

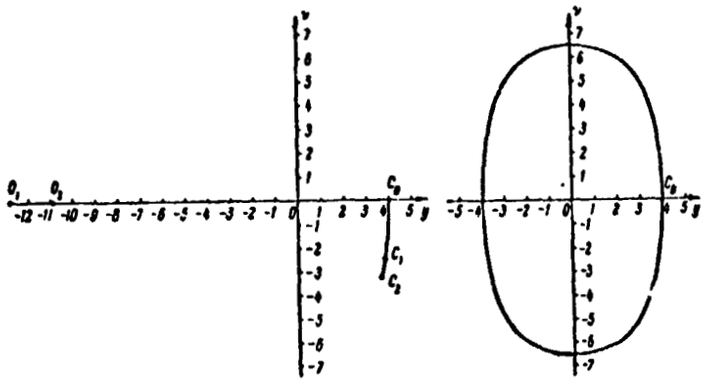

a) b)

Fig. 50.6. Case $\delta = \delta(y)$: a) beginning of formulation; b) phase trajectory.

the functions

$$\delta(y) = -\frac{f(y)}{p^2} \tag{50.18}$$

or

$$\delta(v) = -\frac{f(pv)}{p^2} \tag{50.19}$$

and then take the necessary values of δ directly from the drawing.

Let us use the delta method to formulate the phase trajectories for two particular problems of this type.

a) Free oscillations of a nonlinear conservative system. Let us assume the static characteristic of a nonlinear elastic connection (restoring force) is determined by the equation

$$F(y) = 25y + 5y^3. \tag{50.20}$$

Then the equation for oscillations of the load P = 1000 kg which is connected with this spring has the form

$$\frac{1000}{981}\ddot{y} + 25y + 5y^3 = 0, \tag{50.21}$$

i.e.,

$$\ddot{y} + 24.5y + 4.9y^3 = 0. \tag{50.22}$$

We thus have

$$f(y) = -4.9y^3; \quad p^2 = 24.5 \text{ sec}^{-2} \tag{50.23}$$

and using expression (50.13) /412

$$\delta(y) = 0{,}2y^3. \tag{50.24}$$

Let us compile the phase trajectory describing the motion which begins with the conditions y(0) = 4, v(0) = 0. The initial point of the phase trajectory is designated by the letter C_0 in Figure 50.6, a.

The corresponding value of expression (50.24) equals $\delta_0(4) = 12.8$. This may be used to determine the position of the center O_1 of the first arc. It is drawn with the radius O_1C_0 up to the axis y = 3.8. Thus, the image point C_1 is obtained. In addition, using the expression (50.24) we again find $\delta(3.8) = 11.9$. We note the new center O_2, and we draw the subsequent arc of the circle up to the abscissa y = 3.6 (point C_2). Proceeding in this same way, we may compile the entire phase trajectory. It represents a closed curve with an oval form (Figure 50.6, b)(*).

Using the phase trajectory, we may determine the maximum oscillation velocity. It may be seen from Figure 50.6, b, that $v_{max} \equiv 6.5$ cm. Consequently, we have

$$v_{max} = v_{max} p = 32{,}3 \ \frac{\text{cm}}{\text{sec}}$$

b) Process of establishing self-oscillations. By way of an example, let us draw the phase curve for the establishment of frictional self-oscillations described by the differential equation (48.14). The parameters of the system using the notation of § 48: m = 0.102 kg·sec/cm, c = 1000 kg/cm, $R_* = 10$ kg, $v_0 = 9.5$ cm/sec, $v_* = 10$ cm/sec. Using the formula (48.10), we obtain

$$R_1 = 0.292 \text{ kg·sec/cm}, \ R_2 = 0.285 \text{ kg·sec}^2/\text{cm}, \ R_3 = 0.01 \text{ kg·sec/cm}^3$$

(*) For a linear oscillatory system $\delta(y) \equiv 0$, so that the phase trajectory is a circle. The oval shape of the trajectory shown in Figure 50.6, b, is due to the nonlinearity of the system.

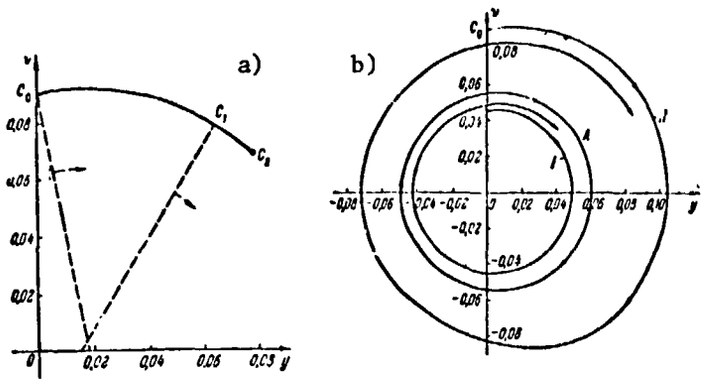

Fig. 50.7. Case $\delta = \delta(v)$: a) beginning of formulation; b) phase trajectory.

and in addition using formula (48.15):

$$r_1 = 2.87 \text{ sec}^{-1},\ r_2 = 2.80 \text{ cm}^{-1},\ r_3 = 0.10 \text{ cm}^2 \text{ sec}.$$

We now determine the frequency of the self-oscillations

$$p = \sqrt{\frac{c}{m}} = 100 \text{ sec}^{-1}$$

We may see from equation (48.14) that

$$f(\dot{y}) = r_1\dot{y} + r_2\dot{y}^2 - r_3\dot{y}^3.$$

Using (50.19), we obtain

$$\delta(v) = -0.029\, v - 2.80\, v^2 + 10\, v^3 \qquad (50.25)$$

and we formulate the phase trajectory, beginning with any (given by the initial conditions) point on the phase plane. Let us set $y_0 = 0$, $v_0 = 0.09$. Then using formula (50.25), $\delta = -0.018$.

Figure 50.7, a shows the beginning of the formulation. The first segment in the phase trajectory has its center at a point with the coordinates 0.018; 0. An arc of the circle is drawn from this center from the initial point C_0 to the point C_1, at which $v = 0.08$. Using formula (50.25), we obtain $\delta = -0.015$. The center of the second arc is located at a point with the coordinates 0.015; 0. From this center, we draw the second arc to the point C_2, at which $v = 0.07$, etc.

The phase trajectory as a whole is shown in Figure 50.7, b, and is /414
designated by II. It represents a convergent spiral. The other phase trajectory, beginning at the point (0; 0.045) is a divergent spiral. It is designated by I. Phase trajectories of the type I and II infinitely approximate a closed trajectory A, which is the limiting cycle.

Curve A is asymmetric, and the disturbance of the symmetry with respect to the vertical axis is particularly pronounced. The maximum and minimum deflection of the system when it moves along the limiting cycle equal 0.06 cm and 0.05 cm, respectively. Thus, the center of oscillations is displaced somewhat in the direction of the y-axis, and the semirange of the oscillations is 0.055 cm. The greatest value is $v = 0.055$ cm, and the maximum velocity is $v_{max} = vp = 100 \cdot 0.055 = 5.5$ cm/sec. These results satisfactorily coincide with the solution (48.24), according to which the amplitude of the self-oscillations equals $A = 0.064$ cm and the maximum velocity is $v_{max} = Ap = 6.4$ cm/sec.

The error in our formulation does not probably exceed 2%, and the results of a graphic solution by means of the delta method are more accurate. The error in the analytical solution is due to the fact that the solution was proposed in the form of harmonic oscillations — (47.25).

V.V. Guretskiy proposed a certain modification of the δ-method, based /415
on the following reasoning. Directly applying the δ-method to a formulation of the phase trajectories of equation $\ddot{x} + f(x) = 0$ means replacing $f(x)$ by a discontinuous function, consisting of rectilinear segments of the same inclination. However, it is more accurate to replace $f(x)$ by a certain continuous broken line. If we now divide the phase plane by the vertical bands, in each of which $f(x)$ is approximated by a segment with the inclination k_i^2, and if we assume that the scale of the ordinate axis equals $\dot{x}/k_i$ in the ith band, then the phase trajectory will consist of arcs of circles. When changing from the ith band to the $i + 1$ th band, the ordinate of the image point changes by a factor of k_i/k_{i+1}. Thus, an accuracy in formulating the

trajectory, which is the same as with the δ-method, is achieved by dividing f(x) by a smaller number of segments, i.e., with a smaller number of computations.

The delta method was proposed in the work: Jacobsen L.S. "On a General Method of Solving Second-Order Ordinary Differential Equations by Phase Plane Displacements" (J. Appl. Mech., Vol. 74, 1952, pp. 543 - 553. See also Chapter 2 in the book by W.J. Cunningham "Introduction to the Theory of Nonlinear Systems" (Gosenergoizdat, Moscow-Leningrad, 1962). A particular case of the delta method is the earlier method of A. Lienard, which is described in all the books on the theory of nonlinear oscillations. This method is applied to the case when the nonlinear function $f(y, \dot{y})$ does not depend on the coordinate y. For the work of V.V. Guretskiy see the collection "XXV nauchnaya konferentsiya LISI", (XXV Scientific Conference of the Leningrad Construction Engineering Institute), Leningrad, 1966.

CAT.-32

*U.S. GOVERNMENT PRINTING OFFICE: 1973-739-154/58